THE ROLE OF CATHEPSIN PROTEASES IN REOVIRUS PATHOGENESIS

By

Elizabeth Rose Meade Johnson

Dissertation

Submitted to the Faculty of the

Graduate School of Vanderbilt University

in partial fulfillment of the requirements

for the degree of

DOCTOR OF PHILOSOPHY

in

Microbiology and Immunology

December, 2009

Nashville, Tennessee

Approved:

Professor Terence Dermody

Professor Mark Boothby

Professor Graham Carpenter

Professor Anne Kenworthy

Professor D. Borden Lacy

To Ken

ACKNOWLEDGEMENTS

I am grateful for the financial support of the Cellular Microbiology Training Grant (Public Health Service Award T32 AI07611) and the Cell Entry of Reovirus Grant (Public Health Service Award R01 AI32539). I offer special thanks to the Lamb Center for Pediatric Research and to the Lamb family for their generosity. Additional support was provided by Public Health Service awards P30 CA68485 for the Vanderbilt-Ingram Cancer Center and P60 DK20593 for the Vanderbilt Diabetes Research and Training Center.

I would like to thank the many people who have contributed directly to this work through their efforts and guidance. Hal Champman, Douglass Hanahan, and Johanna Joyce provided the cathepsin-deficient mice to make the findings possible. John Mort and Nobuhiko Katunuma provided cathepsin L and the CLIK-148 inhibitor of cathepsin L, respectively. These reagents allowed me to extend my findings beyond the cathepsin-deficient background and further probe the effects of cathepsin deficiency on reovirus disease. I am grateful to my committee, Drs. Mark Boothby, Graham Carpenter, Anne Kenworthy, and Borden Lacy. Their probing questions forced me to think more deeply about my project and pushed me to a better understanding of the scientific process. Their comments on my manuscript and experiments strengthened them and helped me develop a compelling story. I also thank Don Rubin for insightful conversation and ideas for extending the research.

The Department of Microbiology and Immunology has provided an atmosphere of collegiality and scientific rigor. Through Research In Progress and the weekly seminar

series I have learned important aspects of scientific presentation and the art of thinking critically about my own science and that of others. Jean Tidwell has been helpful to me on a number of occasions for all things administrative. Dr. Hawiger works tirelessly to promote scientific inquiry of the highest caliber.

I would also like to thank the Division of Pediatric Infectious Diseases. Marijean Rue has provided administrative support and personal assistance while fostering a fun atmosphere. I thank the other support personnel and dish room attendants for their efforts.

I would like to thank the members of the Dermody lab for all their contributions to my training. Dan Ebert and Jackie Campbell set me off on sure footing. The members of the Entry and Pathogenesis Working Groups helped me to maintain my course and provided insight into experiments and techniques for which I am grateful. Pranav Danthi, Melissa Maginnis, Karl Boehme, Annie Antar, and Geoff Holm proved to be valuable resources for help with experimental design. I would also like to thank Kristen Guglielmi, Annie Antar, Melissa Maginnis, and Mine Ikizler for their friendship.

I cannot thank Denise Wetzel enough for the work she has done for me. She keeps the Dermody lab running smoothly, addresses our concerns, and keeps us in the black. She has helped me on many occasions with problems both scientific and administrative.

Of course none of this work would have been possible without Terry Dermody. His strong commitment to developing trainees is rare. He encourages a thoughtful approach to both scientific and career decisions and supports his students and post-doctoral fellows in their chosen endeavors. His love of science is infectious, and he shares it openly with his team. Lab meetings and journal clubs are always an opportunity for learning, whether the topic is directly related to our work or completely off the wall.

His willingness to share project development and writing opportunities with his trainees provides ample opportunity for us to sharpen these skills so necessary for future careers. I am thankful for his guidance and for his direction throughout my graduate work. I look forward to our future interactions and his continuing support.

My family, immediate and extended, has contributed to my life in many ways. They have helped to shape me into the person I have become. My grandparents offered the world and a healthy perspective in which to view it. My sister, Claire, has been my friend. We have shared concerns and parenting tips and her example has made me a better mother. My brother, Ben, is my science companion. I always enjoy our conversations about the many aspects of his work and mine. His approach to life and sense of adventure continue to inspire me! My parents provided invaluable opportunities to learn and grow. They have worked to ensure that I developed into a woman of whom they could be proud. They fostered independence and academic excellence in an environment of love and support.

My graduate experience has been enriched by my daughter, Caroline. She is therapy for the worst of days and the sunshine that lights my life. Her smile is ever-present. Watching her grow from 6 lbs 8 oz to a toddler with ideas and opinions has been the greatest experiment of all. Being a mother has brought new purpose to my work and to my commitment to my career. I look forward to the day when she will choose her own path and hope that the road will be smooth, having been paved by the many women who have come before her.

And finally, I thank Ken. Words cannot describe the understanding and patience that you have shown over the last 7 years. You have committed to helping me achieve my

goals, even as those goals have changed. You have weathered this storm with me and we are stronger for it. I do not know what lies ahead, but knowing you will be with me provides security and strength. As we move on to the next great adventure, thank you.

TABLE OF CONTENTS

LIST OF TABLES

LIST OF FIGURES

CHAPTER I

INTRODUCTION

Introduction

As obligate intracellular parasites, viruses must co-opt basic cellular processes to enter into host cells and deliver their genomes to the appropriate intracellular site (1). Viral entry steps include attachment of the virus to the cell surface, penetration of the virus into the cell interior, disassembly of the viral capsid, and activation of the viral genetic program. These events are essential for the virus to transition from the extracellular environment to the cellular compartment in which viral transcription and replication occur. Entry steps also play key roles in viral pathogenesis, as these events often determine cell tropism within the infected host.

Mammalian orthoreoviruses (reoviruses) are important models for studies of virus cell entry and the pathogenesis of viral disease. Reovirus entry is initiated by attachment to both carbohydrate and proteinaceous cell-surface receptors. Binding events trigger internalization of virions into endosomes where uncoating takes place. Following removal of the viral outer capsid, viral proteins breach the endosomal membrane, releasing the transcriptionally active core into the cytoplasm. Recent work in our lab and others has defined cellular components necessary for uncoating and membrane penetration in cell culture. However, the role of these cellular factors in vivo is not understood. For my dissertation research, I have investigated the function of endosomal

cathepsin proteases, enzymes required for uncoating of the reovirus outer capsid, in reovirus pathogenesis and disease.

Reovirus Structure and Background

Reoviruses are nonenveloped, icosahedral viruses that contain a genome of 10 double-stranded (ds) RNA gene segments encased in two concentric protein shells (3, 5) (Figure I-1). The viral core is composed primarily of the λ1 and σ2 proteins with the λ3, μ2, and λ2 proteins localized to the icosahedral vertices providing polymerase (6-11) and capping (14, 15) functions. The outer capsid is exquisitely designed for stability in the environment. The σ3 protein is most prominent, protruding from the virion in tetrameric and hexameric clusters over the surface of the particle. The σ3 protein forms a heterohexamer with μ1, the viral component responsible for membrane penetration. The interaction of σ3 with μ1 prevents the premature exposure of hydrophobic residues within μ1 and therefore aids in the proper timing of membrane penetration. Trimers of the viral attachment protein σ1 protrude from the pentamers of λ2 at the icosahedral vertices.

There are three reovirus serotypes, which can be differentiated by the capacity of anti-reovirus antisera to neutralize viral infectivity and inhibit hemagglutination (16, 17). The three serotypes are each represented by a prototype strain isolated from a human host: type 1 Lang (T1L), type 2 Jones (T2J), and type 3 Dearing (T3D). Other strains of reovirus commonly used for studies of reovirus entry and pathogenesis include field isolates and viruses selected for resistance to pharmacologic inhibitors of disassembly. In addition, reassortant genetics (18), and now reverse genetics (19), allow for exchange of

genetic material between strains. These techniques allow identification of viral gene segments that segregate with various biological and biochemical phenotypes.

An important control for studies of reovirus entry is the infectious subvirion particle (ISVP) (Figure I-1). ISVPs are a naturally occurring intermediate in the uncoating process (20-23) that can be generated in vitro by treatment of virions with proteases such as chymotrypsin and trypsin (24, 25). These particles are thought to penetrate cells directly at the cell surface as they are resistant to inhibitors of uncoating (21, 26-29) and release ^{51}Cr from preloaded cells (30, 31). Infection by ISVPs in the absence of infection by virions attests to the viability of cells and their capacity to support the stages of reovirus infection beyond uncoating and membrane permeabilization.

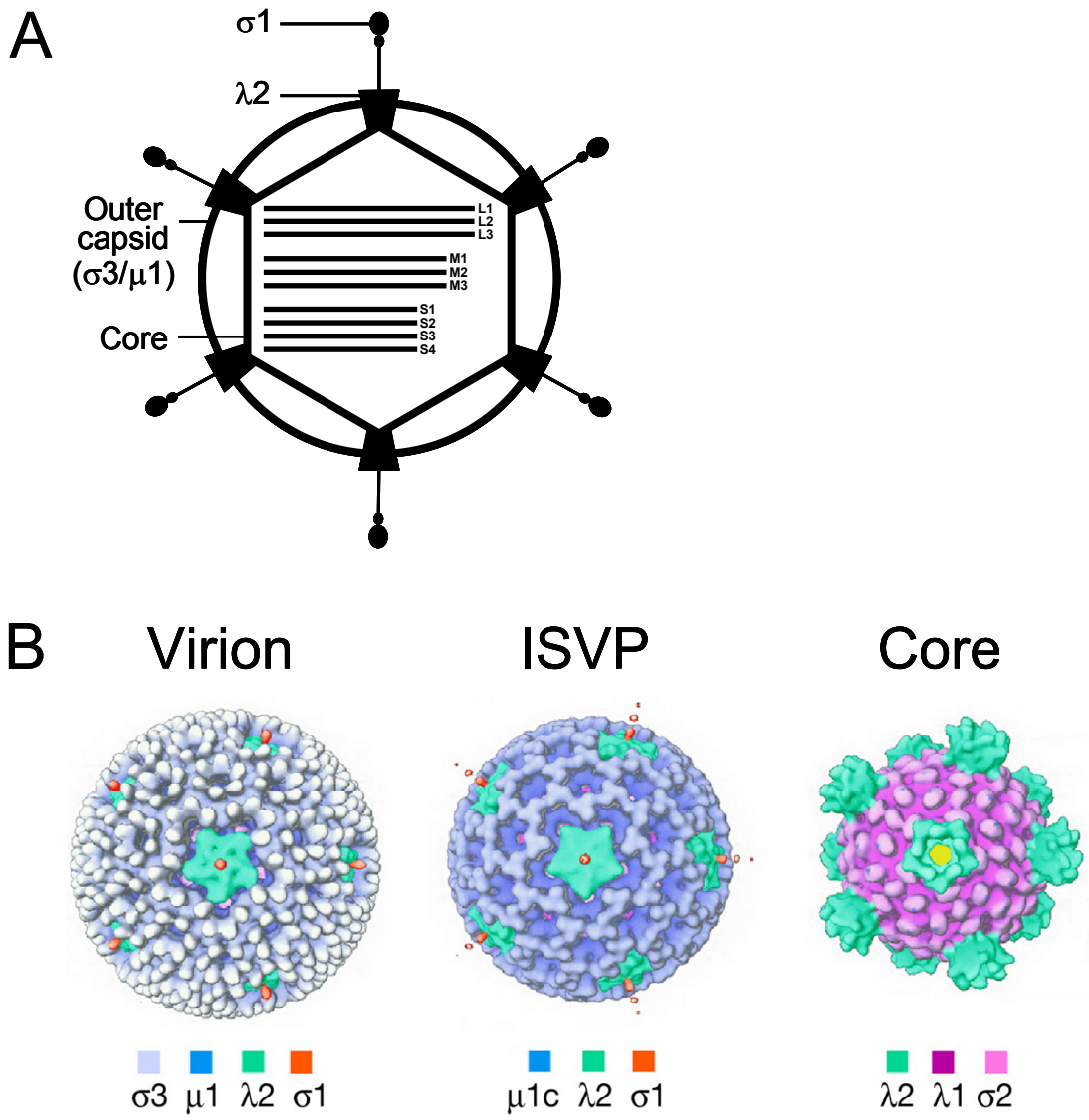

Figure I-1. Reovirus structure. (A) Schematic of a reovirus virion. The outer capsid and core are shown with 10 segments of dsRNA within. (B) Structure of reovirus virions, ISVPs, and cores. Surface-shaded representations of cryo-EM image reconstructions of reovirus are shown, as viewed along a twofold axis of symmetry. Density, representing σ1, can be seen extending from turrets of λ2 at the icosahedral axes of virions and ISVPs. Cores lack σ1. Image adapted from Dryden et al (3).

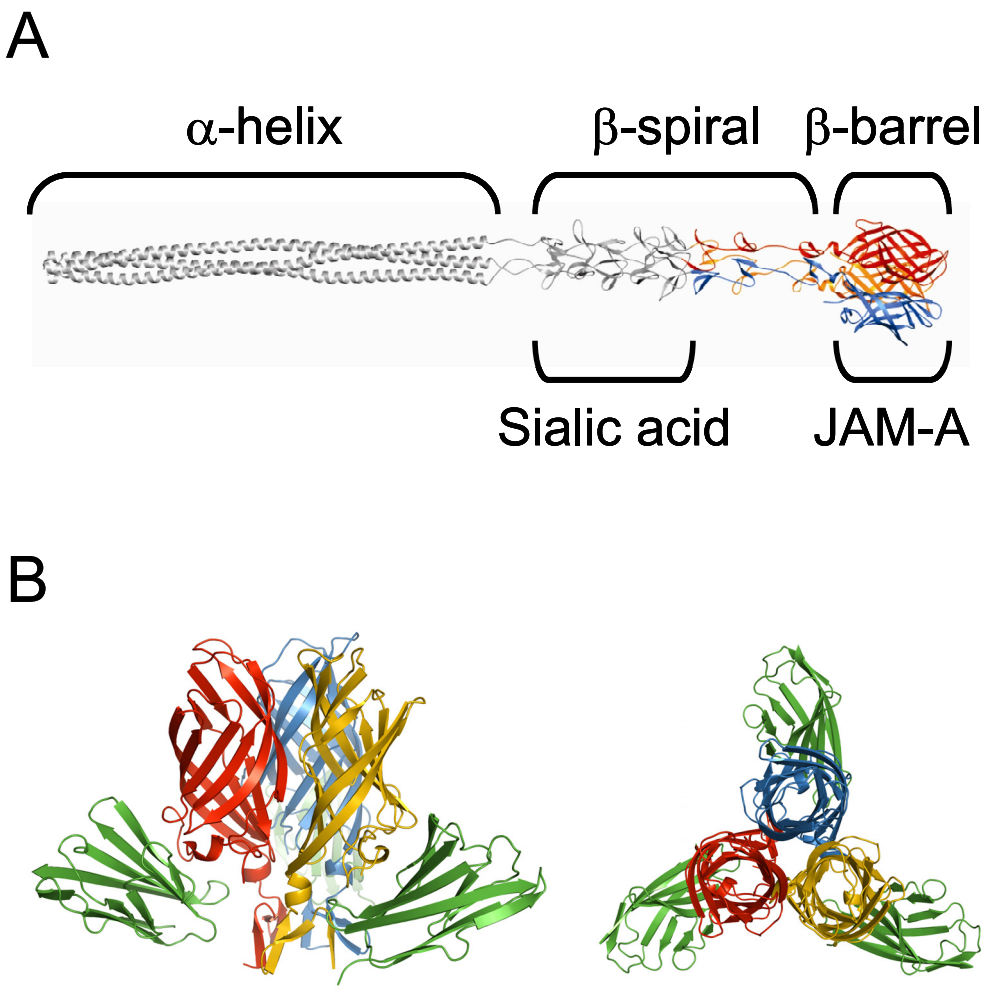

Figure I-2. Crystal structure of σ1 and JAM-A. (A) Ribbon drawing of the σ1 trimer with σ1 monomers shown in red, orange, and blue. Each monomer consists of a head domain formed by a compact β-barrel and a fibrous tail with three β-spiral repeats. Predicted structure of residues 1-245 is shown in grey. Binding sites for JAM-A and sialic acid (predicted) are noted. Image adapted from Chappell et al (2). (B) Ribbon drawing of the σ1 trimer in complex with monomers of the D1 head domain of JAM-A as viewed from the side (left) and three-fold axis of symmetry (right). σ1 monomers shown as in (A) and JAM-A monomers shown in green. Image adapted from Kirchner et al (12).

Reovirus Attachment

Reovirus entry is initiated by the binding of σ1 to its cognate cell-surface receptors. The σ1 protein is a fibrous, trimeric molecule with distinct head-and-tail morphology (Figure I-2 A). Although structural information is available only for the C-terminal half of the molecule (residues 246-455) (2, 32), sequence analysis has facilitated the development of a model of the full-length protein (2). The N-terminal tail region consists of approximately 160 residues of predicted α-helix that anchors σ1 to the virion (33-36) and approximately 150 residues that form triple β-spiral repeats responsible for binding to cell-surface carbohydrate (2). For many type 3 strains, this carbohydrate is sialic acid in either α2,3 or α2,6 linkages (37-39). Interaction with sialic acid is required for hemagglutination (39, 40) and optimal infection of murine L cells (38, 41, 42) and murine erythroleukemia (MEL) cells (43) by strain T3D.

The remaining σ1 sequence forms the head domain, which is composed of two Greek-key motifs that fold into a β-barrel (2, 32). Residues in the loops connecting β-strands D and E, along with residues in the most C-terminal β-spiral, make contacts with junctional adhesion molecule-A (JAM-A) (12) (Figure I-2 B), a member of the immunoglobulin superfamily (44). Human and murine homologs of JAM-A serve as receptors for all three reovirus serotypes, including all strains tested to date (45).

Internalization of Reovirus Virions Is Mediated by β1 Integrins

Following attachment to cell-surface carbohydrate and JAM-A, reovirus is internalized by receptor-mediated endocytosis (21, 22, 46-49). Expression of a JAM-A truncation mutant lacking a cytoplasmic tail allows reovirus to infect nonpermissive cells

(48), suggesting that molecules other than JAM-A mobilize the internalization apparatus that promotes reovirus cell entry. Based on similarities in the structures of the reovirus and adenovirus attachment proteins and receptors (50), it was hypothesized that reovirus and adenovirus employ similar integrin-dependent internalization mechanisms to enter cells. In keeping with this hypothesis, reovirus λ2 protein contains conserved integrin-binding motifs, RGD and KGE (51, 52). These sequences are displayed on surface-exposed loops of λ2 (53), where they could interact with integrins. Interestingly, the λ2-encoding L2 gene segment is genetically linked to viral shedding in infected mice and spread to littermates (54), suggesting a role for λ2 in reovirus-induced disease.

Treatment of cells with antibodies specific for β1 integrin reduces reovirus infection, while antibodies specific for the other integrin subunits expressed on permissive cells, including those specific for α integrin subunits, have no effect (48). However, antibodies specific for β1 integrin do not alter infection by in vitro generated ISVPs (48). These findings suggest that β1 integrin blockade inhibits endocytic uptake of virions. In comparison to β1 integrin-expressing cells, β1-null cells are substantially less susceptible to infection by reovirus virions, while infection by ISVPs is equivalent in both cell types (48). Diminished reovirus replication in β1-null cells correlates with diminished viral uptake, indicating that β1 integrin is required for efficient reovirus cell entry.

Most available evidence suggests that reovirus is internalized by a clathrin-dependent pathway (21, 22, 46, 47, 49). Reovirus virions are observed to colocalize with clathrin in living cells (47), and treatment of cells with chlorpromazine, a clathrin-specific chemical inhibitor (49), inhibits reovirus internalization and infection (49 and E.

Johnson, unpublished observations). However, there is mounting evidence that both clathrin- and caveolin-dependent mechanisms can be employed by some viruses to enter host cells (55, 56). Although there are no published reports of clathrin-independent uptake strategies for reovirus, a role for caveolae in reovirus cell entry has not been conclusively excluded (E. Johnson, unpublished observations and B. Mainou, unpublished observations).

Vesicles containing internalized reovirus virions are transported via microtubules (57) and accumulate in late endosomes (21, 22, 46, 57, 58). In the endocytic compartment, reovirus virions undergo stepwise disassembly forming sequential disassembly intermediates, the first of which is the ISVP (Figures I-1 B and I-3). ISVPs are characterized by the loss of outer-capsid protein σ3, a conformational change in attachment protein σ1, and cleavage of outer-capsid protein μ1 to form particle-associated fragments, δ and φ (25). Following further processing, ISVP-like particles (called ISVP*s) breach the endosomal membrane, leading to release of transcriptionally active core particles, which lack σ1 and μ1 (59, 60), into the cytoplasm. Thus, the disassembly process consists of a highly coordinated series of events that are dependent on host cell functions that act upon discrete components of the viral outer capsid.

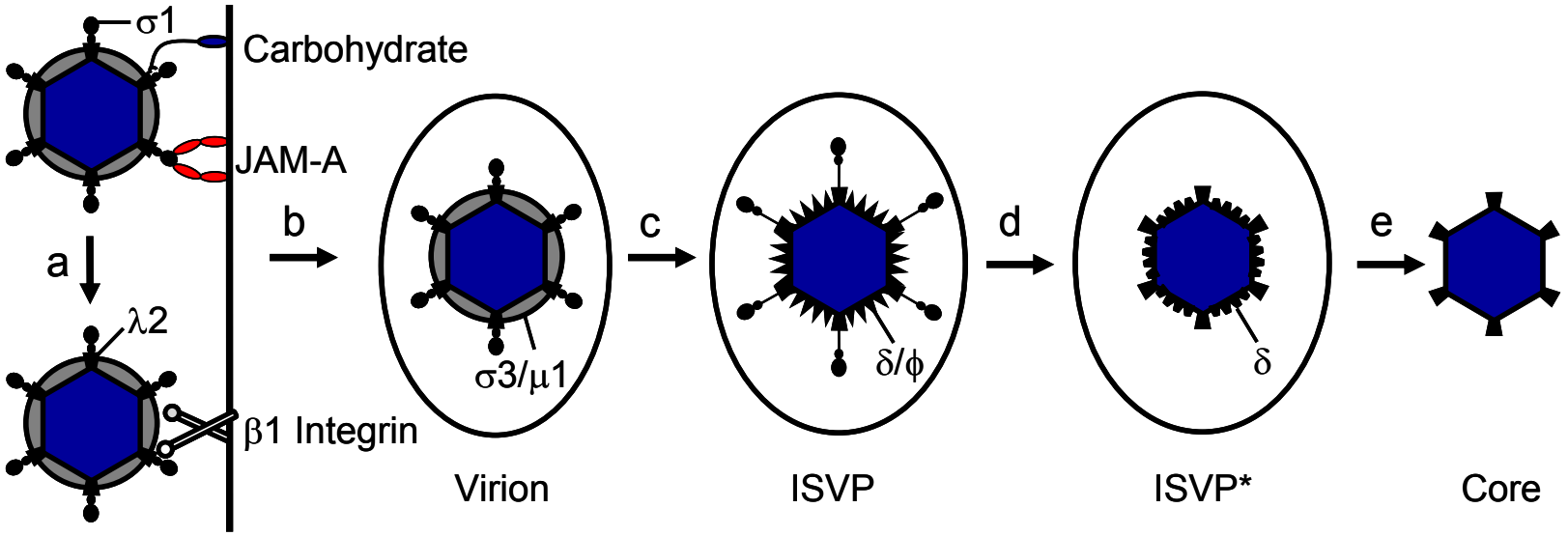

Figure I-3. Stepwise disassembly of reovirus. (a) Following attachment to cell-surface carbohydrate (α-linked sialic acid for type 3 reoviruses) and junctional adhesion molecule-A (JAM-A), reovirus virions enter cells by receptor-mediated endocytosis, a process requiring β1 integrin (b). Within an endocytic compartment, the viral outer-capsid undergoes acid-dependent proteolysis. (c) The first disassembly intermediate is the ISVP, which is characterized by loss of σ3 and cleavage of μ1C into particle-associated fragments δ and φ. (d) The ISVP then undergoes further conformational changes to form the ISVP*. The ISVP* is characterized by conformational rearrangements of the μ1 fragments to expose hydrophobic residues, release of μ1N and φ, and loss of attachment protein σ1. (e) The μ1 cleavage fragments mediate penetration through the endosomal membrane releasing the transcriptionally active core into the cytoplasm.

Reovirus Disassembly Requires Acidic pH and Endocytic Proteases

Treatment of murine L cells (21, 61, 62) or rat insulinoma cells (21, 61, 62) with the weak base ammonium chloride (AC), which raises the pH of endosomes and lysosomes (63, 64), blocks growth of reovirus when infection is initiated with virions. However, ISVPs can infect AC-treated cells (21). This finding indicates that the block to reovirus growth mediated by AC occurs following attachment but prior to disassembly. Concordantly, treatment of L cells with inhibitors of vacuolar proton ATPase activity, such as bafilomycin A1 and concanamycin A, blocks infection by virions but not by ISVPs (65). Thus, acidic pH is required for reovirus disassembly in some types of cells.

Pharmacologic treatments also have been used to demonstrate an important function for endocytic proteases in reovirus disassembly. Treatment of L cells with E64, an inhibitor of cysteine proteases (66), blocks growth of reovirus virions. Similar to findings made in studies using acidification inhibitors, ISVPs generated in vitro can infect E64-treated cells (26, 67-69), suggesting that one or more endocytic cysteine proteases can catalyze reoviruses disassembly. However, pepstatin A, an inhibitor of aspartyl proteases (70), is incapable of blocking reovirus infection and uncoating in multiple cells types (71). Moreover, in vitro treatment of reovirus virions with cathepsin D, an aspartyl protease, does not lead to generation of ISVPs (71). Thus, aspartyl proteases appear to be incapable of mediating virion-to-ISVP conversion.

Studies of Persistent Reovirus Infections

Support for a critical role of cysteine proteases in reovirus disassembly comes from studies of persistent reovirus infections in cultured cells. Although usually cytolytic,

reoviruses are capable of establishing persistent infections in many types of cells in culture (72). These cultures are maintained by horizontal transmission of virus from cell to cell and can be cured of persistent infection by passage in the presence of anti-reovirus serum. Cured (LX) cells, and the viruses isolated from persistently infected L-cell cultures (PI viruses), harbor mutations that affect viral disassembly (72).

Parental L cells support growth of reovirus after infection by virions or in vitro generated ISVPs. In contrast, LX cells do not support growth of reovirus after infection by virions of wildtype virus but do so after infection by PI virus virions or wildtype ISVPs (28, 73). Since LX cells allow growth of wildtype reovirus only when infection is initiated by ISVPs, these cells are altered in the capacity to support steps in viral replication leading to ISVP formation. L cells and LX cells do not differ in the capacity to bind or internalize virions or distribute them to a perinuclear compartment (73). Intravesicular pH is equivalent in both cell types, and virions colocalize with an acid-sensitive fluorophore in both L cells and LX cells. However, LX cells do not support the proteolytic disassembly of the viral outer-capsid following internalization of virus into the endocytic pathway (73, 74), suggesting a defect in proteolytic activity in LX cells.

The major cysteine proteases in the endocytic compartment of fibroblasts such as L cells are cathepsins B, H, and L, with cathepsin L being the most abundant in several cell types (66, 75-78). These enzymes are first produced as inactive proenzyme precursors that are processed to yield single-chain intermediates that are subsequently cleaved in lysosomes to form two-chain mature forms consisting of heavy and light chains (79-84). In LX cells, only the precursor form of cathepsin L is found (73). The mature, double-chain form of cathepsin B is found in these cells; however, the enzyme is

inactive (74). Neither cathepsin B nor cathepsin L is genetically altered in LX cells, indicating an extrinsic block to the function of these enzymes. Mixed lysates of L cells and LX cells lack activity of both cathepsin B and cathepsin L (74), suggesting the presence of an inhibitor of cathepsin function in LX cells. These findings indicate that a mutation in LX cells selected during persistent reovirus infection alters the activity of cathepsin B and cathepsin L, suggesting a critical function for these enzymes in reovirus disassembly in fibroblasts. Consistent with a role for cysteine proteases in reovirus uncoating, treatment of virions with either cathepsin B or cathepsin L in vitro results in the formation of particles that have similar biochemical and growth properties to ISVPs generated by treatment of virions with chymotrypsin or trypsin (4, 73).

Proteases that Mediate Disassembly

The involvement of cathepsin B and cathepsin L in the disassembly of reovirus virions in fibroblasts was confirmed in studies using pharmacologic inhibitors and genetically deficient cell lines (4). Infection of either L cells treated with the cathepsin L inhibitor A-Phe-Tyr(*t*-Bu)-diazomethyl ketone or cathepsin L-deficient mouse embryo fibroblasts results in inefficient proteolytic disassembly and decreased viral yields. In contrast, L cells treated with the cathepsin B inhibitor CA-074Me and cathepsin B-deficient mouse embryo fibroblasts support reovirus disassembly and growth. However, removal of both cathepsin B and cathepsin L activity completely abrogates disassembly and growth of reovirus. Concordantly, cathepsin L mediates reovirus disassembly more efficiently than cathepsin B in vitro (4). These results demonstrate that either cathepsin B

or cathepsin L can promote reovirus entry into murine fibroblasts and indicate that cathepsin L is the primary mediator of reovirus disassembly in these cells.

Cathepsins B and L are expressed in all major organs and mediate unique, tissue-specific activities (85). Cathepsin B modulates pathological trypsinogen activation (86) and apoptosis induced by TNF-α (87). Cathepsin L is required for hair follicle cycling and epidermal homeostasis (88).

The function of several cathepsin proteases intersects in their roles in adaptive immunity. Both cathepsins B (89, 90) and L (91) process endocytosed antigen for display by MHC II molecules. However, cathepsin B-deficient mice (*Ctsb*$^{-/-}$) do not display overt immunodeficiency (85). Involvement of cathepsin L in MHC II presentation has been well characterized. This enzyme cleaves the invariant chain in cortical thymic epithelial cells (92) and is hypothesized to mediate efficient endosomal protein fragmentation to ensure diverse peptide generation in the thymus (93, 94). Through these functions, it serves to facilitate positive selection of CD4+ T cells (95, 96). Cathepsin L also participates in NK1.1+ T cell selection through proteolytic processing in thymocytes (97). As a result, cathepsin L-deficient (*Ctsl*$^{-/-}$) mice have reduced numbers of both CD4+ and NK1.1+ T cells.

Proteases other than cathepsin B and cathepsin L also are capable of ISVP formation. In P388D cells, a macrophage-like cell line, cathepsin S, also a cysteine protease, mediates uncoating of some strains of reovirus (98). Expression of cathepsin S is more limited to cells and tissues of the immune system. It is primarily expressed in bone-marrow-derived, professional antigen-presenting cells (APCs), namely dendritic cells, B cells (95), and macrophages (99). In addition, cathepsin S is active in intestinal

epithelial cells (100), which can act as non-professional APCs. The role of cathepsin S in reovirus disassembly is important because during enteric infection, primary replication is thought to occur in mononuclear cells of Peyer's patches and intestinal epithelium (101-104). Cathepsin S is known to be expressed in mononuclear cells, including alveolar macrophages in the lung (105, 106) and microglial cells in the brain (107).

Like cathepsins B and L, cathepsin S is required for processing internalized antigens by APCs (108). In addition, cathepsin S cleaves the invariant chain in these cells, leading to CD4+ T cell activation (109). Like cathepsin L, cathepsin S participates in NK1.1+ T cell selection in the thymus through proteolytic processing in APCs (110). Thus, cathepsin S-deficient (*Ctss*$^{-/-}$) mice have impairments in both CD4+ and NK1.1+ T cell activities. Cathepsin S also processes antigen in endosomes for cross-presentation via the MHC I pathway (111).

Outer-Capsid Protein σ3 Regulates Reovirus Disassembly

The first step in the disassembly of reovirus virions is the cathepsin-mediated removal of outer-capsid protein σ3. The σ3 protein is a major outer-capsid component that protects the virion from degradation in the environment (112) and forms a protective cap for the μ1 protein (3). The latter function is especially important during entry as μ1 is responsible for penetration of ISVPs into the cytoplasm. By capping the μ1 protein, σ3 controls the timing of penetration: if too early, the resulting particle may not be primed to initiate transcription; if too late, the particle may be proteolytically degraded in the lysosome before it gains access to the cytoplasm where transcription occurs.

The σ3 protein contains two large domains separated by a flexible hinge (3, 113) (Figure I-4 A). The N-terminus of σ3 is in the smaller, virion-proximal lobe, and the C-terminus is in the larger, virion-distal lobe. These domains are not discrete in primary sequence as the peptide chain passes back and forth between the two lobes. A σ3-specific monoclonal antibody that sterically inhibits the σ1-mediated property of sialic acid binding engages the very tip of the virion-distal lobe (114).

Studies of PI viruses have shed light on mechanisms of σ3 cleavage during reovirus disassembly. In contrast to wildtype reoviruses, PI viruses can infect cells treated with either AC (28, 73, 115) or E64 (26). In most cases, growth of PI viruses in the presence of AC or E64 segregates with the S4 gene segment (26, 115), which encodes σ3 (116, 117). In addition, passage of wildtype reovirus in the presence of E64, resulting in selection of E64-resistant viruses (D-EA viruses) (68), or AC, resulting in selection of AC-resistant viruses (ACA-D viruses) (27), enriches populations of viruses that contain mutations in the σ3-encoding S4 gene. Therefore, mutations in σ3 protein confer the capacity of variant reoviruses to grow in the presence of pharmacologic inhibitors of reovirus disassembly.

All PI viruses analyzed to date have a mutation of Tyr to His at residue 354 near the C-terminus of σ3 (26, 115) (Figure I-4 A). This mutation is also selected in D-EA viruses (68) and some ACA-D viruses (27). PI, D-EA, and ACA-D viruses exhibit altered kinetics of disassembly with degradation of σ3 and cleavage of μ1 occurring much more rapidly both in vitro and in cells (27, 68, 115). Image reconstructions of cryo-EM images of PI viruses indicate that the Tyr354 to His mutation leads to an alteration in σ3 structure

at the hinge region between the two lobes (118). These findings suggest that the C-terminus of σ3 regulates susceptibility of the protein to cleavage.

The σ3 C-terminus also dictates strain-specific differences in the susceptibility of σ3 to proteolytic attack (69, 119). The σ3 protein of strain T1L is cleaved more rapidly than that of T3D. Analysis of ISVPs recoated with chimeric σ3 proteins generated from T1L and T3D revealed that the C-terminus is primarily responsible for the rate of σ3 proteolysis. Sequence polymorphisms at residues 344, 347, and 353 in σ3 contribute to this effect (119).

Treatment of reovirus virions in vitro with either cathepsin B or cathepsin L leads to an initial cleavage of σ3 at a terminus (4). Given that sequence polymorphisms in the C-terminus determine susceptibility to proteolysis, the initial cleavage of σ3 probably occurs in this region. During proteolysis by cathepsin L, subsequent cleavages occur between residues 243-244 and 250-251 (4). These cleavage sites are physically located near the C-terminus in the σ3 crystal structure (113) (Figure I-4 A). Because of this proximity, the small end fragment released following initial cathepsin L cleavage likely exposes the other two sites, rendering them susceptible to subsequent cleavage events. The C-terminus therefore appears to act as a "safety latch" that controls access to internal, proteolytically sensitive sites in σ3. Because reovirus disassembly in some cell types is an acid-dependent process, the safety latch might be primed for movement at acidic pH. In viruses with mutations near the C-terminus, such as PI, D-EA, and ACA-D viruses, the safety latch may be altered by structural rearrangements.

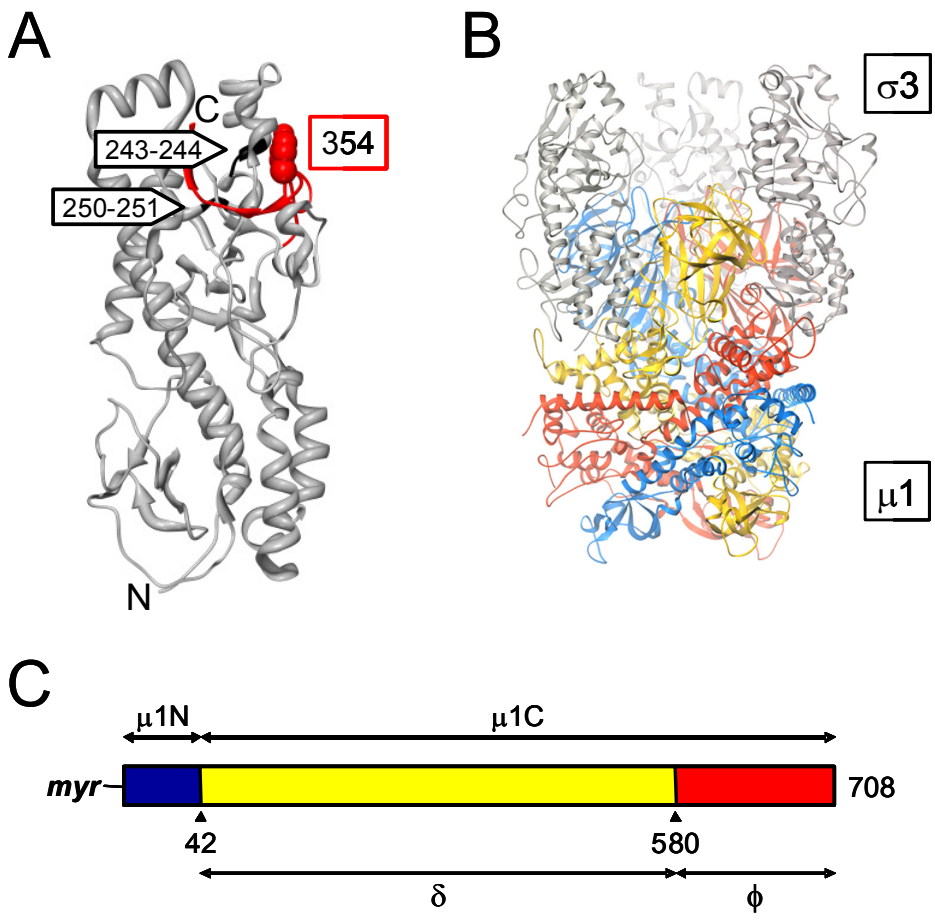

Figure I-4. Crystal structure of outer-capsid proteins σ3 and μ1. (A) Crystal structure of a σ3 monomer as viewed from the side. The C-terminus is highlighted in red with the Tyr at position 354 shown as a space-filling model. Cathepsin L cleavage sites are shown in black with the primary amino acid positions noted. Image adapted from Ebert et al (4). (B) A $\sigma 3_3\mu 1_3$ heterohexamer, viewed from the side. The bottom of the complex would contact σ2 proteins on the surface of the reovirus core. Three σ3 proteins (shown in gray) bind to the upper part of the underlying trimer of μ1 (with individual monomers shown in yellow, red, and blue). The three μ1 chains are wound tightly around each other. Each σ3 contacts two μ1 proteins. Image adapted from Liemann et al (13) (C) Regions of μ1 as determined by cleavage sites. μ1N is colored blue, δ is yellow, and φ is red. The N-terminal myristoylation site and cleavage sites at positions 42 and 580 are indicated.

Outer-Capsid Protein μ1 Mediates Membrane Penetration

Insight into mechanisms employed by reovirus to penetrate into the cytoplasm first came from studies of ISVPs generated in vitro. ISVPs, but not intact virions, release ^{51}Cr from preloaded L cells (46), lyse red blood cells in the presence (67, 69, 120) and absence (121, 122) of cesium ions, and form ion-permeant channels in planar phospholipid bilayers (123). ISVPs also facilitate entry into cells of the toxin alpha-sarcin in the presence of inhibitors of reovirus uncoating (65, 122, 124, 125). These observations suggest that ISVPs are the immediate precursor to the disassembly intermediate that facilitates delivery of the core particle into the cytoplasm.

Following formation of ISVPs in endosomes, transcriptionally active cores, which lack both μ1 and σ1, are released into the cytoplasm (Figure I-3). The mechanism of penetration and the shedding of these outer-capsid proteins has been the focus of recent work. This research has led to the identification of an additional intermediate particle formed subsequent to the ISVP, the ISVP* (124-126).

Most of the μ1 protein on mature virions is autocatalytically cleaved near the N-terminus to generate two fragments, μ1N and μ1C (60, 127) (Figure I-4 C). This cleavage is not required for virion assembly (125) and may occur physiologically during the transition from the ISVP to the ISVP* (128). In ISVPs, μ1C is further cleaved by either endocytic (4, 21) or intestinal (129) proteases to form fragments δ and φ, which remain particle-associated (25). However, the role of this cleavage in viral penetration is not understood, as core particles recoated with mutant forms of μ1 incapable of δ/φ cleavage can establish productive infection (120). In addition, μ1 is not cleaved at the δ/φ junction

in ISVPs generated in the presence of alkyl sulfate detergents (dpSVPs), yet dpSVPs are infectious (67).

Transition from the ISVP to the ISVP* in vitro is triggered by differential cationic concentration or interactions with membranes (124, 126). In contrast to ISVPs, ISVP*s lack σ1 and have an altered conformer of μ1 in which internal hydrophobic residues are exposed. ISVP*s are capable of membrane penetration and transcription initiation (124, 126). The conformational change in μ1 may be the driving force for both the loss of σ1 and the initiation of transcription (13). Mechanisms underlying these events are unknown, but it is possible that μ1 rearrangement induces a conformational change in λ2, the pentameric turret that anchors σ1, causing σ1 release. A μ1-induced conformational change in λ2 also may activate the transcriptional machinery through interactions with either or both of the core proteins λ1 and σ2.

Cleavage of intact μ1 to form μ1N and μ1C is required for generation of ISVP*s (125, 128). Particles recoated with mutant forms of μ1 incapable of μ1N/μ1C cleavage can facilitate each of the entry steps including μ1 conformational changes and transcription initiation but are deficient in membrane penetration (125). In addition to σ1, the N-terminal μ1 fragment, μ1N, is released from the ISVP* and interacts with membranes, most likely through the myristoyl group at the N-terminus (124). Association of μ1N with artificial membranes is sufficient to form small pores (130), although not large enough to facilitate virion translocation (131). The φ fragment of μ1 is also released during ISVP* production and appears to function as a chaperone for μ1N, facilitating membrane penetration (130). The precise mechanism of membrane breach is not known and may result from osmotic lysis as a consequence of multiple small pores in the

endosomal membrane. Alternatively, cellular factors may assist the viral components to build larger endosomal membrane pores.

HSC70 is a cellular chaperone that contributes to removal of the δ fragment from the ISVP* (132). Following the transition from ISVP* to core and viral membrane translocation, δ is lost from the particle and localizes to the cytoplasm (124). The cytoplasmic distribution of δ is diffuse, which differs from the punctate distribution of the released cores. HSC70 is hypothesized to aid the movement of the particle into the cytoplasm concomitant with removal of δ in an ATP-dependent fashion (132).

Amphipathic helices and other hydrophobic residues in μ1 thought to be involved in membrane penetration are located in the center of μ1, including the myristoylated Gly2 at the N-terminus (13). Cleavage of μ1 to μ1N and μ1C does not appear to result in conformational rearrangements, but this cleavage, along with the loss of σ3, may render the μ1 trimer metastable. Since the μ1N/μ1C cleavage sites in the three monomers of the μ1 trimer are adjacent to each other, cleavage may open this area of the molecule by altering protein-protein contacts to allow influx of solvent into an area at the center of the trimer structure. When the steric hindrance imposed by σ3 is released, μ1 may then undergo the conformational alterations necessary to allow membrane penetration.

Pathogenesis of Reovirus Infection in Mice

Newborn mice are exquisitely sensitive to reovirus infection and have been used as the preferred experimental system for studies of reovirus pathogenesis (18). While less is known about the respiratory route of inoculation, infection following peroral inoculation has been well characterized, and basic principles are understood. Proteolytic

enzymes are required for reovirus infection when mice are infected by the peroral route (129, 133). Virions are converted to ISVPs in the intestinal lumen by the resident proteases chymotrypsin and trypsin. ISVPs generated by chymotrypsin or trypsin in vitro or in the gut lumen (129, 133) are similar to ISVPs generated in the endocytic compartment of cells (73, 74). ISVPs produced in this fashion transcytose through intestinal M cells and are released basolaterally (134-137). Underlying dendritic and mononuclear cells of the Peyer's patch stain positive for reovirus antigen (101, 103, 137, 138). These cells may support viral replication or transport virus to other sites such as the mesenteric lymph node.

Subsequent to infection of Peyer's patches, reovirus infects the adjacent epithelial cells of the ileum (104), most likely initiating at the crypts of Lieberkuhn and spreading progressively to the villus tips. Spread of virus to the epithelia may occur via lymphatic or cell-to-cell spread. Epithelial cells are infected from the basolateral surface (104, 139-141), and progeny virions are released apically (104, 139). This mechanism accounts for the efficient spread of virus both within and between hosts. Transport of virus to the basolateral surface of M cells and infection of Peyer's patches also allows virus to spread via hematogenous and lymphatic routes to sites of secondary infection. The release of virus back into the lumen of the gut facilitates viral excretion.

Following infection of the intestine, reovirus spreads to other organs throughout the animal. However, the route of spread varies with serotype and is dependent on σ1 (142-144). T1L spreads from the intestine to the mesenteric lymph nodes and spleen, presumably via hematogenous routes (143). However, T3C9 spreads to the myenteric plexus and vagus nerve and infects the brain via the dorsal motor nucleus of the vagus

within the brain stem (101). Once in the brain, T1 and T3 strains infect different populations of cells. T1L infects primarily ependymal cells (144, 145), causing hydrocephalus (146), whereas T3D infects neurons (101, 144, 145, 147), leading to encephalitis (146, 148).

Reovirus Immunity and Clearance

The immune response to reovirus infection has been studied primarily using adult animals. Various infection models have been explored including different routes of inoculation and virus strains. Studies using peroral inoculation infection models have enhanced our knowledge of the mucosal immune response to viral infection and immune factors that regulate spread and disease within the infected host. Following peroral inoculation with reovirus strains T1L or Type 3 clone 9 (T3C9), there is a strong local T helper cell type 1 (T_H1) response (149-151). Cytotoxic T lymphocytes (CTL), natural killer cells, T_H1 cells, and IgA-producing plasma cells are present in the Peyer's patches and intestinal epithelium (150, 152-156). Viral replication and immune cells also can be found in peripheral lymph nodes and lamina propria (149, 150). IgG2a and IgG2b, antibody isotypes elicited during a T_H1 response, are also prevalent in infected mice (151, 155, 157). The CTL response to reovirus can provide cross-protection against type 1 and type 3 strains of reovirus (154).

To understand the relative importance of the various components of the immune response in clearing viral infection, mice deficient in various components of the immune system have been used. Adult SCID mice infected perorally with reovirus strain T3C9 die within 6 weeks primarily due to liver disease, although there is prolonged replication in

many organs (158-161). However, SCID mice infected intraperitoneally with strain T3D develop chronic infection and survive for approximately 100 days (160). Transfer of pre-immune or non-immune Peyer's patch cells results in decreased virulence following peroral inoculation of SCID mice (158, 159), suggesting that the immune response in the gut is of particular importance in controlling reovirus infection.

To elucidate the role of CD8+ T cells in reovirus infection, β2 microglobulin deficient ($\beta 2^{-/-}$) mice have been used. Infection of adult mice results in normal viral clearance from the intestine and limited spread of the virus to sites of secondary replication (155, 158), indicating that a CTL response is not necessary for control of virus replication and spread following peroral inoculation. However, $\beta 2^{-/-}$ mice exhibit enhanced IgG2a and IgG2b production and increased numbers of CD4+ T cells with respect to wt controls (155), suggesting that these mice compensate for the lack of CTL responses with alternate immune effector mechanisms.

Mice deficient in the production of IgM (MuMT mice), and therefore functional B cells, have been used to determine the importance of B cells in reovirus immunity. These adult mice exhibit delayed clearance of reovirus T3C9 from the intestine (158). This result suggests that a humoral response is necessary for early control of infection, whereas the CTL response is responsible for later clearance.

Depletion of CD4+ and/or CD8+ T cells from neonatal animals using cell-type-specific antibodies has varying effects depending on the strain of mouse used (162). Depletion of both CD4+ and CD8+ T cells from BALB/c pups had no effect on viral infection or clearance following infection with strains T1L, T3C9, or T3D. However, depletion of one or both cell types had more profound effects on NIH Swiss mice and

CAF_1 mice (BALB/c AnNCR x A/JCr F_1 progeny). Following peroral infection with T3C9, depletion of either CD4+ T cells, CD8+ T cells, or both resulted in increased liver disease. Depletion of CD8+ T cells had a more pronounced effect than depletion of CD4+ T cells on viral titer in the heart and liver. Therefore, both the CTL and humoral responses are of critical importance to reovirus immunity in neonatal animals. Whether an IgA or IgG response more effectively mediates timely clearance, however, is debated (149, 150, 158, 162-165).

Most studies of reovirus pathogenesis use neonatal animals. Pre-immune dams are capable of transferring immunity through transplacental transfer and via milk (166). This passive immunity lessens IgA production in the gut of perorally infected pups. However, if the dam is not pre-immune to reovirus, there is no effect on IgA production by her pups despite inevitable infection of the dam from exposure to infected pups. IgA production by pups is equivalent whether nursed by a naive immuno-competent or immuno-deficient dam. Therefore, the primary immune response elicited in the dam does not affect the concurrent primary immune response of her pups. This point is necessary for the interpretation of studies in neonatal animals since pathogenesis studies are conducted in mice with varying levels of immune function.

Significance of the Research

With the knowledge that cathepsin proteases cleave outer-capsid components σ3 and μ1, I sought to determine the role of these proteases in vivo. In addition to reovirus, cathepsins catalyze proteolytic events required for membrane fusion of several important pathogens. Ebola virus requires both cathepsins B and L for efficient cell entry (167),

while SARS coronavirus requires cathepsin L but also can utilize cathepsins B and S (168, 169). Hendra (170) and Nipah (171) viruses use cathepsin L for fusion protein processing, most likely at the stage of virion assembly (172). Despite the importance of cathepsins in viral growth, nothing is known about the function of these proteases in the pathogenesis of viral disease.

Although basic principles of reovirus pathogenesis in mice are known, the role of cellular and viral factors that promote viral cell entry during infection in vivo are largely unexplored. Furthermore, the results of in vivo experiments conducted thus far have not been predictable based upon in vitro results. For example, although JAM-A is required for infection of cells in culture, *JAM-A*$^{-/-}$ mice support reovirus infection in the intestine and brain (147). *JAM-A*$^{-/-}$ mice display a defect in hematogenous dissemination, most likely due to inefficient infection of endothelial cells.

As a means of testing the role of viral factors related to cell entry in vivo, mice were infected intracranially with PI viruses (173). Interestingly, although PI viruses establish persistent infection in culture and display resistance to inhibitors of viral entry, these viruses do not establish persistence in vivo and are eventually cleared. Prolonged replication is not associated with increased virulence or altered tropism within the brain. Interestingly, the virus is not found in organs other than the brain, suggesting that mutations in PI viruses prevent either spread out of the CNS or growth in other organs.

The role of cathepsin proteases B and L in reovirus uncoating in mouse fibroblasts is well established (4, 21, 26, 67-69, 73, 74, 119). The utilization of cathepsin S, however, is limited to specific cell types and virus strains (98). Furthermore, though cathepsin S activity appears to be required for reovirus uncoating in P388D cells, the

process is not optimally efficient as infection by ISVPs is greater than infection by virions (98). Because cellular and viral factors that modulate growth of reovirus in vitro do not exert the same growth phenotype in vivo, it is essential to test hypotheses about their activity as virulence factors using intact animal hosts.

To determine the function of cathepsin proteases in viral virulence, I used mammalian reovirus as a model system. I studied reovirus disease following infection of mice lacking cathepsins B, L, or S. To further investigate whether cathepsin utilization is affected by viral tropism, I used two different strains of virus, T1L and T3SA+. I found that following peroral inoculation, serotype specificity influences the requirement for cathepsin proteases in reovirus disease. Reovirus strain T1L was largely unaffected by cathepsin-deficiency, whereas yields of strain T3SA+ were diminished at sites of secondary replication. Furthermore, treatment of wt mice with an inhibitor of cathepsin L reduces T3SA+ disease severity. These studies demonstrate that cathepsin activity plays a key role in the pathogenesis of some reovirus strains and identify a new target for antiviral drug development.

CHAPTER II

CATHEPSIN PROTEASES ARE REQUIRED FOR EFFICIENT GROWTH OF T3SA+ AT SITES OF SECONDARY REPLICATION

Introduction

Cathepsins B, L, and S catalyze removal of the reovirus outer-capsid and prime the membrane-penetration machinery in the endocytic compartment of host cells (4, 98). However, the role of these enzymes in reovirus pathogenesis is unknown. In this study, I used wildtype (wt) and cathepsin-deficient mice to determine whether cathepsin proteases are individually required for reovirus infection in vivo. I chose reovirus strain T3SA+ for these studies because it is highly pathogenic and, unlike the prototype virus T3D, is capable of spread to all organs following peroral inoculation. It is also capable of binding sialic acid, which correlates with increased virulence in the liver and may contribute to virulence in the brain (174). Results of these experiments demonstrate that cathepsin proteases are required for maximal viral yields at sites of secondary replication and highlight a role for adaptive immunity in reovirus clearance and disease.

Results

Processing of reovirus virions by purified cathepsin proteases. Cathepsins B (4), L (4), and S (98) can catalyze reovirus disassembly in vitro and in certain types of cells. Reovirus strain T3SA+ is a reassortant virus that contains a genome consisting of nine gene segments from strain T1L and the S1 gene segment from strain T3C44-MA (175).

Following peroral inoculation of newborn mice, T3SA+ replicates in the intestine and disseminates systemically from that site to the brain, heart, and liver (174). To determine whether T3SA+ is susceptible to cathepsins B, L, and S, I incubated purified virions with each enzyme over a time course and resolved the resultant digestion mixtures by SDS-PAGE. Following incubation for 24 hours with each protease, complete degradation of σ3 and cleavage of μ1 to δ was observed (Figure II-1). Therefore, treatment of T3SA+ virions with cathepsins B, L, or S results in formation of ISVPs.

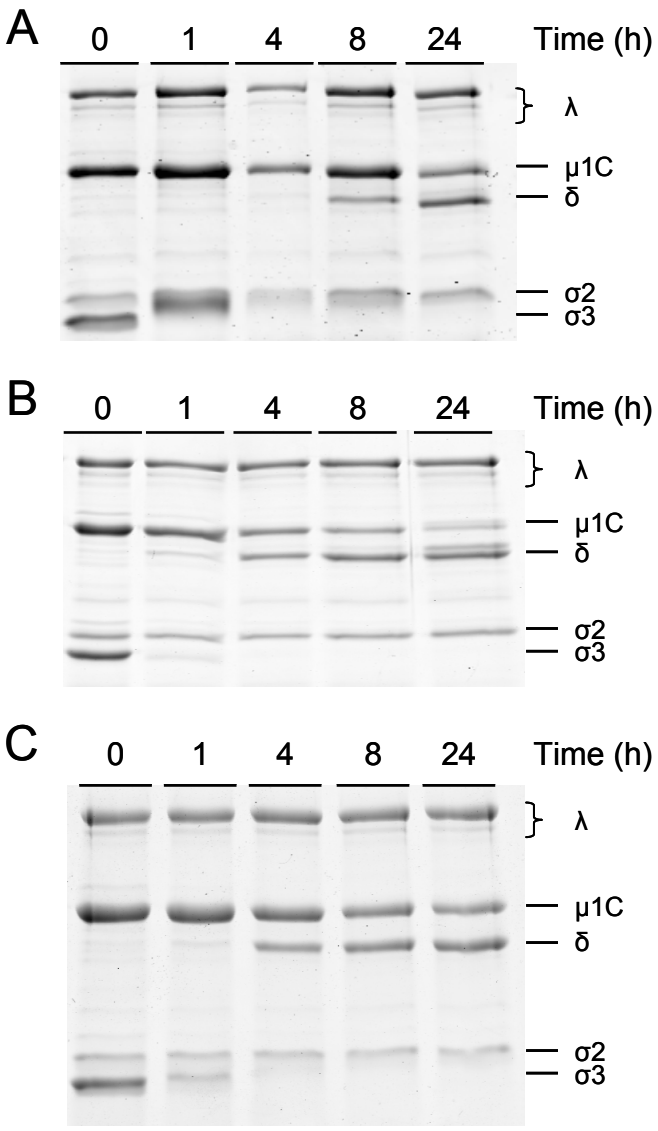

Figure II-1. Treatment of reovirus virions with cathepsins B, L, and S.
Purified virions of T3SA+ were treated with 400 μg/ml cathepsin B (A), 100 μg/ml cathepsin L (B), or 300 μg/ml cathespin S (C) at 37°C for the times shown. Equal numbers of viral particles were loaded into wells of 10% polyacrylamide gels and electrophoresed. Viral proteins are labeled on the right.

Cathepsin deficiency differentially affects survival following reovirus infection. To determine the function of cathepsin proteases in reovirus disease, I inoculated wt, *Ctsb*$^{-/-}$, *Ctsl*$^{-/-}$, and *Ctss*$^{-/-}$ mice perorally with 10^7 plaque-forming units (PFU) of reovirus T3SA+. Mice were monitored for 21 days post-infection for morbidity and mortality. The cathepsin-null mice displayed differential survival patterns in comparison to wt animals. Following a 21-day observation interval, 82% of *Ctsb*$^{-/-}$ mice survived in comparison to 61% for wt mice (Figure II-2 A). In contrast, only 7% and 39% of *Ctsl*$^{-/-}$ and *Ctss*$^{-/-}$ mice, respectively, survived T3SA+ infection. However, the mean survival time for each strain of cathepsin-deficient mice was increased in comparison to wt animals (Table 1). The disease phenotype in all strains did not notably differ, with all strains of mice displaying weakness and lethargy during the period of illness. All pups of wt and cathepsin-deficient strains inoculated with PBS and observed under identical conditions survived and did not display symptoms (data not shown). As a surrogate marker for disease severity, *Ctsb*$^{-/-}$ mice displayed less weight loss in comparison to wt animals (Figure II-2 B). However, *Ctsl*$^{-/-}$ and *Ctss*$^{-/-}$ mice had more weight loss in comparison to wt mice, and subsequent weight gain, indicative of recovery of these juvenile animals, was delayed. The increased weight loss in *Ctsl*$^{-/-}$ and *Ctss*$^{-/-}$ mice is particularly evident in comparison to the weight of mock-infected animals (Figure II-2 C). These findings suggest that despite the increased mortality of *Ctsl*$^{-/-}$ and *Ctss*$^{-/-}$ mice, these animals display slower kinetics of disease development. Thus, expression of cathepsins B, L, and S influences reovirus pathogenesis.

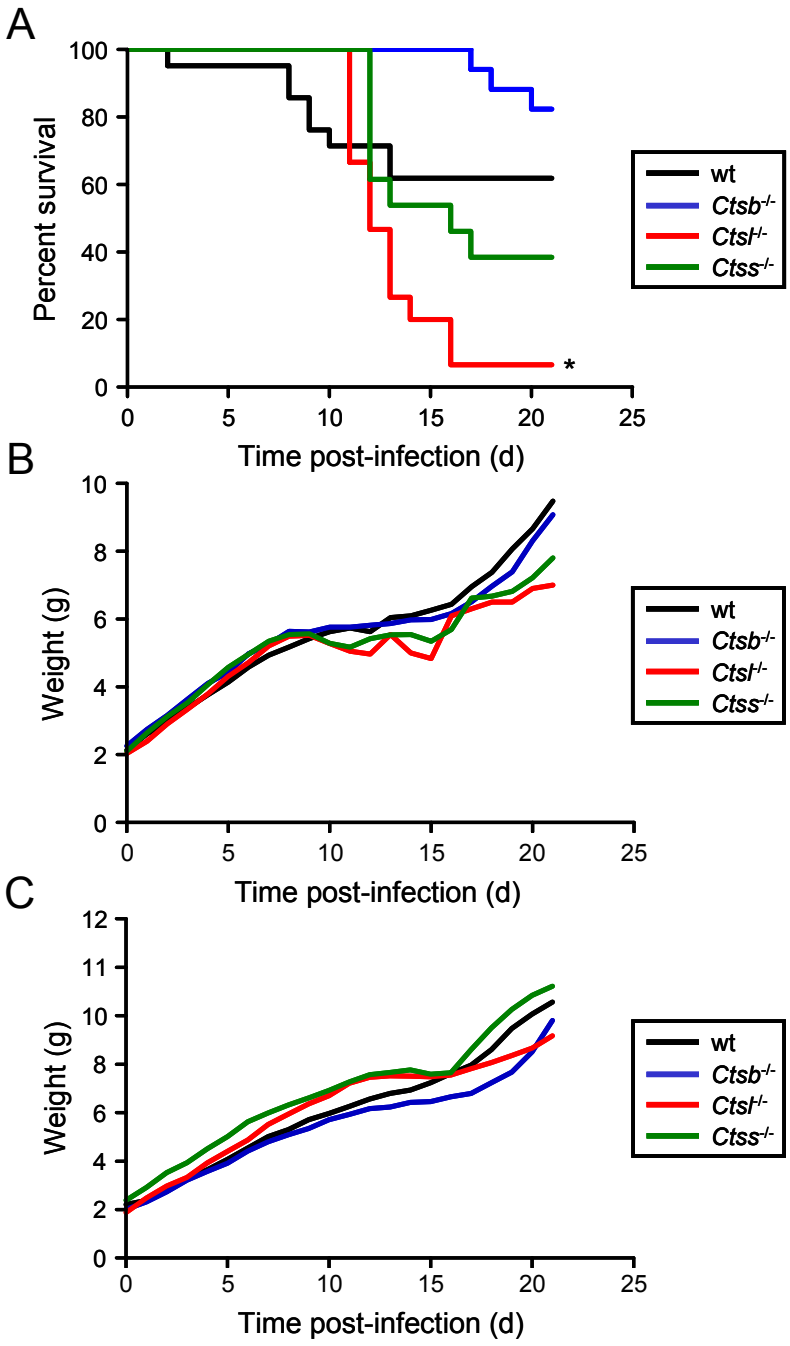

Figure II-2. Survival of wt and cathepsin-deficient mice following peroral inoculation. C57/Bl6 wt and cathepsin-deficient mice, 2-4 d old, were inoculated perorally with 10^7 PFU T3SA+ (A,B) or PBS alone (C). Mice (n = 14 to 21) were monitored for (A) survival and (B,C) weight gain. (A) *, $P <$ 0.01 as determined by log rank test in comparison to wt. (B,C) Results are expressed as mean weight of all living, infected animals. (B) Statistical significance ($P < 0.05$ as determined by student's t test) was achieved in comparison to wt mice for *Ctsb*$^{-/-}$ mice between days 2 and 8; for *Ctsl*$^{-/-}$ mice at days 1, 13, and 14; and for *Ctss*$^{-/-}$ mice at days 4-8, 11, and 14.

Table II-1. Mean survival time following reovirus infection.[a]

Mouse strain	No. of mice	Mortality (%)[b]	Mean survival time (d)[c]	*P* Value[d]
wt	21	38.1	9.0 ± 1.2	
Ctsb $^{-/-}$	17	17.6	18.3 ± 0.9	0.0017
Ctsl $^{-/-}$	15	93.3	12.6 ± 0.5	0.0041
Ctss $^{-/-}$	13	61.5	13.3 ± 0.7	0.0098

[a]C57/Bl6 wt and cathepsin-deficient mice, 2-4 d old, were inoculated perorally with 10^7 PFU T3SA+. Mice were monitored for survival for 21 d.
[b]Mortality, percent animals dead after 21 d.
[c]Mean survival time, as defined by the average day of death for animals that succumbed to infection, in d ± SEM.
[d]*P* value as determined by student's *t* test in comparison to wt.

Peak reovirus titers are diminished in cathepsin-deficient mice. To understand differences in susceptibility to reovirus infection among the cathepsin-deficient mice, I inoculated three-day-old mice perorally with a lower dose of T3SA+, 10^2 PFU, and quantified viral growth in selected organs. In comparison to wt mice, *Ctsb*$^{-/-}$ mice demonstrated equivalent growth of reovirus in the intestine, the site of primary replication, at all time points tested (Figures II-3 A, II-5, and II-6). Although titers were lower at day 4 in the liver of *Ctsb*$^{-/-}$ mice, peak titers at day 8 were equivalent to those in wt mice. In contrast, peak titers in the heart and brain of *Ctsb*$^{-/-}$ mice were lower than those in wt mice, reaching statistical significance at day 12 in the brain. In concordance with these results, *Ctsb*$^{-/-}$ mice exhibited greater weight gain than wt mice at day 12 (Figure II-5), suggesting that lower titers in the heart and brain are associated with diminished disease and lead to enhanced survival. In these experiments, neither wt nor *Ctsb*$^{-/-}$ mice displayed signs of illness or succumbed to infection.

In contrast to *Ctsb*$^{-/-}$ mice, peak titers in all organs of *Ctsl*$^{-/-}$ mice were decreased in comparison to wt mice, reaching statistical significance in the heart at day 8 (Figures II-3 B, II-5, and II-7). However, viral titers in *Ctsl*$^{-/-}$ mice were greater than those in wt mice at days 12, 16, and 20 post-inoculation, reaching statistical significance in the intestine and liver at day 12. As expected from these results, the average weight of *Ctsl*$^{-/-}$ mice was significantly less than that of wt mice at day 20 (Figure II-4). Despite the lower dose of T3SA+ used in these experiments, several *Ctsl*$^{-/-}$ animals displayed overt signs of illness, including weakness and lethargy, and some died.

The kinetics of viral growth in *Ctss*$^{-/-}$ mice were similar to those in *Ctsl*$^{-/-}$ mice. Peak titers in all organs of *Ctss*$^{-/-}$ animals were lower than those in wt mice, reaching statistical significance in the liver at day 4, in the heart at days 4 and 8, and in the brain at day 8 (Figures II-3 C, II-5, and II-8). As in *Ctsl*$^{-/-}$ mice, viral titers did not decrease in *Ctss*$^{-/-}$ mice between days 8 and 12, and titers in the intestine of *Ctss*$^{-/-}$ mice were actually greater than those in wt mice at days 12 and 16. Also, like *Ctsl*$^{-/-}$ mice, *Ctss*$^{-/-}$ mice infected with T3SA+ displayed signs of illness including weakness and lethargy, diminished weight gain (Figure II-4), and mortality. Thus, peak reovirus titers were decreased in all strains of cathepsin-deficient mice, but mice deficient in cathepsin L or cathepsin S had higher viral titers at late times after inoculation.

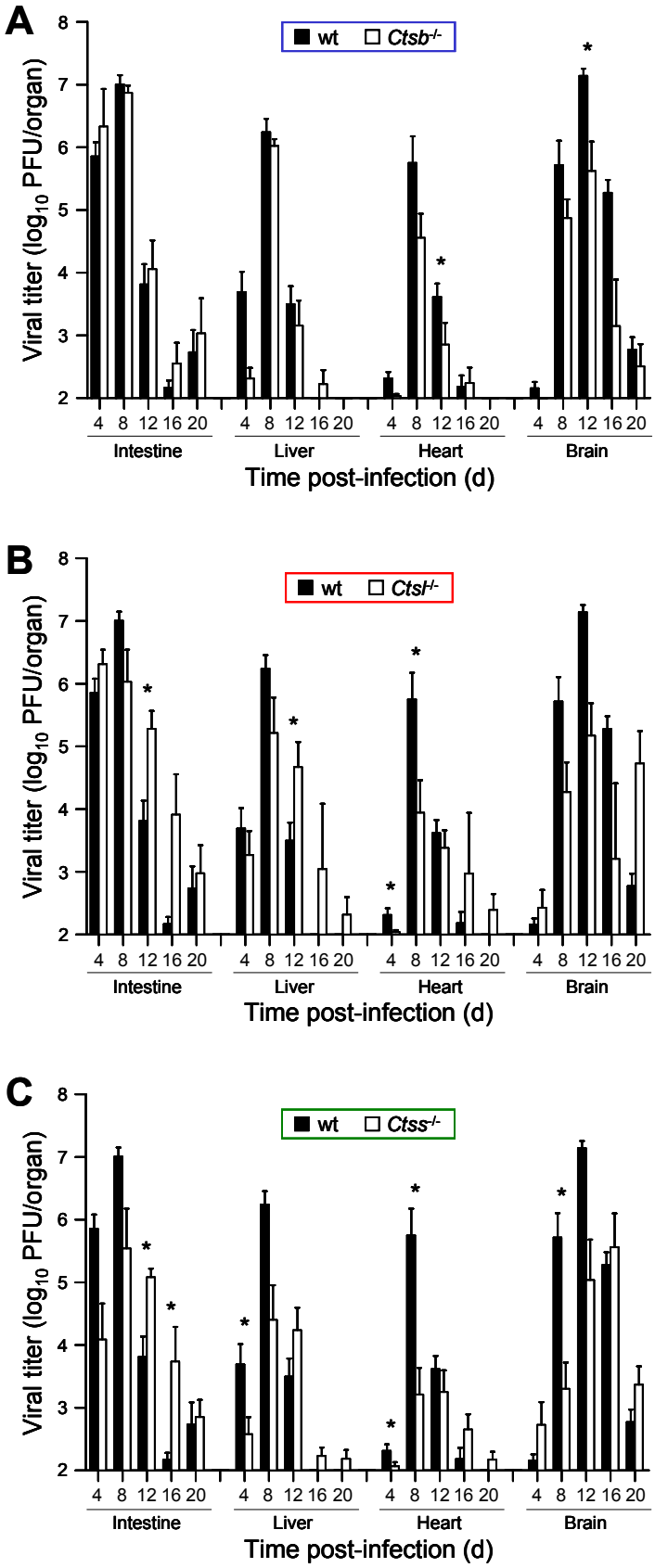

Figure II-3. Reovirus titers in organs of wt and cathepsin-deficient mice following peroral inoculation. C57/Bl6 wt and cathepsin-deficient mice, 2-4 d old, were inoculated perorally with 10^2 PFU T3SA+. Organs were resected at the times shown and homogenized by freeze-thawing and sonication. Viral titers in organ homogenates were determined by plaque assay. Results are presented as mean viral titer in whole organs of 6 to 20 mice. Error bars represent SEM. *, $P < 0.05$ as determined by Mann-Whitney test in comparison to wt at the same time after inoculation. The limit of detection was 10^2 PFU/organ.

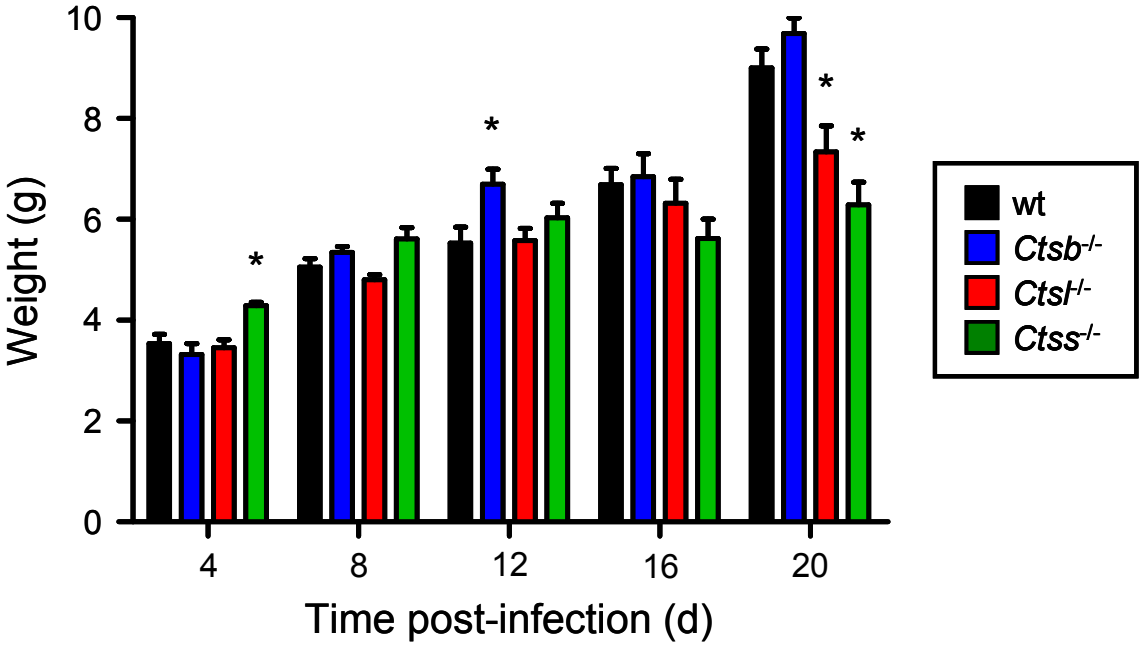

Figure II-4. Weight of mice following peroral inoculation with T3SA+. C57/Bl6 wt and cathepsin-deficient mice, 2-4 d old, were inoculated perorally with 10^2 PFU T3SA+. Mice were weighed only on the d of harvest as indicated. Results are displayed as the mean weight of 6-20 animals. *, $P < 0.05$ as determined by student's *t* test in comparison to wt at the same time after inoculation.

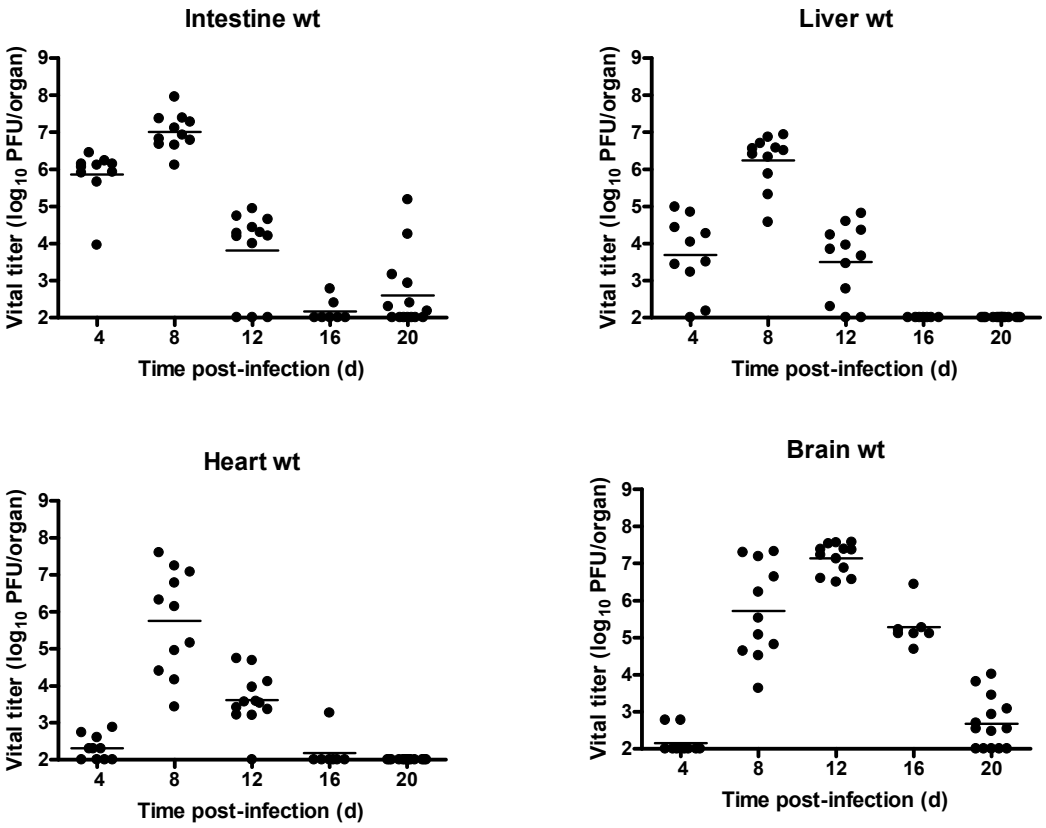

Figure II-5. Reovirus titers in organs of wt mice following peroral inoculation. C57/Bl6 wt mice, 2-4 days old were inoculated perorally with 10^2 PFU T3SA+. Organs were resected at the times shown and homogenized by freeze-thawing and sonication. Viral titers in organ homogenates were determined by plaque assay. Each data point represents one animal. Horizontal bars indicate the arithmetic mean of log-transformed data. The limit of detection was 100 PFU/ml.

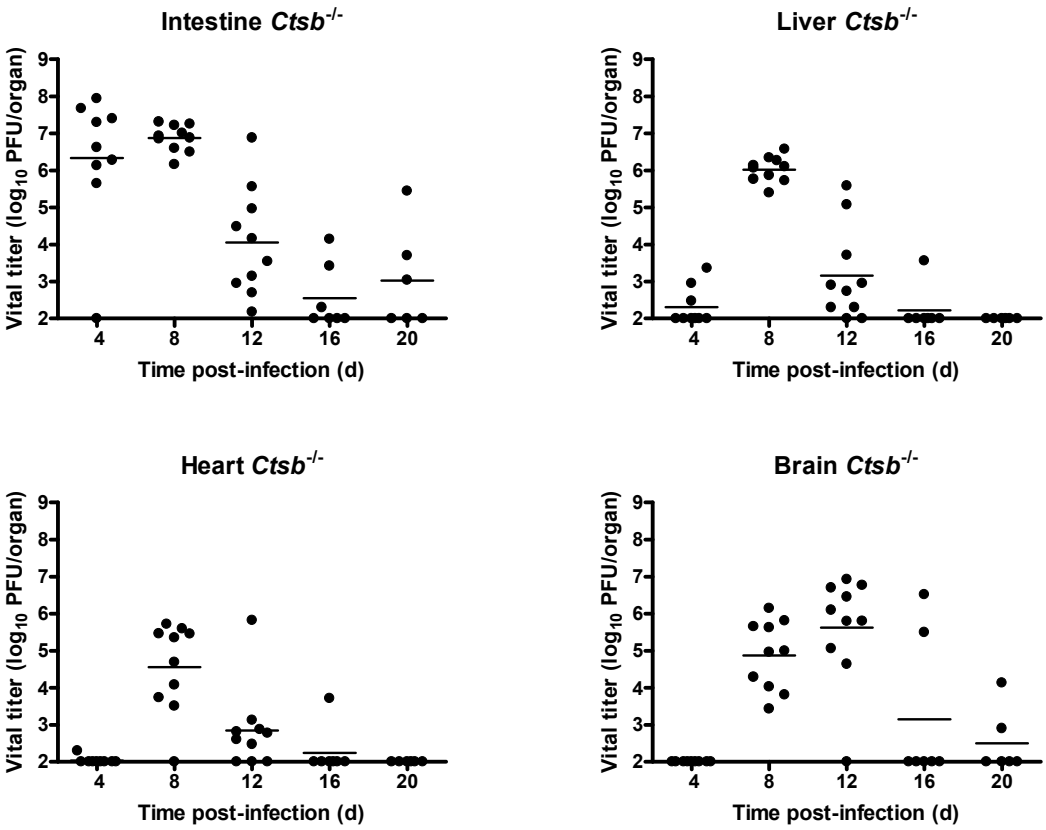

Figure II-6. Reovirus titers in organs of *Ctsb*$^{-/-}$ mice following peroral inoculation. *Ctsb*$^{-/-}$ mice, 2-4 days old were inoculated perorally with 10^2 PFU T3SA+. Organs were resected at the times shown and homogenized by freeze-thawing and sonication. Viral titers in organ homogenates were determined by plaque assay. Each data point represents one animal. Horizontal bars indicate the arithmetic mean of log-transformed data. The limit of detection was 100 PFU/ml.

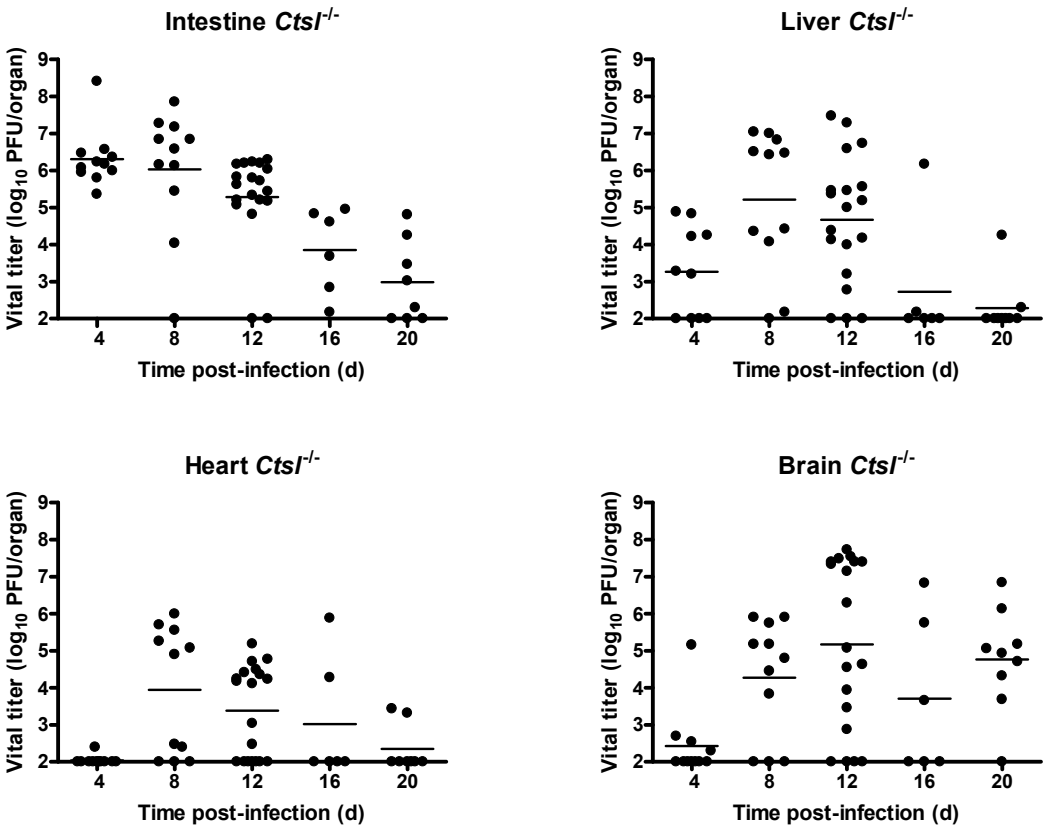

Figure II-7. Reovirus titers in organs of *Ctsl*$^{-/-}$ mice following peroral inoculation. *Ctsl*$^{-/-}$ mice, 2-4 days old were inoculated perorally with 10^2 PFU T3SA+. Organs were resected at the times shown and homogenized by freeze-thawing and sonication. Viral titers in organ homogenates were determined by plaque assay. Each data point represents one animal. Horizontal bars indicate the arithmetic mean of log-transformed data. The limit of detection was 100 PFU/ml.

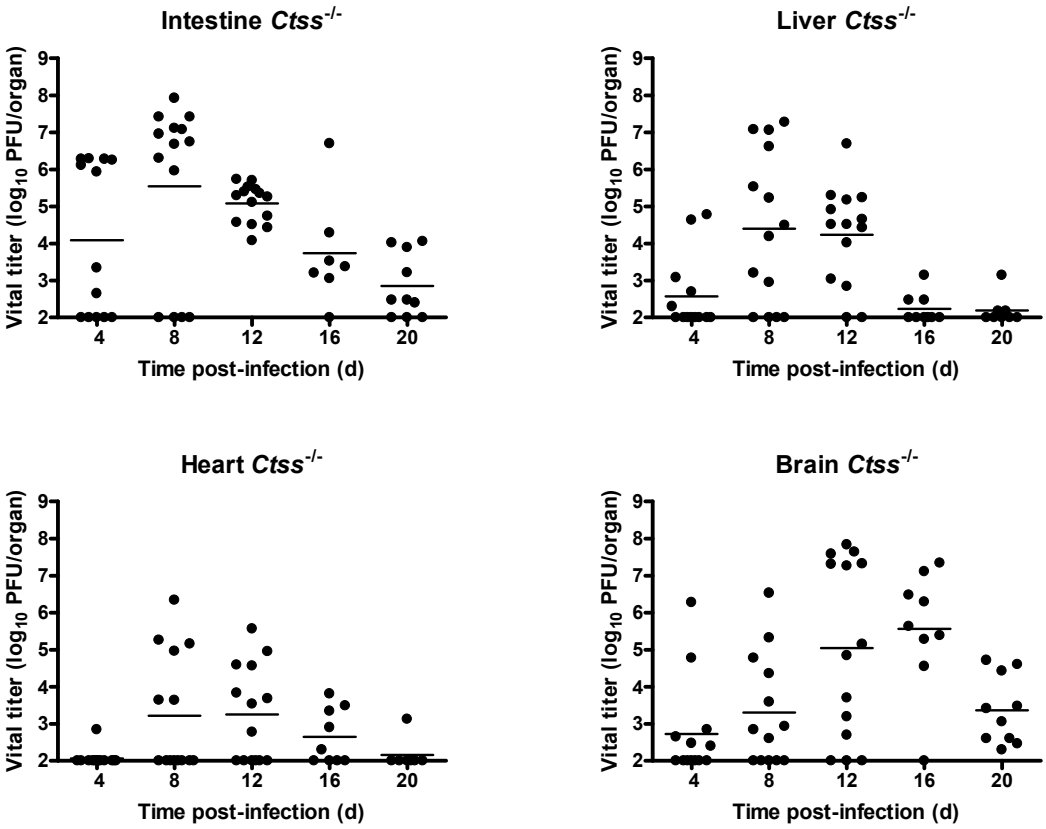

Figure II-8. Reovirus titers in organs of *Ctss*$^{-/-}$ mice following peroral inoculation. *Ctss*$^{-/-}$ mice, 2-4 days old were inoculated perorally with 10^2 PFU T3SA+. Organs were resected at the times shown and homogenized by freeze-thawing and sonication. Viral titers in organ homogenates were determined by plaque assay. Each data point represents one animal. Horizontal bars indicate the arithmetic mean of log-transformed data. The limit of detection was 100 PFU/ml.

Inflammation in the liver is more severe in cathepsin L- and cathepsin S-deficient mice. To better understand why *Ctsl*$^{-/-}$ and *Ctss*$^{-/-}$ mice had increased susceptibility to reovirus infection in comparison to wt or *Ctsb*$^{-/-}$ mice, we examined histologic sections of heart and liver from mice inoculated perorally with 10^6 PFU T3SA+. Animals chosen for histologic analysis were matched for viral titer in the liver. Viral antigen staining in the hearts of all genotypes of mice localized primarily to the subepicardial myocardium with little to moderate involvement of the deeper myocardium (Figure II-9). The extent of inflammatory cell infiltrates associated with infectious foci was consistent across all strains of mice.

In all mouse strains, infection in the liver centered on the bile duct epithelium (Figure II-10), as has been previously reported (174). Viral antigen and inflammation was more pronounced along large portal tracts; however, smaller portal tracts also were involved. Hepatic lobular involvement was present in all strains of mice in regions of increased reovirus antigen staining and inflammation. Although there was variability within each genotype of mice and some overlap between them, inflammation centered at the portal triads was more severe in *Ctsl*$^{-/-}$ and *Ctss*$^{-/-}$ mice in comparison to wt and *Ctsb*$^{-/-}$ mice (see Figure II-10 low magnification insets showing increased numbers of leukocytes in panels C and D versus A and B).

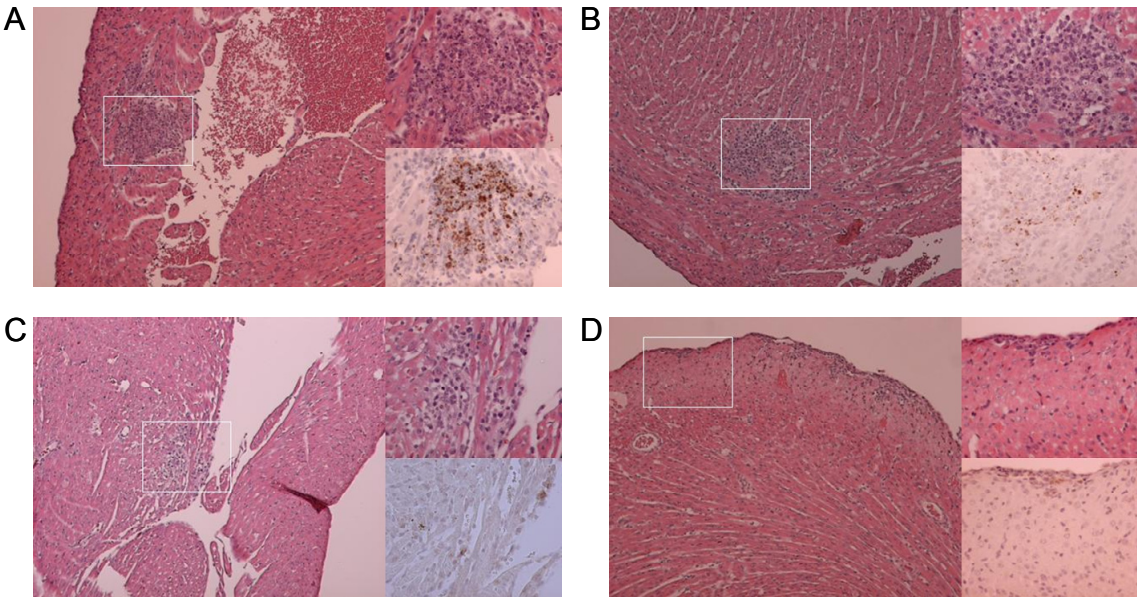

Figure II-9. Histological analysis of reovirus growth in the heart. C57/Bl6 wt and cathepsin-deficient mice, 2-4 days old, were inoculated perorally with 10^6 PFU T3SA+. Hearts were resected at day 8 post-infection and processed for histopathology. Consecutive sections were stained with hematoxylin and eosin or polyclonal reovirus antiserum. Boxes indicate areas of enlargement shown in the panels on the right. Original magnifications 10x and 40x. (A) wt; (B) *Ctsb*$^{-/-}$; (C) *Ctsl*$^{-/-}$; (D) *Ctss*$^{-/-}$.

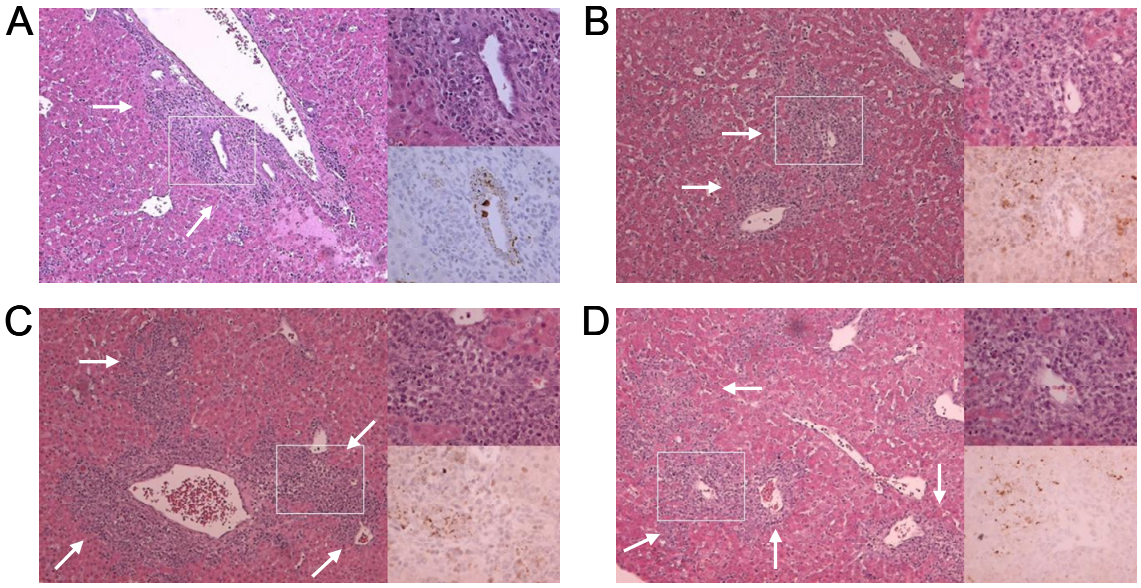

Figure II-10. Histological analysis of reovirus growth in the liver. C57/Bl6 wt and cathepsin-deficient mice, 2-4 d old, were inoculated perorally with 10^6 PFU T3SA+. Livers were resected at d 8 post-infection, and a small wedge of liver was removed for titer determination by plaque assay. The remaining liver was processed for histopathology, and consecutive sections were stained with hematoxylin and eosin or polyclonal reovirus antiserum. Representative samples from titer-matched livers are shown. Boxes indicate areas of enlargement shown in the panels on the right. Arrows indicate areas of inflammation. Original magnifications 10x and 40x.
(A) wt; (B) *Ctsb*$^{-/-}$; (C) *Ctsl*$^{-/-}$; (D) *Ctss*$^{-/-}$.

Table II-2. Bilirubin and liver enzyme levels in serum following reovirus infection.[a]

	Mock-Infected				Reovirus-Infected			
Mouse Strain	TBIL	ALK	ALT	AST	TBIL	ALK	ALT	AST
wt	1.5	634	127	461	0.9 (0.3)	768 (140.8)	295 (224.8)	495 (231.2)
Ctsb $^{-/-}$	2.0	475	73	417	1.9 (0.2)	783 (109.0)	97.5 (31.1)	460.5 (105.1)
Ctsl $^{-/-}$	1.5	567	57	409	9.2* (1.1)	1282.4 (300.3)	60 (20.8)	439 (43.8)
Ctss $^{-/-}$	0.9	574	99	330	6.9* (2.0)	1709* (258.9)	858 (665.5)	2083.75 (856.8)

[a] C57/Bl6 wt and cathepsin-deficient mice, 2-4 d old, were inoculated perorally with PBS alone or 10^6 PFU T3SA+. At d 12 post-inoculation, the liver was resected and blood was collected. A small wedge of liver was removed for titer determination by plaque assay. Mean values from 2 mock-infected mice or 3-5 reovirus-infected mice with approximately equivalent viral titer in the liver are shown. TBIL, total bilirubin (mg/dl); ALK, alkaline phosphatase (u/l); ALT, alanine aminotransferase (u/l); AST, aspartate aminotransferase (u/l). *, $P < 0.05$ as determined by student's *t* test in comparison to wt. SEM is shown in parentheses.

Liver enzyme levels are increased in Ctsl$^{-/-}$ and Ctss$^{-/-}$ mice. To obtain biochemical evidence of biliary or hepatic injury in reovirus-infected mice, we assessed levels of total bilirubin (TBIL), alkaline phosphatase (ALK), alanine aminotransferase (ALT), and aspartate aminotransferase (AST) in mice that were either mock-infected or infected with 10^6 PFU T3SA+. No biomarker of liver injury was elevated in mock-infected mice at any time point or in any strain of reovirus-infected mice at day 8 post-infection. In contrast, levels of TBIL and ALK were increased in *Ctsl*$^{-/-}$ mice and levels of all four markers were increased in *Ctss*$^{-/-}$ mice at day 12 post-infection (Table 2). These results indicate more severe hepatobiliary damage in reovirus-infected *Ctsl*$^{-/-}$ and *Ctss*$^{-/-}$ mice in comparison to wt and *Ctsb*$^{-/-}$ animals.

Hematogenous dissemination of reovirus is unaffected by absence of a single cathepsin protease following peroral inoculation. I thought it possible that the capacity of reovirus to either disseminate to sites of secondary infection in cathepsin-deficient mice or establish infection once reaching those sites might be reduced. To distinguish between these possibilities, I quantified viral titers in the blood following peroral inoculation. Newborn mice were inoculated perorally with 10^6 PFU of T3SA+, and blood was collected at various times after inoculation. Reovirus established viremia in all strains of mice (Figure II-11 A and B), reaching titers that were approximately equivalent in all strains tested (Figure II-11 B). Furthermore, the percentage of mice with detectable viremia correlated with the percentage of mice with detectable titer in the intestine (Figures II-5 - II-8, and II-11 A). Therefore, lack of a single cathepsin protease does not appear to alter the efficiency of reovirus hematogenous dissemination in mice.

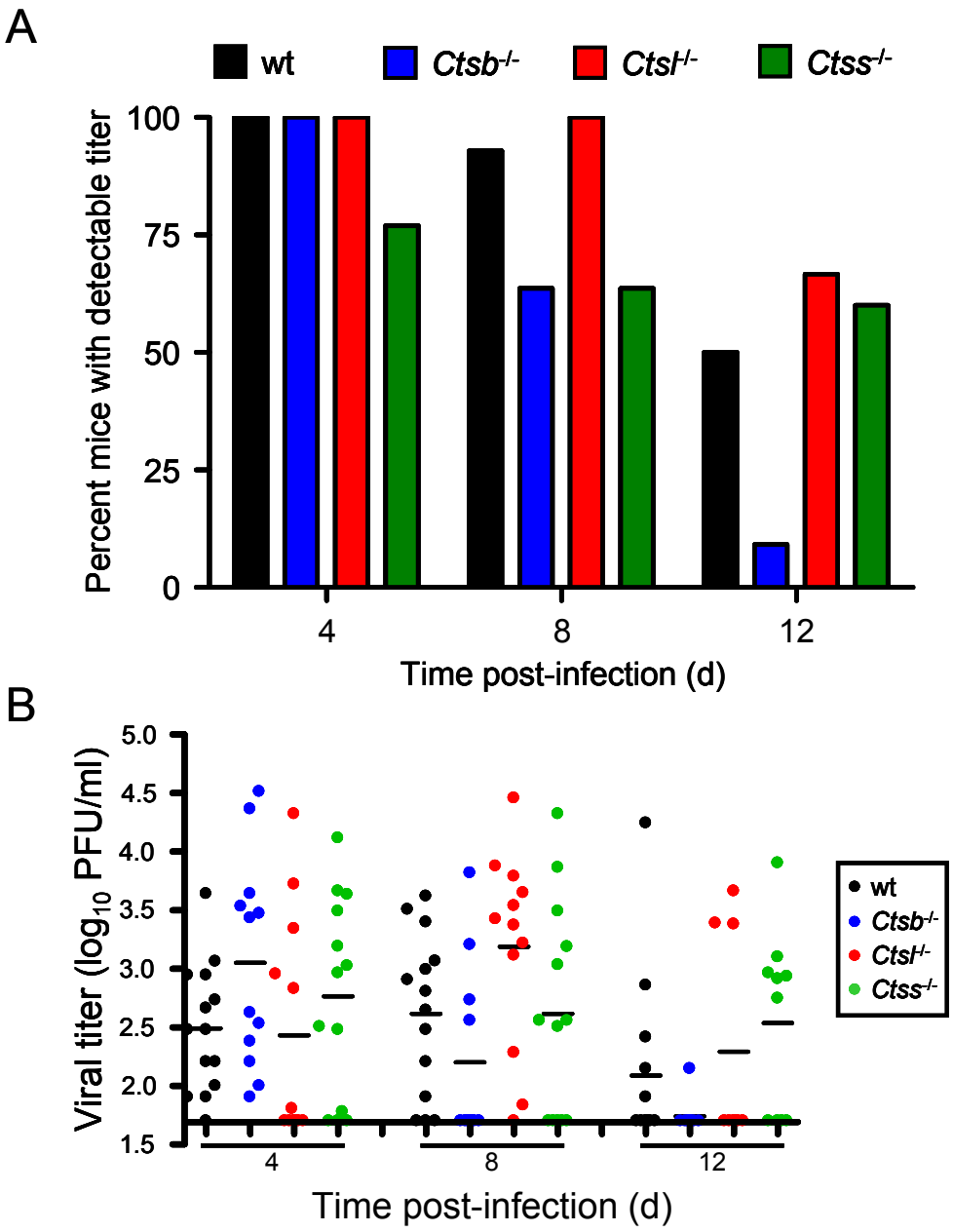

Figure II-11. Viremia in wt and cathepsin-deficient mice following peroral inoculation. C57/Bl6 wt and cathepsin-deficient mice, 2-4 d old, were inoculated perorally with 10^6 PFU T3SA+. Blood was collected at the times shown and homogenized by freeze-thawing and sonication. Viral titers in blood were determined by plaque assay. The limit of detection was 50 PFU/ml. N = 9 to 14 mice. (A) Results are presented as percent animals with detectable titer in the blood. (B) Each data point represents one animal. Horizontal bars indicate the arithmetic mean of log-transformed data.

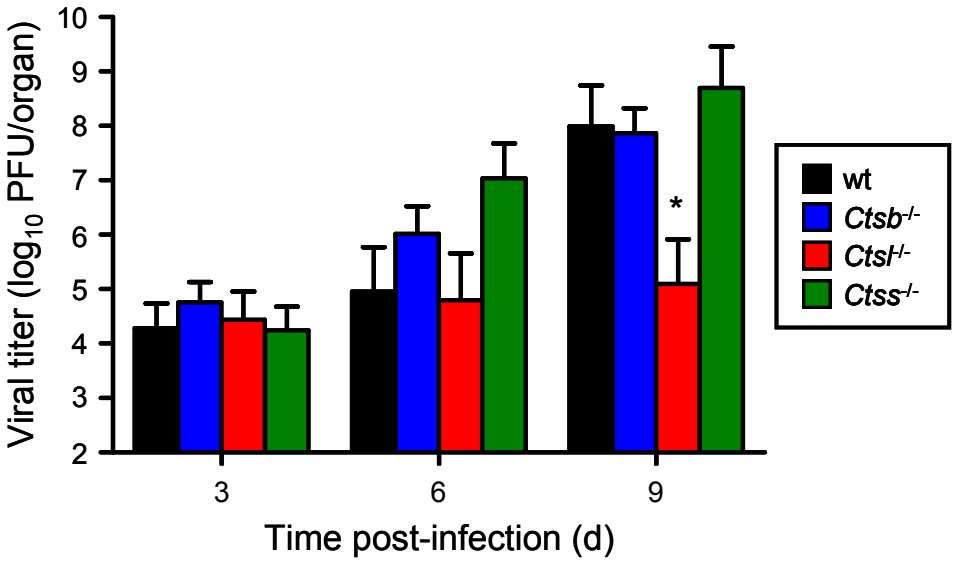

Figure II-12. Viral growth in the brain of wt and cathepsin-deficient mice following intracranial inoculation. C57/Bl6 wt and cathepsin-deficient mice, 2-4 d old, were inoculated intracranially with 10^2 PFU T3SA+. Brains were resected at the times shown and homogenized by freeze-thawing and sonication. Viral titers in brain homogenates were determined by plaque assay. Results are expressed as mean viral titer in the brains of 9 to 13 mice. Error bars represent SEM. *, $P < 0.05$ as determined by Mann-Whitney test in comparison to wt at the same time after inoculation. The limit of detection was 10^2 PFU/brain.

Growth of reovirus in the brain is diminished in cathepsin L-deficient mice following intracranial inoculation. To determine the effect of cathepsin deficiency on the capacity of reovirus to grow at a site of secondary replication, I quantified viral titers in the brain following intracranial inoculation of wt and cathepsin-deficient mice. This site was chosen for ease of direct inoculation. Titers of T3SA+ in the brains of wt, *Ctsb*$^{-/-}$, and *Ctss*$^{-/-}$ mice did not differ statistically (Figure II-12), suggesting that cathepsins B and S are not required for reovirus growth in the brain following direct inoculation into that site. However, titers of T3SA+ in the brains of *Ctsl*$^{-/-}$ mice were significantly lower on

day 9 post-inoculation, suggesting that cathepsin L is required for efficient growth of reovirus in the brain. Thus, cathepsin L contributes to reovirus tropism for the CNS.

Discussion

Reovirus virions are uncoated in late endosomes or lysosomes by cathepsins B (4), L (4), or S (98). I reasoned that deficiency in the proteases that catalyze uncoating might lead to decreased viral growth and diminished disease severity. Only mice deficient in expression of cathepsin B fit this profile. *Ctsb*$^{-/-}$ mice had increased survival in comparison to wt mice when infected with a high dose of reovirus, whereas *Ctsl*$^{-/-}$ and *Ctss*$^{-/-}$ mice displayed decreased survival. In concordance with this observation, reovirus produced lower titers at sites of secondary replication in *Ctsb*$^{-/-}$ mice than in wt mice, and *Ctsb*$^{-/-}$ mice displayed greater weight gain. These results suggest that cathepsin B is required for reovirus to establish high-titer infection and exert pathological effects.

The decreased survival of *Ctsl*$^{-/-}$ and *Ctss*$^{-/-}$ mice in comparison to wt mice raised the possibility that viral loads might be higher in these animals. However, reovirus produced lower peak titers at sites of secondary replication in both genotypes of mice in comparison to both wt and *Ctsb*$^{-/-}$ mice. Diminished survival in *Ctsl*$^{-/-}$ and *Ctss*$^{-/-}$ mice is likely attributable to defects in immune function in these animals (96) with resultant failure to resolve viral infection. Indeed, viral titers in the intestine at day twelve were significantly higher in both *Ctsl*$^{-/-}$ and *Ctss*$^{-/-}$ mice than those in wt animals. As viral titers in wt mice decreased from day 8 to 12, viral titers in *Ctsl*$^{-/-}$ and *Ctss*$^{-/-}$ mice did not. I think it most likely that the absence of functional CD4+ T cells leads to inefficient viral clearance. Consequently, tissue injury is sustained for a longer period of time. This

conclusion is supported by the kinetics of survival following infection. Although *Ctsl*$^{-/-}$ and *Ctss*$^{-/-}$ mice die at higher frequency than wt mice, survival times of the cathepsin-deficient mice are prolonged. Thus, the immune deficiency displayed by mice lacking cathepsin L or cathepsin S is associated with enhanced reovirus virulence.

It is noteworthy that reovirus titers at sites of secondary replication in the population of *Ctsl*$^{-/-}$ and *Ctss*$^{-/-}$ mice examined have a nearly bimodal distribution (Figures II-7 and II-8). This finding is particularly evident in the heart and liver at days 8 and 12 and in the brain at days 8, 12, and 16. There is a population of animals with titers equivalent to wt and a population of almost equivalent size with titers at or below the limit of detection. The distribution of data points is wider in these genotypes than in wt or *Ctsb*$^{-/-}$ mice (Figures II-5 and II-6). However, titers in the intestine of *Ctsl*$^{-/-}$ and *Ctss*$^{-/-}$ mice are only slightly bimodal, with a lower percentage of mice harboring undetectable levels of virus at that site. These findings suggest that despite reaching a critical threshold of virus in the intestine of *Ctsl*$^{-/-}$ and *Ctss*$^{-/-}$ mice, either spread to or growth at sites of secondary replication is dependent on individual cathepsins. These data also suggest that at least in some animals, redundancy in cathepsin function allows nearly wt levels of viral growth. Furthermore, cathepsins B and L are not required for optimal growth in the intestine, most likely due to the presence of chymotrypsin in the lumen of the intestine.

The paradox that *Ctsl*$^{-/-}$ and *Ctss*$^{-/-}$ mice display increased disease severity and mortality despite lower peak titers suggests that *Ctsl*$^{-/-}$ and *Ctss*$^{-/-}$ mice are more susceptible to the pathologic effects of reovirus infection than are wt mice. The disease phenotype of these mice included lethargy and oily hair effect (174, 176, 177), a syndrome associated with viral replication in intrahepatic bile duct epithelium, biliary

obstruction, and fat malabsorption (174, 176, 178-180). However, the disease symptoms did not include spastic movements of the extremities, overt seizures, or paralysis, indicative of encephalitis. I think that death of reovirus-infected animals lacking cathepsin L or cathepsin S resulted from damage to the liver and heart. Histological analysis of the heart did not reveal striking differences in pathological injury in the different strains of mice, perhaps due to the high viral loads in the hearts of all mice. However, the increase in inflammatory infiltrate surrounding portal triads coupled with the results of liver enzyme profiling support the conclusion that damage to the liver contributed to the poor outcome of reovirus-infected *Ctsl*$^{-/-}$ and *Ctss*$^{-/-}$ mice.

The observation that cathepsin-deficient mice inoculated with reovirus had lower titers at sites of secondary replication prompted us to investigate how individual cathepsins promote viral pathogenesis. I envision two possibilities. First, cathepsin expression might allow the virus to disseminate systemically in the host. Second, cathepsin expression might be required for growth at sites of secondary replication once those sites are reached. All strains of mice had detectable virus in the blood, suggesting that cathepsin deficiency does not block reovirus spread from the intestine into the bloodstream. However, these proteases could be required for reovirus exit from the bloodstream into the surrounding tissues, for example by promoting viral growth in endothelium or extravasation of infected lymphocytes from blood vessels into host tissues.

While cathepsins B and S are dispensable for reovirus growth in the brain, cathepsin L is not. Following intracranial inoculation, titers in *Ctsl*$^{-/-}$ mice were decreased in comparison to all other strains. Cathepsin S is required for maximal growth of reovirus

in the intestine as titers of reovirus in the intestine of *Ctss*$^{-/-}$ mice are less than those in all other strains. It is possible that decreased titer in the intestine of *Ctss*$^{-/-}$ mice is insufficient to allow efficient viral dissemination to sites of secondary replication. However, peak reovirus titers in the brain of *Ctss*$^{-/-}$ mice following peroral inoculation are greater than those of *Ctsb*$^{-/-}$ mice, suggesting that viral spread is independent of titer in the intestine. The site in the intestine from which the majority of viral titer originates is not known, nor is it apparent whether this virus population is responsible for spread to other organs. The virus that spreads within the host most likely arises from infected Peyer's patches. However, if infection of intestinal epithelium produces a majority of detectable virus titer, this occurrence would separate the populations of virus contributing to spread and titer. Therefore, it is possible that lymphatic or hematogenous spread can occur despite low viral loads in the intestine. There is precedence for this concept. Virus that spreads within mice infected with murine cytomegalovirus does not originate from the liver, the organ with the highest viral titer (181). Cathepsin S is expressed in intestinal epithelial cells (100), which may promote reovirus replication at that site. Therefore, cathepsin S may be important for reovirus growth at other sites of secondary replication, including the heart and liver, at which sites peak titers are less that those in wt mice. Cathepsin B also may be important for growth in the heart, as titers in the heart of *Ctsb*$^{-/-}$ mice are decreased in comparison to those in wt mice, while titers in the intestine and liver are not. It is noteworthy that in mouse fibroblasts, although both cathepsins B and L can mediate reovirus uncoating, cathepsin L is more efficient (4). Our data following both peroral and intracranial inoculation support this conclusion in that peak titers in all

organs tested are lower in *Ctsl*$^{-/-}$ mice than in *Ctsb*$^{-/-}$ mice. These findings suggest that cathepsin L is required for efficient reovirus growth in tissues other than the intestine.

I have shown that cathepsin proteases are required for efficient reovirus infection in mice. Cathepsins promote optimal growth at specific sites of reovirus replication in the host and influence survival following reovirus infection. Organ-specific differences in infection of cathepsin-deficient mice highlight distinct roles for these proteases in vivo.

CHAPTER III

CATHEPSIN PROTEASES ARE NOT REQUIRED FOR GROWTH OF T1L IN VIVO

Introduction

Different reovirus strains display differential tropism and disease patterns in vivo. These differences have been genetically ascribed to various gene segments using reassortant genetics. For example, the extent of growth and tissue injury in the heart and lungs is determined by genes encoding the proteins of the viral vertex including L1 (λ3), L2 (λ2), and M1 (μ2) (160). Tropism in the CNS is determined by the S1 gene segment (145), which encodes the attachment protein σ1 and the nonstructural protein σ1s (182-184). Interestingly for my studies, S1 also influences hepatic tropism and resultant liver disease (176). Peroral infection with some type 3 strains, but not T1L, leads to liver disease that is similar to biliary atresia in human infants and characterized by oily hair effect (174, 176-180). This difference in disease presentation is not related to virulence or growth of virus in the liver, as the effect does not correlate with LD_{50} value or titer of virus in the liver (176). However, reovirus strains capable of causing this disease infect bile duct epithelial cells, whereas other strains infect hepatocytes in a more diffuse pattern (176). This variation in infectivity is determined by differences in the capacity to bind sialic acid (174).

The distinct cell types infected by different strains of reovirus might express altered cathepsin activity. Although the relative tissue distribution of the cathepsin proteases is known, their activity within specific cell types is less well understood. I

hypothesized that if differences in cathepsin activity exist in the different cell types infected by reovirus strains, the effect of cathepsin deficiency on reovirus infection in vivo would differ among strains.

To test this hypothesis, I infected cathepsin-deficient mice with a prototype serotype 1 strain, T1L. This virus shares 9 gene segments with T3SA+ (175) but differs in its S1 gene segment. Because the outer-capsid proteins σ3 and μ1 are identical to those of T3SA+, T1L is equally susceptible to cathepsin cleavage in vitro. However, the difference in the σ1 protein, which confers serotype specificity, causes T1L and T3SA+ to exhibit great differences in animal pathogenesis. T1L is much less virulent than T3SA+ (146, 174) and has different tropism patterns in the CNS (101, 144, 145, 147) and liver (174, 176).

Results

To study the role of cathepsins B, L, and S in the pathogenesis of T1L infection, I inoculated three-day-old mice perorally with 10^4 PFU of T1L and quantified viral growth in selected organs. Although titers in the intestine, the primary site of replication, of *Ctsb*$^{-/-}$ mice were lower than those in wt mice at day 4 post-infection, peak titers were equivalent (Figures III-1 A, III-2, and III-3). A similar pattern was observed in the liver, heart, and brain. However, at day 12 post-infection, titers in the intestine and liver were slightly higher in *Ctsb*$^{-/-}$ mice than wt mice. In keeping with these findings, *Ctsb*$^{-/-}$ mice exhibited poor weight gain at 12 days post-infection in comparison to wt mice (Figure III-1 B).

In contrast to *Ctsb*$^{-/-}$ mice, peak titers in all organs of *Ctsl*$^{-/-}$ mice were equivalent to or greater than titers in wt mice, reaching statistical significance in the liver at day 8 (Figures III-1 A, III-2, and III-4). Furthermore, viral titers in *Ctsl*$^{-/-}$ mice were greater than those in wt mice at day 12 post-inoculation in all organs, reaching statistical significance in the intestine and liver. Accordingly, *Ctsl*$^{-/-}$ mice had poor weight gain throughout the experiment, as the average weight was lower than that of wt mice at all timepoints tested (Figure III-1 B).

Peak titers in *Ctss*$^{-/-}$ mice were equivalent to wt in all organs tested (Figures III-1 A, III-2, and III-5). However, titers at sites of secondary replication were higher in *Ctss*$^{-/-}$ mice at days 4 and 12 post-inoculation than those in wt mice, reaching statistical significance in the liver on day 4 and in the liver and heart on day 12. As expected from these results, the average weight of *Ctss*$^{-/-}$ mice was lower than wt mice at days 8 and 12 post-infection (Figure III-1 B).

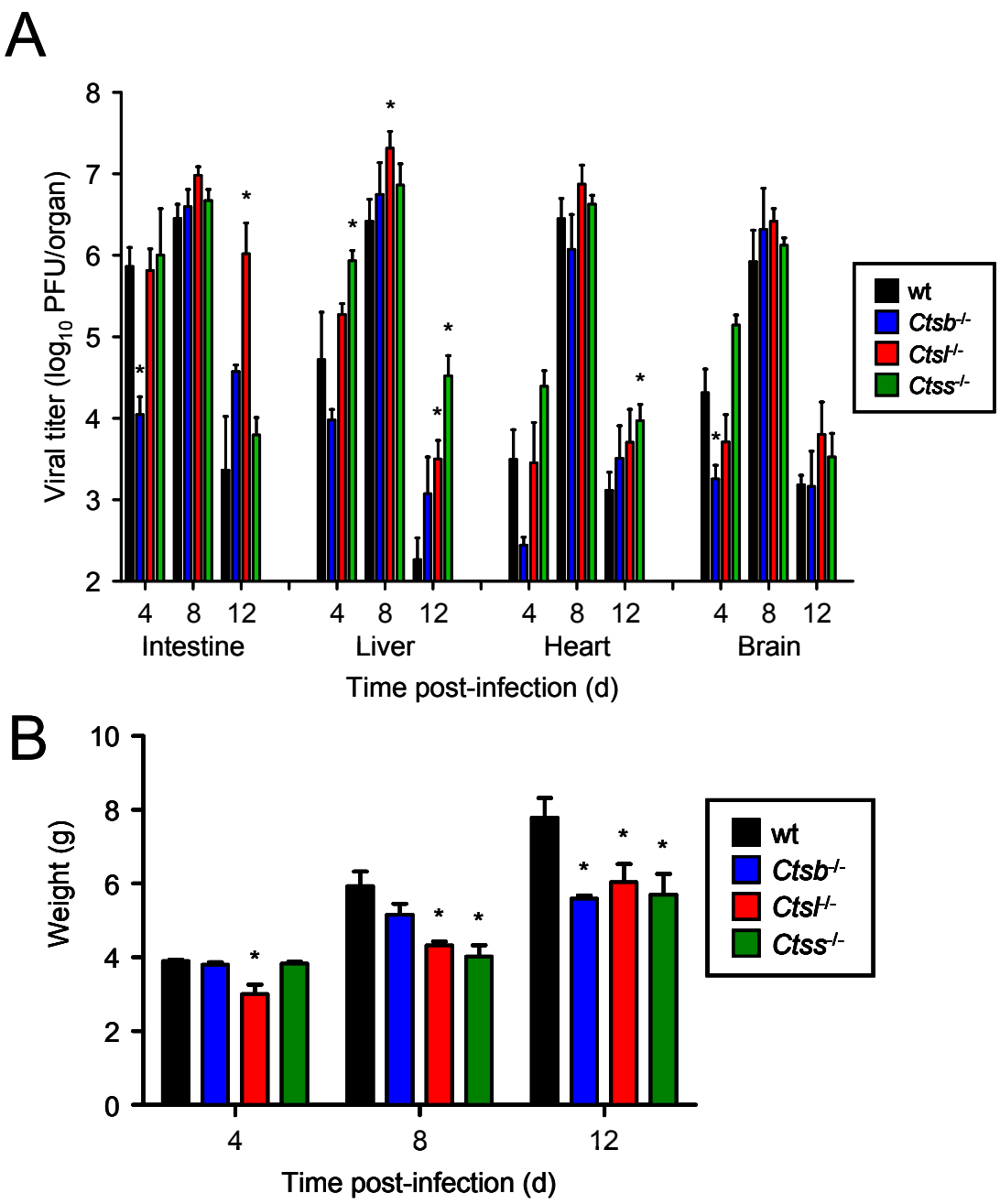

Figure III-1. Infection of wt and cathepsin-deficient mice with T1L. C57/Bl6 wt and cathepsin-deficient mice (n = 4 to 7), 2-4 days old, were inoculated perorally with 10^4 PFU T1L. (A) Organs were resected at the times shown and homogenized by freeze-thawing and sonication. Viral titers in organ homogenates were determined by plaque assay. Results are expressed as mean viral titer in whole organs. Error bars represent SEM. *, $P < 0.05$ as determined by Mann-Whitney test in comparison to wt at the same time after inoculation. The limit of detection was 10^2 PFU/organ. (B) Mice were weighed at the times shown. Results are expressed as mean weight of infected animals.

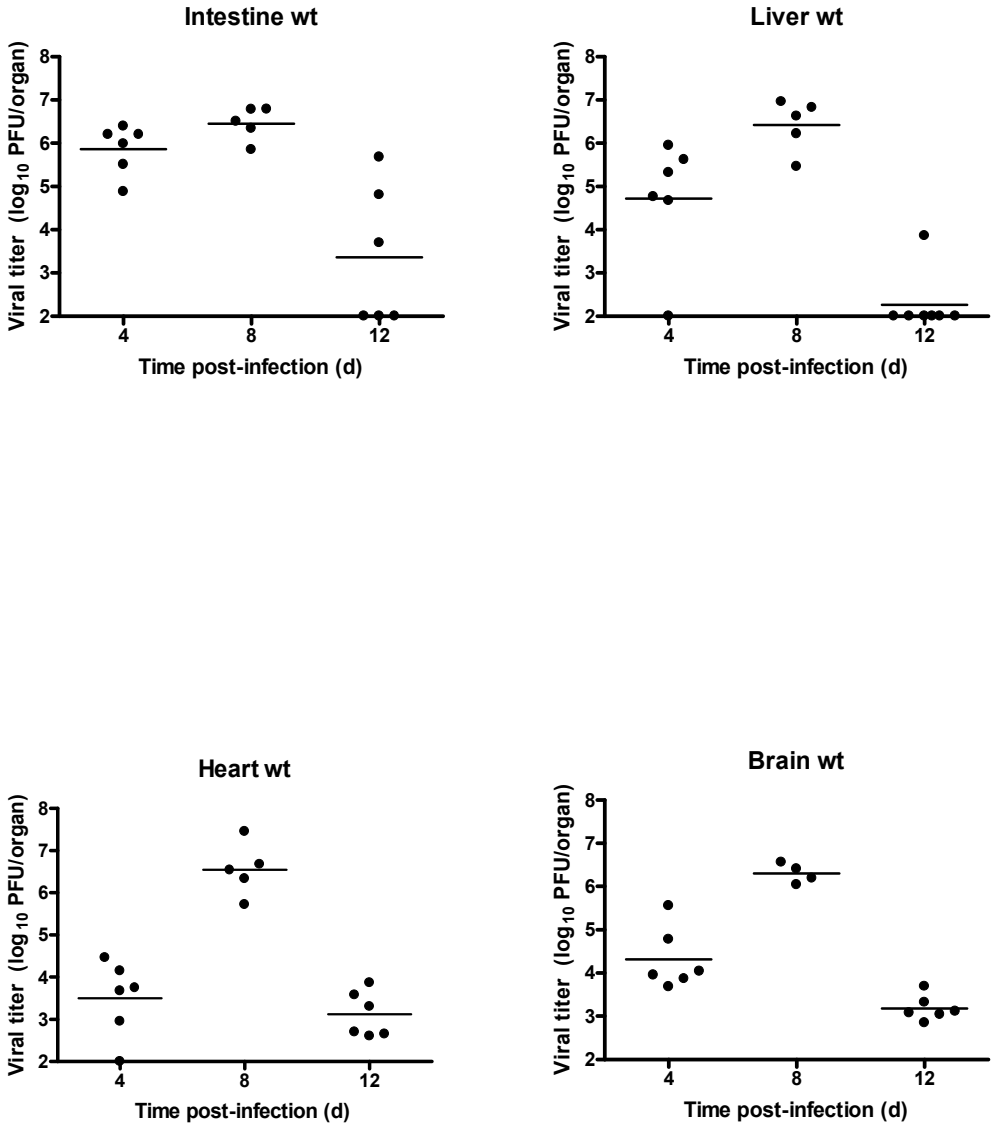

Figure III-2. Reovirus titers in organs of wt mice following peroral infection with T1L. C57/Bl6 wt mice (n = 4 to 7), 2-4 days old, were inoculated perorally with 10^4 PFU T1L. Organs were resected at the times shown and homogenized by freeze-thawing and sonication. Viral titers in organ homogenates were determined by plaque assay. Each data point represents one animal. Horizontal bars indicate the arithmetic mean of log-transformed data. The limit of detection was 10^2 PFU/organ.

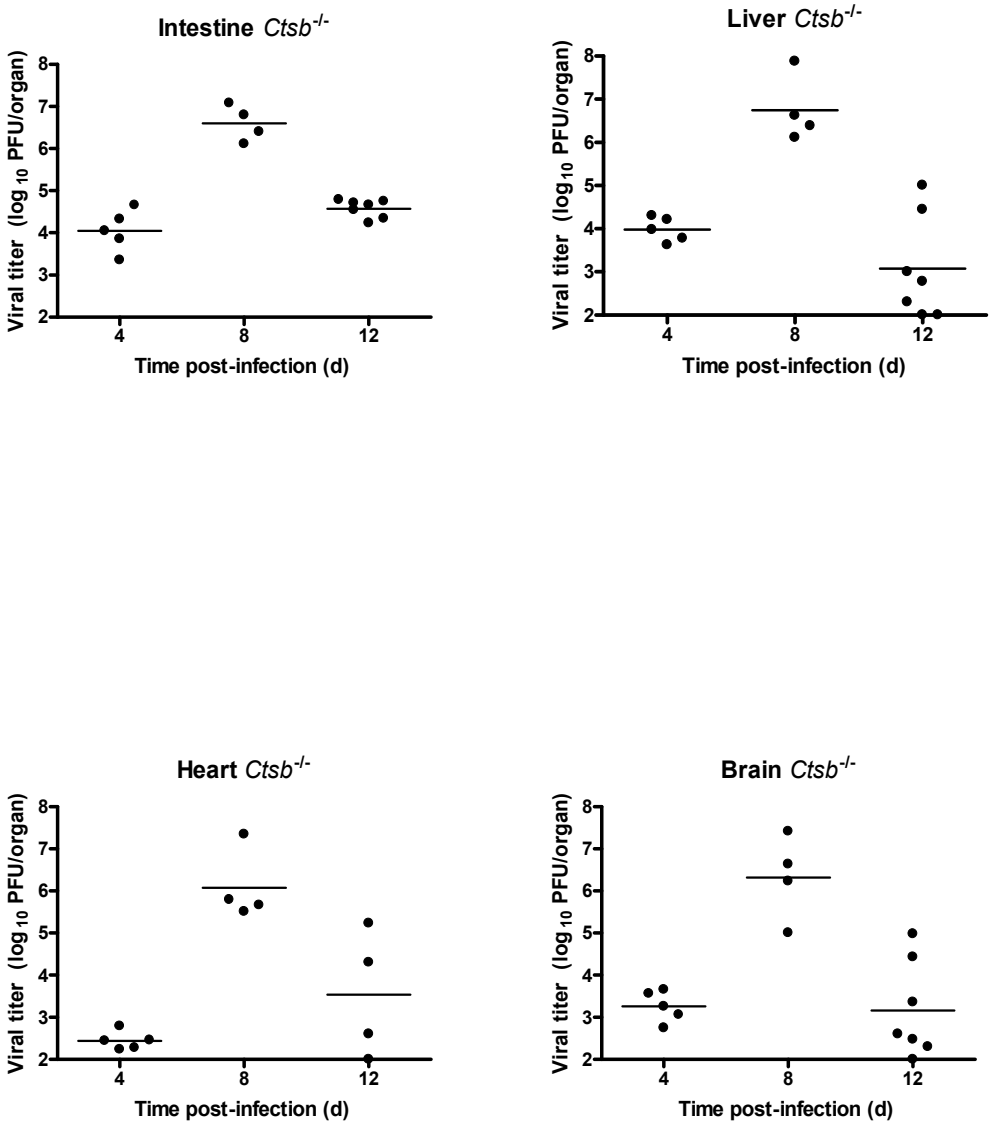

Figure III-3. Reovirus titers in organs of *Ctsb*$^{-/-}$ mice following peroral infection with T1L. *Ctsb*$^{-/-}$ mice (n = 4 to 7), 2-4 days old, were inoculated perorally with 10^4 PFU T1L. Organs were resected at the times shown and homogenized by freeze-thawing and sonication. Viral titers in organ homogenates were determined by plaque assay. Each data point represents one animal. Horizontal bars indicate the arithmetic mean of log-transformed data. The limit of detection was 10^2 PFU/organ.

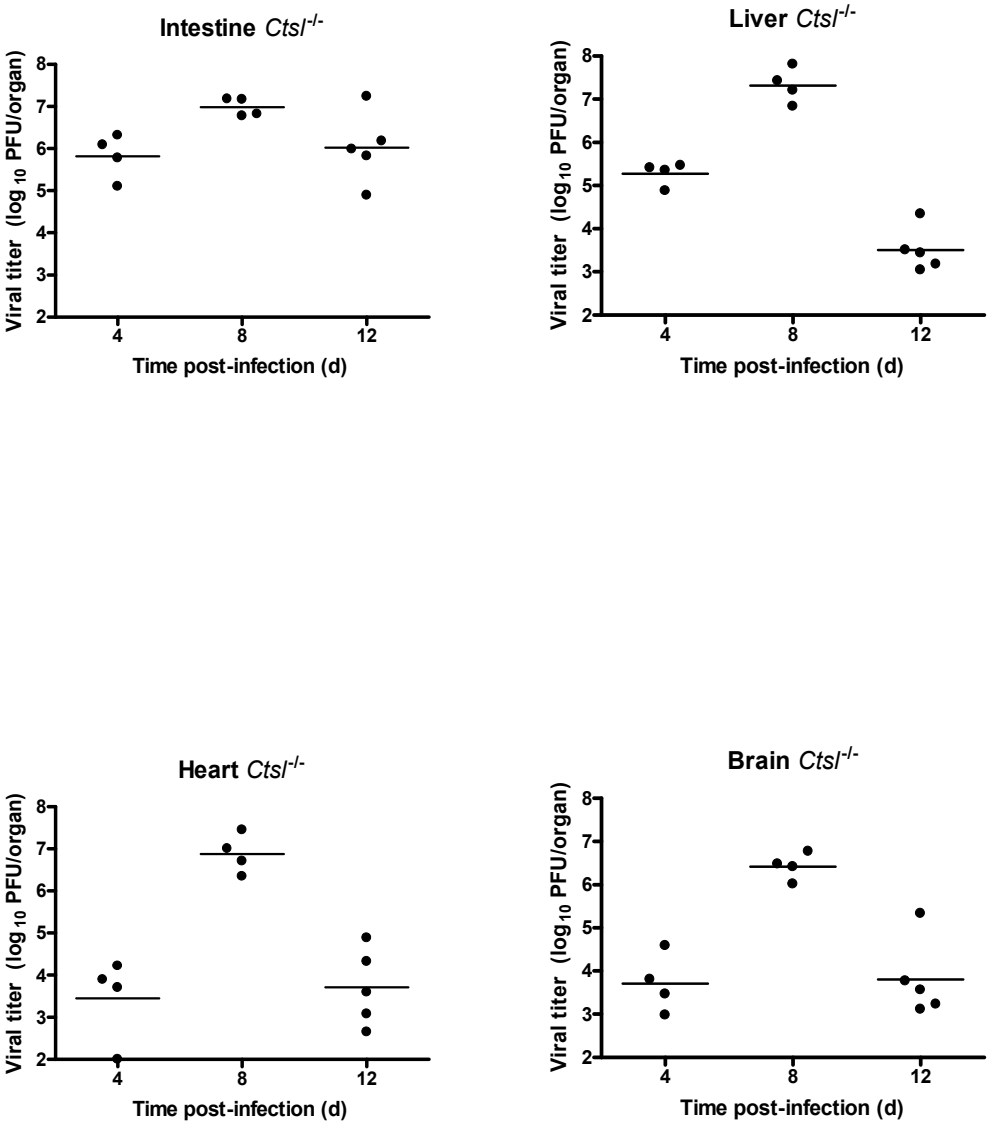

Figure III-4. Reovirus titers in organs of *Ctsl*$^{-/-}$ mice following peroral infection with T1L. *Ctsl*$^{-/-}$ mice (n = 4 to 7), 2-4 days old, were inoculated perorally with 10^4 PFU T1L. Organs were resected at the times shown and homogenized by freeze-thawing and sonication. Viral titers in organ homogenates were determined by plaque assay. Each data point represents one animal. Horizontal bars indicate the arithmetic mean of log-transformed data. The limit of detection was 10^2 PFU/organ.

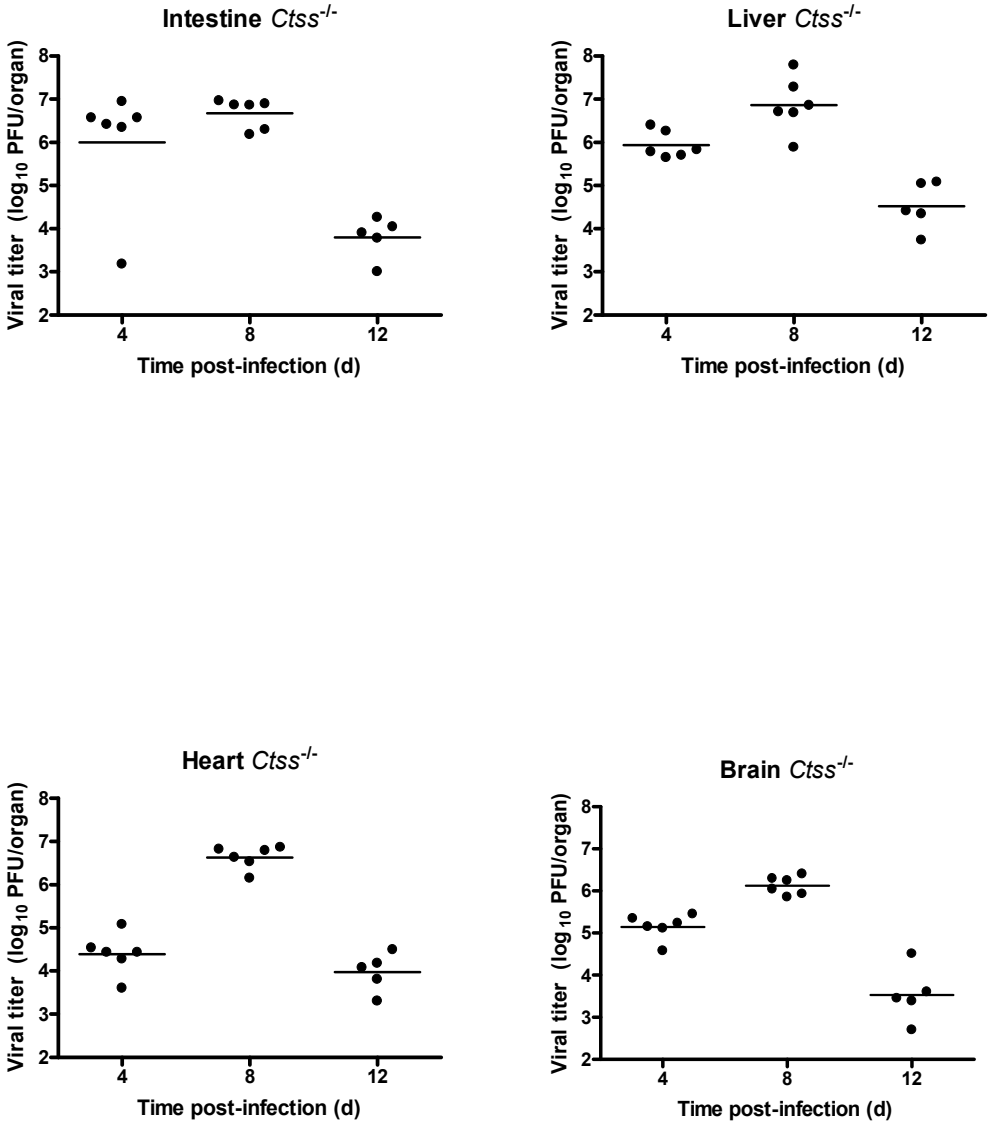

Figure III-5. Reovirus titers in organs of *Ctss*$^{-/-}$ mice following peroral infection with T1L. *Ctss*$^{-/-}$ mice (n = 4 to 7), 2-4 days old, were inoculated perorally with 10^4 PFU T1L. Organs were resected at the times shown and homogenized by freeze-thawing and sonication. Viral titers in organ homogenates were determined by plaque assay. Each data point represents one animal. Horizontal bars indicate the arithmetic mean of log-transformed data. The limit of detection was 10^2 PFU/organ.

Discussion

Data presented in this chapter indicate that viral tropism does affect the requirement for cathepsin proteases for maximal viral replication. I discovered dramatic differences in the pathogenesis of reovirus following infection of cathepsin-deficient mice with T1L in comparison to mice infected with T3SA+. In general, whereas cathepsin expression is required for peak growth of T3SA+ at sites of secondary replication, deficiency of a single cathepsin does not diminish growth of T1L. Cathepsin B may be required for initial infection events in the gastrointestinal tract for T1L, since *Ctsb*$^{-/-}$ mice had lower viral titers in the intestine at day 4. However, peak titers are equivalent in all organs tested at day 8, suggesting that cathepsin B alone is not required for productive infection of any organ.

Cathepsins L and S also are individually dispensable for growth of T1L in vivo. In contrast to *Ctsb*$^{-/-}$ mice, there was no delay in establishing infection in the intestine of *Ctsl*$^{-/-}$ and *Ctss*$^{-/-}$ mice. In fact, titers of T1L are higher in the liver of *Ctsl*$^{-/-}$ mice at day 4. Furthermore, peak titers in all organs tested of *Ctsl*$^{-/-}$ and *Ctss*$^{-/-}$ mice are equivalent to or greater than peak titers in wt mice.

It is intriguing that infection with T1L is not hampered by the loss of a single cathepsin, whereas infection with T3SA+ is substantially diminished. There are several possible explanations for this observation. First, T1L and T3SA+ differ in the route of spread from the intestine to target tissues. Whereas T1L uses hematogenous routes (143), T3SA+ uses both hematogenous and neural pathways (101, 147). Titers of T3SA+ in the blood of cathepsin-deficient mice did not differ from those in wt mice, suggesting that if hematogenous spread is defective in these mice, it would be blocked at the stage of exit

of the virus from the bloodstream into the target tissue. Alternatively, hematogenous spread may not be affected by lack of a single cathepsin, but neural spread may be altered. Titers in the brains of *Ctsl*$^{-/-}$ mice are lower than those in other genotypes of mice following intracranial inoculation of T3SA+. It is possible that cathepsin function is required for optimal spread of reovirus through neural routes. The capacity of T1L to infect all target organs equally in cathepsin-deficient and wt mice demonstrates that hematogenous spread of this virus is not affected.

Second, T1L and T3SA+ differ in cell and tissue tropism. In the brain, T1L infects ependymal cells (144, 145), whereas T3SA+ infects neurons (101, 144, 145, 147). In the liver, T1L infects hepatocytes (176), whereas infection with T3SA+ initiates at the bile duct epithelium (174, 176). Perhaps the cell types infected by T3SA+ are more sensitive to loss of cathepsin function than those infected by T1L.

Both T1L and T3SA+ are cleared more slowly from the intestine and sites of secondary replication in cathepsin L- and cathepsin S-deficient mice. While viral titers of T1L and T3SA+ in organs of wt mice decrease between days 8 and 12, titers do not diminish in these knock-out mice. At day 12 post-infection, titers of T1L are significantly higher in the intestine and heart of *Ctsl*$^{-/-}$ mice and in the liver and heart of *Ctss*$^{-/-}$ mice in comparison to wt mice. At the same timepoint, titers of T3SA+ are significantly higher in the intestine and liver of *Ctsl*$^{-/-}$ mice and the intestine of *Ctss*$^{-/-}$ mice in comparison to wt mice. The increased titers of T3SA+ at day 12 in cathepsin L- and cathepsin S-deficient mice occurs despite lower peak titers in these same organs at day 8 post-infection. This result is most likely due to a deficiency in CD4+ T cell help. Both *Ctsl*$^{-/-}$ and *Ctss*$^{-/-}$ mice display decreased CD4+ T cell activity due to inefficient cleavage of the invariant chain

in thymocytes (92) and peripheral APCs (108, 185), respectively. This deficiency in *Ctss*$^{-/-}$ mice is known to result in decreased germinal center formation and antibody class switching, particularly to isotype IgG2a (185). This antibody isotype has been implicated in clearance of reovirus in T3C9-infected adult mice lacking a functional IgM (158). It is also possible that an effective CD4+ T cell response is necessary for the development of the CD8+ T cell response to reovirus.

Adult SCID mice infected perorally with T1L develop lethal hepatitis and display lesions only in the liver despite the presence of virus in all organs tested (159). Neither *Ctsl*$^{-/-}$ nor *Ctss*$^{-/-}$ mice efficiently clear infection with either T1L or T3SA+ from the liver (though the differences between the cathepsin-deficient and wt mice may not always be statistically significant). Transfer of Peyer's patch cells from immune competent mice to SCID mice attenuates T1L infection (159), suggesting that the adaptive immune response in the intestine is essential for control of viral growth and spread. The requirement for intact adaptive immunity in the intestine is particularly intriguing, as *Ctsl*$^{-/-}$ mice appear unable to control infection with T1L at this site. Viral titer in the intestine of *Ctsl*$^{-/-}$ mice does not decrease from days 8 to 12 post-infection, when titers remain extraordinarily high. Infection with T3SA+ is also poorly controlled in the intestine of *Ctsl*$^{-/-}$ mice. Titers at sites of secondary replication of both *Ctsl*$^{-/-}$ and *Ctss*$^{-/-}$ mice decrease more slowly than in wt mice following infection with both T1L and T3SA+. Thus the lack of intact adaptive immunity in *Ctsl*$^{-/-}$ and *Ctss*$^{-/-}$ mice may be responsible for their poor control of reovirus infection at both the primary and secondary sites of replication following peroral inoculation.

In contrast to infection with T3SA+, expression of cathepsins B, L, and S individually does not appear to be required for efficient growth of T1L in any organ tested. It is likely that the deficiency in immune function exhibited by these mice leads to increased replication of T1L and inefficient clearance. Thus, in addition to providing the enzymatic mechanism for reovirus uncoating, these enzymes indirectly control reovirus infection by acting as critical determinants of immune function. Redundancy in cathepsin activity for viral replication allows reovirus to infect mice lacking a single cathepsin. However, absence of redundancy in cathepsin activity for immune function renders cathepsin-deficient animals severely immunocompromised.

CHAPTER IV

TREATMENT OF MICE WITH AN INHIBITOR OF CATHEPSIN L AMELIORATES REOVIRUS T3SA+ INFECTION IN VIVO

Introduction

Cathepsin-specific inhibitors are important tools for studies of cathepsin proteases. Techniques such as computer-graphic analysis of crystal structures and the generation of small-molecule libraries have facilitated the design of broad-spectrum inhibitors for families of proteases (e.g., E-64, a pan cysteine-containing protease inhibitor) and inhibitors of specific members of a protease family. One such compound, CLIK-148, inhibits cathepsin L specifically (186, 187). This compound was developed by altering the structure of E-64 using differences in the substrate-binding pockets of cathepsins B, L, and S as a guide. Inhibitors active against specific cathepsin proteases are useful for studies to better understand substrate specificity and to determine functions of cathepsins in vivo. The pleiotropic effects associated with genetic cathepsin deficiency complicate the interpretation of in vivo results. Furthermore, given the large number of human pathogens that exploit cathepsin proteases for infection, these inhibitors could be developed as antiviral therapeutics. To determine whether a cathepsin inhibitor can block reovirus infection, I treated wt mice with CLIK-148 during infection with T3SA+. Results from these experiments demonstrate that cathepsin inhibition diminishes reovirus disease.

Results

Treatment with an inhibitor of cathepsin L promotes survival following reovirus infection. Since titers of reovirus in organs of cathepsin-deficient mice are lower than those in wt mice, but mortality is increased in *Ctsl*$^{-/-}$ and *Ctss*$^{-/-}$ mice, I hypothesized that the immune defects accompanying cathepsin L and cathepsin S deficiency might mask a cathepsin requirement for efficient viral growth. Therefore, I sought to determine whether reovirus disease could be ameliorated in wt mice by treatment with an inhibitor of cathepsin L, CLIK-148, which blocks cathepsin L in vivo (186, 188). Mice were treated with CLIK-148 at a dose of approximately 100 μg/g body weight via intraperitoneal injection 1 hour prior to peroral inoculation with 10^7 PFU T3SA+ and then every 24 hours for 7 days. In comparison to mice treated with vehicle alone, a significantly greater percentage of mice treated with CLIK-148 survived (Figure IV-1 A). At day 21, 40% of CLIK-148-treated mice succumbed, whereas 80% of vehicle-treated mice died. As a surrogate marker for disease, CLIK-148-treated mice exhibited only minimal weight loss followed by substantial weight gain through the course of the experiment, whereas vehicle-treated mice exhibited more severe weight loss and gained weight more slowly during the recovery phase (Figure IV-1 B). Mock-infected mice treated with CLIK-148 or vehicle alone showed no signs of drug toxicity and had survival rates of 100% (data not shown). These results suggest that treatment with a cathepsin inhibitor dampens the severity of reovirus disease.

Treatment with an inhibitor of cathepsin L diminishes reovirus growth at sites of secondary replication. To determine whether the cause of diminished mortality following

treatment with CLIK-148 is related to viral growth, I quantified viral titers in various organs in wt mice treated with CLIK-148. Mice were treated with CLIK-148 at a dose of approximately 100 μg/g body weight via intraperitoneal injection 1 hour prior to peroral inoculation with 10 PFU T3SA+ and then every 24 hours for 7 days. On day 8 post-infection, organs were harvested and titers determined by plaque assay. Although titers in vehicle-treated and CLIK-148-treated mice were equivalent in the intestine, titers were reduced at sites of secondary replication in the CLIK-148-treated mice in comparison to vehicle-treated mice (Figure IV-2). More striking, perhaps, of the 5 CLIK-148-treated animals with detectable titer in the intestine, only 2 exhibited virus dissemination to other organs. However, of the 7 vehicle-treated mice with detectable titer in the intestine, 6 had disseminated virus. Thus, pharmacologic blockade of cathepsin L activity diminishes reovirus dissemination to sites of secondary replication.

Treatment with CLIK-148 inhibits reovirus entry into cells. To characterize the block to infection imposed by CLIK-148, murine L cells were treated with varying concentrations of CLIK-148 prior to infection with T3SA+ virions and in vitro generated ISVPs. ISVPs are capable of penetrating cells at the plasma membrane and are resistant to blocks of the entry an uncoating processes (21, 26-28, 115). In comparison to growth in untreated cells, treatment with 100μM CLIK-148 diminished viral yields by 1 log (Figure IV-3). Treatment with 200 μM E64, which blocks the activity of both cathepsins B and L (66), diminished viral yield by 2 logs. The decreased inhibition by CLIK-148 in comparison to E64 results from the presence of cathepsin B activity in these cells. Infection by ISVPs was not decreased in cells treated with either agent, demonstrating

that the block imposed by CLIK-148 is at a stage associated with entry. These results are in agreement with those obtained previously using other inhibitors of cathepsin L (4, 26).

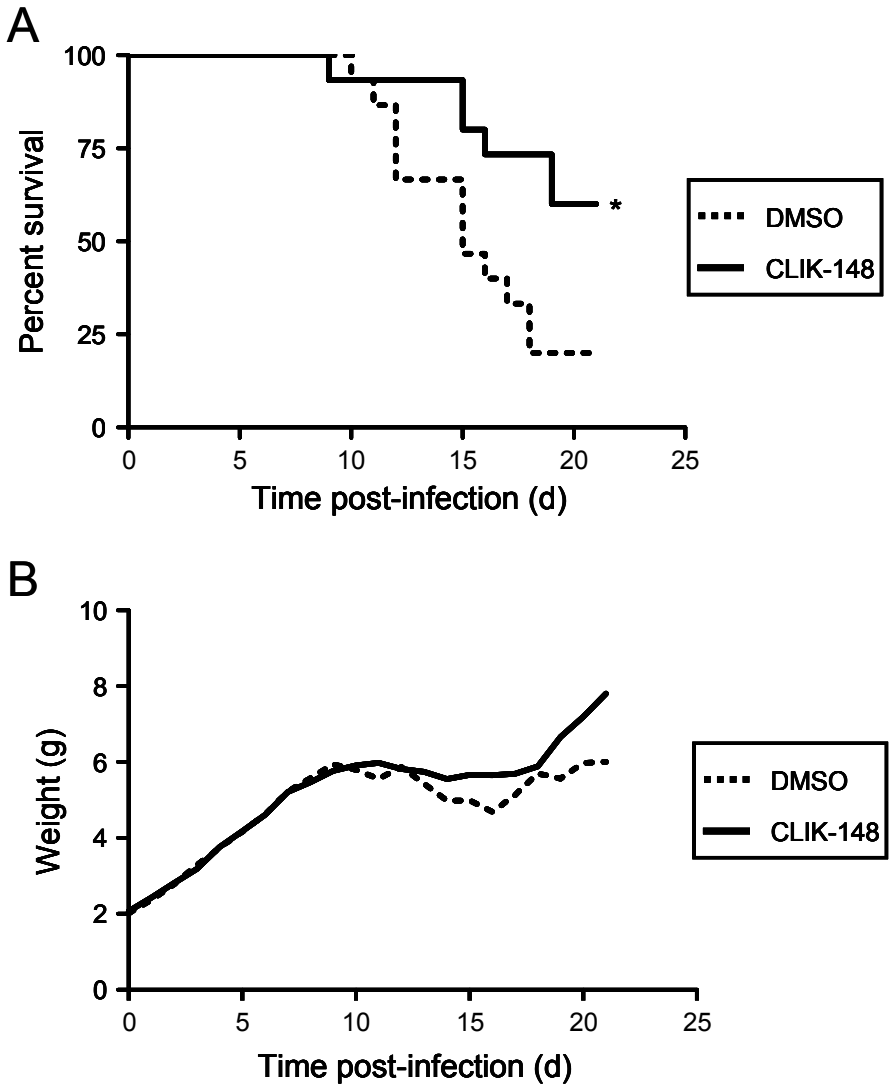

Figure IV-1. Survival following treatment with an inhibitor of cathepsin L. C57/Bl6 wt mice, 2-4 d old, were inoculated intraperitoneally with CLIK-148 at a dose of 100 μg/g average litter body weight or vehicle control 1 h prior to peroral inoculation with 10^7 PFU T3SA+. Mice were treated intraperitoneally with CLIK-148 thereafter for 7 d. Mice (n = 15) were monitored for (A) survival and (B) weight gain. (A) *, $P < 0.05$ as determined by log rank test in comparison to vehicle-treated mice. (B) All live mice were weighed each day.

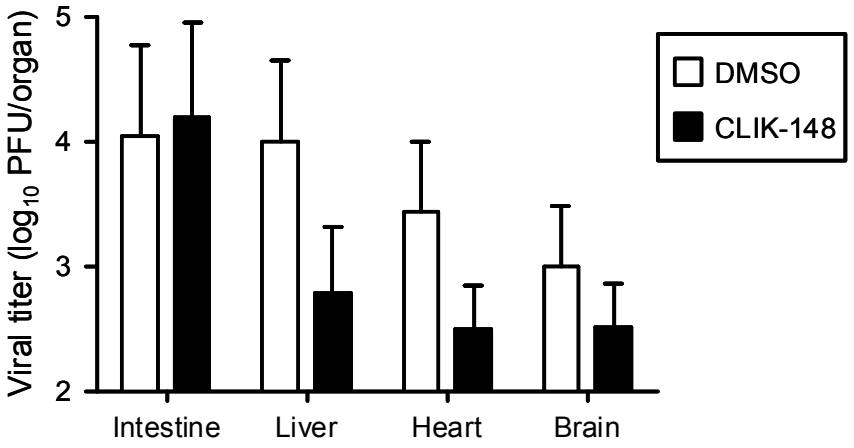

Figure IV-2. Viral titers following treatment with CLIK-148. C57/Bl6 wt mice, 2-4 d old, were inoculated intraperitoneally with CLIK-148 at a dose of 100 µg/g average litter body weight or vehicle control 1 h prior to peroral inoculation with 10 PFU T3SA+. Mice were treated intraperitoneally with CLIK-148 thereafter for 7 d. Mice (n = 9-10) were euthanized at d 8 post-inoculation, and viral titer in organs was determined by plaque assay. Error bars represent SEM.

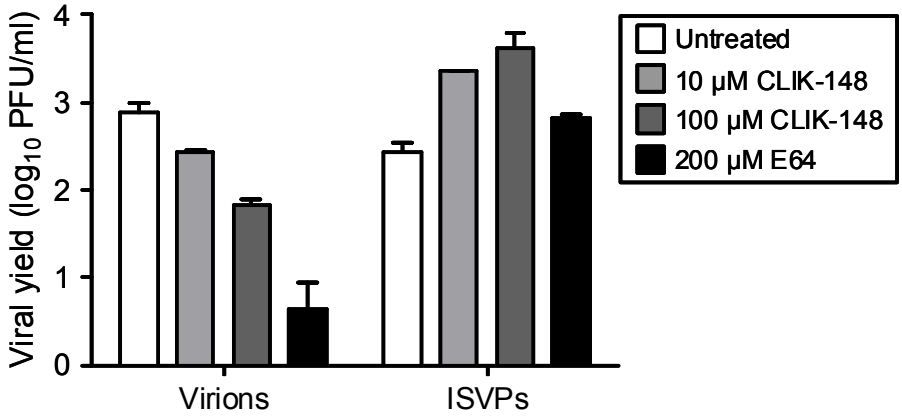

Figure IV-3. Infection of L cells following treatment with CLIK-148. Monolayers of L cells were preincubated for 4 h in medium with or without CLIK-148 or E64 at the concentrations shown. The medium was removed, and cells were adsorbed with T3SA+ virions or ISVPs at an MOI of 2 PFU per cell. After 1 h, the inoculum was removed, fresh medium with or without CLIK-148 or E64 was added, and cells were incubated for 0 or 24 h. Viral titers in cell lysates were determined by plaque assay. The results are presented as mean viral yields, calculated by dividing the titer at 24 h by the titer at 0 h for each concentration of CLIK-148 or E64 for duplicate wells.

Discussion

To eliminate the confounding variables present in the gene-deletion experiments, I sought to determine the effect of a cathepsin inhibitor on reovirus pathogenesis. CLIK-148, a derivative of the pan-cysteine protease inhibitor E-64, inhibits cathepsin L in vivo (186, 188). Mice treated with CLIK-148 had increased resistance to reovirus infection in comparison to vehicle-treated controls as assessed by both survival and viral titers at sites of secondary replication. Because survival was increased in CLIK-148-treated mice but decreased in *Ctsl*$^{-/-}$ mice, I conclude that the inhibition of viral replication is specific and that immune functions are preserved. Furthermore, since the mice treated with CLIK-148 did not display defects in fur growth characteristic of *Ctsl*$^{-/-}$ mice (88), I conclude that pharmacologic inhibition of cathepsin L is not as complete as genetic ablation.

Successful pharmacologic attenuation of reovirus disease with a cathepsin inhibitor raises the possibility that cathepsin-inhibitor therapy could be effective for other viruses that require cathepsin proteolysis for cell entry. Ebola virus (167), Nipah virus (171, 189), Hendra virus (170), and SARS CoV (168) utilize cathepsin proteases to enter cells. Treatment of cells with chloroquine inhibits Hendra and Nipah virus infection (190), most likely via interference with viral fusion glycoprotein processing by cathepsin L. The absence of inhibitor-associated toxicity in this study and others (186, 188), along with the efficacy of CLIK-148 treatment in the amelioration of disease (this study), suggests that cathepsin inhibitors should be evaluated for therapeutic efficacy against these viruses.

CHAPTER V

SUMMARY AND FUTURE DIRECTIONS

Despite their role in the entry of several important human and animal pathogens (167-172), the function of cathepsin proteases in viral infection of a host was previously unexplored. Reovirus offers an ideal experimental system to define how host factors influence viral pathogenesis. In this study, I found that cathepsins B, L, and S influence reovirus disease in a serotype-dependent manner (Table V-1). Although these enzymes are individually required for development of peak viral titers at sites of secondary replication following infection with reovirus strain T3SA+, they are not individually required for maximal growth of strain T1L. Following infection with T3SA+, survival is enhanced in mice lacking cathepsin B but diminished in mice lacking cathepsins L or S, likely reflecting the differential importance of these cathepsins in adaptive immunity. Importantly, treatment with an inhibitor of cathepsin activity, which uncouples cathepsin functions in reovirus disassembly and immunity, enhances survival. These findings indicate a key role for cathepsin proteases in viral pathogenesis.

Table V-1. Reovirus pathogenesis in cathepsin-deficient mice.

Results following infection with T3SA+

Genotype	Peroral[a]								Intracranial[a]
	Survival	Mean survival time	Replication in intestine	Replication in liver	Replication in heart	Replication in brain	Clearance	Viremia	Replication in brain
Ctsb $^{-/-b}$	↑	↑	↔	↔	↓	↓	↔	↔	↔
Ctsl $^{-/-b}$	↓	↑	↓	↓	↓	↓	↓	↔	↓
Ctss $^{-/-b}$	↓	↑	↓	↓	↓	↓	↓	↔	↔
wt + CLIK-148[c]	↑	ND	↔	↓	↓	↓	ND	ND	ND

Results following infection with T1L

Genotype	Peroral[a]				
	Replication in intestine	Replication in liver	Replication in heart	Replication in brain	Clearance
Ctsb $^{-/-b}$	↔	↔	↔	↔	↔
Ctsl $^{-/-b}$	↔	↑	↔	↔	↓
Ctss $^{-/-b}$	↔	↔	↔	↔	↓

[a] Route of inoculation
[b] In comparison to wt mice
[c] In comparison to wt mice treated with DMSO
ND, not determined

Cathepsin Proteases Influence Reovirus Pathogenesis in a Strain-Specific Manner

Although members of the cathepsin family show some redundancy of function, there exist specific roles for each protease. Therefore, I hypothesized that the proteases capable of mediating reovirus disassembly would serve nonredundant functions in reovirus pathogenesis by virtue of their specialized host functions. I found that, following infection with T3SA+, cathepsins B, L, and S are individually required for maximal viral growth at sites of secondary replication (Chapter II). Furthermore, the average survival time was increased in cathepsin-deficient mice in comparison to wt mice, presumably due to the lower viral yield at these sites. However, *Ctsl*$^{-/-}$ and *Ctss*$^{-/-}$ mice displayed decreased survival in comparison to wt and *Ctsb*$^{-/-}$ mice following both high- and low-

dose infections. They also displayed an increase in damage to the liver. These differences are presumably due to the requirement for cathepsins L and S for fully functional adaptive immunity. Furthermore, cathepsin L appears to play a specific role in reovirus infection of the CNS, as titers of T3SA+ were decreased in the brains of *Ctsl*$^{-/-}$ mice following intracranial inoculation.

To complement studies using genetically-deficient mice, I also studied reovirus pathogenesis using wt mice treated with CLIK-148, an inhibitor of cathepsin L. Results of these experiments (Chapter IV) show an increase in survival of CLIK-148-treated mice in comparison to vehicle-treated animals. This finding contrasts with the results gathered in experiments using *Ctsl*$^{-/-}$ mice. However, as in *Ctsl*$^{-/-}$ mice, viral titers at sites of secondary replication were decreased in CLIK-148-treated mice in comparison to vehicle-treated mice. Therefore, following infection with serotype 3 reovirus, cathepsin proteases influence reovirus pathogenesis in a cathepsin-specific manner.

The effect of cathepsin deficiency on the growth of T1L, a serotype 1 strain, differed from that of T3SA+ (Chapter III). Peak titers were not decreased in cathepsin-deficient mice and, in some instances, titers were increased. However, both strains were cleared more slowly in infected *Ctsl*$^{-/-}$ and *Ctss*$^{-/-}$ mice compared to wt controls. This observation most likely is a consequence of poor immune function in these mice.

The work presented herein establishes several insights into reovirus pathogenesis and the role of cathepsin proteases in viral infection. (i) Despite the presence of proteases such as chymotrypsin in the lumen of the gut, cathepsin S is required for maximal infection by T3SA+ at this site. Cathepsin S is expressed primarily in cells of the immune system (96) and also in intestinal epithelial cells (100). The decreased replication of

T3SA+ in the intestine of *Ctss*$^{-/-}$ mice suggests that the route of egress of the virus into intestinal epithelial cells is not apical but basolateral. By entering and exiting intestinal epithelial cells from the side opposite the lumen of the gut, exposure to chymotrypsin would not occur and infection of these cells would require disassembly in endosomes. Alternatively, the low titers of T3SA+ in the intestine of *Ctss*$^{-/-}$ mice may reflect the necessity for this protease to mediate infection of lymphocytes of the Peyer's patches. (ii) Redundancy of cathepsin function allows reovirus to infect all organs, though to varying degrees. However, other cathepsins cannot compensate for the specific role of cathepsins L and S in immune function. (iii) The requirement for individual cathepsins for maximal yields of T3SA+ at sites of secondary replication may be a result of the requirement for specific cathepsin activity for growth at those sites. Alternatively, cathepsins may be important for transport of the virus into infected tissues or along nerves. (iv) Serotype specificity of the virus influences the requirement for cathepsin activity for maximal infection, but serotype does not affect the requirement for cathepsin activity for proper immune function against the virus.

These findings raise new questions about cathepsin function in reovirus pathogenesis. For example, what influences the strain-specific differences in infectivity of T1L and T3SA+ in cathepsin-deficient mice? Why is the growth of T3SA+ most dramatically affected at sites of secondary replication? Why is cathepsin L required for maximal growth of T3SA+ in the brain? What is the role of the immune system in liver disease following reovirus infection? How does the protease susceptibility of viral proteins influence reovirus pathogenesis? Future experiments will address these questions.

Titers of T3SA+ are Reduced in the Brains of Cathepsin-Deficient Mice

Reovirus serotypes differ in the cell types they infect in vivo. This difference is particularly prominent in the brain where type 1 strains infect ependymal cells (144, 145) and type 3 strains infect neurons (101, 144, 145, 147). The variation in susceptibility to cathepsin deficiency between T1L and T3SA+ growth in the brain may be attributable to the distinct cell types infected by these strains. If ependymal cells are more capable than neurons to compensate for the loss of a single cathepsin, reovirus would grow more efficiently in these cells than in neurons from cathepsin-deficient mice. This compensation would be possible if the activity of cathepsins B, L, and S is greater in ependymal cells than in neurons. To determine whether cathepsin activity differs between these cell types, neurons and ependymal cells should be isolated (191) and the activity of cathepsins B, L, and S in each cell type measured using fluorogenic substrates (4, 186). The experiment should be conducted with cells isolated from wt and cathepsin-deficient mice. Measurement of cathepsin activity in cells from cathepsin-deficient mice will allow us to determine whether ependymal cells upregulate the activity of certain cathepsins in the absence of another. Results of these experiments will provide insight into the susceptibility of virus growth and lead to further studies to identify mechanisms of cathepsin regulation.

That T3SA+, but not T1L, is less infectious in the brain of cathepsin-deficient mice in comparison to wt mice raises the possibility that cathepsins contribute to neural spread to the brain from the primary site of infection. Both in vivo and in vitro approaches can be used to address this question. Type 3 reoviruses disseminate via neural routes to the brain following hind-limb inoculation (144, 147, 192). We can track

progression through the CNS by measuring viral titer in different parts of the CNS, namely the inferior spinal chord, superior spinal chord, and brain. Initial growth in the muscle of the hind-limb also should be confirmed. If the block to T3SA+ infection in the brain occurs during neural spread from the hind-limb, then viral titers will be diminished in the upper regions of the CNS in cathepsin-deficient mice but not in wt mice.

Virus spread within the CNS of cathepsin-deficient mice could be blocked at one of several stages. Possible points of hindrance include entry into neurons, transmission of virus between neurons, or egress from infected neurons into target cells. To determine whether cathepsins are required for reovirus entry into neurons, neurons should be isolated from wt and cathepsin-deficient mice and tested for the capacity to support the growth of T3SA+ virions and ISVPs. If the block to reovirus infection is related to entry events, neurons from cathepsin-deficient mice would be diminished in the capacity to support reovirus growth following infection with virions but not ISVPs.

Reovirus spreads through motor and sensory neurons (193) and autonomic neurons (101) via retrograde and anterograde movement. The virus enters motor neurons via motor nerve terminals (194) and travels through neurons using microtubule-associated system of fast axonal transport (144). The virus then replicates within the cell bodies of neurons (144, 194).

To further characterize the block to neuronal spread, compartmentalized neuron chambers (Figure V-1) (195-197) will be used. This system allows axons from neural cell bodies seeded in an isolated “soma” chamber to cross barriers and enter a distal “neurite” chamber where isolated target cells can be seeded. Use of these chambers will allow analysis of viral spread between neurons and from neurons to target cells.

To determine whether virus transmission between neurons is restricted in cathepsin-deficient mice, superior cervical ganglia (SCG) isolated from day E15 wt and cathepsin-deficient mice will be plated in the soma chamber and their axons allowed to grow into the neurite chamber for 10 days. Target cell neurons will then be plated in the neurite chamber. One day after plating of target neurons, before they are able to extend their axons into adjacent chambers, virus will be added to the soma chamber to infect the neurons with extended axons. Virus spread to the target neurons will be measured 48 hours post-inoculation by fluorescence focus assay. To determine whether virus spreads from axons into target cells, murine L929 cells should be seeded in the neurite chamber as target cells. These studies will reveal information about the role of cathepsins in neuronal transport.

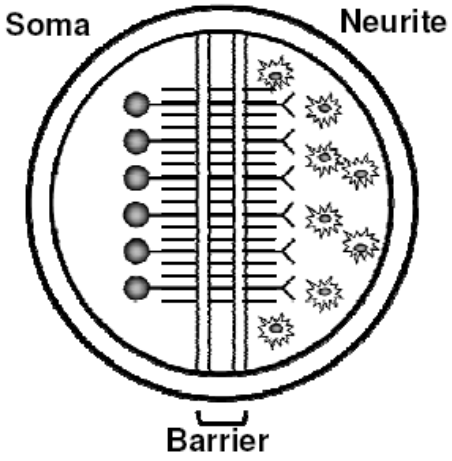

Figure V-1. Compartmentalized neuron chamber. The tripartite system consists of a Teflon chamber sealed onto a tissue culture dish with vacuum grease. Neurons are seeded in the soma chamber. Axons extend through the mid barrier and penetrate the neurite chamber where target cells are seeded.

Adaptive Immunity Controls Reovirus Disease

Cathepsins L and S play active roles in the development of adaptive immunity. Cathepsin L is required for positive selection of CD4+ T cells in the thymus, most likely though the combined action of processing the invariant chain in cortical thymic epithelial cells (92) and fragmentation of endosomal proteins, thereby promoting diverse peptide generation for display by MHC II on these cells (93). Cathepsin S is required for cleavage of the invariant chain in APCs (109) and processing antigenic endosomal proteins (108), thereby contributing to the activation of CD4+ T cells. Diminished T cell help contributes to a decrease in germinal center formation and antibody isotype class switching (185). *Ctsl*$^{-/-}$ and *Ctss*$^{-/-}$ mice fail to clear reovirus as quickly as wt and *Ctsb*$^{-/-}$ mice (Chapters II and III). I hypothesize that this defect in clearance is due to a deficiency in CD4+ T cell activity. To test this hypothesis, it will be necessary to define the role of CD4+ T cells in reovirus infection in the context of cathepsin deficiency.

An important first step in these studies is to determine the level of activation of CD4+ T cells in the context of reovirus infection in wt and cathepsin L- and cathepsin S-deficient mice. To do this, wt, *Ctsl*$^{-/-}$, and *Ctss*$^{-/-}$ mice will be infected with reovirus strain T3SA+ or mock infected. Two weeks post-infection, spleen cells and blood will be harvested. The number of CD4+ T cells will be quantified by flow cytometry, and total CD4+ T cells will be enumerated. The number of CD4+ T cells that have differentiated to T_H1 or T_H2 also will be determined by intracellular cytokine staining for IL-2 and IL-4, respectively.

It is unknown whether the alteration in CD4+ T cell helper functions of *Ctsl*$^{-/-}$ and *Ctss*$^{-/-}$ mice affects humoral or cytotoxic immunity during reovirus infection. To test the

effect of decreased CD4+ T cell help on humoral immunity, anti-reovirus antibody levels of wt, *Ctsl*$^{-/-}$, and *Ctss*$^{-/-}$ mice will be investigated. Mice of these three genotypes will be mock-infected or infected with strain T3SA+. Two weeks post-inoculation, serum will be collected, and the amount of reovirus-specific IgG, IgG1, IgG2a, and IgA will be measured by ELISA.

To test the effect of cathepsin L and cathepsin S deficiency on cell-mediated immunity, mice will be infected with T3SA+, and the CD8+ T-cell response will be measured. Two weeks post-inoculation, isolated splenocytes will be activated by co-culture with T3SA+-infected fibroblasts, and the level of activation in CD8+ T cells will be measured by intracellular cytokine staining for INFγ followed by flow cytometry.

These experiments will enhance knowledge about the role of cathepsins in adaptive immunity in the context of viral infection. This information is especially important as cathepsin inhibitors are currently being investigated as therapies for osteoporosis (198) and could be targets for the treatment of Alzheimer's disease (199) and cancer (200). An understanding of how long-term cathepsin inhibition affects the immune system is important for the safe use of these drugs.

Liver Damage Contributes to the death of Cathepsin L- and Cathepsin S-Deficient Mice

Following infection with T3SA+, *Ctsl*$^{-/-}$ and *Ctss*$^{-/-}$ mice display decreased survival and increased damage to the liver in comparison to wt and *Ctsb*$^{-/-}$ mice (Chapter II). This liver injury most likely contributes to the poor outcome of these animals. However, it is not known whether the damage to the liver results from virus-induced injury or from an aberrant immune response. T3SA+ infection in the liver originates at

the bile-duct epithelium and spreads to neighboring hepatocytes (174 and this study). The infection causes an infiltration of inflammatory cells; however, the identity of these cells and their specific effects on liver function are unknown. The influx of cells into the portal triad results in the collapse of bile ducts, which in turn results in a build-up of bile in the liver (174 and this study). Without bile secretion into the intestine, fat absorption in the intestine is diminished, which leads to numerous pathological consequences (174, 176, 178-180).

Information about the involvement of cathepsin proteases in virus-induced innate immunity is lacking. Cathepsin B is involved in the trafficking of TNF-α-containing vesicles to the plasma membrane in macrophages following stimulation by LPS (201). Cathepsin L is involved in regulating AKT/GSK3β in the heart, most likely through regulation of NF-κB (202). Various cathepsins, including cathepsins B, L, and S, have been implicated in the processing of TLR 9 following stimulation with CpG DNA (203). These findings suggest that cathepsins serve important functions in innate immunity and that their activities could contribute to the pathogenesis of reovirus disease independently of their function in uncoating.

To better understand the nature of the inflammatory infiltrate at sites of reovirus infection in the liver, histological analysis will be performed. Cathepsin-deficient and wt mice will be infected with 10^6 PFU T3SA+. At day 12 post-inoculation, mice will be harvested and livers resected, fixed, and embedded. Sections of tissue will be stained for reovirus antigen and various hallmarks of inflammation. These would include cytokines such as TNF-α and interferons and cell-specific markers to identify natural killer cells, neutrophils, macrophages, and dendritic cells. Sections also will be stained for CD8+ T

cells to determine the extent of the local adaptive immune response. Information gathered from this experiment will provide clues about the nature of the local immune response. If the inflammatory response in *Ctsl*$^{-/-}$ and *Ctss*$^{-/-}$ mice differs from that in wt and *Ctsb*$^{-/-}$ mice, further steps will be taken to discover the implications of these differences. One possible difference is the lack of expression of IL-10. This cytokine is produced by CD8+ T cells to inhibit the function of NK cells. In the absence of T cell help, *Ctsl*$^{-/-}$ and *Ctss*$^{-/-}$ mice may have fewer CD8+ T cells at the site of infection and, therefore, the signal to limit the inflammatory response may be diminished. An exacerbated inflammatory response could lead to increased damage of hepatocytes and bile-duct epithelia. Thus, information about differences in the innate immune response to reovirus in cathepsin-deficient mice will provide insight into the role of individual cathepsins in innate immunity and viral disease.

Cleavage Susceptibility of σ3 Regulates Uncoating and Pathogenesis

Reovirus disassembly is initiated by the proteolytic removal of σ3 (21, 26), which leads to conformational changes in μ1 that allow viral penetration into the cytoplasm (25, 124-126). Endocytic protease cathepsin L cleaves σ3 internally between residues 243-244 and 250-251 and at an unidentified site near the C terminus (4) (Figure I-4). I hypothesize that a surface-exposed loop in the C-terminus of σ3 is cleaved first, allowing cathepsin L to access a pocket containing the internal cleavage sites (4). Cathepsin L preferentially cleaves following a bulky hydrophobic residue at the P2 position and a basic residue at the P1 position (204). The σ3 cleavage sites between amino acids 243-244 and 250-251 confirm this preference at the P2 (Leu242 and Phe249) but not the P1 (Val243 and

Gly250) positions (4). It is not understood how variance from an optimal cleavage site influences the susceptibility of σ3 to proteolysis. Furthermore, it is not known whether both internal cleavage sites are used, nor whether the cleavage events are temporally related.

Identification of the C-terminal cathepsin L cleavage site in σ3. The C-terminal cleavage site in σ3 will be identified following limited proteolysis of T3D virions with cathepsin L (4). Digestion mixtures will be subjected to SDS-PAGE, and bands corresponding to full-length σ3 and the large N-terminal σ3 fragment, which can be readily detected (4), will be excised from the gel, trypsinized by in-gel digestion, and analyzed by MALDI-TOF/TOF mass spectrometry. The two MS spectra will be compared, and peptide peaks that differ between the spectra will be sequenced by MS/MS to identify the cleavage site. Alternatively, digestion products will be fractionated by reverse-phase HPLC to isolate the small C-terminal σ3 fragment, which will be sequenced using nanoLC-MS/MS mass spectrometry. Once the C-terminal cleavage site is identified, we will use reverse genetics to generate mutant viruses in which the P1 and P2 positions have been altered to modulate cleavage (205). Mutant viruses will be tested for infectivity (175) and susceptibility to cleavage by cathepsin L in vitro (4). These experiments will determine whether cleavage of σ3 at the C-terminus controls access to the internal cleavage sites and thus regulates reovirus disassembly.

Analysis of internal cathepsin L cleavage sites in σ3. To determine contributions of the internal σ3 cleavage sites to reovirus disassembly, the P1 and P2 positions at each

site will be substituted with the residues shown in Table V-2. The resultant σ3 CS mutants will be recovered by reverse genetics and tested for infection of *Ctsb*$^{-/-}$ and *Ctsl*$^{-/-}$ MEFs and susceptibility to cleavage by cathepsins B and L in vitro (4). We anticipate that σ3 CS mutants with arginine substitutions at the P1 positions will be more susceptible to cathepsin L but display wt susceptibility to cathepsin B. Such mutants should infect wt cells more efficiently than wt virus but exhibit wt infectivity in *Ctsl*$^{-/-}$ cells. Conversely, σ3 CS mutants with alanine substitutions at the P2 positions should be resistant to cathepsin L but not cathepsin B. Since either cathepsin B or cathepsin L can catalyze reovirus disassembly in fibroblasts (4), these σ3 CS mutants should infect cells lacking cathepsin L but not those lacking cathepsin B. Use of both cell types, coupled with in vitro analyses of proteolysis, will allow us to determine the functional importance of the cathepsin L cleavage sites in σ3 and provide insight into mechanisms used by endocytic proteases to catalyze viral disassembly.

Table V-2. Planned mutations of σ3 cleavage-site residues.

Mutant	P2-242	P1-243	P2-249	P1-250	Anticipated result
Wildtype	L	V	F	G	
σ3 CS1	**A**	V	F	G	Diminished utilization of 243-244
σ3 CS2	L	V	**A**	G	Diminished utilization of 250-251
σ3 CS3	**A**	V	**A**	G	Diminished utilization of both 243-244 and 250-251
σ3 CS4	**F**	V	**L**	G	No change in cleavage site utilization or perhaps a reversal in the temporal relationship of the cleavage events
σ3 CS5	L	**R**	F	G	Enhanced utilization of 243-244
σ3 CS6	L	V	F	**R**	Enhanced utilization of 250-251
σ3 CS7	L	**R**	F	**R**	Enhanced utilization of both 243-244 and 250-251

Pharmacologic inhibition of cathepsin activity. I found that treatment of mice with CLIK-148, an inhibitor of cathepsin L, lessens the severity of reovirus disease. To extend this finding and provide rationale for the development of cathepsin inhibitors as

antiviral therapeutics, we must determine whether inhibitors of other cathepsins would also inhibit reovirus infection and whether the drugs are effective if administered after infection is established.

To determine whether inhibition of cathepsins B and S attenuates reovirus disease, we will test CA-074 and CLIK-60, which have been used in mice to selectively inhibit cathepsins B (206) and S (207), respectively, for the capacity to diminish reovirus infection and pathology. Wildtype mice will be inoculated perorally with reovirus strain T3SA+ and treated by intraperitoneal administration with CA-074, CLIK-60, or DMSO. Inhibition of cathepsin activity in harvested tissues will be confirmed using fluorogenic substrates (74). Uninfected animals will be treated with each inhibitor alone as a control for drug toxicity. In our initial experiments, inhibitor treatment will begin on the day of inoculation and continue for 7 days post-inoculation. Combinations of these inhibitors will also be tested for toxicity and efficacy against reovirus.

To determine whether the inhibitors can be administered after infection is established, treatment will be initiated at successively longer intervals following inoculation. These experiments will establish whether cathepsin inhibitors can serve as antiviral agents.

Pathogenesis of σ3 CS mutant viruses. To determine whether alterations in viral capsid proteolysis by cathepsin L influence reovirus pathogenesis, we will compare wt and σ3 CS mutant viruses for pathologic outcome following infection of wt and cathepsin-deficient mice. We anticipate that virulence of cathepsin L-insensitive σ3 CS mutant viruses in wt mice will be altered to an extent similar to wt virus in *Ctsl*$^{-/-}$ mice,

which would confirm a requirement for cathepsin L in reovirus pathogenesis. However, because of cathepsin L insensitivity, these σ3 CS mutant viruses should be substantially more attenuated than wt virus in either *Ctsb*$^{-/-}$ or *Ctss*$^{-/-}$ mice. Virulence of cathepsin L-hypersensitive σ3 CS mutant viruses is more difficult to predict. These 3 CS mutant viruses may be more virulent than wt virus as a consequence of enhanced cleavage susceptibility or attenuated due to alterations in capsid stability.

Collectively, these experiments will determine whether strategic alterations in σ3 affecting cathepsin L sensitivity influence reovirus pathogenesis. In addition to defining mechanisms of reovirus disassembly, this work is relevant to the use of reovirus as an oncolytic agent. Enhanced replication of reovirus in transformed cells is in part attributable to endocytic protease activity (208). Alteration of the cathepsin L cleavage sites may make it possible to engineer reovirus vectors with enhanced tumor cell killing and diminished toxicity. Moreover, these experiments will advance knowledge about substrate utilization by cathepsin L, which will allow refined prediction of cathepsin L cleavage sites and foster the design of new cathepsin L inhibitors.

CHAPTER VI

MATERIALS AND METHODS

Cells and viruses. L929 cells were maintained in Joklik's minimal essential medium supplemented to contain 10% fetal bovine serum (FBS), 2 mM L-glutamine, 100 U/ml penicillin, 100 μg/ml streptomycin, and 25 ng/ml amphotericin B. T3SA+ is a reassortant virus containing the S1 gene segment of strain T3C44MA and the remaining nine gene segments of strain T1L (175). Virus was purified after growth in L929 cells by CsCl-gradient centrifugation (209). Viral titers were determined by plaque assay (210).

Treatment of virions with purified cathepsins. Purified reovirus virions at a concentration of 10^{12} particles per ml in reaction buffer B-L (50 mM sodium acetate [pH 5.0], 15 mM $MgCl_2$, 100 mM NaCl, 5 mM DTT) were treated with 400 μg/ml bovine spleen cathepsin B (Calbiochem-Novabiochem) or 100 μg/ml purified recombinant human cathepsin L (211) at 37°C for various intervals. Alternatively, purified virions at a concentration of 10^{12} particles per ml in reaction buffer S (50 mM sodium acetate [pH 6.0], 15 mM $MgCl_2$, 100 mM NaCl) were treated with 300 μg/ml purified recombinant human cathepsin S (Calbiochem) at 37°C for various intervals. Proteolysis was terminated by incubation of reaction mixtures on ice and addition of 1 mM E64. A 30-μl aliquot of each reaction was incubated with 7 μl 6x sample buffer (350 mM Tris [pH6.8], 9.3% DTT, 10% SDS, 0.012% bromophenol blue) at 100°C for 5 min. Samples were

loaded into wells of 10% polyacrylamide gels and electrophoresed. After electrophoresis, gels were fixed and stained using colloidal Coomassie blue (Invitrogen, Carlsbad, CA).

Mice. C57Bl/6J mice (wt) were obtained from Jackson Laboratory. *Ctsb*$^{-/-}$ (86, 212) and *Ctsl*$^{-/-}$ mice (88), each backcrossed to a C57Bl/6 background at least 8 times, were provided by D. Hanahan (San Francisco, CA). *Ctss*$^{-/-}$ mice, backcrossed at least 10 times to a C57Bl/6 background (110), were provided by H. Chapman (San Francisco, CA).

Infection of mice. Newborn mice, 2-4 days old, weighing approximately 2 g were inoculated perorally or intracranially with purified reovirus virions diluted in PBS. Peroral inoculations (50 µl) were delivered intragastrically (213). Intracranial inoculations (5 µl) were delivered to the left cerebral hemisphere using a Hamilton syringe and 30-gauge needle (214). For analysis of virulence, mice were monitored for weight loss and symptoms of disease for 21 days post-inoculation and euthanized when found to be moribund (defined by rapid or shallow breathing, severe lethargy, or paralysis). For analysis of viral replication, mice were euthanized at various intervals following inoculation, and organs were harvested into 1 ml of PBS before freezing, thawing, and homogenization by sonication. For analysis of viremia, mice were euthanized and decapitated at various intervals following inoculation. Whole blood was collected from the neck into a 1 ml syringe containing 100 µl Alsever's solution (Sigma) and frozen, thawed, and sonicated. Viral titers in organ and blood homogenates were determined by plaque assay (215). Animal husbandry and experimental procedures were

performed in accordance with Public Health Service policy and approved by the Vanderbilt University School of Medicine Institutional Animal Care and Use Committee.

Treatment of mice with an inhibitor of cathepsin L. Mice were inoculated intraperitoneally with approximately 100 μg/g average litter weight of CLIK-148 in DMSO or DMSO alone. One hour following treatment, mice were inoculated perorally with PBS or reovirus T3SA+. Mice were subsequently treated with CLIK-148 daily for 7 days. Analysis of virulence was conducted for 21 days or mice were euthanized at 8 days post-inoculation and organs resected for determination of viral titer as described. Pups with obvious injury from intraperitoneal injections or that died within 6 days post-inoculation were eliminated from the study.

Statistical analysis. For survival experiments, curves were obtained using the Kaplan-Meier method and compared by the log-rank test. For experiments in which viral titers were determined in an organ or blood, the Mann-Whitney test was used to calculate two-tailed *P* values. This test is appropriate for experimental data that display a non-Gaussian distribution (216). Mann-Whitney analysis lacks the power of the *t* test and, therefore, statistical significance is achieved less frequently using this method. All statistical analyses were performed using GraphPad Prism software.

Histology. Newborn mice, 2-4 days old, weighing approximately 2 g were inoculated perorally with purified reovirus virions diluted in PBS. At various intervals following inoculation, mice were euthanized, organs were resected, and a wedge of liver

was removed for titer determination by plaque assay. Remaining organs were incubated in 10% formalin at room temperature for 24 h, followed by incubation in 70% ethanol at room temperature. Fixed organs were embedded in paraffin, and 5-μm sections were prepared. Consecutively obtained sections were stained with hematoxylin and eosin for evaluation of histopathologic changes or processed for immunohistochemical detection of reovirus protein (217).

Quantitation of serum hepatic enzymes. Newborn mice, 2-4 days old, weighing approximately 2 g were inoculated perorally with purified reovirus virions diluted in PBS. At various intervals following inoculation, mice were euthanized and decapitated. Blood was collected and allowed to coagulate, and serum was separated by centrifugation. Sera were stored at -20°C, protected from light, and submitted in batches to Charles River Research Animal Diagnostic Services (Wilmington, MA). A small wedge of liver was resected concurrently with blood collection for correlative titer determination by plaque assay.

Growth of reovirus in vitro in the presence of cathepsin inhibitors. Monolayers of L cells ($2x10^5$ cells) in 24-well plates were preincubated in medium supplemented to contain 10-100 μM CLIK-148 or 200 μM E64 for 4 h. The medium was removed, and cells were adsorbed with T3SA+ or ISVPs of T3SA+ at an MOI of 2 PFU per cell. After incubation at 4°C for 1 h, the inoculum was removed, cells were washed with phosphate-buffered saline, and 1 ml fresh medium supplemented with CLIK-148 or E64 was added.

After incubation at 37°C for 0 or 24 h, cells were frozen and thawed twice, and viral titers in cell lysates were determined by plaque assay.

APPENDIX

A. JUNCTIONAL ADHESION MOLECULE A SERVES AS A RECEPTOR FOR PROTOTYPE AND FIELD-ISOLATE STRAINS OF MAMMALIAN REOVIRUS

The discovery that JAM-A is a receptor for reovirus was originally made using prototype strains T1L and T3D and reassortant viruses T3SA- and T3SA+ (218). This study demonstrated that JAM-A also serves as a receptor for other serotypes of reovirus and non-prototype strains. My involvement in this project was to help with plaque-purification and cultivation of virus stocks and to conduct infectivity studies using the prototype and field-isolate strains.

JOURNAL OF VIROLOGY, July 2005, p. 7967–7978 Vol. 79, No. 13
0022-538X/05/$08.00+0 doi:10.1128/JVI.79.13.7967–7978.2005

Junctional Adhesion Molecule A Serves as a Receptor for Prototype and Field-Isolate Strains of Mammalian Reovirus

Jacquelyn A. Campbell,[1,2] Pierre Schelling,[3] J. Denise Wetzel,[2,4] Elizabeth M. Johnson,[1,2] J. Craig Forrest,[1,2] Greame A. R. Wilson,[5] Michel Aurrand-Lions,[6] Beat A. Imhof,[6] Thilo Stehle,[3] and Terence S. Dermody[1,2,4]*

Departments of Microbiology and Immunology[1] and Pediatrics[4] and Elizabeth B. Lamb Center for Pediatric Research,[2] Vanderbilt University School of Medicine, Nashville, Tennessee 37232; Amgen Inc., Thousand Oaks, California 91320[5]; Department of Pathology, Centre Medical Universitaire, Geneva, Switzerland[6]; and Laboratory of Developmental Immunology, Massachusetts General Hospital and Harvard Medical School, Boston, Massachusetts 02114[3]

Received 6 January 2005/Accepted 17 March 2005

Reovirus infections are initiated by the binding of viral attachment protein σ1 to receptors on the surface of host cells. The σ1 protein is an elongated fiber comprised of an N-terminal tail that inserts into the virion and a C-terminal head that extends from the virion surface. The prototype reovirus strains type 1 Lang/53 (T1L/53) and type 3 Dearing/55 (T3D/55) use junctional adhesion molecule A (JAM-A) as a receptor. The C-terminal half of the T3D/55 σ1 protein interacts directly with JAM-A, but the determinants of receptor-binding specificity have not been identified. In this study, we investigated whether JAM-A also mediates the attachment of the prototype reovirus strain type 2 Jones/55 (T2J/55) and a panel of field-isolate strains representing each of the three serotypes. Antibodies specific for JAM-A were capable of inhibiting infections of HeLa cells by T1L/53, T2J/55, and T3D/55, demonstrating that strains of all three serotypes use JAM-A as a receptor. To corroborate these findings, we introduced JAM-A or the structurally related JAM family members JAM-B and JAM-C into Chinese hamster ovary cells, which are poorly permissive for reovirus infection. Both prototype and field-isolate reovirus strains were capable of infecting cells transfected with JAM-A but not those transfected with JAM-B or JAM-C. A sequence analysis of the σ1-encoding S1 gene segment of the strains chosen for study revealed little conservation in the deduced σ1 amino acid sequences among the three serotypes. This contrasts markedly with the observed sequence variability within each serotype, which is confined to a small number of amino acids. Mapping of these residues onto the crystal structure of σ1 identified regions of conservation and variability, suggesting a likely mode of JAM-A binding via a conserved surface at the base of the σ1 head domain.

Mammalian orthoreoviruses (referred to as reoviruses in this article) are nonenveloped viruses with genomes of 10 discrete segments of double-stranded RNA (reviewed in reference 41). There are at least three serotypes of reoviruses, which can be differentiated by the capacity of antireovirus antisera to neutralize viral infectivity and inhibit hemagglutination (47, 50). Each of the reovirus serotypes is represented by a prototype strain, namely, type 1 Lang/53 (T1L/53), type 2 Jones/55 (T2J/55), and type 3 Dearing/55 (T3D/55). Reoviruses appear to infect most mammalian species, but disease is restricted to the very young (reviewed in reference 63). Reovirus infections of newborn mice have been used as the preferred experimental system for studies of reovirus pathogenesis. Sequence polymorphisms in reovirus attachment protein σ1 play an important role in determining sites of reovirus infection in the infected host (4, 32, 69, 70).

The σ1 protein is an elongated trimer with a head-and-tail morphology. The N-terminal σ1 tail partially inserts into the virion via "turrets" formed by the pentameric λ2 protein, while the C-terminal σ1 head projects away from the virion surface (1, 25, 26). A crystal structure of the C-terminal half of T3D/55 σ1 revealed that the head contains three β-barrel domains (one from each trimer), each of which is constructed from eight antiparallel β-strands (16). Sequence analysis and structural modeling have suggested that the N-terminal half of the tail is formed from an α-helical coiled coil (6, 21, 40) and the C-terminal half is formed from a triple β-spiral (16, 56). The overall structural topology of the β-spiral and head domains of σ1 is strikingly similar to that of the adenovirus attachment protein, fiber (16, 37, 56).

There are two distinct receptor-binding regions in σ1. A region in the fibrous tail domain of type 3 σ1 binds to α-linked sialic acid (2, 14, 15, 18). A distinct region in the type 1 σ1 tail domain also binds to cell surface carbohydrates (14), and recent evidence suggests that sialic acid may be involved in the binding of T1L/53 to intestinal cells (30). A second receptor-binding site is located in the head domains of both the type 1 and type 3 σ1 proteins (3, 39).

An expression-cloning approach was used to identify junctional adhesion molecule A (JAM-A) as a receptor for the prototype strains T1L/53 and T3D/55 (3). JAM-A is a 35-kDa type I transmembrane protein that is a member of the immunoglobulin superfamily (34, 36). JAM-A contains two immunoglobulin-like domains, a single transmembrane region, and a short cytoplasmic tail. JAM-A is expressed in a variety of

* Corresponding author. Mailing address: Lamb Center for Pediatric Research, D7235 MCN, Vanderbilt University School of Medicine, Nashville, TN 37232. Phone: (615) 343-9943. Fax: (615) 343-9723. E-mail: terry.dermody@vanderbilt.edu.

tissues, including epithelial and endothelial barriers (34, 36, 43), where it is thought to regulate tight-junction permeability and mediate leukocyte trafficking (17, 34, 36, 43).

The crystal structures of the murine (m) and human (h) homologs of JAM-A, both of which are functional reovirus receptors (3), indicate that JAM-A forms homodimers via extensive hydrophobic and ionic contacts between apposing membrane-distal (D1) immunoglobulin-like domains (33, 44). Residues that facilitate interdimer interactions are strictly conserved between mJAM-A and hJAM-A (33, 44). JAM-A dimers are thought to be physiologically relevant, perhaps functioning in tight-junction barrier integrity or the diapedesis of inflammatory cells (8, 33, 44). Recent biochemical studies of reovirus–JAM-A interactions suggested that σ1 binds to a monomeric version of JAM-A and contacts residues in the vicinity of the JAM-A dimer interface (24). This strategy of cell attachment is strikingly similar to that used by adenovirus fiber to bind to the coxsackievirus and adenovirus receptor (CAR) (10, 66), an immunoglobulin superfamily member that shares considerable structural homology with JAM-A (57).

For this study, we determined whether JAM-A serves as a receptor for the prototype type 2 strain T2J/55 and a panel of four type 1, two type 2, and four type 3 field-isolate strains. The results indicate that JAM-A, but not the related JAM family members JAM-B and JAM-C, is a receptor for prototype and field-isolate strains of the three reovirus serotypes. An analysis of conserved and variable sequences in the σ1 head, together with existing structural information for σ1 and JAM-A, suggested an especially high tolerance for surface variation in the protein while maintaining the specificity for receptor utilization. These findings enhance our understanding of the molecular basis of reovirus binding to JAM-A and provide clues about the mechanisms of reovirus attachment.

MATERIALS AND METHODS

Cells, viruses, and antibodies. Spinner-adapted murine L929 (L) cells were grown in either suspension or monolayer cultures in Joklik's modified Eagle's minimal essential medium (Irvine Scientific, Santa Ana, Calif.) supplemented to contain 5% fetal bovine serum (Gibco-BRL, Gaithersburg, Md.), 2 mM L-glutamine, 100 U of penicillin per ml, 100 mg of streptomycin per ml, and 0.25 mg of amphotericin per ml (Gibco-BRL). HeLa cells were maintained in monolayer cultures in Dulbecco's minimal essential medium (Gibco-BRL) supplemented to contain 10% fetal bovine serum, L-glutamine, and antibiotics as described for L cells. Chinese hamster ovary (CHO) cells were maintained in Ham's F12 medium supplemented with fetal bovine serum, L-glutamine, and antibiotics as described for HeLa cells.

The prototype reovirus strains T1L/53, T2J/55, and T3D/55 are laboratory stocks. The field-isolate reovirus strains used in this study are shown in Table 1. Variant K, a neutralization-resistant variant of T3D/55, was selected and characterized as previously described (7, 54, 55). Viral stocks were prepared by plaque purification and passage in L cells (67). Purified virions were prepared by using second- and third-passage L-cell lysate stocks as previously described (26, 49). Viral particle concentrations were determined by measurements of the optical density at 260 nm, using a conversion factor of 2.1×10^{12} viral particles per optical density unit (52). The particle-to-PFU ratio of stocks used for viral infectivity assays was approximately 250 to 1.

Rabbit hCAR-specific antiserum was provided by Jeffrey Bergelson (University of Pennsylvania). Rabbit polyclonal hJAM-B- and hJAM-C-specific antisera were generated as previously described (28). The murine hJAM-A-specific monoclonal antibody (MAb) J10.4 was purified from mouse ascites by using protein A-Sepharose (34). The immunoglobulin G (IgG) fractions of polyclonal rabbit antisera raised against T1L/53 and T3D/55 (71) were purified by using protein A-Sepharose (2). A mixture of these sera was capable of recognizing all strains of reovirus used in this study.

TABLE 1. Strains used for studies of JAM-A utilization by reoviruses

Virus strain[a]	Abbreviation	GenBank accession no.	Reference
T1/Human/Ohio/Lang/1953	T1L/53	M35963	45, 50
T1/Bovine/Maryland/clone23/1959	T1C23/59	AY862134	31
T1/Bovine/Maryland/clone50/1960	T1C50/60	AY862133	31
T1/Human/Netherlands/1/1984	T1Neth/84	AY862136	29
T1/Human/Netherlands/1/1985	T1Neth/85	AY862135	29
T2/Human/Ohio/Jones/1955	T2J/55	M35964	46, 50
T2/Human/Netherlands/1/1973	T2Neth/73	AY862137	29
T2/Human/Netherlands/1/1984	T2Neth/84	AY862138	29
T3/Human/Ohio/Dearing/1955	T3D/55	NC_004277	46, 50
T3/Human/Wash.D.C./clone93/1955	T3C93/55	L37675	31
T3/Human/Wash.D.C./clone87/1957[b]	T3C87/57	L37677	48
T3/Bovine/Maryland/clone18/1961	T3C18/61	L37684	31
T3/Murine/France/clone9/1961	T3C9/61	L37676	31

[a] Strain nomenclature is as follows: serotype/species of origin/place of origin/strain designation/year of isolation.
[b] This strain has also been designated T3/Human/Wash.D.C./Abney/1957.

Fluorescent-focus assays of viral infectivity. Monolayers of HeLa cells in 96-well plates (Costar, Cambridge, Mass.) (3×10^4 cells per well) were pretreated for 1 h with phosphate-buffered saline (PBS), hCAR-specific antiserum, or the hJAM-A-specific MAb J10.4 at various concentrations prior to the adsorption of virus at room temperature for 1 h. Following removal of the inoculum, the cells were washed with PBS and incubated at 37°C for 20 h to permit the completion of a single round of viral replication. Monolayers were fixed with 1 ml of methanol at −20°C for a minimum of 30 min, washed twice with PBS, blocked with 2.5% immunoglobulin-free bovine serum albumin (Sigma-Aldrich, St. Louis, Mo.) in PBS, and incubated at room temperature for 1 h with protein-A–affinity-purified polyclonal rabbit antireovirus serum at a 1:800 dilution in PBS–0.5% Triton X-100. The monolayers were washed twice with PBS–0.5% Triton X-100 and incubated with a 1:1,000 dilution of goat anti-rabbit immunoglobulin conjugated with the Alexa Fluor 546 fluorophore (Molecular Probes, Eugene, Oreg.). The monolayers were washed twice with PBS, and infected cells were visualized by indirect immunofluorescence using an Axiovert 200 inverted microscope modified for fluorescence microscopy (Carl Zeiss, New York, N.Y.). Infected cells were identified by the presence of intense cytoplasmic fluorescence that was excluded from the nucleus. No background staining of uninfected control monolayers was noted. Reovirus antigen-positive cells were quantified by counting the fluorescent cells in at least three random fields of view per well in triplicate at a magnification of ×20.

Transient transfection and infection of CHO cells. CHO cells were transiently transfected with an empty vector or with plasmids encoding receptor constructs by the use of Lipofectamine PLUS reagent (Invitrogen, San Diego, Calif.) as previously described (3). After 24 h of incubation to allow receptor expression, transfected cells were allowed to adsorb to the virus at a multiplicity of infection (MOI) of 1 fluorescent focus unit (FFU) per cell, incubated for an additional 20 h, fixed with methanol, and stained for reovirus proteins by use of an anti-reovirus serum at a 1:800 dilution. Images were captured at a magnification of ×20 with a Zeiss Axiovert 200 inverted microscope.

Flow cytometric analysis of receptor expression. CHO cells were transiently transfected with receptor constructs, incubated for 24 h, and detached from the plates by incubation with 20 mM EDTA in PBS. Cells (10^6) were incubated with the hCAR-specific antiserum, the hJAM-A-specific MAb J10.4, or an antibody specific for hJAM-B or hJAM-C (28), washed with PBS, and incubated with a phycoerythrin-conjugated goat anti-rabbit or anti-rat IgG secondary antibody (Molecular Probes) at a 1:1,000 dilution on ice for 30 min. The cells were washed twice with PBS and analyzed with a FACScan flow cytometer (Becton-Dickinson, Palo Alto, Calif.).

Sequence analysis of the S1 gene. Viral genomes were extracted from infected L-cell lysates by the use of Trizol (Life Technologies, Rockville, Md.) according to the protocol supplied by the manufacturer. S1 gene segments were amplified by reverse transcription-PCR (RT-PCR) using 10 U of avian myeloblastosis virus reverse transcriptase (Promega Biosciences, San Luis Obispo, Calif.), 2.5 U *Taq* DNA polymerase (Promega Biosciences), and primers complementary to the 5′ and 3′ nontranslated regions of the S1 genes of the reovirus prototype strains. The type 1 S1 forward primer was 5′ GGATCCGCTATTCGCGCCTATGG

ATG, and the reverse primer was 5′ GGGTTCGCGCTAGATTCA. The type 2 S1 forward primer was 5′ GCTATTCGCACTCATGTCGGATCTAGTGC AGC, and the reverse primer was 5′ GATGAGTCGCCACTGTGCCGAGT GGA. The type 1 5′ forward primer contained nucleotides that resulted in a primer-derived sequence for the first two amino acids (M and D), and the type 2 5′ forward primer contained nucleotides that resulted in a primer-derived sequence for the first six amino acids (M, S, D, L, V, and Q). The amplification products were cloned into the pCR 2.1 vector (Invitrogen). Sequences of at least two independent RT-PCR clones for each S1 gene segment were determined by automated sequencing.

Phylogenetic analysis of S1 gene nucleotide sequences. Sequences were aligned by using the program ClustalX (62). Phylogenetic trees were constructed from variations in the σ1-encoding S1 gene nucleotide sequences by the maximum parsimony method using the heuristic search algorithm within the program PAUP v4.0b10 (58). Trees were rooted at the midpoint. The branching orders of the phylograms were verified statistically by resampling the data 1,000 times in a bootstrap analysis using the branch and bound algorithm as applied in PAUP.

Sequence alignment and structural modeling methods. Sequences were aligned by using the program ClustalW (http://www.ebi.ac.uk/clustalw/). Alignments were rendered in ALSCRIPT (5), using different colors to highlight different degrees of sequence similarity. Sequence changes were mapped onto the crystal structure of T3D/55 σ1 (16) by using the program GRASP (42).

RESULTS

JAM-A serves as a receptor for prototype strains of the three reovirus serotypes. Our previous work indicated that JAM-A serves as a receptor for the prototype reovirus strains T1L/53 and T3D/55 (3). To confirm these observations and to test whether JAM-A is used as a receptor by T2J/55, we treated HeLa cells with PBS, an hCAR-specific antiserum as a control, or the hJAM-A-specific MAb J10.4 prior to viral adsorption. Infected cells were quantified by indirect immunofluorescence using an antireovirus serum (Fig. 1A). The treatment of cells with the CAR-specific antiserum had no effect on the capacity of the prototype strains to infect HeLa cells. In sharp contrast, the treatment with MAb J10.4 resulted in a concentration-dependent inhibition of infection for all three strains. The minimum concentrations of MAb J10.4 required to reduce the infectivities of these strains by 50% were between 0.1 and 1.0 μg per ml (Fig. 1B). The infectivities of all three strains were reduced approximately 90% following the treatment of cells with 100 μg per ml MAb J10.4.

JAM-B and JAM-C do not serve as receptors for prototype strains of reovirus. JAM-A is the only JAM family member tested to date that functions as a receptor for T1L/53 (44). To determine whether other JAM family members in addition to JAM-A serve as reovirus receptors for other reovirus prototype strains, we transfected CHO cells, which are poorly permissive for reovirus infection (24), with a cDNA encoding hJAM-A, hJAM-B, or hJAM-C. Cells also were transfected with hCAR as a negative control. After confirmation of the cell surface expression of the receptor constructs (Fig. 2A), the transfected cells were tested for the capacity to support reovirus infection. Infected cells were quantified by indirect immunofluorescence using an antireovirus serum (Fig. 2B). Only CHO cells transfected with hJAM-A were capable of supporting an efficient infection of each of the three prototype reovirus strains, whereas cells transfected with hJAM-B and hJAM-C did not support the infection of any of these strains in excess of that supported by cells transfected with hCAR (Fig. 2C). Therefore, the JAM family member JAM-A, but not JAM-B or JAM-C, functions as a receptor for prototype strains of reovirus.

JAM-A serves as a receptor for field-isolate strains of reovirus. Strains of each of the three reovirus serotypes have been isolated from many mammalian hosts over a period in excess of 50 years (29, 31). A type 3 reovirus strain isolated from the cerebrospinal fluid of a child with meningitis is capable of using JAM-A as a receptor (64). However, the receptor-binding properties of other field-isolate strains have not been reported. To determine whether JAM-A is used as a receptor by other field-isolate strains of reovirus, we transfected CHO cells with hJAM-A, hJAM-B, or hJAM-C and tested them for the capacity to support reovirus infection. Ten strains, encompassing four type 1, two type 2, and four type 3 viruses (Table 1), were used in these experiments. In parallel with the findings for prototype reovirus strains, each of the field-isolate strains tested was capable of utilizing hJAM-A, but not hJAM-B or hJAM-C, as a receptor (Fig. 3).

Analysis of deduced σ1 amino acid sequences for JAM-A-binding reovirus strains. To gain insight into the σ1 residues that mediate interactions between reoviruses and JAM-A, we analyzed the amino acid sequences of the σ1 proteins of the 3 prototype and 10 field-isolate strains chosen for study. For these experiments, we determined the σ1-encoding S1 gene sequences of the strains T1C23/59, T1C50/60, T1Neth/84, T1Neth/85, T2Neth/73, and T2Neth/84 and compared these sequences to those reported previously (Table 1). RT-PCR primers complementary to the nontranslated regions of the type 1 and type 2 S1 genes were designed to facilitate the amplification of entire S1 genes from infected L-cell lysates.

To define the evolutionary relationships of the S1 gene sequences determined for this study with those of the other reovirus strains sequenced to date, we constructed phylogenetic trees by using variation in the σ1-encoding S1 gene nucleotide sequences and the maximum parsimony method as applied in the program PAUP (Fig. 4). The most noteworthy feature of the S1 phylogenetic tree is that the strains clustered into distinct lineages based on their serotypes. A phylogenetic tree generated by using the same data set and the neighbor-joining algorithm of the phylogenetic analysis program MacVector (MacVector 2001, version 7.1.1) had a topology identical to that of the tree generated by PAUP (data not shown). Therefore, our phylogenetic analysis indicates that the S1 genes of reovirus strains cluster tightly into three lineages defined by serotype. Concordantly, changes in the deduced amino acid sequences of the σ1 protein within a given serotype are confined to a small number of residues. Since each of the strains investigated for this study was capable of using JAM-A as a receptor, the locations of these changes provide clues about areas that can vary in surface structure without impeding the capacity to engage this molecule. Thus, these changes define areas that are unlikely to interact with JAM-A.

Sequence variability within type 3 σ1 protein. Structural information is available for the T3D/55 σ1 protein (16). We therefore carried out a structure-based comparison of the deduced amino acid sequences of the σ1 proteins of type 3 field-isolate strains with that of the prototype T3D/55 to define regions of conserved and variable sequences within a serotype (Fig. 5). Substantial variability is seen between residues 240 and 250, a region that lies just N-terminal to the first β-spiral repeat in the crystallized fragment and is disordered in the crystal structure. The σ1 fragment was obtained by trypsin

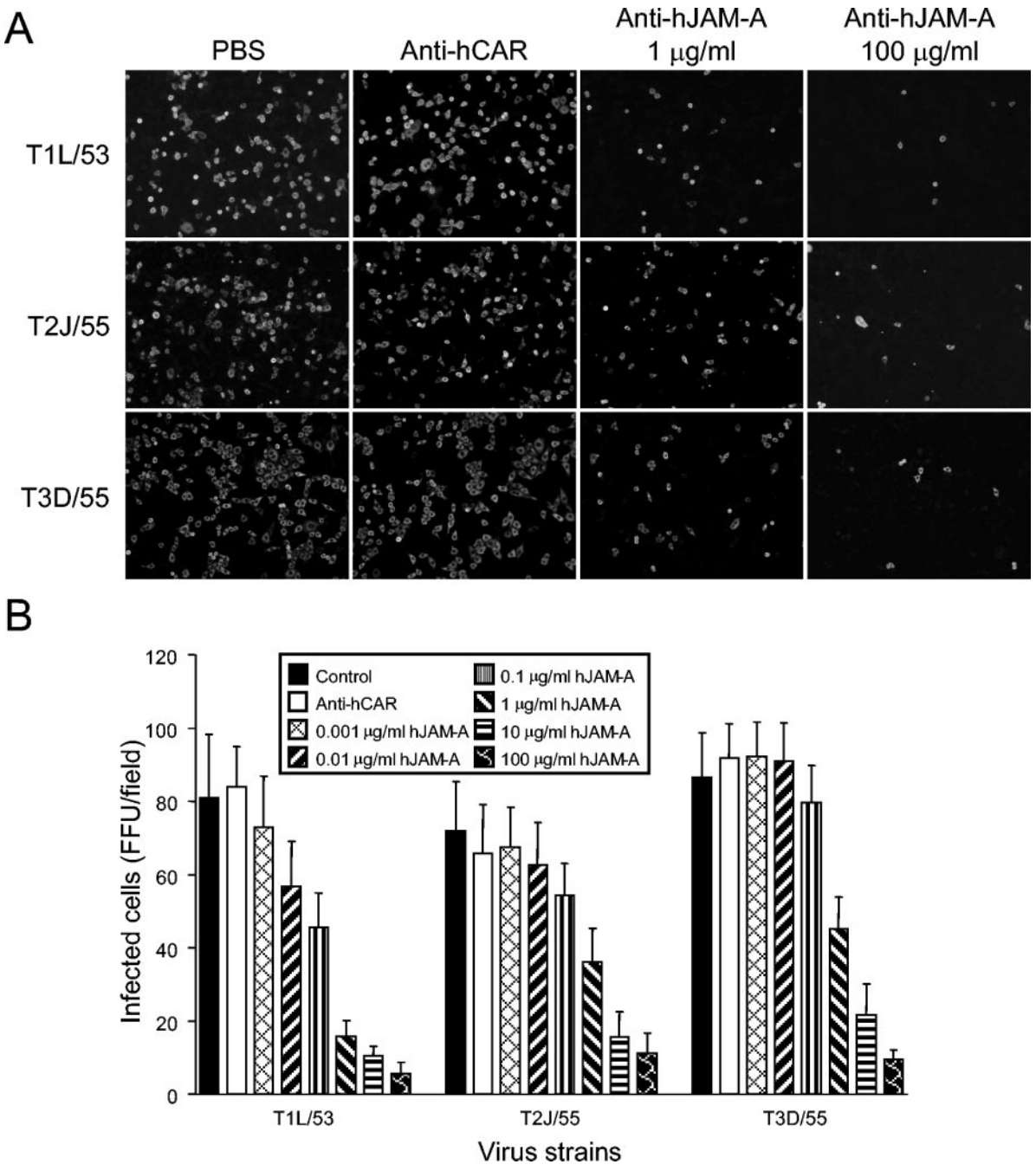

FIG. 1. JAM-A blockade reduces infection of prototype reovirus strains. HeLa cells at equivalent degrees of confluence were pretreated with PBS, an hCAR-specific antiserum as a control, or the hJAM-A-specific MAb J10.4 prior to adsorption with T1L/53, T2J/55, or T3D/55 at an MOI of 0.1 FFU per cell. After incubation for 20 h, the cells were fixed and permeabilized with methanol. Newly synthesized viral proteins were detected by the incubation of cells with a polyclonal rabbit antireovirus serum followed by incubation with an anti-rabbit immunoglobulin–Alexa-546 serum for the visualization of infected cells by indirect immunofluorescence. (A) Representative fields of view. (B) Reovirus-infected cells were quantified by counting fluorescent cells in a minimum of three random fields of view per well for three wells at a magnification of ×20. The results are presented as the mean FFU per field. Error bars indicate standard deviations.

cleavage of a longer construct after residue Arg245 (16). The fact that trypsin cleaves σ1 at only this position suggests that Arg245 lies in an exposed loop that likely possesses some flexibility. Exposed areas in the second and third β-spiral repeats of the crystallized fragment also contain several substitutions. Because these areas are variable, they are unlikely to contribute significantly to JAM-A binding.

Most of the remaining substitutions are located at the top of the σ1 trimer, forming a highly variable "plateau" that is also unlikely to bind to JAM-A. Some of the observed variations on

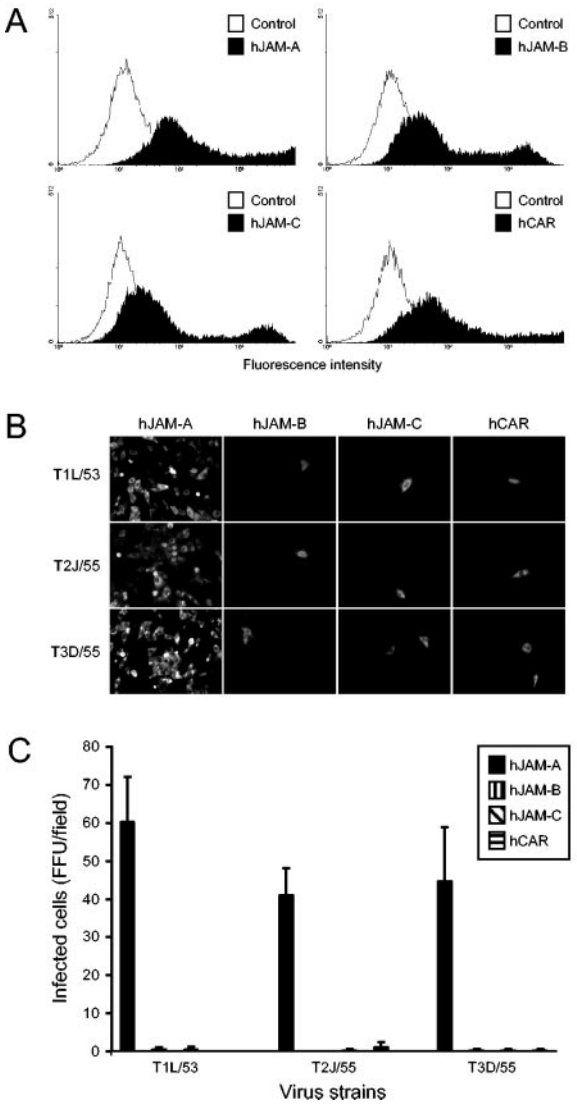

FIG. 2. CHO cells transfected with hJAM-A support growth of prototype reovirus strains. (A) CHO cells were transiently transfected with a plasmid encoding hCAR, hJAM-A, hJAM-B, or hJAM-C. Following incubation for 24 h to permit receptor expression, cells were incubated with receptor-specific MAbs, and the cell surface expression of receptor constructs was assessed by flow cytometry. (B) Transfected CHO cells at equivalent degrees of confluence were adsorbed with T1L/53, T2J/55, or T3D/55 at an MOI of 0.1 FFU per cell. Reovirus proteins were detected by indirect immunofluorescence at 20 h postinfection. Representative fields of view are shown. Magnification, ×20. (C) Reovirus-infected cells were quantified by counting fluorescent cells in five random fields of view per well for three wells. The results are presented as the mean FFU per field. Error bars indicate standard deviations.

the plateau are anticipated to alter the structure of the molecule. For example, the replacement of Ser435 with Met in T3D9/61 and T3D18/61 is likely to cause significant structural changes, as Ser435 is partially buried in the T3D/55 structure (16). Because they are exposed at the protein surface, the polymorphisms seen on the plateau may allow viral escape from antibody recognition. In contrast, the lower portion of the head domain is highly invariant, suggesting that the base of the σ1 head is primarily responsible for interactions with JAM-A.

Sequence variability within σ1 proteins of the three reovirus serotypes. An alignment of the deduced σ1 amino acid sequences for all of the strains chosen for study showed that only 36 of the 210 residues in the crystallized fragment of T3D/55 σ1 (16) are conserved (Fig. 6). There is substantially more variability among the serotypes than that within each serotype. Mapping of the conserved residues onto the crystal structure of T3D/55 σ1 showed that many of these residues are buried, especially those located at the base of the σ1 head-trimer interface (Fig. 6). A large fraction of the remaining conserved residues cluster in a single, solvent-exposed region at the lower edge of the β-barrel. Again, the regions that are most variable within type 3 σ1 (the β-spiral region and the "top" of the trimer) are also most variable among the different serotypes. In contrast, an extended, contiguous area of conserved residues is located at the base of the head domain, and additional, smaller areas of conservation are found along the side of this domain. Because these regions are conserved in the JAM-A-binding strains investigated here, they mark potential contact points for this receptor.

The large conserved area at the base of the head domain is formed primarily by a stretch of residues (Asn369 to Glu384 in T3D/55 σ1) within a 3_{10} helix and a long loop between β-strands D and E (16) (Fig. 6). This region also includes Trp421 at the end of β-strand F. The conserved region is fairly hydrophobic, with the side chains of Val371, Leu379, and Trp421 accounting for a large portion of the surface area predicted to be involved in JAM-A binding. A second, smaller cluster of conserved residues (Leu331, Trp333, Ile360, and His438 in T3D/55 σ1) lies above this putative JAM-A-binding surface, near the top of the trimer (Fig. 6). While most of the side chains of these residues are buried, the structural features of this cluster may contribute to receptor engagement. The remaining surface area of the σ1 trimer, especially near the top of the head and the head-to-head contacts, is almost entirely devoid of conserved residues.

A neutralization-resistant variant of reovirus T3D/55 uses JAM-A as a receptor. Variants of T3D/55 selected for their resistance to neutralization by the use of MAb 9BG5 (55) have a mutation at Asp340 or Glu419 in the σ1 head (7) (Fig. 5B). These variants have alterations in central nervous system (CNS) tropism following infections of newborn mice (54). The single mutation in variant K of σ1, Glu419 to Lys (7), segregates genetically with the altered growth and tropism of this virus in the murine CNS (32). To determine whether a neutralization-resistant variant of T3D/55 retained the capacity to use JAM-A as a receptor, we treated HeLa cells with PBS, an hCAR-specific antiserum as a negative control, or the hJAM-A-specific MAb J10.4 prior to infection with variant K. Infected cells were quantified by indirect immunofluorescence using an antireovirus serum (Fig. 7). The treatment of cells with increasing concentrations of the JAM-A-specific MAb J10.4 resulted in a dose-dependent inhibition of viral infection, while the CAR-specific antiserum had no effect on viral infectivity. At the maximal concentration of MAb J10.4 used (100 μg per ml), infectivity was nearly abolished, demonstrating that variant K is capable of using JAM-A as a receptor (Fig. 7).

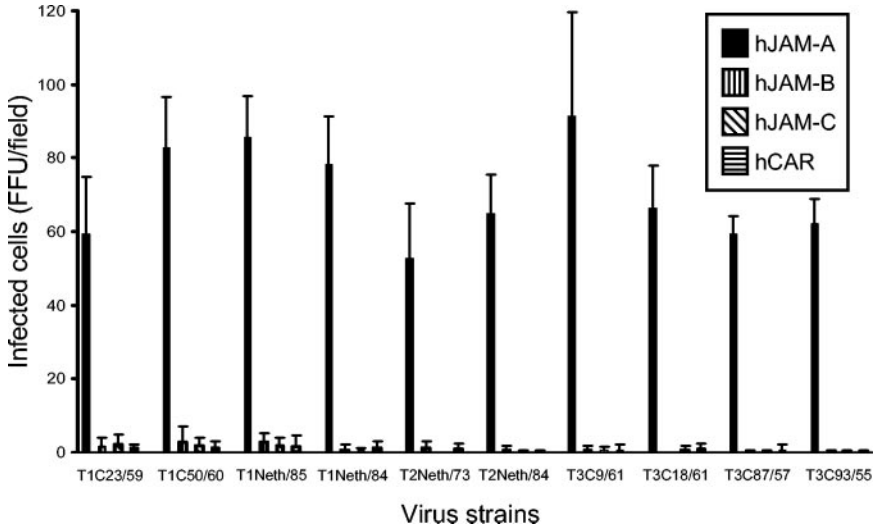

FIG. 3. Expression of JAM-A confers infectivity on field-isolate reovirus strains. CHO cells were transiently transfected with a plasmid encoding hCAR, hJAM-A, hJAM-B, or hJAM-C. Following incubation for 24 h to permit receptor expression, the cells were adsorbed with the indicated field-isolate strains at an MOI of 1 FFU per cell. Reovirus proteins were detected by indirect immunofluorescence at 20 h postinfection and quantified by counting of the fluorescent cells in three random fields of view per well for three wells. The results are presented as the mean FFU per field. Error bars indicate standard deviations.

Thus, the mechanism of the altered pathogenicity of variant K appears to be independent of JAM-A utilization.

DISCUSSION

An examination of receptor usage by diverse virus families, including arenaviruses (11, 53), adenoviruses (9, 27, 51, 72), and measles virus (20, 35, 61), has led to the discovery that receptor usage by some viruses varies based on the viral clade, serotype, or adaptation to passaging in cell culture. We undertook this study to determine whether JAM-A is used as a receptor by both prototype and field-isolate strains of reoviruses. The results demonstrate that each of the prototype and field-isolate reovirus strains tested, regardless of their serotype, species, or geographical region of isolation, is capable of utilizing JAM-A as a receptor.

Prior to this work, sequence information for the S1 gene segments of type 1 and type 2 reovirus strains was limited to the prototype strains T1L/53 and T2J/55. In this study, we determined the S1 sequences of four type 1 and two type 2 field-isolate strains. A phylogenetic analysis of the deduced σ1-encoding S1 gene sequences revealed that these reovirus field-isolate strains are associated with discrete lineages defined by serotype. Given that all reovirus strains tested to date

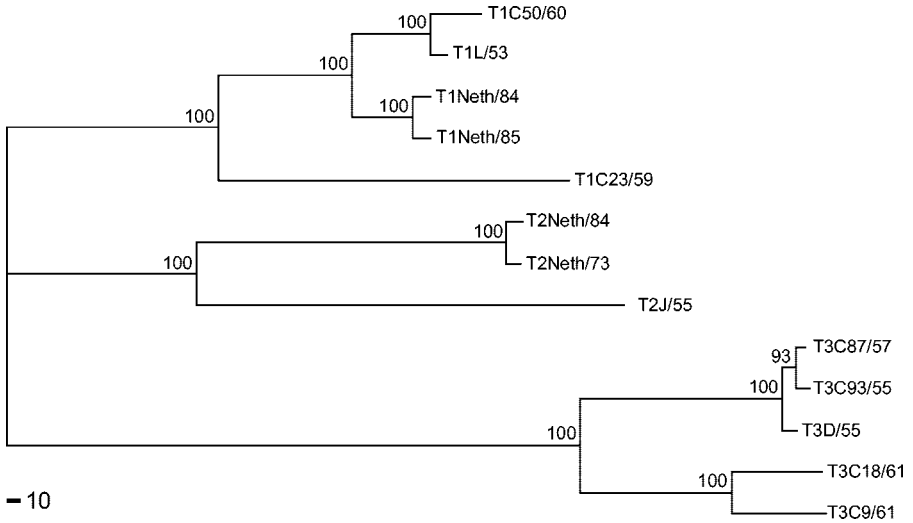

FIG. 4. Phylogenetic relationships among S1 gene nucleotide sequences of 13 reovirus strains. A phylogenetic tree for the σ1-encoding S1 gene sequences of the strains shown in Table 1 was constructed by using the maximum parsimony method as applied in the program PAUP. The tree is rooted at its midpoint. Bootstrap values of >50% (indicated as a percentage of 1,000 repetitions) for major branches are shown at the nodes. Bar, distance resulting from 10 nucleotide changes.

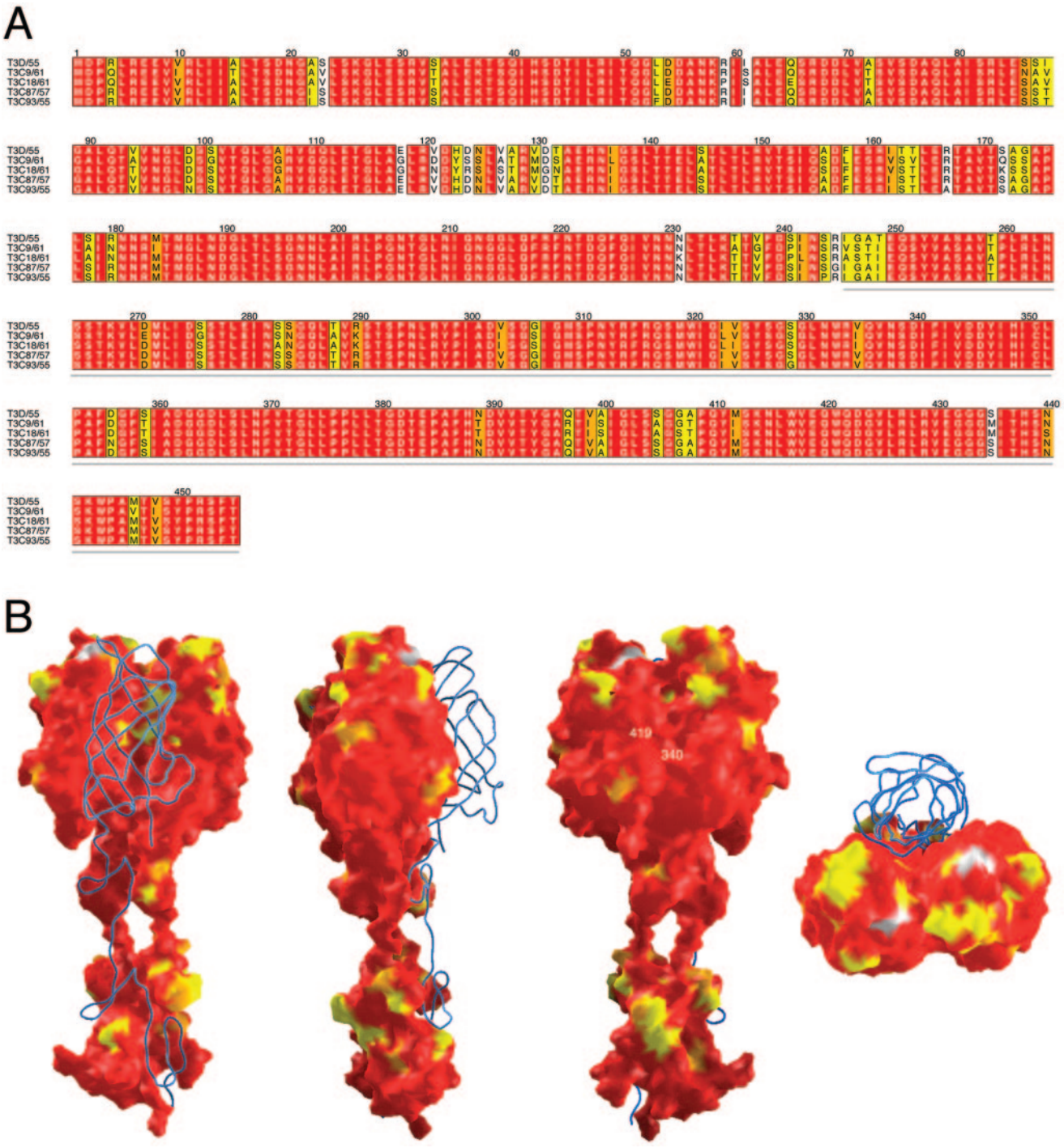

FIG. 5. Sequence conservation and structural variability within the type 3 σ1 protein. (A) Alignment of deduced amino acid sequences of the σ1 proteins of prototype strain T3D/55 and four type 3 field-isolate strains. The alignment was generated by using the program ALSCRIPT (5), with default conservation parameters applied according to the following color scheme: red, identical residues; orange, conserved residues at 80% conservation; yellow, conserved residues at 60% conservation; white, nonconserved residues. The 80% conservation threshold identifies closely related amino acids (e.g., Ile and Leu), whereas the 60% threshold identifies more distantly related amino acids (e.g., Ser and Ala, both of which have small side chains). The amino acid positions in the alignment are numbered above the sequences. The gray line indicates residues present in the crystallized fragment of T3D/55 σ1 (16). (B) Structure of the σ1 trimer, with residues colored according to the same color code as that used for panel A. Four different views are shown. For each of the views, two σ1 monomers are shown in surface representation, and the other is depicted as a blue ribbon tracing corresponding to the α-carbon backbone. The first three views each differ by 90° along a vertical axis; the fourth view shows the molecule in the third view after rotation by 90° along a horizontal axis. The positions of residues 340 and 419 are marked in the third panel from the left.

A

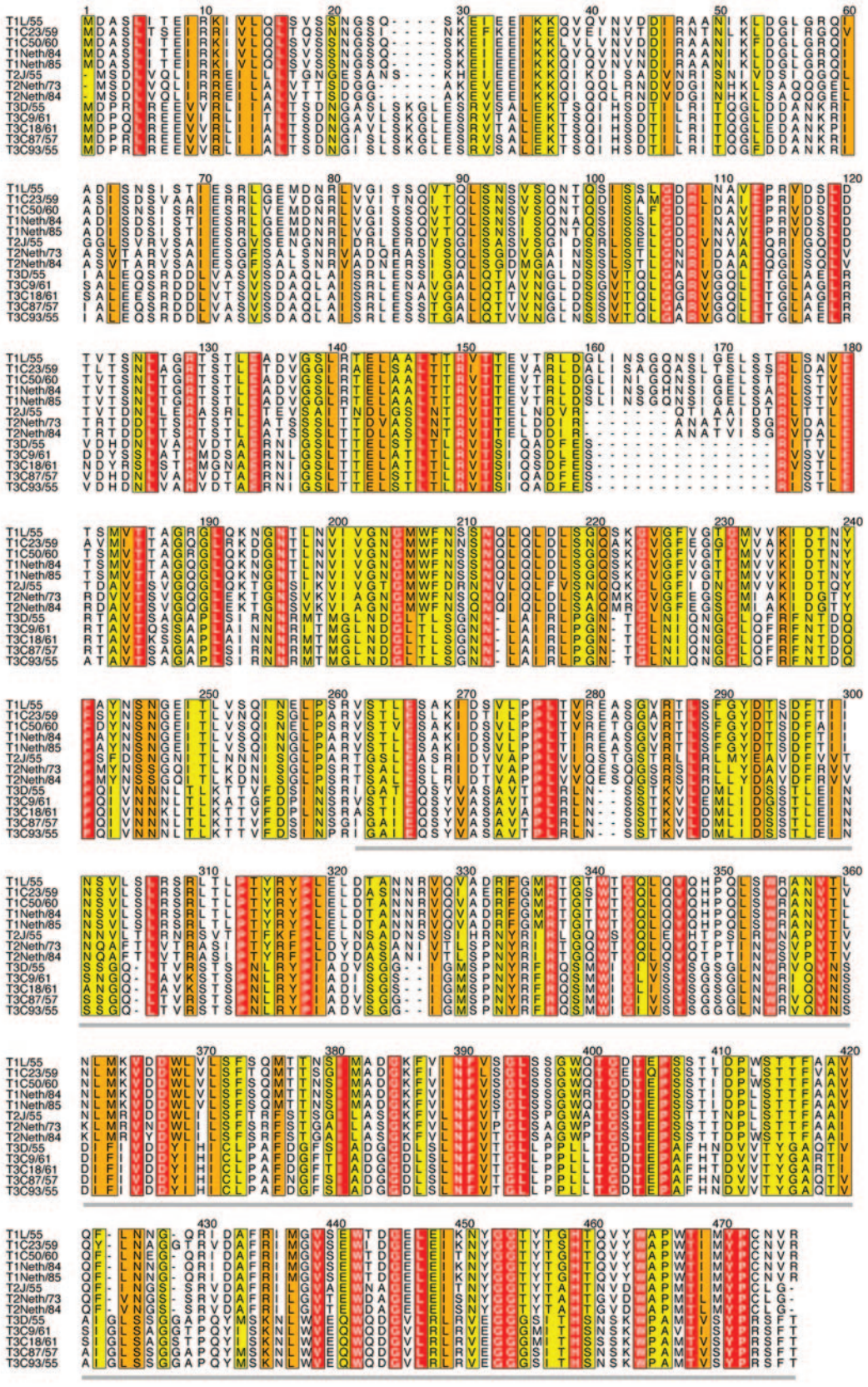

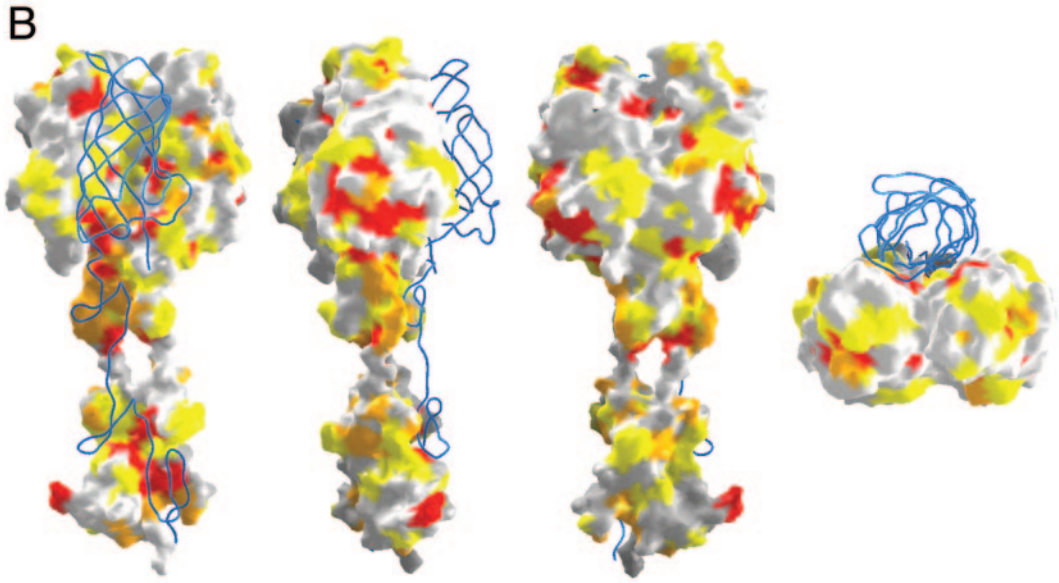

FIG. 6. Sequence conservation and structural variability within the σ1 proteins of the three reovirus serotypes. (A) Alignment of deduced amino acid sequences of the σ1 proteins of 3 prototype and 10 field-isolate reovirus strains. The alignment was generated by using ALSCRIPT and the scheme described in the legend to Fig. 5. Gaps in the aligned sequences are indicated by dots. (B) Mapping of residues onto the σ1 structure, using the same color code as that depicted in Fig. 5. The four views correspond to those in Fig. 5B.

are capable of using JAM-A as a receptor, it seems plausible that σ1 interacts with JAM-A through residues that are conserved among the serotypes, including the newly characterized type 1 and type 2 field-isolate strains. The observation that JAM-A is used as a receptor by all reovirus strains tested was unexpected since the σ1 protein is highly divergent among the three serotypes. For example, a sequence analysis of the prototype strains revealed that the σ1 head domains of T1L/53 and T2J/55 share 50% identical residues, while those of T1L/53 and T3D/55 share only 27% of their residues.

Substantial evidence has accumulated to suggest that the σ1 head domain binds to cellular receptors. Truncated forms of σ1 containing only the head domain are capable of specific cell interactions (22, 23). Concordantly, proteolysis of T3D/55 virions leads to the release of a C-terminal receptor-binding fragment of σ1 (residues 246 to 455) (13) and a resultant loss in infectivity (39). This fragment of σ1 is capable of binding to JAM-A on a biosensor surface with an affinity in the nanomolar range (3). Preliminary findings from our laboratory indicate that an even smaller fragment of T3D/55 σ1, corresponding to the head domain and a single β-spiral repeat, is capable of binding to JAM-A (K. M. Guglielmi, P. Schelling, T. Stehle, and T. S. Dermody, unpublished observations). Thus, the σ1 head promotes interactions with JAM-A that are distinct from the interactions with sialic acid mediated by the σ1 tail.

While most of the residues conserved among the σ1 proteins of the strains tested are scattered throughout the molecule, an examination of the σ1 surface revealed a single extended patch of conserved residues at the lower edge of the σ1 head. We think that this region may form part of a JAM-A-binding surface. This conserved region is formed mostly by residues in the vicinity of a long loop connecting β-strands D and E of the eight-stranded β-barrel that forms the σ1 head. Although it is easily accessible to ligands, this site is somewhat recessed into

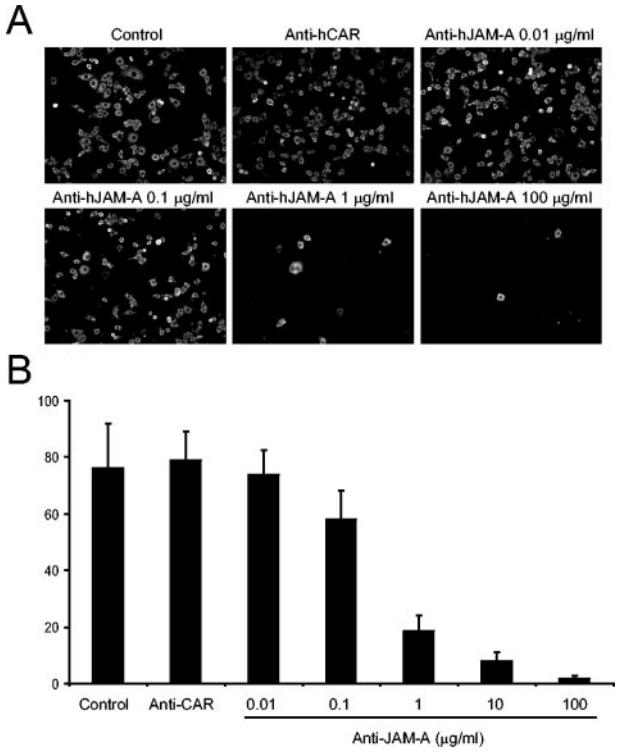

FIG. 7. JAM-A is used as a receptor for a neutralization-resistant variant of reovirus T3D/55. HeLa cells at equivalent degrees of confluence were pretreated with PBS, an hCAR-specific antiserum, or the hJAM-A-specific MAb J10.4 prior to adsorption with variant K at an MOI of 1 FFU per cell. Reovirus proteins were detected by indirect immunofluorescence at 20 h postinfection. (A) Representative fields of view. (B) Reovirus-infected cells were quantified by counting fluorescent cells in three random fields of view per well for three wells. The results are presented as the mean FFU per field. Error bars indicate standard deviations.

the protein surface and is surrounded by protruding, nonconserved residues on all three edges of the trimer. Only residues from a single monomer contribute to the putative JAM-A-binding region and its borders, and the regions are not involved in σ1 intersubunit contacts. Thus, the location of conserved residues within the trimer suggests that each σ1 monomer can independently bind to a JAM-A molecule.

Although it may serve as the primary contact point for the receptor, the putative JAM-A-binding site in σ1 is relatively small, measuring about 15 Å long and 10 Å wide. Most other interactions between viral ligands and proteinaceous receptors cover somewhat larger areas. It is therefore likely that additional regions of σ1 contribute to interactions with JAM-A. We noted that the putative JAM-A-binding site lies at the lower edge of a large, concave surface formed by β-strands B, A, D, and G of σ1. Residues on this surface, which almost entirely covers one side of the β-barrel, would easily be accessible to a receptor and do not participate in intersubunit contacts. The top of the σ1 head is formed by three prominent protrusions, with one coming from each β-barrel. These protrusions are entirely devoid of conserved residues among the serotypes and also exhibit significant sequence drift within type 3 σ1 proteins. It is therefore highly unlikely that the top of the σ1 head participates in receptor binding, again implicating regions on the side of each β-barrel as the most likely areas of contact with JAM-A.

Neutralization-resistant variants of the reovirus T3D/55 selected by using the σ1-specific MAb 9BG5 contain mutations in the σ1 head that segregate genetically with alterations in neural tropism (7, 32, 54, 55). Since reovirus tropism in the murine CNS is determined at least in part by σ1-receptor interactions (19, 60), it is possible that the antibody-selected mutations in the σ1 head alter receptor binding. However, we found that variant K, which has a Glu-to-Lys mutation at amino acid 419, uses JAM-A as a receptor. This observation suggests that the mutation in σ1 of variant K alters the interactions of this strain with cell surface receptors other than JAM-A or influences a postattachment step in reovirus replication. It is noteworthy that amino acid 419 is adjacent to the σ1 head trimer interface in the vicinity of amino acid 340 (16) (Fig. 5), which is also targeted for mutation in neutralization-resistant variants of T3D/55 (7). It is possible that mutations at these sites alter σ1 subunit interactions required for viral assembly or disassembly.

Reovirus serotypes exhibit striking differences in tropism and pathogenesis in the murine CNS. Type 1 reoviruses spread to the CNS hematogenously and infect ependymal cells (65, 70), resulting in subacute hydrocephalus (69). In contrast, type 3 reoviruses spread to the CNS by neural routes and infect neurons (38, 65, 70), causing lethal encephalitis (59, 69). An analysis of reassortant viruses containing gene segments derived from T1L/53 and T3D/55 demonstrated that the pathway of viral spread in the host (65) and tropism for neural tissues (19, 70) segregate with the σ1-encoding S1 gene. These findings suggest that σ1 determines the CNS cell types that serve as targets for reovirus infection, presumably by its capacity to bind to receptors expressed by specific CNS cells. Since all strains of reovirus tested are capable of utilizing JAM-A as a receptor, the engagement of JAM-A alone does not explain the differences in tropism and virulence displayed by the different reovirus serotypes in the murine CNS. It is possible that JAM-A serves as a serotype-independent reovirus receptor at some sites within the host and that other receptors, perhaps carbohydrate in nature, confer serotype-dependent tropism. In support of a role for cell surface carbohydrates in reovirus disease, the capacity to bind sialic acid enhances the spread of type 3 reoviruses within the host and targets the virus to bile duct epithelial cells, leading to obstructive jaundice (4). It is also possible that serotype-dependent differences in pathogenesis are influenced by one or more postbinding events.

The role of JAM-A utilization in reovirus infections in vivo is not known. JAM-A is expressed on many cell types, including intestinal epithelium, bile duct epithelium, lung epithelium, leukocytes, and CNS endothelial cells (36), which serve as sites of reovirus infection in mice (68). It will be interesting to determine whether JAM-A functions as a reovirus receptor at these sites in infected animals. Mice with a targeted disruption of the JAM-A gene are viable and fertile (12). These mice exhibit an accelerated migration of dendritic cells to lymph nodes, which is associated with enhanced contact hypersensitivity (12). No other developmental or immune abnormalities have been noted. Studies of reovirus infections using JAM-A-deficient animals should clarify the function of JAM-A in reovirus pathogenesis and disease.

ACKNOWLEDGMENTS

We thank members of our laboratory for many useful discussions and Annie Antar, Jim Chappell, and Kristen Guglielmi for reviews of the manuscript. We are grateful to Jeff Bergelson for providing the hCAR-specific serum, Chuck Parkos for providing the hJAM-A-specific MAb J10.4, and the Nashville Veterans Affairs Hospital Flow Cytometry Facility for assistance and data analysis. We are grateful to Kevin Coombs, Max Nibert, and Ken Tyler for kindly contributing stocks of reovirus field-isolate strains.

This research was supported by Public Health Service awards T32 CA09385 (J.A.C. and J.C.F.), R01 AI38296 (T.S.D.), and R01 GM67853 (T.S. and T.S.D.) and by the Elizabeth B. Lamb Center for Pediatric Research. Additional support was provided by Public Health Service awards CA68485 to the Vanderbilt Cancer Center and DK20593 to the Vanderbilt Diabetes Research and Training Center.

REFERENCES

1. **Banerjea, A. C., K. A. Brechling, C. A. Ray, H. Erikson, D. J. Pickup, and W. K. Joklik.** 1988. High-level synthesis of biologically active reovirus protein sigma 1 in a mammalian expression vector system. Virology **167:**601–612.
2. **Barton, E. S., J. L. Connolly, J. C. Forrest, J. D. Chappell, and T. S. Dermody.** 2001. Utilization of sialic acid as a coreceptor enhances reovirus attachment by multistep adhesion strengthening. J. Biol. Chem. **276:**2200–2211.
3. **Barton, E. S., J. C. Forrest, J. L. Connolly, J. D. Chappell, Y. Liu, F. Schnell, A. Nusrat, C. A. Parkos, and T. S. Dermody.** 2001. Junction adhesion molecule is a receptor for reovirus. Cell **104:**441–451.
4. **Barton, E. S., B. E. Youree, D. H. Ebert, J. C. Forrest, J. L. Connolly, T. Valyi-Nagy, K. Washington, J. D. Wetzel, and T. S. Dermody.** 2003. Utilization of sialic acid as a coreceptor is required for reovirus-induced biliary disease. J. Clin. Investig. **111:**1823–1833.
5. **Barton, G. J.** 1993. ALSCRIPT: a tool to format multiple sequence alignments. Protein Eng. **6:**37–40.
6. **Bassel-Duby, R., A. Jayasuriya, D. Chatterjee, N. Sonenberg, J. V. Maizel, Jr., and B. N. Fields.** 1985. Sequence of reovirus haemagglutinin predicts a coiled-coil structure. Nature **315:**421–423.
7. **Bassel-Duby, R., D. R. Spriggs, K. L. Tyler, and B. N. Fields.** 1986. Identification of attenuating mutations on the reovirus type 3 S1 double-stranded RNA segment with a rapid sequencing technique. J. Virol. **60:**64–67.
8. **Bazzoni, G., O. M. Martinez-Estrada, F. Mueller, P. Nelboeck, G. Schmid, T. Bartfai, E. Dejana, and M. Brockhaus.** 2000. Homophilic interaction of junctional adhesion molecule. J. Biol. Chem. **275:**30970–30976.
9. **Bergelson, J. M., J. A. Cunningham, G. Droguett, E. A. Kurt-Jones, A. Krithivas, J. S. Hong, M. S. Horwitz, R. L. Crowell, and R. W. Finberg.** 1997.

Isolation of a common receptor for coxsackie B viruses and adenoviruses 2 and 5. Science **275:**1320–1323.
10. **Bewley, M. C., K. Springer, Y. B. Zhang, P. Freimuth, and J. M. Flanagan.** 1999. Structural analysis of the mechanism of adenovirus binding to its human cellular receptor, CAR. Science **286:**1579–1583.
11. **Cao, W., M. D. Henry, P. Borrow, H. Yamada, J. H. Elder, E. V. Ravkov, S. T. Nichol, R. W. Compans, K. P. Campbell, and M. B. Oldstone.** 1998. Identification of alpha-dystroglycan as a receptor for lymphocytic choriomeningitis virus and Lassa fever virus. Science **282:**2079–2081.
12. **Cera, M. R., A. Del Prete, A. Vecchi, M. Corada, I. Martin-Padura, T. Motoike, P. Tonetti, G. Bazzoni, W. Vermi, F. Gentili, S. Bernasconi, T. N. Sato, A. Mantovani, and E. Dejana.** 2004. Increased DC trafficking to lymph nodes and contact hypersensitivity in junctional adhesion molecule-A-deficient mice. J. Clin. Investig. **114:**729–738.
13. **Chappell, J. D., E. S. Barton, T. H. Smith, G. S. Baer, D. T. Duong, M. L. Nibert, and T. S. Dermody.** 1998. Cleavage susceptibility of reovirus attachment protein σ1 during proteolytic disassembly of virions is determined by a sequence polymorphism in the σ1 neck. J. Virol. **72:**8205–8213.
14. **Chappell, J. D., J. L. Duong, B. W. Wright, and T. S. Dermody.** 2000. Identification of carbohydrate-binding domains in the attachment proteins of type 1 and type 3 reoviruses. J. Virol. **74:**8472–8479.
15. **Chappell, J. D., V. L. Gunn, J. D. Wetzel, G. S. Baer, and T. S. Dermody.** 1997. Mutations in type 3 reovirus that determine binding to sialic acid are contained in the fibrous tail domain of viral attachment protein σ1. J. Virol. **71:**1834–1841.
16. **Chappell, J. D., A. Prota, T. S. Dermody, and T. Stehle.** 2002. Crystal structure of reovirus attachment protein σ1 reveals evolutionary relationship to adenovirus fiber. EMBO J. **21:**1–11.
17. **Del Maschio, A., A. De Luigi, I. Martin-Padura, M. Brockhaus, T. Bartfai, P. Fruscella, L. Adorini, G. Martino, R. Furlan, M. G. De Simoni, and E. Dejana.** 1999. Leukocyte recruitment in the cerebrospinal fluid of mice with experimental meningitis is inhibited by an antibody to junctional adhesion molecule (JAM). J. Exp. Med. **190:**1351–1356.
18. **Dermody, T. S., M. L. Nibert, R. Bassel-Duby, and B. N. Fields.** 1990. A σ1 region important for hemagglutination by serotype 3 reovirus strains. J. Virol. **64:**5173–5176.
19. **Dichter, M. A., and H. L. Weiner.** 1984. Infection of neuronal cell cultures with reovirus mimics in vitro patterns of neurotropism. Ann. Neurol. **16:**603–610.
20. **Dörig, R. E., A. Marcil, A. Chopra, and C. D. Richardson.** 1993. The human CD46 molecule is a receptor for measles virus (Edmonston strain). Cell **75:**295–305.
21. **Duncan, R., D. Horne, L. W. Cashdollar, W. K. Joklik, and P. W. K. Lee.** 1990. Identification of conserved domains in the cell attachment proteins of the three serotypes of reovirus. Virology **174:**399–409.
22. **Duncan, R., D. Horne, J. E. Strong, G. Leone, R. T. Pon, M. C. Yeung, and P. W. K. Lee.** 1991. Conformational and functional analysis of the C-terminal globular head of the reovirus cell attachment protein. Virology **182:**810–819.
23. **Duncan, R., and P. W. K. Lee.** 1994. Localization of two protease-sensitive regions separating distinct domains in the reovirus cell-attachment protein sigma 1. Virology **203:**149–152.
24. **Forrest, J. C., J. A. Campbell, P. Schelling, T. Stehle, and T. S. Dermody.** 2003. Structure-function analysis of reovirus binding to junctional adhesion molecule 1. Implications for the mechanism of reovirus attachment. J. Biol. Chem. **278:**48434–48444.
25. **Fraser, R. D. B., D. B. Furlong, B. L. Trus, M. L. Nibert, B. N. Fields, and A. C. Steven.** 1990. Molecular structure of the cell-attachment protein of reovirus: correlation of computer-processed electron micrographs with sequence-based predictions. J. Virol. **64:**2990–3000.
26. **Furlong, D. B., M. L. Nibert, and B. N. Fields.** 1988. Sigma 1 protein of mammalian reoviruses extends from the surfaces of viral particles. J. Virol. **62:**246–256.
27. **Gaggar, A., D. M. Shayakhmetov, and A. Lieber.** 2003. CD46 is a cellular receptor for group B adenoviruses. Nat. Med. **9:**1408–1412.
28. **Gliki, G., K. Ebnet, M. Aurrand-Lions, B. A. Imhof, and R. H. Adams.** 2004. Spermatid differentiation requires the assembly of a cell polarity complex downstream of junctional adhesion molecule-C. Nature **431:**320–324.
29. **Goral, M. I., M. Mochow-Grundy, and T. S. Dermody.** 1996. Sequence diversity within the reovirus S3 gene: reoviruses evolve independently of host species, geographic locale, and date of isolation. Virology **216:**265–271.
30. **Helander, A., K. J. Silvey, N. J. Mantis, A. B. Hutchings, K. Chandran, W. T. Lucas, M. L. Nibert, and M. R. Neutra.** 2003. The viral sigma1 protein and glycoconjugates containing alpha2-3-linked sialic acid are involved in type 1 reovirus adherence to M cell apical surfaces. J. Virol. **77:**7964–7977.
31. **Hrdy, D. B., L. Rosen, and B. N. Fields.** 1979. Polymorphism of the migration of double-stranded RNA segments of reovirus isolates from humans, cattle, and mice. J. Virol. **31:**104–111.
32. **Kaye, K. M., D. R. Spriggs, R. Bassel-Duby, B. N. Fields, and K. L. Tyler.** 1986. Genetic basis for altered pathogenesis of an immune-selected antigenic variant of reovirus type 3 Dearing. J. Virol. **59:**90–97.
33. **Kostrewa, D., M. Brockhaus, A. D'Arcy, G. E. Dale, P. Nelboeck, G. Schmid, F. Mueller, G. Bazzoni, E. Dejana, T. Bartfai, F. K. Winkler, and M. Hennig.** 2001. X-ray structure of junctional adhesion molecule: structural basis for homophilic adhesion via a novel dimerization motif. EMBO J. **20:**4391–4398.
34. **Liu, Y., A. Nusrat, F. J. Schnell, T. A. Reaves, S. Walsh, M. Ponchet, and C. A. Parkos.** 2000. Human junction adhesion molecule regulates tight junction resealing in epithelia. J. Cell Sci. **113:**2363–2374.
35. **Manchester, M., D. S. Eto, A. Valsamakis, P. B. Liton, R. Fernandez-Munoz, P. A. Rota, W. J. Bellini, D. N. Forthal, and M. B. A. Oldstone.** 2000. Clinical isolates of measles virus use CD46 as a cellular receptor. J. Virol. **74:**3967–3974.
36. **Martin-Padura, I., S. Lostaglio, M. Schneemann, L. Williams, M. Romano, P. Fruscella, C. Panzeri, A. Stoppacciaro, L. Ruco, A. Villa, D. Simmons, and E. Dejana.** 1998. Junctional adhesion molecule, a novel member of the immunoglobulin superfamily that distributes at intercellular junctions and modulates monocyte transmigration. J. Cell Biol. **142:**117–127.
37. **Mercier, G. T., J. A. Campbell, J. D. Chappell, T. Stehle, T. S. Dermody, and M. A. Barry.** 2004. A chimeric adenovirus vector encoding reovirus attachment protein σ1 targets cells expressing junctional adhesion molecule 1. Proc. Natl. Acad. Sci. USA **101:**6188–6193.
38. **Morrison, L. A., R. L. Sidman, and B. N. Fields.** 1991. Direct spread of reovirus from the intestinal lumen to the central nervous system through vagal autonomic nerve fibers. Proc. Natl. Acad. Sci. USA **88:**3852–3856.
39. **Nibert, M. L., J. D. Chappell, and T. S. Dermody.** 1995. Infectious subvirion particles of reovirus type 3 Dearing exhibit a loss in infectivity and contain a cleaved σ1 protein. J. Virol. **69:**5057–5067.
40. **Nibert, M. L., T. S. Dermody, and B. N. Fields.** 1990. Structure of the reovirus cell-attachment protein: a model for the domain organization of σ1. J. Virol. **64:**2976–2989.
41. **Nibert, M. L., and L. A. Schiff.** 2001. Reoviruses and their replication, p. 1679–1728. *In* D. M. Knipe, P. M. Howley, D. E. Griffin, R. A. Lamb, M. A. Martin, B. Roizman, and S. E. Straus (ed.), Fields virology, 4th ed. Lippincott-Raven, Philadelphia, Pa.
42. **Nicholls, A., K. A. Sharp, and B. Honig.** 1991. Protein folding and association: insights from the interfacial and thermodynamic properties of hydrocarbons. Proteins **11:**281–296.
43. **Ozaki, H., K. Ishii, H. Horiuchi, H. Arai, T. Kawamoto, K. Okawa, A. Iwamatsu, and T. Kita.** 1999. Cutting edge: combined treatment of TNF-alpha and IFN-gamma causes redistribution of junctional adhesion molecule in human endothelial cells. J. Immunol. **163:**553–557.
44. **Prota, A. E., J. A. Campbell, P. Schelling, J. C. Forrest, T. R. Peters, M. J. Watson, M. Aurrand-Lions, B. Imhof, T. S. Dermody, and T. Stehle.** 2003. Crystal structure of human junctional adhesion molecule 1: implications for reovirus binding. Proc. Natl. Acad. Sci. USA **100:**5366–5371.
45. **Ramos-Alvarez, M., and A. B. Sabin.** 1954. Characteristics of poliomyelitis and other enteric viruses recovered in tissue culture from healthy American children. Proc. Soc. Exp. Biol. **87:**655–661.
46. **Ramos-Alvarez, M., and A. B. Sabin.** 1958. Enteropathogenic viruses and bacteria. Role in summer diarrheal diseases of infancy and early childhood. JAMA **167:**147–158.
47. **Rosen, L.** 1960. Serologic grouping of reovirus by hemagglutination-inhibition. Am. J. Hyg. **71:**242–249.
48. **Rosen, L., J. F. Hovis, F. M. Mastrota, J. A. Bell, and R. J. Huebner.** 1960. Observations on a newly recognized virus (Abney) of the reovirus family. Am. J. Hyg. **71:**258–265.
49. **Rubin, D. H., D. B. Weiner, C. Dworkin, M. I. Greene, G. G. Maul, and W. V. Williams.** 1992. Receptor utilization by reovirus type 3: distinct binding sites on thymoma and fibroblast cell lines result in differential compartmentalization of virions. Microb. Pathog. **12:**351–365.
50. **Sabin, A. B.** 1959. Reoviruses: a new group of respiratory and enteric viruses formerly classified as ECHO type 10 is described. Science **130:**1387–1389.
51. **Segerman, A., J. P. Atkinson, M. Marttila, V. Dennerquist, G. Wadell, and N. Arnberg.** 2003. Adenovirus type 11 uses CD46 as a cellular receptor. J. Virol. **77:**9183–9191.
52. **Smith, R. E., H. J. Zweerink, and W. K. Joklik.** 1969. Polypeptide components of virions, top component and cores of reovirus type 3. Virology **39:**791–810.
53. **Spiropoulou, C. F., S. Kunz, P. E. Rollin, K. P. Campbell, and M. B. Oldstone.** 2002. New World arenavirus clade C, but not clade A and B viruses, utilizes alpha-dystroglycan as its major receptor. J. Virol. **76:**5140–5146.
54. **Spriggs, D. R., R. T. Bronson, and B. N. Fields.** 1983. Hemagglutinin variants of reovirus type 3 have altered central nervous system tropism. Science **220:**505–507.
55. **Spriggs, D. R., and B. N. Fields.** 1982. Attenuated reovirus type 3 strains generated by selection of haemagglutinin antigenic variants. Nature **297:**68–70.
56. **Stehle, T., and T. S. Dermody.** 2003. Structural evidence for common functions and ancestry of the reovirus and adenovirus attachment proteins. Rev. Med. Virol. **13:**123–132.
57. **Stehle, T., and T. S. Dermody.** 2004. Structural similarities in the cellular receptors used by adenovirus and reovirus. Viral Immunol. **17:**129–143.
58. **Swofford, D. L.** 2002. PAUP—phylogenetic analysis using parsimony (and other methods), version 4.0b10. Sinauer Associates, Sunderland, Mass.

59. **Tardieu, M., M. L. Powers, and H. L. Weiner.** 1983. Age-dependent susceptibility to reovirus type 3 encephalitis: role of viral and host factors. Ann. Neurol. **13:**602–607.
60. **Tardieu, M., and H. L. Weiner.** 1982. Viral receptors on isolated murine and human ependymal cells. Science **215:**419–421.
61. **Tatsuo, H., N. Ono, K. Tanaka, and Y. Yanagi.** 2000. SLAM (CDw150) is a cellular receptor for measles virus. Nature **406:**893–897.
62. **Thompson, J. D., T. J. Gibson, F. Plewniak, F. Jeanmougin, and D. G. Higgins.** 1997. The CLUSTAL_X windows interface: flexible strategies for multiple sequence alignment aided by quality analysis tools. Nucleic Acids Res. **25:**4876–4882.
63. **Tyler, K. L.** 2001. Mammalian reoviruses, p. 1729–1745. *In* D. M. Knipe, P. M. Howley, D. E. Griffin, R. A. Lamb, M. A. Martin, B. Roizman, and S. E. Straus (ed.), Fields virology, 4th ed. Lippincott-Raven, Philadelphia, Pa.
64. **Tyler, K. L., E. S. Barton, M. L. Ibach, C. Robinson, T. Valyi-Nagy, J. A. Campbell, P. Clarke, S. M. O'Donnell, J. D. Wetzel, and T. S. Dermody.** 2004. Isolation and molecular characterization of a novel type 3 reovirus from a child with meningitis. J. Infect. Dis. **189:**1664–1675.
65. **Tyler, K. L., D. A. McPhee, and B. N. Fields.** 1986. Distinct pathways of viral spread in the host determined by reovirus S1 gene segment. Science **233:** 770–774.
66. **van Raaij, M. J., E. Chouin, H. van der Zandt, J. M. Bergelson, and S. Cusack.** 2000. Dimeric structure of the coxsackievirus and adenovirus receptor D1 domain at 1.7 A resolution. Structure Fold Des. **8:**1147–1155.
67. **Virgin, H. W., IV, R. Bassel-Duby, B. N. Fields, and K. L. Tyler.** 1988. Antibody protects against lethal infection with the neurally spreading reovirus type 3 (Dearing). J. Virol. **62:**4594–4604.
68. **Virgin, H. W., K. L. Tyler, and T. S. Dermody.** 1997. Reovirus, p. 669–699. *In* N. Nathanson (ed.), Viral pathogenesis. Lippincott-Raven, New York, N.Y.
69. **Weiner, H. L., D. Drayna, D. R. Averill, Jr., and B. N. Fields.** 1977. Molecular basis of reovirus virulence: role of the S1 gene. Proc. Natl. Acad. Sci. USA **74:**5744–5748.
70. **Weiner, H. L., M. L. Powers, and B. N. Fields.** 1980. Absolute linkage of virulence and central nervous system tropism of reoviruses to viral hemagglutinin. J. Infect. Dis. **141:**609–616.
71. **Wetzel, J. D., J. D. Chappell, A. B. Fogo, and T. S. Dermody.** 1997. Efficiency of viral entry determines the capacity of murine erythroleukemia cells to support persistent infections by mammalian reoviruses. J. Virol. **71:**299–306.
72. **Wu, E., S. A. Trauger, L. Pache, T. M. Mullen, D. J. von Seggern, G. Siuzdak, and G. R. Nemerow.** 2004. Membrane cofactor protein is a receptor for adenoviruses associated with epidemic keratoconjunctivitis. J. Virol. **78:**3897–3905.

B. A PLASMID-BASED REVERSE GENETICS SYSTEM FOR ANIMAL DOUBLE-STRANDED RNA VIRUSES

Prior to the publication of this report, an entirely plasmid-based reverse-genetics system did not exist for any dsRNA virus of the *Reoviridae* family. Development of this strategy enabled the selective introduction of desired mutations in each viral gene segment and recovery of the resultant mutant viruses. In addition to reporting the design of the reverse genetics system, experiments using mutant viruses were described in this paper. These viruses were tested in vitro and in vivo for various traits including outer-capsid protease susceptibility and pathogenesis in mice. My contribution to this manuscript included infection of mice with viruses containing mutations in the attachment protein σ1 that altered susceptibility of σ1 to intestinal proteases.

Cell Host & Microbe
Resource

A Plasmid-Based Reverse Genetics System for Animal Double-Stranded RNA Viruses

Takeshi Kobayashi,[1,2] Annukka A.R. Antar,[2,3,5] Karl W. Boehme,[1,2,5] Pranav Danthi,[1,2,5] Elizabeth A. Eby,[2,3,5] Kristen M. Guglielmi,[2,3,5] Geoffrey H. Holm,[1,2,5] Elizabeth M. Johnson,[2,3,5] Melissa S. Maginnis,[2,3,5] Sam Naik,[2,4,5] Wesley B. Skelton,[1,2,5] J. Denise Wetzel,[1,2,5] Gregory J. Wilson,[1,2,5] James D. Chappell,[1,2,4,*] and Terence S. Dermody[1,2,3,*]
[1] Department of Pediatrics
[2] Elizabeth B. Lamb Center for Pediatric Research
[3] Department of Microbiology and Immunology
[4] Department of Pathology
Vanderbilt University School of Medicine, Nashville, TN 37232, USA
[5] These authors contributed equally to this work.
*Correspondence: jim.chappell@vanderbilt.edu (J.D.C.), terry.dermody@vanderbilt.edu (T.S.D.)
DOI 10.1016/j.chom.2007.03.003

SUMMARY

Mammalian orthoreoviruses (reoviruses) are highly tractable experimental models for studies of double-stranded (ds) RNA virus replication and pathogenesis. Reoviruses infect respiratory and intestinal epithelium and disseminate systemically in newborn animals. Until now, a strategy to rescue infectious virus from cloned cDNA has not been available for any member of the *Reoviridae* family of dsRNA viruses. We report the generation of viable reovirus following plasmid transfection of murine L929 (L) cells using a strategy free of helper virus and independent of selection. We used the reovirus reverse genetics system to introduce mutations into viral capsid proteins σ1 and σ3 and to rescue a virus that expresses a green fluorescent protein (GFP) transgene, thus demonstrating the tractability of this technology. The plasmid-based reverse genetics approach described here can be exploited for studies of reovirus replication and pathogenesis and used to develop reovirus as a vaccine vector.

INTRODUCTION

Reoviruses are members of the *Reoviridae* family, which includes several genera that cause disease in humans and animals. Chief among these are the rotaviruses, which are the most common cause of viral gastroenteritis in human infants (Kapikian et al., 2001). Reoviruses infect the respiratory and gastrointestinal tracts of virtually all mammals, including humans (Tyler, 2001). However, disease associated with reovirus infection occurs primarily in the very young (Tyler et al., 2004). Reoviruses are highly virulent in newborn mice, the preferred experimental system for studies of reovirus pathogenesis, and produce injury to a variety of host tissues, including the central nervous system (CNS), heart, and liver (Tyler, 2001).

Reoviruses contain a genome of 10 dsRNA gene segments enclosed in two concentric protein shells, termed *outer capsid* and *core*. Reovirus infection is initiated by viral attachment to host cells via the filamentous attachment protein σ1 (Furlong et al., 1988). The σ1 protein engages cell-surface carbohydrate (Chappell et al., 1997, 2000) and junctional adhesion molecule-A (JAM-A) (Barton et al., 2001b; Campbell et al., 2005), an integral component of intercellular tight junctions (Martin-Padura et al., 1998). Following attachment to the cell surface, reovirus internalization is mediated by β1 integrins (Maginnis et al., 2006), most likely via clathrin-dependent endocytosis (Ehrlich et al., 2004). In the endocytic compartment, viral outer-capsid proteins σ3 and μ1/μ1C are cleaved by acid-dependent cysteine proteases (Baer and Dermody, 1997; Ebert et al., 2002), resulting in generation of infectious subvirion particles (ISVPs) (Borsa et al., 1981). During ISVP formation, σ3 is removed and a hydrophobic conformer of μ1/μ1C is exposed, facilitating endosomal membrane penetration and delivery of transcriptionally active reovirus core particles into the cytoplasm (Chandran et al., 2002; Odegard et al., 2004), where the remainder of the replication cycle occurs.

With the exception of dsRNA viruses, a plasmid-based reverse genetics system exists for all major groups of animal RNA viruses, including bornaviruses, bunyaviruses, coronaviruses, flaviviruses, orthomyxoviruses, paramyxoviruses, picornaviruses, and rhabdoviruses (Table S1 in the Supplemental Data available with this article online). Despite extensive efforts in several laboratories, generation of an animal dsRNA virus entirely from cloned cDNAs has not been achieved. This critical technological gap is perhaps the single most important limitation to studies of these viruses. Previous efforts on reovirus and rotavirus reverse genetics have resulted in entirely RNA-based (Roner et al., 1997) or partially plasmid-based (Komoto et al., 2006) systems that permit replacement of one or two viral genes. These approaches have been used to

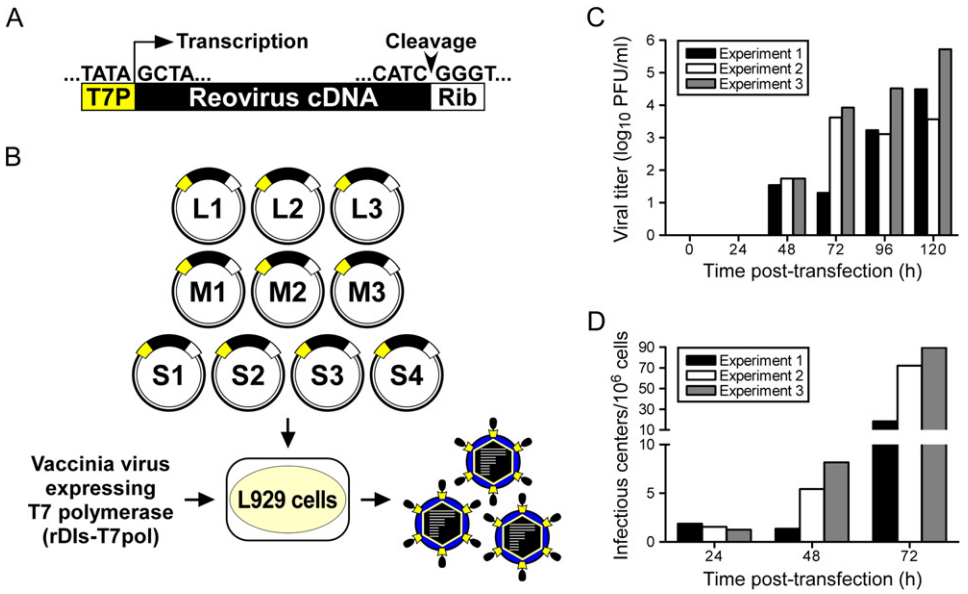

Figure 1. Experimental Strategy to Generate Reovirus from Cloned cDNA

(A) Prototype reovirus gene segment cDNA in plasmid. Cloned cDNAs representing each of the ten full-length reovirus RNA gene segments are flanked by the bacteriophage T7 RNA polymerase promoter (T7P) and the antigenomic hepatitis delta virus (HDV) ribozyme (Rib).

(B) Schematic of approach. The ten reovirus cDNA constructs are transfected into murine L cells expressing T7 RNA polymerase from recombinant vaccinia virus strain rDIs-T7pol, which is replication defective. Nascent transcripts correspond to viral mRNAs containing the native 5′ end. Self cleavage by the HDV ribozyme generates the native viral 3′ end. Following 5 days of incubation, transfected cells are lysed by freeze-thaw, and viable viruses rescued from cloned cDNAs are isolated by plaque assay using L cells.

(C) Kinetics of virus production following plasmid transfection of L cells. Cells were transfected with plasmid DNA according to the protocol in (B) and lysed at the intervals shown. Viral titers in cell lysates were determined by plaque assay.

(D) Infectious center assay following plasmid transfection of L cells. Cells were transfected with plasmid DNA, trypsinized at the intervals shown post-transfection, washed, counted, diluted, and applied directly to monolayers of untreated L cells. The number of the infectious centers was determined by plaque assay.

rescue temperature-sensitive reovirus strains (Roner et al., 1997), define packaging signals in reovirus RNAs (Roner and Steele, 2007), and isolate rotaviruses containing engineered changes in the viral attachment protein (Komoto et al., 2006). However, neither the reovirus nor rotavirus reverse genetics systems in their current configurations permit selective introduction and recovery of desired mutations in each viral gene segment.

We report the development of an entirely plasmid-based reverse genetics system for mammalian reovirus in which viable viruses are generated from cloned cDNAs. Neither helper virus nor coexpression of viral replication proteins is required for recovery of wild-type (WT) virus or engineered viral mutants. Point mutations introduced into viral capsid proteins σ1 and σ3 were used to define sequences that govern susceptibility to cleavage by intestinal proteases. We also recovered a recombinant virus that expresses green fluorescent protein (GFP) by replacement of the σ3 open reading frame (ORF) with GFP. The establishment of plasmid-based reverse genetics for reovirus will allow heretofore technically unapproachable problems in dsRNA virus biology to be studied, provide a platform for development of analogous marker rescue systems for other segmented dsRNA viruses, and foster exploration of reovirus as a vaccine vector to elicit protective immunity against a variety of mucosal pathogens.

RESULTS

Generation of Viable Reovirus from Cloned cDNA

To generate recombinant reovirus from cloned cDNAs, plasmids encoding each of the ten viral gene segments were engineered to facilitate transcription of full-length viral mRNAs under control of the bacteriophage T7 RNA polymerase promoter, which directs transcription initiation preferentially from a juxtaposed guanosine residue (Milligan et al., 1987). As all reovirus (+)-sense RNAs are terminated with a 5′ guanosine (Furuichi et al., 1975a, 1975b), plasmid-generated transcripts are anticipated to possess native 5′ ends (Roner and Joklik, 2001) (Figure 1A). Murine L929 fibroblast (L) cells, which efficiently support reovirus replication (Barton et al., 2001a), were infected with the attenuated, T7 RNA polymerase-expressing vaccinia virus strain rDIs-T7pol 1 hr prior to transfection with the ten reovirus cDNA plasmids (Figure 1B). Nascent transcripts were synthesized with the hepatitis delta virus (HDV) ribozyme fused to the 3′ terminus, which is expected to generate a native 3′ end upon autocatalytic removal (Roner and Joklik, 2001) (Figure 1A). Thus, this

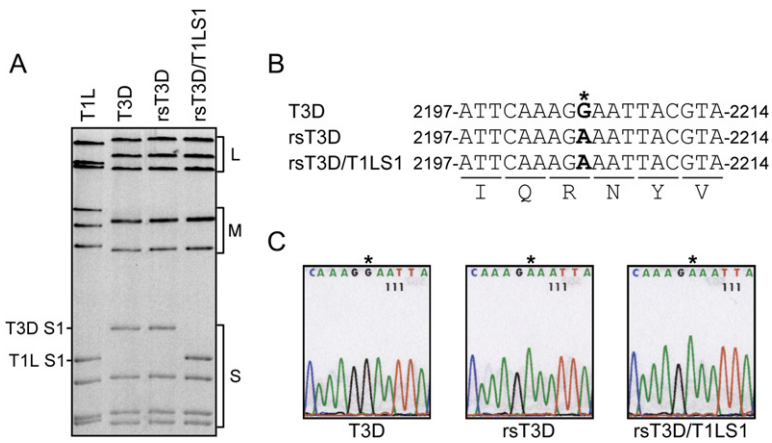

Figure 2. Rescue of rsT3D and rsT3D/T1LS1

(A) Electropherotypes of T1L, T3D, rsT3D, and rsT3D/T1LS1. Viral dsRNA was extracted from purified virions and electrophoresed in an SDS-polyacrylamide gel, followed by ethidium bromide staining to visualize viral gene segments. Size classes of gene segments (L, M, S) are indicated.

(B) Recombinant viruses contain a novel mutation in the L1 gene. The single nucleotide difference in L1 unique to rsT3D and rsT3D/T1LS1 is shown in the alignment as an asterisk. The G→A substitution at position 2205 is a signature change engineered into the cloned T3D L1 cDNA used for marker rescue.

(C) Sequence analysis of L1 gene RT-PCR products from rescued reoviruses. A fragment of the L1 gene was amplified by one-step RT-PCR performed using viral dsRNA extracted from purified virions of T3D, rsT3D, and rsT3D/T1LS1. Products were subjected to direct sequence analysis and compared to the L1 sequence of T3D. Shown are sequence chromatograms demonstrating G→A substitution at position 2205 of the rsT3D and rsT3D/T1LS1 L1 genes.

expression strategy should yield ten unique reovirus mRNA species competent to complete all steps in the viral RNA life cycle. Accordingly, rescued viruses were recovered from cell-culture supernatants by plaque assay on L cell monolayers (Figure 1C).

To ensure that viruses isolated following plasmid transfection represented single clones, and to preclude contamination of reovirus stocks by rDIs-T7pol, all viruses were isolated by plaque purification using L cell monolayers. rDIs-T7pol is replication defective and produces no detectable growth in mammalian cells (Ishii et al., 2002). Concordantly, no viral plaques arose on L cell monolayers when the cotransfections were prepared with nine of the ten reovirus marker-rescue plasmids (data not shown). Furthermore, vaccinia virus proteins were not detected by immunoblot analysis of second-passage stocks of plaque-purified reoviruses (data not shown).

Infectious center assays were performed to assess the efficiency of reovirus infection in plasmid-transfected L cells. At 24–48 hr posttransfection, times corresponding to the primary round of infection, eight or fewer infectious centers per 10^6 cells were detected (Figure 1D). The number of infectious centers increased substantially between 48 and 72 hr posttransfection to 18 to 90 per 10^6 cells, suggesting that a secondary round of infection had ensued by the 72 hr time point. Viral titer in transfection lysates was below the limit of detection (~10 PFU/ml) at 24 hr but was detectable at 48 hr and increased logarithmically at time points thereafter (Figure 1C). The ratio of viral PFU in transfection lysates to infectious centers was ~10 to 100 at 48 and 72 hr. These results indicate that initiation of productive reovirus replication from transfected plasmids is inefficient, with approximately 1 cell per 10^5 to 10^6 cells giving rise to, on average, 10 to 100 viable virus particles that establish infection of the culture. In our experiments, yields of WT virus 5 days after plasmid transfection are regularly in the range of 10^4–10^6 PFU/ml (Figure 1C).

Separation of reovirus genomic dsRNA using SDS-PAGE produces unique electrophoretic patterns that can be used to discriminate different viral strains (Barton et al., 2001a). To confirm that viruses isolated using the plasmid-based rescue procedure contained the expected combination of gene segments, genomic dsRNA isolated from recombinant strain (rs) T3D and rsT3D/T1LS1 was resolved in SDS-polyacrylamide gels and visualized by ethidium bromide staining (Figure 2A). The electropherotype of rsT3D was indistinguishable from that of strain T3D, the origin of the cloned cDNA sequences used to generate rsT3D. Likewise, rsT3D/T1LS1 displayed an electropherotype consistent with nine cloned gene segments derived from T3D and a single cloned gene segment, S1, derived from strain T1L. To exclude the possibility of contamination, a silent point mutation, G to A at nucleotide 2205, was introduced into the L1 gene of all virus strains generated from cloned cDNAs (Figure 2B). This change has not been observed in any reported T3D L1 sequence (Wiener and Joklik, 1989) and serves as a signature for viruses derived through plasmid-based rescue. As anticipated, sequence analysis of rsT3D and rsT3D/T1LS1 revealed the expected G to A substitution (Figure 2C), confirming the plasmid origins of these isolates.

Characterization of Reoviruses Generated by Plasmid Transfection

Reoviruses replicate and assemble within cytoplasmic inclusions in infected cells (Fields, 1971). Viral inclusions contain dsRNA (Silverstein and Schur, 1970), viral proteins (Fields, 1971), and both complete and incomplete viral particles (Fields, 1971). Reovirus strain T3D forms large globular inclusions that localize to the perinuclear space (Parker et al., 2002). To determine whether rsT3D forms viral inclusions in a manner similar to native T3D, cells were infected with T3D and rsT3D and processed 18 hr postinfection for image analysis by confocal microscopy (Figure 3A). Both T3D and rsT3D formed morphologically indistinguishable large globular inclusions that were

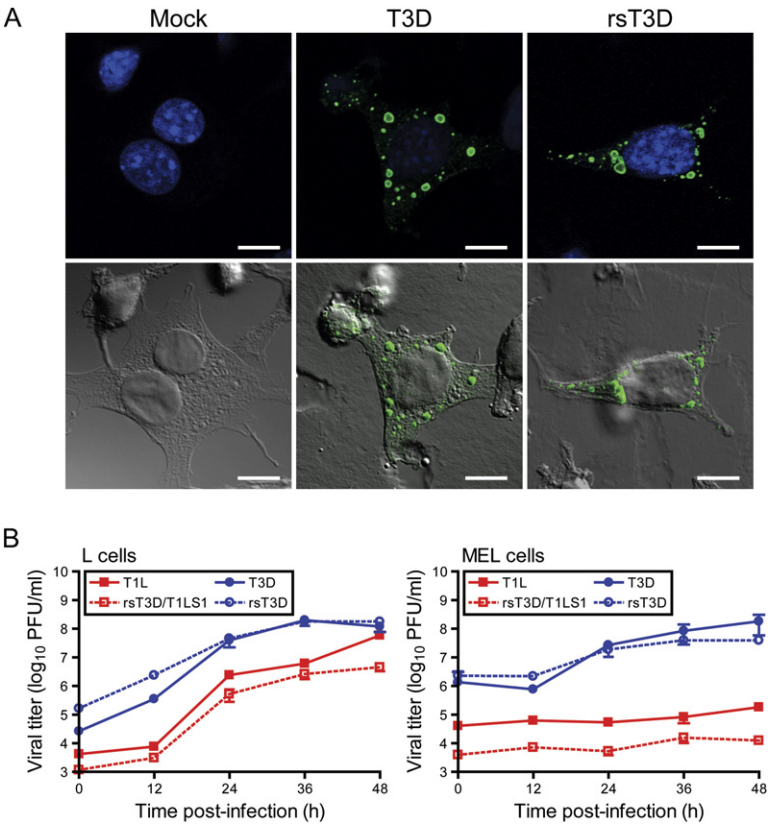

Figure 3. Infectivity of Native and Recombinant Reoviruses

(A) Immunofluorescence of cells infected with T3D and rsT3D. L cells were mock infected or infected with either T3D or rsT3D, stained at 18 hr postinfection with anti-μNS antiserum to visualize reovirus inclusions (green) and TO-PRO3 to visualize nuclei (blue), and imaged by confocal laser scanning microscopy. Representative digital fluorescence (top panel) and DIC images (bottom panel) for mock-, T3D-, and rsT3D-infected cells are shown. Scale bar, 10 μM.

(B) One-step growth curve for T1L, T3D, rsT3D, and rsT3D/T1LS1 in L cells (left) and MEL cells (right). Cells were infected with virus, incubated for the intervals shown, and lysed by freeze-thaw. Viral titers in cell lysates were determined by plaque assay. The results are presented as the mean viral titers for triplicate experiments. Error bars indicate SD.

localized to the perinuclear compartment. We conclude that recombinant rsT3D recapitulates a hallmark of native T3D infection in cultured cells.

To confirm that the recombinant viruses exhibit replication kinetics similar to the native strains, T1L, T3D, rsT3D, and rsT3D/T1LS1 were tested for infection of L cells and MEL cells (Figure 3B). L cells support replication of all reovirus strains tested in our laboratory. In contrast, MEL cells support replication of only sialic acid-binding reovirus strains (Rubin et al., 1992; Chappell et al., 1997). T1L, rsT3D/T1LS1, T3D, and rsT3D produced ~1000-fold yields of viral progeny in L cells. However, only sialic acid-binding strains T3D and rsT3D were capable of efficiently infecting MEL cells, producing yields in each case of ~100-fold, whereas strains T1L and rsT3D/T1LS1 produced minimal yields of viral progeny in these cells (<10-fold). Together, these data indicate that recombinant reoviruses display replication characteristics indistinguishable from native strains.

Susceptibility of Attachment Protein σ1 to Proteolytic Cleavage Attenuates Reovirus Intestinal Infection and Systemic Spread

The σ1 protein exhibits strain-specific differences in susceptibility to cleavage following in vitro treatment with intestinal proteases to generate ISVPs (Nibert et al., 1995; Chappell et al., 1998). This difference in cleavage susceptibility segregates with a single amino acid polymorphism in the tail domain of σ1 (Figure 4A). Strains with a threonine at residue 249 in σ1 are susceptible to cleavage by trypsin after Arg245, whereas those with an isoleucine at residue 249 are resistant to cleavage (Chappell et al., 1998). The importance of sequence polymorphism at residue 249 has been confirmed in studies using expressed protein (Chappell et al., 1998) and recoated core particles (Chandran et al., 2001) but not with intact virions.

To determine whether the single Thr-Ile polymorphism at residue 249 in σ1 protein is sufficient to alter σ1 cleavage susceptibility during treatment of virions with intestinal proteases to generate ISVPs, we used plasmid-based rescue to generate rsT3D-σ1T249I, which differs from rsT3D by the presence of an isoleucine in σ1 at residue 249 (Table S2). Purified virions of rsT3D and rsT3D-σ1T249I were treated with trypsin and analyzed by SDS-PAGE. As expected, a digestion pattern consistent with formation of ISVPs (loss of σ3 protein and generation of the δ fragment of μ1C protein) was observed for both viruses (Figure 4B). However, the stability of rsT3D and rsT3D-σ1T249I σ1 proteins differed. The band corresponding to rsT3D σ1 diminished in intensity immediately after trypsin addition until it was eventually undetectable (Figure 4B). However, the rsT3D-σ1T249I σ1 band was intact even after 60 min of digestion. Thus, the T249I polymorphism is an independent determinant of σ1 cleavage susceptibility.

Proteolytic cleavage of σ1 at a site adjacent to Thr249 releases the JAM-A-binding σ1 head domain, leading to

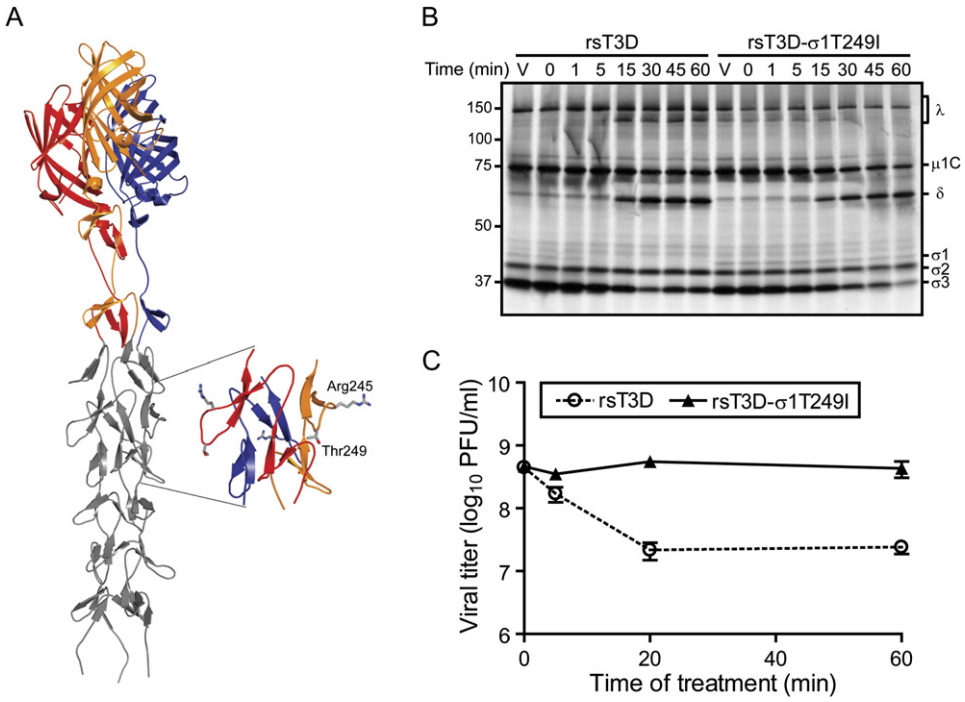

Figure 4. The σ1 Protein of rsT3D-σ1T249I Is Resistant to Trypsin

(A) Model of σ1 generated by adding five β spiral repeats to the N terminus of the crystallized fragment of σ1 (Chappell et al., 2002). The three monomers in the crystallized fragment are shown in red, yellow, and blue; the model is shown in gray. The inset shows an enlarged view of the β spiral region in σ1 that influences susceptibility of the molecule to cleavage by intestinal proteases (Chappell et al., 1998). Side chains of Arg245 and Thr249 are depicted in ball-and-stick representation.

(B) Electrophoretic analysis of viral structural proteins of rsT3D and rsT3D-σ1T249I during treatment with trypsin to generate ISVPs. Purified ^{35}S-methionine-labeled virions were treated with trypsin for the indicated intervals and loaded into wells of a 4%–20% polyacrylamide gradient gel. After electrophoresis, the gel was prepared for fluorography and exposed to film. Samples of untreated virions appear in the lanes labeled "V." Viral proteins are labeled. Positions of molecular weight standards (in kDa) are indicated. The experiments shown are representative of two performed for each virus.

(C) Infectivity of rsT3D and rsT3D-σ1T249I during treatment with trypsin to generate ISVPs. Purified virions were treated with trypsin at 37°C for the intervals shown. Titers of virus in the treatment mixtures were determined by plaque assay. The results are presented as the mean viral titers for triplicate experiments. Error bars indicate SD.

diminished viral infectivity (Nibert et al., 1995). To test whether rsT3D and rsT3D-σ1T249I differ in infectivity after protease treatment to generate ISVPs, purified virions of each strain were exposed to trypsin for various intervals, and titers of infectious virus in the treatment mixtures were determined by plaque assay (Figure 4C). As observed with WT T3D in previous experiments (Nibert et al., 1995), rsT3D lost infectious titer rapidly after protease treatment. In contrast, titers of rsT3D-σ1T249I remained relatively stable throughout the assay time course. Loss of infectivity of rsT3D correlated with kinetics of σ1 cleavage (compare Figures 4B and 4C), indicating that changes in viral infectivity after trypsin treatment are governed by the cleavage state of σ1. Furthermore, both phenotypes are linked to a single σ1 polymorphism at amino acid 249.

Reovirus strains T1L and T3D differ in the capacity to infect the murine intestine after peroral (PO) inoculation (Bodkin et al., 1989), a property that segregates with the viral S1 (encoding σ1 and σ1s) and L2 (encoding λ2) genes (Bodkin and Fields, 1989). Exposure of T3D to an intestinal wash results in σ1 cleavage (Chappell et al., 1998), raising the possibility that failure of T3D to infect the intestine is in part attributable to σ1 cleavage susceptibility. To test whether susceptibility of σ1 to proteolytic cleavage is associated with diminished T3D growth in animals, we assessed the capacity of rsT3D and rsT3D-σ1T249I to infect the intestine and disseminate systemically following PO inoculation (Figure 5A). Newborn mice were inoculated perorally with each strain, and viral titers in the intestine and brain were determined at 4, 8, and 12 days after inoculation. At all time points tested, titers of rsT3D-σ1T249I in the intestine were greater than those produced by rsT3D. Furthermore, rsT3D-σ1T249I produced greater titers in the brain at days 8 and 12 than did rsT3D. However, when inoculated by the intracranial (IC) route, rsT3D and rsT3D-σ1T249I produced equivalent titers (Figure 5B), although rsT3D reached peak titers at earlier time points than did rsT3D-σ1T249I. These findings indicate that a Thr-Ile polymorphism at amino acid 249 in T3D σ1 controls viral growth in the murine intestine and systemic spread to the CNS.

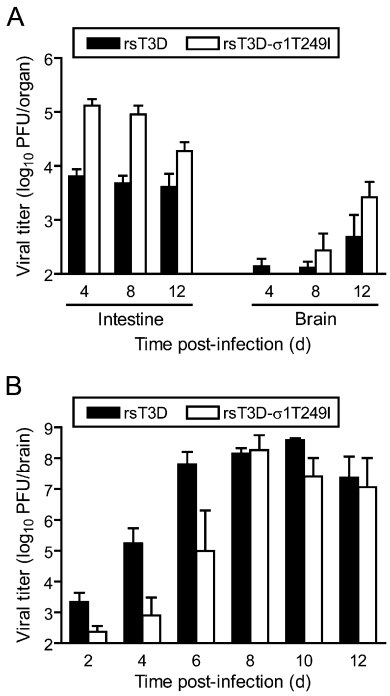

Figure 5. rsT3D-σ1T249I Infects the Murine Intestine and Disseminates to the CNS

Titers of rsT3D and rsT3D-σ1T249I after either PO (A) or IC (B) inoculation. Mice were inoculated with virus and euthanized at the indicated times postinoculation. Viral titers in organ homogenates were determined by plaque assay. The limit of detection was 100 PFU/ml of organ homogenate. Each data point represents the average viral titer from 3 to 12 mice. Error bars indicate SD.

Regulation of Reovirus Disassembly by a Single Polymorphism in Outer-Capsid Protein σ3

Previous studies identified a tyrosine-to-histidine substitution at amino acid 354 in T3D σ3 as a key regulator of the kinetics of virion-to-ISVP conversion in vitro (Wetzel et al., 1997) and viral resistance to growth inhibition by the cysteine protease inhibitor E64 (Baer and Dermody, 1997; Ebert et al., 2001). Tyr354 is located in the virion-distal lobe of σ3 adjacent to sites in the protein that are cleaved during formation of ISVPs (Ebert et al., 2002) (Figure 6A). The importance of this residue in viral replication has been deduced by analysis of reassortant viruses containing WT and mutant σ3 proteins (Wetzel et al., 1997; Ebert et al., 2001; Clark et al., 2006) and analysis of ISVPs recoated with WT and mutant forms of σ3 (Wilson et al., 2002; Clark et al., 2006).

To determine whether the Y354H mutation in σ3 is sufficient to confer enhanced virion-to-ISVP conversion and resistance to E64, we generated rsT3D-σ3Y354H (Table S2) and compared this virus to rsT3D for kinetics of σ3 proteolysis following protease treatment in vitro. Virions of each strain were treated with chymotrypsin for various intervals and processed for analysis of viral structural proteins by SDS-PAGE (Figure 6B). Treatment of rsT3D and rsT3D-σ3Y354H virions with chymotrypsin resulted in degradation of σ3 and cleavage of μ1C to form δ, indicative of ISVP formation. Proteolysis of rsT3D-σ3Y354H σ3 during chymotrypsin treatment occurred with substantially faster kinetics than that of rsT3D σ3. This result indicates that amino acid 354 in σ3 protein is an independent determinant of virion susceptibility to proteolytic digestion and likely functions as an autonomous regulator of viral disassembly in cellular endosomes.

The role of σ3 mutation Y354H in virion disassembly in cyto was investigated by quantifying yields of rsT3D and rsT3D-σ3Y354H after 24 hr of growth in L cells treated with 0–200 μM E64 (Figure 6C). Both strains produced yields of ~1000 fold following growth in untreated cells. However, yields of rsT3D-σ3Y354H were ~100-fold greater than those of rsT3D following growth in cells treated with 200 μM E64 (the highest concentration tested). Therefore, a single mutation in σ3, Y354H, regulates resistance of reovirus to an inhibitor of cysteine proteases within cellular endosomes.

Transduction of GFP by a Recombinant Reovirus

To determine whether reoviruses capable of expressing a foreign gene can be recovered following plasmid transfection, we introduced sequences encoding GFP into the σ3 ORF of the T3D S4 plasmid (Figure 7A). In this configuration, GFP is expressed as a fusion protein incorporating amino acids 1–39 of σ3 protein at the N terminus. Recombinant virus rsT3D/S4-GFP was recovered following plasmid transfection of L cells stably expressing WT σ3 protein, which is required for propagation of this strain (Figure S1). RT-PCR analysis using primers specific for T3D S4 and GFP confirmed incorporation of a recombinant S4-GFP gene segment into rsT3D/S4-GFP (Figure 7B). Infection of L cells with rsT3D/S4-GFP resulted in expression of GFP and viral inclusion-forming proteins μNS and σNS but not σ3 (Figures 7C and 7D). The capacity of rsT3D/S4-GFP to express GFP was not altered through four passages (data not shown). These results demonstrate that reovirus can be engineered to express foreign genes.

DISCUSSION

The absence of DNA intermediates in the life cycle of RNA viruses poses a technical challenge to genetic analysis of viral phenotypes. Prior to the development of reverse genetics, or "marker rescue," for RNA viruses of animals, in which plasmid-borne cDNAs of viral genomes initiate synthesis of replication-competent RNAs, classical Darwinian methods were used to select viral mutants that could be subjected to correlative genetic studies—so-called "forward genetics." However, reverse genetics technology permits testing of tightly focused, rational hypotheses about complex questions of virus structure, virus-cell interactions, and viral pathogenesis through direct engineering of the viral genome without a need to devise complicated selection strategies for isolation of viral mutants. Furthermore, reverse genetics of RNA viruses has supported rapid generation of vaccines against these and other infectious agents and propelled their use as gene

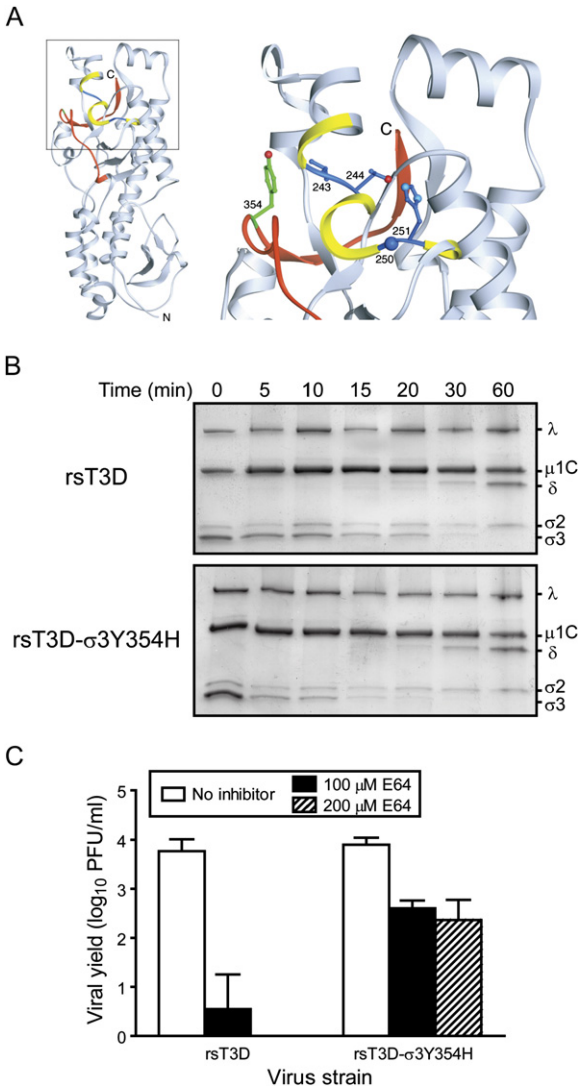

Figure 6. A Single Mutation in Outer-Capsid Protein σ3 Accelerates Proteolytic Disassembly of Reovirus

(A) Crystal structure of T3D σ3 (Olland et al., 2001), in which cathepsin L cleavage sites are depicted in blue between amino acids 243 and 244 and between 250 and 251 (Ebert et al., 2002). Surrounding residues, from amino acids 241 to 253, are shown in yellow. The C-terminal residues of σ3, from amino acids 340–365, are colored red. Tyr354, which is altered in several PI (Wetzel et al., 1997), D-EA (Ebert et al., 2001), and ACA-D viruses (Clark et al., 2006), is shown in green. The virion-distal end of σ3 is at the top of the figure, and the virion-proximal end and N terminus are at the bottom. The inset shows an enlarged view of the boxed region of σ3 using the same color scheme. Side chains of amino acids 243, 244, 250, 251, and 354 are depicted in ball-and-stick representation.

(B) Chymotrypsin treatment of rsT3D and rsT3D-σ3Y354H. Purified virions were treated with chymotrypsin for the indicated intervals and loaded into wells of 10% polyacrylamide gels. After electrophoresis, the gels were stained with Coomassie blue. Viral proteins are labeled. The experiments shown are representative of two performed for each virus.

(C) Growth of rsT3D and rsT3D-σ3Y354H in L cells treated with E64. L cells were preincubated in medium with or without E64 at the concentrations shown. The medium was removed, cells were adsorbed with virus for 1 hr, and fresh medium with or without E64 was added. After 24 hr incubation, viral titers in cell lysates were determined by plaque assay. The results are presented as the mean viral yields, calculated by dividing titer at 24 hr by titer at 0 hr for each concentration of E64, for triplicate experiments. Error bars indicate SD.

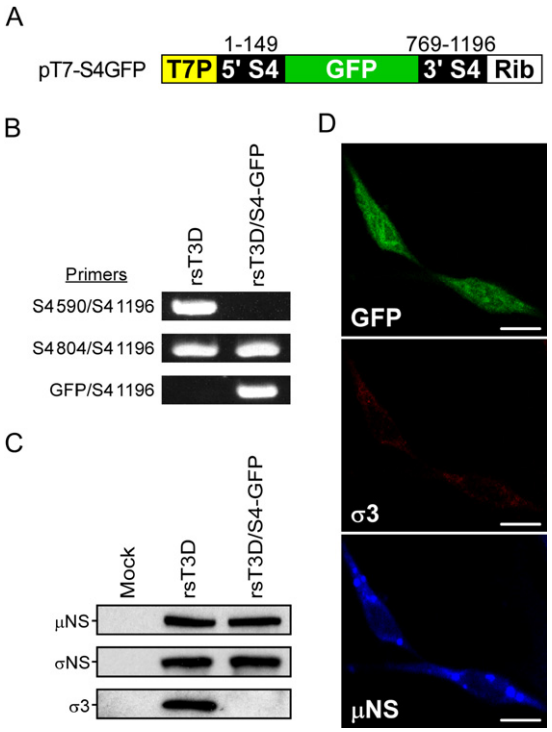

Figure 7. Expression of GFP by rsT3D/S4-GFP

(A) Schematic of pT7-S4GFP. The GFP ORF is flanked by S4 gene nucleotides 1–149 and 769–1196.

(B) RT-PCR analysis of rsT3D and rsT3D/S4-GFP. Viral dsRNA was extracted from purified virions and subjected to RT-PCR using primers specific for T3D S4 and GFP sequences. Numbers delineate the S4 RNA nucleotide position corresponding to the 5′ end of S4-specific primers.

(C) Viral protein expression in cells infected with rsT3D/S4-GFP. L cells were infected with rsT3D or rsT3D/S4-GFP at an MOI of 1 PFU per cell and incubated for 24 hr. Cell lysates were analyzed by immunoblotting using antibodies specific for μNS, σNS, and σ3 proteins.

(D) Image analysis of cells infected with rsT3D/S4-GFP. L cells were infected with rsT3D/S4-GFP, stained with antibodies specific for μNS (blue) and σ3 (red) proteins at 24 hr postinfection, and imaged by confocal laser scanning microscopy. Scale bar, 10 μM.

delivery vehicles (Blaney et al., 2006; Horimoto and Kawaoka, 2006; Riezebos-Brilman et al., 2006).

We developed a fully plasmid-based reverse genetics technology for mammalian reoviruses. This system permits selective introduction of desired mutations into cloned cDNAs encoding each of the ten viral gene segments, followed by isolation of mutant viruses from cells transfected with the plasmid constructs. Moreover, gene segment cDNAs can be manipulated to facilitate expression of a transgene. Importantly, recombinant viruses are generated without a requirement for helper virus and free of any selection. Thus, this new technology provides

a means to directly and precisely engineer the viral genome in the context of infectious virus.

We used the newly developed plasmid-based reovirus reverse genetics system to engineer mutations in the σ1 and σ3 proteins. These proteins form part of the viral outer capsid, which is responsible for numerous major events in reovirus interaction with the cell and host, including attachment, disassembly within endosomes, penetration of cell membranes, induction of apoptosis, growth in the intestine, pathways of spread, neurovirulence, and tropism within the CNS (for reviews, see Chandran and Nibert, 2003; O'Donnell et al., 2003; Guglielmi et al., 2006). Therefore, we initially applied reverse genetics technology to the study of outer-capsid proteins to better understand how these proteins mediate critical steps in reovirus replication and disease.

The infectivity of ISVPs of reovirus strain T1L in L cells is approximately 10-fold greater than that of T3D ISVPs (Nibert et al., 1995). This difference in infectivity is hypothesized to be a direct result of σ1 cleavage (Nibert et al., 1995; Chappell et al., 1998), presumably due to removal of the JAM-A-binding region of the molecule. Although the T249I substitution in expressed T3D σ1 renders it resistant to cleavage by trypsin (Chappell et al., 1998), until now it has not been possible to define the role of σ1 cleavage in T3D infectivity for lack of means to generate a mutant T3D virus with the T249I change. This virus has been generated using reverse genetics, and our findings indicate that cleavage susceptibility of viral attachment protein σ1 due to a single polymorphism at amino acid position 249 is the basis for reduced infectivity of T3D ISVPs relative to virions (Figure 4C) and contributes to diminished growth of T3D in the murine intestine following PO inoculation (Figure 5A).

Previous studies of T3D-derived reovirus strains with altered disassembly kinetics point to a critical role for sequences in the virion-distal, C-terminal lobe of σ3 in susceptibility to acid-dependent proteolysis. A C-terminal Y354H mutation in σ3 protein of strain T3D was selected during persistent infection of L cells (PI viruses) (Wetzel et al., 1997) and by serial passage of virus in L cells treated with either E64 (D-EA viruses) (Ebert et al., 2001) or ammonium chloride (ACA-D viruses) (Clark et al., 2006). Using reovirus reverse genetics, the Y354H substitution was introduced into a WT T3D genetic background, and the resultant virus, rsT3D-σ3Y354H, demonstrated accelerated kinetics of σ3 cleavage (Figure 6B) and diminished sensitivity to the growth-inhibitory effects of E64 (Figure 6C). Residue 354 is located in a position thought to be important for controlling access to protease-hypersensitive regions in σ3, residues 208–214 and 238–242, thereby influencing σ3 cleavage kinetics (Jané-Valbuena et al., 2002). Therefore, it appears that residue 354 in σ3 is a gatekeeper for the viral outer capsid, serving to regulate the balance between viral stability and an irreversible, proteolytically triggered disassembly cascade committing the virion particle to either replication or inactivation.

We exploited the reovirus reverse genetics system to develop a gene-delivery vehicle by replacing the σ3 ORF in the S4 plasmid with a GFP-encoding cDNA (Figure 7). The resultant virus, rsT3D/S4-GFP, expresses GFP through successive passages in cell culture. These results reveal the potential for exploitation of reovirus as a gene-transduction vector with application in the development of new mucosal vaccines, more effective oncolytic agents (Coffey et al., 1998), and high-level expression of foreign genes in animal cells. Ideal reovirus vectors will contain stable σ1 proteins and combine excellent extracellular stability with highly efficient intracellular disassembly. We find that each of these parameters can be independently adjusted through strategic alterations in outer-capsid proteins. Manipulation of inner-capsid proteins and the genomic RNA itself should allow construction of viruses able to circumvent other aspects of virus-cell and virus-host interactions that pose potential barriers to antigen and gene delivery by reovirus.

Our results indicate that productive viral infection is established in a small fraction of L cells, approximately 1 in 10^5–10^6 cells, transfected with plasmids encoding the ten reovirus gene segments (Figure 1D). Thus, the reovirus plasmid-based marker rescue system is suited to the isolation of viable viral clones by plaque assay, followed by expansion in cell culture to attain quantities of virus sufficient for phenotypic analyses. Manipulations that severely cripple viral replication or particle assembly are more challenging to study because these changes may prohibit virus isolation. However, recovery of a GFP-expressing virus, rsT3D/S4-GFP, demonstrates that marker rescue of lethal mutations is possible by transcomplementation (in this case with WT σ3 protein) (Figure 7 and Figure S1). This result also agrees with our previous finding that inhibition of reovirus replication by RNAi-mediated reduction of viral protein synthesis is reversible by transcomplementation with ectopically expressed WT protein (Kobayashi et al., 2006). Furthermore, transcomplementation allows precise definition through systematic mutational analysis of functional domains in reovirus proteins that are essential for viral replication (Kobayashi et al., 2006). It should be possible to apply this technique to the new marker rescue system for delineation of structure-function relationships in reovirus proteins and RNA.

Quantitative success of plasmid-initiated reovirus infection in this reverse genetics system probably is not limited by the amount of template or transfection efficiency, since the molar ratio of plasmid to target cell is approximately 5×10^4, and increasing the amount of plasmid does not effect higher viral yields from cotransfection lysates (data not shown). Furthermore, it does not appear that infection efficiency is limited by the absence of viral replication proteins during early steps of replication because high-level expression of the replication proteins μ2, μNS, and σNS, which collaborate to form viral inclusions in infected cells (Mbisa et al., 2000; Broering et al., 2002; Becker et al., 2003; Miller et al., 2003), did not enhance viral recovery (data not shown). Perhaps the presence of other viral or cellular factors associated with natural infection by intact virion particles is required for maximal reovirus infectivity.

Presently, no entirely plasmid-based reverse genetics system has been described for any other dsRNA virus of animals. Although each genus within this constellation of viruses bears unique biologic characteristics and physiochemical properties, there are nonetheless numerous unifying features of virion particle structure and replication mechanisms that should allow principles and techniques established in this study to be applied broadly across the group. We expect that new insights into mammalian reovirus replication learned with the use of this reverse genetics system will be quickly extrapolated to other *Reoviridae* family members, leading to accelerated development of analogous marker-rescue technologies for those viruses.

EXPERIMENTAL PROCEDURES

Cells and Viruses

L cells and HeLa cells were maintained as described (Barton et al., 2001a). Reovirus strains T1L and T3D are laboratory stocks originally obtained from Dr. Bernard Fields. Virus was purified after growth in L cells by CsCl-gradient centrifugation (Furlong et al., 1988). Purified ^{35}S-methionine-labeled virions were prepared as described (Nibert et al., 1995). Attenuated vaccinia virus strain rDIs-T7pol expressing T7 RNA polymerase was propagated in chick embryo fibroblasts as described (Ishii et al., 2002).

Plasmid Construction

Full-length reovirus cDNAs were amplified by RT-PCR using viral dsRNA extracted from purified virions as template. Amplified cDNAs were initially cloned into pBluescript II SK (−) (Stratagene) for the T3D L1, L2, and L3 genes or pCR 2.1 (Invitrogen) for the T3D M1, M2, M3, S1, S2, S3, and S4 genes and the T1L S1 gene (Table S3). To generate pT7-L1T3D, pT7-L2T3D, pT7-L3T3D, pT7-M1T3D, pT7-M2T3D, pT7-M3T3D, pT7-S2T3D, pT7-S3T3D, and pT7-S4T3D, viral cDNA-containing fragments were subcloned into p3E5EGFP (Watanabe et al., 2004). Viral cDNAs fused at their native 5′ termini to the phage T7 RNA polymerase promoter were inserted into p3E5EGFP by partial or complete replacement of plasmid sequences encoding GFP and the Ebola virus leader and trailer, resulting in ligation of native 3′ termini to the HDV ribozyme sequence. To generate pBacT7-S1T3D and pBacT7-S1T1L, encoding the T3D S1 and T1L S1 genes, respectively, S1 cDNAs fused to the T7 promoter and a portion of the HDV ribozyme were first cloned into the BseRI site of p3E5EGFP, and fragments containing the S1 gene flanked 5′ by the T7 promoter and 3′ by the HDV ribozyme and T7 terminator sequences were subcloned into the XbaI site of pBacPAK8 (Clontech). pBacT7-S1T3D and pT7-S4T3D were used as templates to generate mutant constructs pBacT7-S1T3DT249I and pT7-S4T3DY354H, respectively, by introduction of specific nucleotide substitutions using the QuickChange site-directed mutagenesis kit (Stratagene) (Table S4). To generate pT7-S4GFP, S4 nucleotide sequences 150–768 within pT7-S4T3D were replaced with the GFP ORF. Nucleotide sequences of recombinant plasmids were confirmed by DNA sequencing. Detailed description of cloning strategies is provided in the Supplemental Data.

Plasmid Transfection and Recovery of Recombinant Virus

Monolayers of L cells at approximately 90% confluence (3×10^6 cells) in 60 mm dishes (Costar) were infected with rDIs-T7pol at an MOI of ~0.5 $TCID_{50}$. At 1 hr postinfection, cells were cotransfected with ten plasmid constructs representing the cloned T3D genome—pT7-L1T3D (2 μg), pT7-L2T3D (2 μg), pT7-L3T3D (2 μg), pT7-M1T3D (1.75 μg), pT7-M2T3D (1.75 μg), pT7-M3T3D (1.75 μg), pBacT7-S1T3D (2 μg), pT7-S2T3D (1.5 μg), pT7-S3T3D (1.5 μg), and pT7-S4T3D (1.5 μg)—using 3 μl of TransIT-LT1 transfection reagent (Mirus) per microgram of plasmid DNA. Following 0–5 days of incubation, recombinant virus was isolated from transfected cells by plaque purification on monolayers of L cells (Virgin et al., 1988). Electrophoretic analysis of viral dsRNA was performed as described (Wilson et al., 1996). Confirmation of mutations in the S1, S4, and L1 genes of recombinant viruses was performed using the Onestep RT-PCR kit (Qiagen), gene-specific primer sets, and viral dsRNA extracted from purified virions as template. PCR products were analyzed following electrophoresis in Tris-borate-EDTA agarose gels or purified and subjected directly to sequence analysis.

Infectious Center and Viral Yield Assays

L cells were cotransfected with ten plasmids corresponding to the T3D genome as described. For infectious center assays, transfected cells were released from plates by trypsin treatment at various intervals posttransfection, washed, counted, diluted, and applied directly to monolayers of untreated L cells (Dermody et al., 1995), which were processed for plaque assay (Virgin et al., 1988). For viral yield assays, transfected L cells were lysed by freezing and thawing, and viral titers in cell lysates were determined by plaque assay (Virgin et al., 1988).

Immunofluorescence Detection of Reovirus Infection

Parental L cells or L cell transfectants selected for stable expression of σ3 protein (5×10^4) were plated on glass coverslips in 24-well plates (Costar) and infected at an MOI of 10,000 (T3D and rsT3D) or 20,000 (rsT3D/S4-GFP) particles per cell. Following incubation at 37°C for various intervals, cells were fixed and stained for μNS and σ3 proteins as described (Maginnis et al., 2006). Images were acquired using a Zeiss LSM 510 META inverted confocal system (Carl Zeiss) with a Zeiss inverted Axiovert 200M microscope and a Plan-APOCHROMAT 63×/1.4 NA oil immersion DIC objective. Images were processed using MetaMorph image analysis software (Molecular Devices).

Infectivity of Recombinant Viruses

Monolayers of L or L-σ3 cells (2.5 to 5×10^5) in 24-well plates or suspension cultures of MEL cells (5×10^5 cells/ml) were infected with virus at an MOI of 1–2 PFU/cell. After 1 hr adsorption at room temperature, the inoculum was removed, cells were washed twice with PBS, and fresh medium was added. Cells were incubated at 37°C for various intervals, and viral titers in cell lysates were determined by plaque assay (Virgin et al., 1988).

Analysis of Viral Capsid Proteins after Protease Treatment

Purified virions at a concentration of either 2×10^{12} particles/ml (trypsin) or 9×10^{12} particles/ml (chymotrypsin) were digested with either 50 μg/ml of N α-p-tosyl-L-sulfonyl phenylalanyl chloromethyl ketone-treated bovine trypsin (Sigma) or 200 μg/ml of *Nα-p*-tosyl-L-lysine chloromethyl ketone-treated bovine α-chymotrypsin (Sigma) for various intervals at either 25°C (trypsin) or 8°C (chymotrypsin) as described (Nibert et al., 1995; Wetzel et al., 1997). Protease digestion was stopped by adding either 0.5 mg/ml soybean trypsin inhibitor (trypsin) (Sigma) or 5 mM phenylmethyl-sulfonyl fluoride (chymotrypsin) (Sigma) to the treatment mixtures and cooling at 0°C. Viral proteins were resolved by SDS-PAGE and visualized by either autoradiography (Nibert et al., 1995) or staining with Coomassie blue (Wetzel et al., 1997).

Infection of Mice

Newborn C57/BL6 mice weighing 2.0–2.5 grams (2–4 days old) were inoculated perorally or intracranially with 10^3 or 10^2 PFU, respectively, of purified reovirus virions diluted in PBS. PO inoculations (50 μl) were delivered intragastrically as described (Rubin and Fields, 1980). IC inoculations (5 μl) were delivered to the left cerebral hemisphere using a Hamilton syringe and 30-gauge needle (Tyler et al., 1985). At various intervals following inoculation, mice were euthanized, and organs were harvested into 1 ml of PBS and homogenized by freezing, thawing, and sonication. Viral titers in organ homogenates were determined by plaque assay (Virgin et al., 1988). Animal husbandry and experimental procedures were performed in accordance with Public Health Service policy and approved by the Vanderbilt University School of Medicine Institutional Animal Care and Use Committee.

Growth of Virus in Cells Treated with E64

Monolayers of L cells (2×10^5) in 24-well plates were preincubated in medium supplemented with 0–200 μM E64 (Sigma) for 4 hr. The medium was removed, and cells were adsorbed with virus at an MOI of 2 PFU/cell. After incubation at 4°C for 1 hr, the inoculum was removed, cells were washed with PBS, and 1 ml of fresh medium supplemented with 0 to 200 μM E64 was added. Cells were incubated at 37°C for 24 hr and frozen and thawed twice. Viral titers in cell lysates were determined by plaque assay (Virgin et al., 1988).

Generation of σ3-Expressing Cells

L cells stably expressing σ3 protein (L-σ3 cells) were selected by transfection of cells with pCXN-S4T3D, which encodes the entire T3D σ3 ORF, and incubation in the presence of 1 mg/ml of geneticin (Invitrogen).

Supplemental Data

The Supplemental Data include Supplemental Experimental Procedures, four supplemental tables, and one supplemental figure and can be found with this article online at http://www.cellhostandmicrobe.com/cgi/content/full/1/2/147/DC1/.

ACKNOWLEDGMENTS

We thank Erik Barton, Craig Forrest, and Tim Peters for review of the manuscript and Dirk Reiter, Johannes Schilling, and Thilo Stehle for assistance in preparation of the figures. We thank Yoshihiro Kawaoka for plasmid p3E5EGFP and Tatsuo Miyamura and Koji Ishii for vaccinia virus rDIs-T7pol. This research was supported by a fellowship from the Naito Foundation (T.K.), Public Health Service awards T32 GM07347 (A.A.R.A. and E.A.E.), T32 CA09385 (K.W.B.), T32 GM08554 (K.M.G.), T32 AI49824 and F32 AI71440 (G.H.H.), T32 AI07611 (E.M.J.), T32 AI07281 (M.S.M.), K08 AI62862 (J.D.C.), R01 AI32539, and R37 AI38296, and the Elizabeth B. Lamb Center for Pediatric Research. Additional support was provided by Public Health Service awards P30 CA68485 for the Vanderbilt-Ingram Cancer Center and P60 DK20593 for the Vanderbilt Diabetes Research and Training Center.

Received: December 29, 2006
Revised: February 16, 2007
Accepted: March 19, 2007
Published: April 18, 2007

REFERENCES

Baer, G.S., and Dermody, T.S. (1997). Mutations in reovirus outercapsid protein σ3 selected during persistent infections of L cells confer resistance to protease inhibitor E64. J. Virol. *71*, 4921–4928.

Barton, E.S., Connolly, J.L., Forrest, J.C., Chappell, J.D., and Dermody, T.S. (2001a). Utilization of sialic acid as a coreceptor enhances reovirus attachment by multistep adhesion strengthening. J. Biol. Chem. *276*, 2200–2211.

Barton, E.S., Forrest, J.C., Connolly, J.L., Chappell, J.D., Liu, Y., Schnell, F., Nusrat, A., Parkos, C.A., and Dermody, T.S. (2001b). Junction adhesion molecule is a receptor for reovirus. Cell *104*, 441–451.

Becker, M.M., Peters, T.R., and Dermody, T.S. (2003). Reovirus σNS and μNS proteins form cytoplasmic inclusion structures in the absence of viral infection. J. Virol. *77*, 5948–5963.

Blaney, J.E., Jr., Durbin, A.P., Murphy, B.R., and Whitehead, S.S. (2006). Development of a live attenuated dengue virus vaccine using reverse genetics. Viral Immunol. *19*, 10–32.

Bodkin, D.K., and Fields, B.N. (1989). Growth and survival of reovirus in intestinal tissue: Role of the L2 and S1 genes. J. Virol. *63*, 1188–1193.

Bodkin, D.K., Nibert, M.L., and Fields, B.N. (1989). Proteolytic digestion of reovirus in the intestinal lumens of neonatal mice. J. Virol. *63*, 4676–4681.

Borsa, J., Sargent, M.D., Lievaart, P.A., and Copps, T.P. (1981). Reovirus: Evidence for a second step in the intracellular uncoating and transcriptase activation process. Virology *111*, 191–200.

Broering, T.J., Parker, J.S., Joyce, P.L., Kim, J., and Nibert, M.L. (2002). Mammalian reovirus nonstructural protein μNS forms large inclusions and colocalizes with reovirus microtubule-associated protein μ2 in transfected cells. J. Virol. *76*, 8285–8297.

Campbell, J.A., Shelling, P., Wetzel, J.D., Johnson, E.M., Wilson, G.A.R., Forrest, J.C., Aurrand-Lions, M., Imhof, B., Stehle, T., and Dermody, T.S. (2005). Junctional adhesion molecule-A serves as a receptor for prototype and field-isolate strains of mammalian reovirus. J. Virol. *79*, 7967–7978.

Chandran, K., and Nibert, M.L. (2003). Animal cell invasion by a large nonenveloped virus: Reovirus delivers the goods. Trends Microbiol. *11*, 374–382.

Chandran, K., Zhang, X., Olson, N.H., Walker, S.B., Chappell, J.D., Dermody, T.S., Baker, T.S., and Nibert, M.L. (2001). Complete in vitro assembly of the reovirus outer capsid produces highly infectious particles suitable for genetic studies of the receptor-binding protein. J. Virol. *75*, 5335–5342.

Chandran, K., Farsetta, D.L., and Nibert, M.L. (2002). Strategy for nonenveloped virus entry: A hydrophobic conformer of the reovirus membrane penetration protein μ1 mediates membrane disruption. J. Virol. *76*, 9920–9933.

Chappell, J.D., Gunn, V.L., Wetzel, J.D., Baer, G.S., and Dermody, T.S. (1997). Mutations in type 3 reovirus that determine binding to sialic acid are contained in the fibrous tail domain of viral attachment protein σ1. J. Virol. *71*, 1834–1841.

Chappell, J.D., Barton, E.S., Smith, T.H., Baer, G.S., Duong, D.T., Nibert, M.L., and Dermody, T.S. (1998). Cleavage susceptibility of reovirus attachment protein σ1 during proteolytic disassembly of virions is determined by a sequence polymorphism in the σ1 neck. J. Virol. *72*, 8205–8213.

Chappell, J.D., Duong, J.L., Wright, B.W., and Dermody, T.S. (2000). Identification of carbohydrate-binding domains in the attachment proteins of type 1 and type 3 reoviruses. J. Virol. *74*, 8472–8479.

Chappell, J.D., Prota, A., Dermody, T.S., and Stehle, T. (2002). Crystal structure of reovirus attachment protein σ1 reveals evolutionary relationship to adenovirus fiber. EMBO J. *21*, 1–11.

Clark, K.M., Wetzel, J.D., Bayley, J., Ebert, D.H., McAbee, S.A., Stoneman, E.K., Baer, G.S., Zhu, Y., Wilson, G.J., Prasad, B.V.V., and Dermody, T.S. (2006). Reovirus variants selected for resistance to ammonium chloride have mutations in viral outer-capsid protein σ3. J. Virol. *80*, 671–681.

Coffey, M.C., Strong, J.E., Forsyth, P.A., and Lee, P.W. (1998). Reovirus therapy of tumors with activated Ras pathway. Science *282*, 1332–1334.

Dermody, T.S., Chappell, J.D., Hofler, J.G., Kramp, W., and Tyler, K.L. (1995). Eradication of persistent reovirus infection from a B-cell hybridoma. Virology *212*, 272–276.

Ebert, D.H., Wetzel, J.D., Brumbaugh, D.E., Chance, S.R., Stobie, L.E., Baer, G.S., and Dermody, T.S. (2001). Adaptation of reovirus to growth in the presence of protease inhibitor E64 segregates with a mutation in the carboxy terminus of viral outer-capsid protein σ3. J. Virol. *75*, 3197–3206.

Ebert, D.H., Deussing, J., Peters, C., and Dermody, T.S. (2002). Cathepsin L and cathepsin B mediate reovirus disassembly in murine fibroblast cells. J. Biol. Chem. *277*, 24609–24617.

Ehrlich, M., Boll, W., Van Oijen, A., Hariharan, R., Chandran, K., Nibert, M.L., and Kirchhausen, T. (2004). Endocytosis by random initiation and stabilization of clathrin-coated pits. Cell *118*, 591–605.

Fields, B.N. (1971). Temperature-sensitive mutants of reovirus type 3 features of genetic recombination. Virology *46*, 142–148.

Furlong, D.B., Nibert, M.L., and Fields, B.N. (1988). Sigma 1 protein of mammalian reoviruses extends from the surfaces of viral particles. J. Virol. *62*, 246–256.

Furuichi, Y., Morgan, M., Muthukrishnan, S., and Shatkin, A.J. (1975a). Reovirus messenger RNA contains a methylated blocked 5′-terminal structure M7G(5′)ppp(5′)GmpCp-. Proc. Natl. Acad. Sci. USA *72*, 362–366.

Furuichi, Y., Muthukrishnan, S., and Shatkin, A.J. (1975b). 5′-Terminal $M^7G(5')ppp(5')G^mp$ in vivo: Identification in reovirus genome RNA. Proc. Natl. Acad. Sci. USA *72*, 742–745.

Guglielmi, K.M., Johnson, E.M., Stehle, T., and Dermody, T.S. (2006). Attachment and cell entry of mammalian orthoreovirus. Curr. Top. Microbiol. Immunol. *309*, 1–38.

Horimoto, T., and Kawaoka, Y. (2006). Strategies for developing vaccines against H5N1 influenza A viruses. Trends Mol. Med. *12*, 506–514.

Ishii, K., Ueda, Y., Matsuo, K., Matsuura, Y., Kitamura, T., Kato, K., Izumi, Y., Someya, K., Ohsu, T., Honda, M., and Miyamura, T. (2002). Structural analysis of vaccinia virus DIs strain: Application as a new replication-deficient viral vector. Virology *302*, 433–444.

Jané-Valbuena, J., Breun, L.A., Schiff, L.A., and Nibert, M.L. (2002). Sites and determinants of early cleavages in the proteolytic processing pathway of reovirus surface protein σ3. J. Virol. *76*, 5184–5197.

Kapikian, A., Hoshino, Y., and Chanock, R. (2001). Rotaviruses. In Fields Virology, D.M. Knipe and P.M. Howley, eds. (Philadelphia: Lippincott-Raven), pp. 1787–1833.

Kobayashi, T., Chappell, J.D., Danthi, P., and Dermody, T.S. (2006). Gene-specific inhibition of reovirus replication by RNA interference. J. Virol. *80*, 9053–9063.

Komoto, S., Sasaki, J., and Taniguchi, K. (2006). Reverse genetics system for introduction of site-specific mutations into the double-stranded RNA genome of infectious rotavirus. Proc. Natl. Acad. Sci. USA *103*, 4646–4651.

Maginnis, M.S., Forrest, J.C., Kopecky-Bromberg, S.A., Dickeson, S.K., Santoro, S.A., Zutter, M.M., Nemerow, G.R., Bergelson, J.M., and Dermody, T.S. (2006). β1 integrin mediates internalization of mammalian reovirus. J. Virol. *80*, 2760–2770.

Martin-Padura, I., Lostaglio, S., Schneemann, M., Williams, L., Romano, M., Fruscella, P., Panzeri, C., Stoppacciaro, A., Ruco, L., Villa, A., et al. (1998). Junctional adhesion molecule, a novel member of the immunoglobulin superfamily that distributes at intercellular junctions and modulates monocyte transmigration. J. Cell Biol. *142*, 117–127.

Mbisa, J.L., Becker, M.M., Zou, S., Dermody, T.S., and Brown, E.G. (2000). Reovirus μ2 protein determines strain-specific differences in the rate of viral inclusion formation in L929 cells. Virology *272*, 16–26.

Miller, C.L., Broering, T.J., Parker, J.S., Arnold, M.M., and Nibert, M.L. (2003). Reovirus σNS protein localizes to inclusions through an association requiring the μNS amino terminus. J. Virol. *77*, 4566–4576.

Milligan, J.F., Groebe, D.R., Witherell, G.W., and Uhlenbeck, O.C. (1987). Oligoribonucleotide synthesis using T7 RNA polymerase and synthetic DNA templates. Nucleic Acids Res. *15*, 8783–8798.

Nibert, M.L., Chappell, J.D., and Dermody, T.S. (1995). Infectious subvirion particles of reovirus type 3 Dearing exhibit a loss in infectivity and contain a cleaved σ1 protein. J. Virol. *69*, 5057–5067.

Odegard, A.L., Chandran, K., Zhang, X., Parker, J.S., Baker, T.S., and Nibert, M.L. (2004). Putative autocleavage of outer capsid protein μ1, allowing release of myristoylated peptide μ1N during particle uncoating, is critical for cell entry by reovirus. J. Virol. *78*, 8732–8745.

O'Donnell, S.M., Hansberger, M.W., and Dermody, T.S. (2003). Viral and cellular determinants of apoptosis induced by mammalian reovirus. Int. Rev. Immunol. *22*, 477–503.

Olland, A.M., Jané-Valbuena, J., Schiff, L.A., Nibert, M.L., and Harrison, S.C. (2001). Structure of the reovirus outer capsid and dsRNA-binding protein σ3 at 1.8 Å resolution. EMBO J. *20*, 979–989.

Parker, J.S., Broering, T.J., Kim, J., Higgins, D.E., and Nibert, M.L. (2002). Reovirus core protein μ2 determines the filamentous morphology of viral inclusion bodies by interacting with and stabilizing microtubules. J. Virol. *76*, 4483–4496.

Riezebos-Brilman, A., de Mare, A., Bungener, L., Huckriede, A., Wilschut, J., and Daemen, T. (2006). Recombinant alphaviruses as vectors for anti-tumour and anti-microbial immunotherapy. J. Clin. Virol. *35*, 233–243.

Roner, M.R., and Joklik, W.K. (2001). Reovirus reverse genetics: Incorporation of the CAT gene into the reovirus genome. Proc. Natl. Acad. Sci. USA *98*, 8036–8041.

Roner, M.R., and Steele, B.G. (2007). Localizing the reovirus packaging signals using an engineered m1 and s2 ssRNA. Virology *358*, 89–97.

Roner, M.R., Nepliouev, I., Sherry, B., and Joklik, W.K. (1997). Construction and characterization of a reovirus double temperature-sensitive mutant. Proc. Natl. Acad. Sci. USA *94*, 6826–6830.

Rubin, D.H., and Fields, B.N. (1980). Molecular basis of reovirus virulence: Role of the M2 gene. J. Exp. Med. *152*, 853–868.

Rubin, D.H., Wetzel, J.D., Williams, W.V., Cohen, J.A., Dworkin, C., and Dermody, T.S. (1992). Binding of type 3 reovirus by a domain of the σ1 protein important for hemagglutination leads to infection of murine erythroleukemia cells. J. Clin. Invest. *90*, 2536–2542.

Silverstein, S.C., and Schur, P.H. (1970). Immunofluorescent localization of double-stranded RNA in reovirus-infected cells. Virology *41*, 564–566.

Tyler, K.L. (2001). Mammalian reoviruses. In Fields Virology, D.M. Knipe and P.M. Howley, eds. (Philadelphia: Lippincott Williams & Wilkins), pp. 1729–1745.

Tyler, K.L., Bronson, R.T., Byers, K.B., and Fields, B.N. (1985). Molecular basis of viral neurotropism: Experimental reovirus infection. Neurology *35*, 88–92.

Tyler, K.L., Barton, E.S., Ibach, M.L., Robinson, C., Valyi-Nagy, T., Campbell, J.A., Clarke, P., O'Donnell, S.M., Wetzel, J.D., and Dermody, T.S. (2004). Isolation and molecular characterization of a novel type 3 reovirus from a child with meningitis. J. Infect. Dis. *189*, 1664–1675.

Virgin, H.W., IV, Bassel-Duby, R., Fields, B.N., and Tyler, K.L. (1988). Antibody protects against lethal infection with the neurally spreading reovirus type 3 (Dearing). J. Virol. *62*, 4594–4604.

Watanabe, S., Watanabe, T., Noda, T., Takada, A., Feldmann, H., Jasenosky, L.D., and Kawaoka, Y. (2004). Production of novel Ebola virus-like particles from cDNAs: An alternative to Ebola virus generation by reverse genetics. J. Virol. *78*, 999–1005.

Wetzel, J.D., Wilson, G.J., Baer, G.S., Dunnigan, L.R., Wright, J.P., Tang, D.S.H., and Dermody, T.S. (1997). Reovirus variants selected during persistent infections of L cells contain mutations in the viral S1 and S4 genes and are altered in viral disassembly. J. Virol. *71*, 1362–1369.

Wiener, J.R., and Joklik, W.K. (1989). The sequences of the reovirus serotype *1*, 2, and 3 L1 genome segments and analysis of the mode of divergence of the reovirus serotypes. Virology *169*, 194–203.

Wilson, G.J., Wetzel, J.D., Puryear, W., Bassel-Duby, R., and Dermody, T.S. (1996). Persistent reovirus infections of L cells select mutations in viral attachment protein σ1 that alter oligomer stability. J. Virol. *70*, 6598–6606.

Wilson, G.J., Nason, E.L., Hardy, C.S., Ebert, D.H., Wetzel, J.D., Prasad, B.V.V., and Dermody, T.S. (2002). A single mutation in the carboxy terminus of reovirus outer-capsid protein σ3 confers enhanced kinetics of σ3 proteolysis, resistance to inhibitors of viral disassembly, and alterations in σ3 structure. J. Virol. *76*, 9832–9843.

Accession Numbers

GenBank accession numbers for cDNAs corresponding to the T3D L1, L2, L3, M1, M2, M3, S1, S2, S3, and S4 genes and the T1L S1 gene are provided in Table S3.

C. NPXY MOTIFS IN THE β1 INTEGRIN CYTOPLASMIC TAIL ARE REQUIRED FOR FUNCTIONAL REOVIRUS ENTRY

Reovirus cell entry is mediated by binding to cell-surface carbohydrate and JAM-A and internalization by β1 integrin (45, 48, 175, 218). The cytoplasmic tail of β1 integrin contains two NPXY motifs that bind adaptor molecules during clathrin-mediated endocytosis and serve as sorting signals in the endocytic pathway (219-223). We hypothesized that the NPXY motifs in β1 integrin mediate internalization and transport of virus to late endosomes where uncoating takes place. Using imaging techniques and pharmacologic inhibitors, we showed that cells expressing wt β1 integrin were capable of internalizing virus to the proper endocytic compartment, allowing virus uncoating and productive infection. Cells expressing a mutant form of β1 in which the NPXY tyrosine residues were changed to phenylalanine were capable of internalizing virus but not supporting productive reovirus infection. Viral internalization by wt cells was inhibited by the drug chlorpromazine, which blocks clathrin-mediated endocytosis, but internalization by mutant cells was not. I participated in this work by developing assays, particularly infection of cells following treatment with chlorpromazine and the corresponding transferrin uptake assay used as a control.

JOURNAL OF VIROLOGY, Apr. 2008, p. 3181–3191 Vol. 82, No. 7
0022-538X/08/$08.00+0 doi:10.1128/JVI.01612-07

NPXY Motifs in the β1 Integrin Cytoplasmic Tail Are Required for Functional Reovirus Entry▽

Melissa S. Maginnis,[1,2,3] Bernardo A. Mainou,[2,3] Aaron Derdowski,[3] Elizabeth M. Johnson,[1,2] Roy Zent,[4,5] and Terence S. Dermody[1,2,3]*

Departments of Microbiology and Immunology,[1] Pediatrics,[3] and Medicine[4] and Elizabeth B. Lamb Center for Pediatric Research,[2] Vanderbilt University School of Medicine, and Department of Medicine, Veterans Affairs Hospital,[5] Nashville, Tennessee 37232

Received 24 July 2007/Accepted 15 January 2008

Reovirus cell entry is mediated by attachment to cell surface carbohydrate and junctional adhesion molecule A (JAM-A) and internalization by β1 integrin. The β1 integrin cytoplasmic tail contains two NPXY motifs, which function in recruitment of adaptor proteins and clathrin for endocytosis and serve as sorting signals for internalized cargo. As reovirus infection requires disassembly in the endocytic compartment, we investigated the role of the β1 integrin NPXY motifs in reovirus internalization. In comparison to wild-type cells (β1+/+ cells), reovirus infectivity was significantly reduced in cells expressing mutant β1 integrin in which the NPXY motifs were altered to NPXF (β1+/+Y783F/Y795F cells). However, reovirus displayed equivalent binding and internalization levels following adsorption to β1+/+ cells and β1+/+Y783F/Y795F cells, suggesting that the NPXY motifs are essential for transport of reovirus within the endocytic pathway. Reovirus entry into β1+/+ cells was blocked by chlorpromazine, an inhibitor of clathrin-mediated endocytosis, while entry into β1+/+ Y783F/Y795F cells was unaffected. Furthermore, virus was distributed to morphologically distinct endocytic organelles in β1+/+ and β1+/+Y783F/Y795F cells, providing further evidence that the β1 integrin NPXY motifs mediate sorting of reovirus in the endocytic pathway. Thus, NPXY motifs in the β1 integrin cytoplasmic tail are required for functional reovirus entry, which indicates a key role for these sequences in endocytosis of a pathogenic virus.

Virus entry into host cells requires interactions between viral capsid constituents and receptors expressed on the cell surface. Many viruses utilize distinct cellular molecules to mediate the functions of attachment and internalization (36). Mammalian reoviruses are nonenveloped, double-stranded RNA (dsRNA) viruses that infect a broad range of hosts in nature (55). Reoviruses are pathogenic in newborn mice, infecting most organs, including the central nervous system, heart, and liver (65). Reoviruses first attach to the cell surface by binding to carbohydrate (4), which is α2,3- or α2,6-linked sialic acid for serotype 3 reovirus strains (19, 46, 47). All reovirus serotypes bind to proteinaceous receptor junctional adhesion molecule A (JAM-A) to mediate high-affinity attachment (5, 14, 50). Following receptor binding, reovirus is internalized into cells via a mechanism involving β1 integrin (34).

The process by which reovirus enters cells is poorly understood. Data gathered from thin-section electron microscopy (EM) images (11, 12, 52, 59) and video fluorescence microscopy (24) suggest that reovirus is internalized by clathrin-dependent endocytosis. However, these studies were performed using imaging techniques that did not address the role of clathrin in productive reovirus infection. Within minutes of internalization, reovirus undergoes stepwise disassembly, which in fibroblasts is dependent on acidic pH (35, 59) and endosomal cysteine-containing proteases cathepsins B and L (23). Viral disassembly leads to generation of well-defined intermediates, the first of which is the infectious subvirion particle (ISVP) (12, 17, 57, 59). ISVPs are characterized by the loss of outer capsid protein σ3 and cleavage of outer capsid protein μ1 to form particle-associated fragments δ and ϕ. Following formation of ISVPs, σ1 is shed and the μ1 cleavage fragments undergo conformational rearrangement, yielding the ISVP* (15, 16). ISVP*s penetrate endosomes to deliver transcriptionally active viral cores into the cytoplasm (40, 42). Although the precise mechanism of membrane penetration is not well understood, ISVP*s are thought to breach the endosomal membrane by a process that requires μ1-mediated formation of small pores (1). The cellular compartment in which reovirus disassembly takes place is unknown, yet cathepsins B and L generally reside in late endosomes or lysosomes (62), suggesting that reovirus disassembly occurs in these endocytic organelles.

Integrins are heterodimeric cell surface molecules consisting of α and β subunits (32). Integrin heterodimers mediate cell adhesion to the extracellular matrix, regulate cell trafficking, and transduce both inside-out and outside-in signaling events (31). In addition to reovirus, several other pathogenic microorganisms use the adhesion and signaling properties of various integrins to bind or enter host cells, including adenovirus (αvβ3 and αvβ5) (72), cytomegalovirus (α2β1, α6β1, αvβ3) (25), echovirus (α2β1) (6), rotavirus (αvβ3, α2β1, α4β1) (27, 30), West Nile virus (αvβ3) (20), and *Yersinia pseudotuberculosis* (β1) (33). Little is known about the internalization and the endocytic trafficking of β1 integrin and its cognate cargo. The β1 integrin cytoplasmic domain is approximately 47 amino acids in length and contains two Asn-Pro-any amino acid-tyrosine (NPXY) motifs (51), with tyrosine residues at amino

* Corresponding author. Mailing address: Lamb Center for Pediatric Research, D7235 MCN, Vanderbilt University School of Medicine, Nashville, TN 37232. Phone: (615) 343-9943. Fax: (615) 343-9723. E-mail: terry.dermody@vanderbilt.edu.

▽ Published ahead of print on 23 January 2008.

acid positions 783 and 795 (51). NPXY motifs are potential sites of tyrosine phosphorylation (53) and serve as endocytic sorting signals that can be recognized by adaptor proteins and clathrin (8, 9, 37, 38, 43). The function of NPXY motifs in cargo internalization was first deduced in studies of familial hypercholesterolemia, a disorder in which low-density lipoprotein (LDL) cholesterol levels are elevated, leading to premature atherosclerosis (22). This disease results from a tyrosine-to-phenylalanine mutation in the NPXY motif of the LDL receptor (22). The NPXY-to-F mutation renders the receptor incapable of recognition by adaptor protein disabled 2 (Dab2), which is engaged by adaptor protein 2 (AP-2) for clathrin-mediated endocytosis (38).

To determine the function of the β1 integrin NPXY motifs in reovirus entry and infection, we used β1−/− cells stably expressing either wild-type β1 integrin or β1 integrin with altered NPXY motifs. Mutation of the β1 integrin NPXY motifs to NPXF prevents tyrosine phosphorylation but does not affect β1 integrin surface expression, the capacity of β1 to form heterodimers with α integrin partners, fibronectin assembly, or cell adhesion (54). However, β1 integrin NPXY-to-F mutation results in increased focal contacts, shorter actin filaments, and impaired cell motility (54). We found that reovirus particles enter into β1+/+ cells via a chlorpromazine-sensitive mechanism and are delivered to vesicles that morphologically resemble endosomes and lysosomes, while a chlorpromazine-resistant mechanism is utilized in cells with altered NPXY motifs that do not lead to productive infection. These findings indicate that the β1 integrin NPXY motifs are required for functional reovirus entry and provide new insights into mechanisms by which β1 integrin delivers cargo to the endocytic compartment.

MATERIALS AND METHODS

Cells, viruses, and antibodies. Spinner-adapted murine L929 (L) cells were grown in either suspension or monolayer cultures in Joklik's modified Eagle's minimal essential medium (Sigma-Aldrich, St. Louis, MO) supplemented to contain 5% fetal bovine serum, 2 mM L-glutamine, 100 U of penicillin per ml, 100 U of streptomycin per ml, and 0.25 mg amphotericin per ml (Gibco Invitrogen Corp., Grand Island, NY). GD25, GD25β1A, GD25β1AY783F, GD25β1AY795F, and GD25β1AY783F/Y795F cells (69, 70) were obtained from Deane Mosher (University of Wisconsin, Madison) and maintained in Dulbecco's minimal essential medium (Gibco Invitrogen) supplemented to contain 10% fetal bovine serum, 100 U of penicillin per ml, and 100 U of streptomycin per ml. Medium for all GD25β1A cells was supplemented to contain 10 μg of puromycin (Sigma-Aldrich) per ml to maintain β1 integrin expression (69, 70).

Reovirus strain type 1 Lang (T1L) is a laboratory stock. Working stocks of virus were prepared by plaque purification and passage using L cells (66). Purified virions were generated from second-passage L-cell lysate virus stocks. Virus was purified from infected cell lysates by Freon extraction and CsCl gradient centrifugation as described previously (26). Bands corresponding to the density of reovirus particles (1.36 g/cm^3) were collected and dialyzed against virion storage buffer (150 mM NaCl, 15 mM MgCl2, 10 mM Tris [pH 7.4]). The reovirus particle concentration was determined from the equivalence of 1 unit of optical density at 260 nm to 2.1×10^{12} particles (58). The viral titer was determined by fluorescent focus assay (4). ISVPs were generated by the treatment of 2×10^{11} particles with 200 μg of α-chymotrypsin (Sigma-Aldrich) in a 100-μl volume of virion storage buffer at 37°C for 30 min (2). Reactions were terminated by the addition of 1.0 mM phenylmethylsulfonyl fluoride (Sigma-Aldrich).

Immunoglobulin G (IgG) fractions of rabbit antisera raised against T1L and type 3 Dearing (71) were purified by protein A Sepharose as described previously (4). Fluorescently conjugated secondary Alexa antibodies were obtained from Molecular Probes (Invitrogen, San Diego, CA). R-phycoerythrin-conjugated secondary antibodies were obtained from BD Biosciences Pharmingen (Franklin Lakes, NJ). Murine β1 integrin-specific monoclonal antibody (MAb) MAB1997 (Chemicon, Temecula, CA) and JAM-A-specific MAb H202-106-7-4 (provided by Beat Imof, Université de Genève) were used to assess cell surface expression of β1 integrin and JAM-A by flow cytometry. IgG controls used for flow cytometry were purchased from Chemicon.

Flow cytometric analysis. Cells were detached from plates using phosphate-buffered saline (PBS)-EDTA (20 mM EDTA), washed, and centrifuged at $1,000 \times g$ to form a pellet. Cells were resuspended with antibodies in PBS-bovine serum albumin (BSA) (Sigma-Aldrich) (5% BSA) and incubated at 4°C for 1 h. Cells were washed twice and incubated with an appropriate secondary antibody conjugated to R-phycoerythrin (BD Biosciences Pharmingen) at 4°C for 1 h. Cells were washed, resuspended in PBS, and analyzed by flow cytometry. Reovirus binding to cells was analyzed by adsorbing cells with T1L particles at 4°C for 1 h. Cells were washed and stained with reovirus polyclonal antisera and an appropriate secondary antibody conjugated to Alexa 546 (Invitrogen) and analyzed by flow cytometry.

Fluorescent focus assay of viral infection. Cells plated in 24-well plates (Costar; Corning Life Sciences, Corning, NY) were either untreated or treated with 5 μg per ml chlorpromazine (Alexis Biochemicals, Lausen, Switzerland) at 37°C for 3 h. Cells were adsorbed with virions or ISVPs in incomplete medium (without serum and antibiotics) at 4°C for 1 h. Inocula were removed, cells were washed, and complete medium with or without chlorpromazine was added. Infected cells were incubated at 37°C for 20 h to allow a single cycle of viral replication. Cells were fixed with cold, absolute methanol at −20°C for at least 30 min. Fixed cells were washed with PBS, incubated with PBS-BSA (5% BSA) for at least 15 min, and incubated with reovirus-specific polyclonal antiserum (1:500) in PBS containing 0.5% Triton X-100 (TX-100) at room temperature for 1 h. Cells were washed twice and incubated with an Alexa Fluor 488- or 546-labeled anti-rabbit IgG (1:1,000) in PBS-TX-100 (0.5% TX-100) at room temperature for 1 h. Cells were washed twice and visualized by indirect immunofluorescence at a magnification of ×20 using an Axiovert 200 fluorescence microscope (Carl Zeiss, New York, NY). Infected cells (fluorescent focus units [FFU]) were identified by diffuse cytoplasmic fluorescence staining that was excluded from the nucleus. Reovirus-infected cells were quantified by counting random fields in equivalently confluent monolayers for three to five fields of view for triplicate wells (4).

Confocal imaging of reovirus internalization. Cells plated on coverslips in 24-well plates (Costar) were adsorbed with reovirus virions in incomplete medium and incubated at 4°C for 1 h. Cells were washed and fixed or nonadherent reovirus was aspirated and replaced with complete medium and incubated at 37°C. At various intervals, cells were washed with PBS and fixed with 10% formalin (Laboratory Supply Company, Louisville, KY) for 20 min, followed by washing with PBS. Cells were treated with 1% TX-100 for 5 min and incubated with PBS-BGT (PBS, 0.5% BSA, 0.1% glycine, and 0.05% Tween 20) for 10 min. Cells were incubated with reovirus-specific polyclonal antiserum (1:500) in PBS-BGT for 1 h, washed with PBS-BGT, and incubated with donkey anti-rabbit immunoglobulin conjugated to Alexa Fluor 488 (Molecular Probes) (1:1,000) to visualize reovirus and phalloidin conjugated to Alexa Fluor 546 (Molecular Probes) (1:100) to visualize actin for 1 h in PBS-BGT. Cell nuclei were visualized by incubating cells with To-Pro 3 conjugated to Alexa Fluor 642 (Molecular Probes) (1:1,000) in PBS-BGT for 20 min. Cells were washed extensively with PBS-BGT, and coverslips were removed from wells and placed on slides using Aqua-Poly/Mount mounting medium (Polysciences, Inc., Warrington, PA). Images were captured using a Zeiss LSM 510 Meta laser-scanning confocal microscope. Three-dimensional image reconstructions were generated from multiple images collected in the Z plane and compiled using Zeiss imaging software.

Quantitation of virus internalization. Virus internalization was quantified as a function of pixel intensity using Metamorph software (Universal Imagining, Downingtown, PA). Confocal images were collected and analyzed for internalized reovirus particles by capturing multiple images in the Z plane and determining the center of the cell based on cell thickness as analyzed using Zeiss imaging software. Cells analyzed for quantitative purposes were selected at random and counted by an observer blinded to the conditions of the experiment. The intracellular space was outlined using the trace tool to exclude the plasma membrane, which was identified by intense actin staining. The region measurement function was used to quantify intensity of green pixels in the trace region for each cell.

Confocal imaging of transferrin internalization. Cells were plated on coverslips in 24-well plates and incubated at 37°C overnight in complete medium. Following incubation in incomplete medium at 37°C for 30 min, cells were untreated or treated with 5 μg per ml chlorpromazine at 37°C for 3 h. Cells were incubated with 2.5 μg per ml Alexa Fluor 488-conjugated transferrin (Molecular Probes) in the presence or absence of 5 μg per ml chlorpromazine in incomplete

medium at 37°C for 10 min. The medium was removed, and cells were washed once with PBS, once with an acid wash (0.2 M acetic acid, 0.5 M NaCl in distilled H_2O [diH_2O]), and twice with PBS. Cells were fixed with 10% formalin and prepared for confocal microscopy. Transferrin internalization was quantified using Metamorph software (Universal Imaging) as described for virus internalization.

EM. Cells plated in 60-mm dishes (Costar) were prechilled at 4°C for 1 h, adsorbed with reovirus virions in incomplete medium, and incubated at 4°C for 1 h. Cells were washed twice with PBS, and cells were harvested or nonadherent virus was aspirated and replaced with warm, complete medium and incubated at 37°C. At 10-min intervals, cells were harvested on ice in 1 ml of PBS using a cell lifter (Costar) and transferred to a 1.5-ml microcentrifuge tube. Cells were pelleted at 1,000 × *g* at 4°C for 5 min. The supernatant was removed, and 1 ml of 2% glutaraldehyde was placed over the cell pellet. Cells were incubated at room temperature for 90 min. Glutaraldehyde was removed and replaced with fresh 2% glutaraldehyde and incubated overnight at 4°C. Cells were washed three times in PBS, transferred to 1% osmium tetroxide in diH_2O for 1 h, and washed three times in diH_2O. Cells were stained en bloc in 1% aqueous uranyl acetate for 1 h and washed three times in diH_2O. Cells were dehydrated by using a graded series of ethanol washes and by increasing the incubation times in each solution starting with 30% for 5 min, followed by two washes with 50% for 5 min, 70% for 5 min, 95% for 10 min, and absolute ethanol for 15 min. Cells were passed through propylene oxide, transferred to a 1:1 araldite:propylene oxide mixture, and embedded in Araldite embedding medium (Electron Microscopy Sciences, Hatfield, PA). Ultra-thin serial sections (50 to 60 nm) were obtained using a Leica UCT Ultracut microtome (Leica Microsystems, Vienna, Austria), transferred to Formvar-coated grids, and examined using a Phillips CM10 transmission EM (FEI Company, Hillsboro, OR) equipped with an Advantage Plus Digital charge-coupled-device system for CM10 transmission EM (Advanced Microscopy Techniques, Danvers, MA).

Reovirus localization with lysosomal markers. Cells were plated on coverslips in 24-well plates and incubated with 75 nM Lysotracker-Red DND-99 dye (Molecular Probes) in incomplete medium at 37°C for 30 min. Cells were prechilled at 4°C for 1 h, adsorbed with reovirus virions in incomplete medium, and incubated at 4°C for 1 h. Cells were washed on ice three times with PBS, nonadherent reovirus was removed, and complete medium was added. Following incubation at 37°C for various intervals, cells were washed with PBS, fixed with 10% formalin, and prepared for confocal immunofluorescence microscopy. Images were analyzed for colocalization of Lysotracker-Red DND-99 dye and reovirus virions using ImageJ software (version 1.37v; W. S. Rasband, National Institutes of Health, Bethesda, MD) Colocalize RGB plug-in.

Statistical analysis. Means for at least triplicate samples were compared by using unpaired Student's *t* test (Microsoft Excel, Redmond, WA). *P* values of <0.05 were considered to be statistically significant.

RESULTS

Reovirus infection is diminished in cells expressing β1 integrin with altered NPXY motifs. To determine whether the NPXY motifs in the cytoplasmic domain of β1 integrin are required for functional reovirus entry, we tested cells with mutations in the β1 integrin NPXY motifs for the capacity to support reovirus infection. GD25 (β1−/−) cells are embryonic stem cells derived from β1-null mouse embryos, while GD25β1A (β1+/+) cells stably express full-length, wild-type β1 integrin (70). GD25β1AY783F (β1+/+Y783F), GD25β1AY795F (β1+/+Y795F), and GD25β1AY783F/Y795F (β1+/+Y783F/Y795F) cells stably express β1 integrin in which the tyrosine residues of the NPXY motifs at amino acid positions 783 and 795 have been substituted with phenylalanine (69, 70). Cell surface expression of β1 integrin by β1−/−, β1+/+, β1+/+Y783F, β1+/+Y795F, and β1+/+Y783F/Y795F cells was assessed using flow cytometry (Fig. 1A). With the exception of β1−/− cells, these cell lines expressed equivalent levels of cell surface β1 integrin. Importantly for our studies of reovirus infection, these cells also expressed equivalent levels of cell surface JAM-A (Fig. 1A). To test for attachment of reovirus to cells expressing wild-type and mutant β1 integrin, cells were incubated with reovirus particles, and binding was detected using flow cytometry (Fig. 1B). Reovirus bound equivalently to all cell types, suggesting that reovirus attachment is not affected by mutation of the β1 integrin NPXY motifs to NPXF.

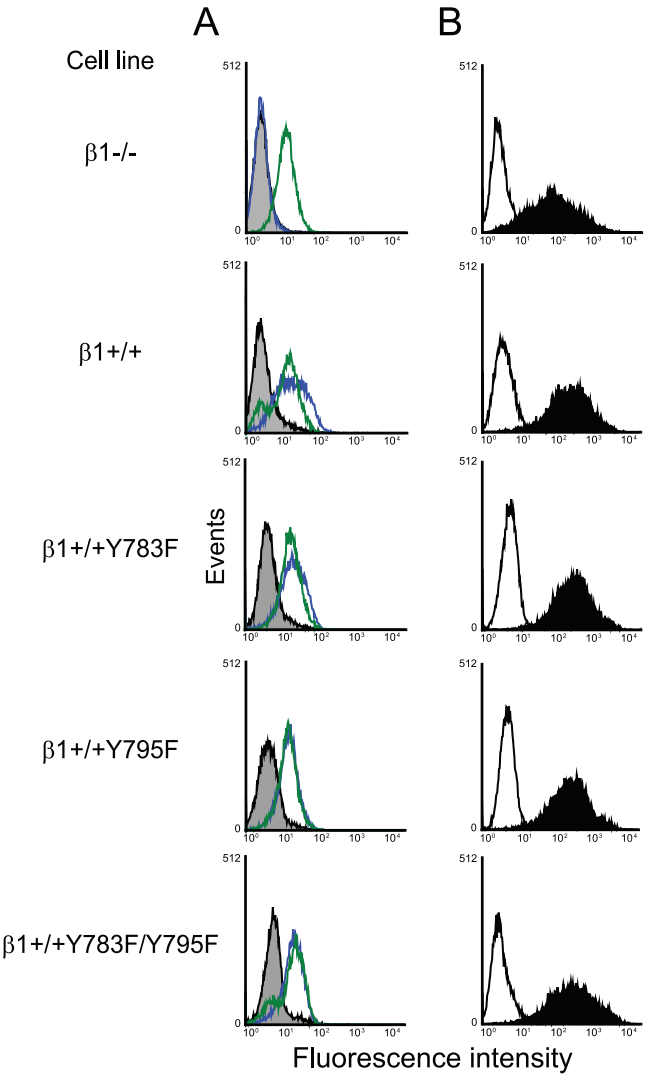

FIG. 1. Reovirus exhibits equivalent binding to β1−/−, β1+/+, and β1+/+ cells with altered NPXY motifs. (A) GD25 (β1−/−), GD25β1A (β1+/+), GD25β1AY783F (β1+/+Y783F), GD25β1AY795F (β1+/+Y795F), and GD25β1AY783F/Y795F (β1+/+Y783F/Y795F) cells were detached from plates using 20 mM EDTA, washed, collected by centrifugation, and incubated with antibodies specific for either murine β1 integrin (blue), murine JAM-A (green), or an IgG control antibody (gray). Cell surface expression of these molecules was detected by flow cytometry. Data are expressed as fluorescence intensity. (B) β1−/−, β1+/+, β1+/+Y783F, β1+/+Y795F, and β1+/+Y783F/Y795F cells were detached from plates using 20 mM EDTA, washed, collected by centrifugation, and incubated with 10^4 particles per cell of reovirus T1L in incomplete medium (filled) or incomplete medium alone (open) at 4°C for 1 h to allow attachment. Cells were washed and incubated with reovirus-specific antiserum. Reovirus binding was detected by flow cytometry. Data are expressed as fluorescence intensity.

To determine whether mutations in the β1 integrin NPXY motifs alter reovirus infection, cells were adsorbed with reovirus virions or ISVPs, and infectivity was scored by indirect immunofluorescence (Fig. 2). In comparison to β1+/+ cells,

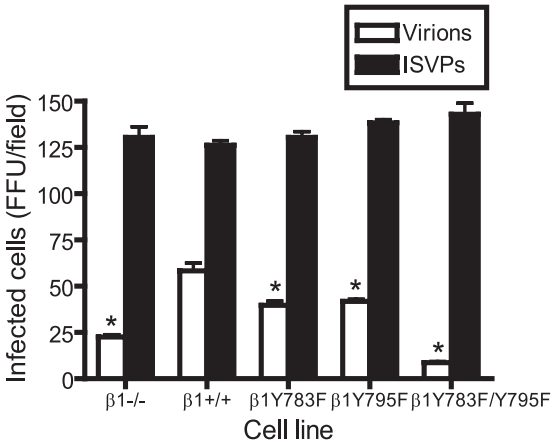

FIG. 2. Reovirus infection is diminished in cells with altered β1 integrin NPXY motifs. β1−/−, β1+/+, β1+/+Y783F, β1+/+Y795F, and β1+/+Y783F/Y795F cells were adsorbed with T1L virions or ISVPs at an MOI of 1 FFU per cell at 4°C for 1 h. Cells were washed with PBS, incubated in complete medium at 37°C for 20 h, fixed, and stained by indirect immunofluorescence. Infected cells were quantified by counting cells exhibiting cytoplasmic staining in five visual fields of equivalently confluent monolayers for triplicate samples. The results are expressed as mean FFU per visual field for triplicate samples. Error bars indicate standard deviations. These data are representative of results of three individual experiments performed in triplicate. *, $P < 0.05$ in comparison to β1+/+ cells.

β1−/−, β1+/+Y783F, β1+/+Y795F, and β1+/+Y783F/Y795F cells were less susceptible to infection by reovirus virions (Fig. 2). While reovirus infection was significantly reduced in β1+/+Y783F and β1+/+Y795F cells, infection was most dramatically diminished in β1+/+Y783F/Y795F cells, to an extent even greater than in β1−/− cells (Fig. 2). ISVPs, which bind to JAM-A (5) but bypass a requirement for endocytosis and disassembly (2, 59), were capable of infecting all cell types (Fig. 2). Equivalent infection by ISVPs suggests that the block to reovirus infection in cells expressing mutant β1 integrin occurs subsequent to viral attachment but preceding capsid disassembly.

Reovirus virions are internalized into the cytoplasm of β1+/+Y783F/Y795F cells. To determine whether the block to reovirus infection in β1+/+Y783F/Y795F cells is due to a defect in internalization, β1−/−, β1+/+, and β1+/+Y783F/Y795F cells were adsorbed with reovirus particles at 4°C for 1 h to allow virus binding and then incubated at 37°C to allow internalization over a time course concurrent with reovirus entry. At 0, 15, and 30 min, cells were fixed, stained using reovirus-specific antiserum, and examined for reovirus particles by confocal immunofluorescence microscopy. Representative confocal micrographic images of β1−/−, β1+/+, and β1+/+Y783F/Y795F cells infected with reovirus and fixed at 30 min postadsorption are shown in Fig. 3A. Although reovirus particles were observed in the cytoplasm of all cell types, there was a notable decrease in β1−/− cells, as described previously (34). Surprisingly, reovirus particles were internalized into both β1+/+ and β1+/+Y783F/Y795F cells (Fig. 3A). To determine the distribution of reovirus particles internalized into β1+/+ and β1+/+Y783F/Y795F cells, multiple confocal micrograph images in the Z plane were collected and examined using Z-stack analysis and three-dimensional image reconstructions (data not shown). Comparisons of the two cell types revealed that reovirus particles were distributed throughout the nonnuclear compartment of β1+/+Y783F/Y795F cells in a pattern similar to that for β1+/+ cells. To directly quantify the fluorescence intensity of internalized reovirus particles, confocal micrographs were obtained over a time course and analyzed using Metamorph imaging software. The average pixel intensity representing reovirus particles was significantly greater in β1+/+ and β1+/+Y783F/Y795F cells than in β1−/− cells (Fig. 3B). These findings indicate that reovirus particles are internalized into β1+/+ and β1+/+Y783F/Y795F cells, and in both cases, the number of particles internalized exceeds that for β1−/− cells.

Reovirus uptake into β1+/+ cells is blocked by chlorpromazine. To determine the mechanism required for functional reovirus entry, β1+/+ cells were pretreated with chlorpromazine, which inhibits clathrin assembly at the plasma membrane by interfering with AP-2 localization to membranes and forcing clathrin lattices to form on endosomal membranes (67). Treatment of cells with chlorpromazine blocks clathrin-dependent endocytosis of a number of viruses, including hepatitis C virus (7), polyomavirus JC virus (49), and vesicular stomatitis virus (60). Cells were infected with reovirus virions or ISVPs in the presence or absence of chlorpromazine and scored for infection by indirect immunofluorescence (Fig. 4A). Treatment of cells with 5 μg per ml of chlorpromazine decreased viral infectivity by greater than 80% following adsorption with virions (Fig. 4A). However, infectivity was unaffected by chlorpromazine treatment following adsorption with ISVPs, suggesting that diminished infectivity by reovirus is caused by a block to entry. Failure of chlorpromazine to inhibit infection by ISVPs also indicates that the concentration of chlorpromazine used in these experiments does not affect viral attachment or the capacity of cells to support the reovirus replication cycle. As a control, chlorpromazine treatment of β1+/+ cells diminished the uptake of transferrin (Fig. 4B and C), which is internalized by clathrin-dependent endocytosis (29, 48). Chlorpromazine also blocked reovirus infection and transferrin uptake in experiments using HeLa cells and L cells (data not shown). Thus, reovirus virions use a chlorpromazine-sensitive pathway, most likely clathrin-mediated endocytosis, to enter cells.

β1 integrin NPXY motifs are required for functional reovirus uptake. To determine the role of the β1 integrin NPXY motifs in reovirus endocytosis, β1+/+ and β1+/+Y783F/Y795F cells were either treated with chlorpromazine or left untreated, adsorbed with reovirus particles at 4°C for 1 h to allow virus binding, and incubated at 37°C to allow internalization. At 0 and 20 min postadsorption, cells were fixed, stained using reovirus-specific antiserum, and examined by confocal immunofluorescence microscopy. Representative confocal micrographic images of β1+/+ and β1+/+Y783F/Y795F cells at 20 min postadsorption are shown in Fig. 5A. The fluorescence intensities of reovirus particles internalized into β1+/+ and β1+/+Y783F/Y795F cells were quantified by averaging the pixel intensities for representative confocal micrographs by using Metamorph imaging software (Fig. 5B). In β1+/+ cells treated with chlorpromazine, the average pixel intensity representing reovirus particles was significantly diminished in comparison to that in untreated β1+/+ cells (Fig. 5B). However, chlorpromazine treatment did not diminish the

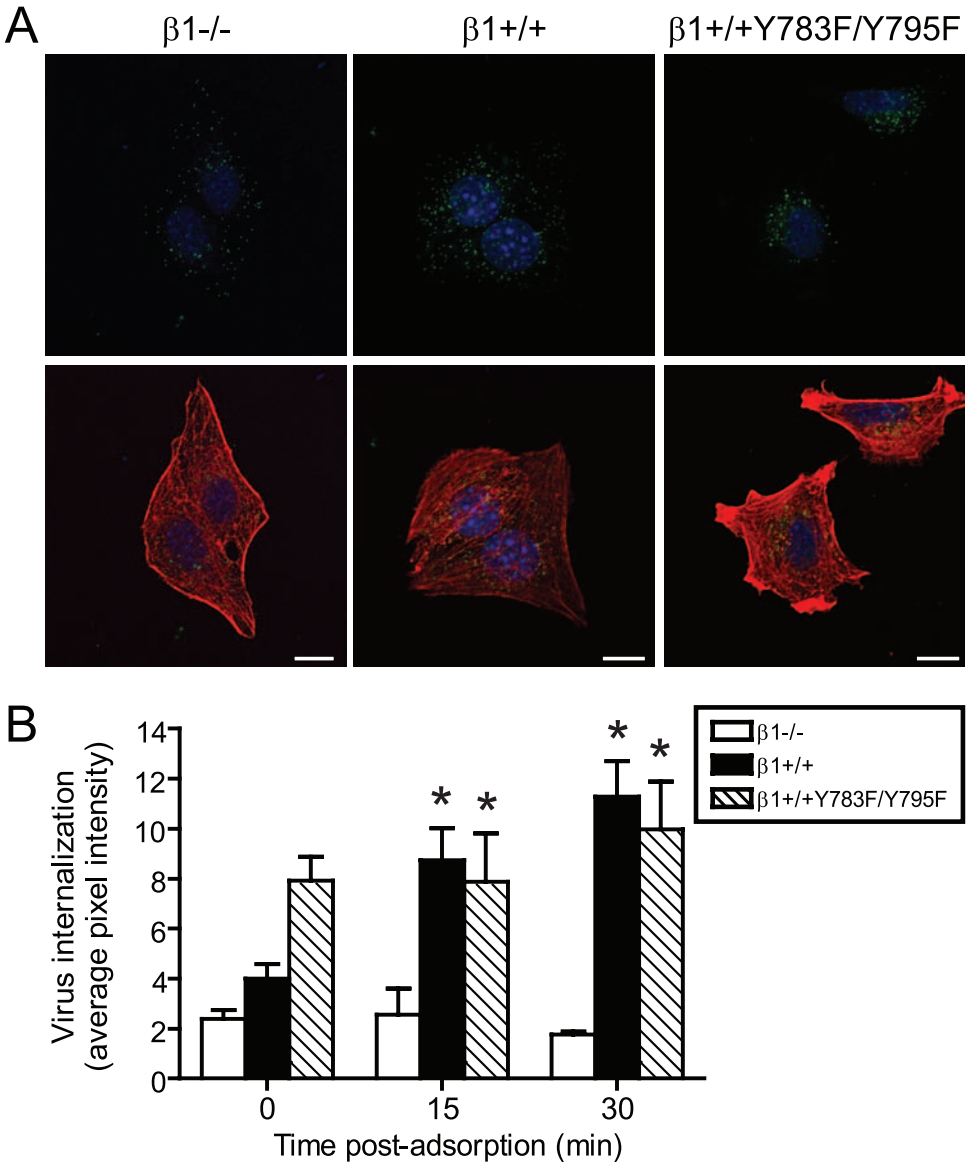

FIG. 3. Reovirus is internalized into β1+/+ and β1+/+Y783F/Y795F cells. β1−/−, β1+/+, and β1+/+Y783F/Y795F cells were adsorbed with 5×10^4 particles per cell of T1L virions and incubated at 4°C for 1 h. Nonadherent virus was removed, warm medium was added, and cells were incubated at 37°C. Cells were fixed over a time course, stained for reovirus (green), actin (red), and DNA (blue), and imaged using confocal immunofluorescence microscopy. (A) Representative digital fluorescence images of cells fixed at 30 min postadsorption are shown. Scale bars, 10 μm. (B) Fluorescent particles internalized into the cytoplasm were analyzed to determine the average pixel intensity of fluorescent particles per cell. Fluorescent particles localized at the cell periphery were excluded from the analysis. The results are expressed as the average pixel intensity per cell for five cells at each time point. Error bars indicate standard errors of the means. *, $P < 0.05$ in comparison to β1−/− cells.

pixel intensity in β1+/+Y783F/Y795F cells, indicating that reovirus internalization into β1+/+Y783F/Y795F cells is not inhibited by chlorpromazine (Fig. 5B). These data demonstrate that the reovirus uptake pathway in β1+/+ cells is chlorpromazine sensitive, whereas reovirus internalization into β1+/+Y783F/Y795F cells is mediated by an alternative uptake mechanism that is not sensitive to chlorpromazine and does not give rise to productive infection.

Intracellular trafficking of reovirus virions. To define the fate of reovirus virions in the endocytic pathway during internalization and disassembly, we performed an ultrastructural analysis of reovirus-infected cells. β1−/−, β1+/+, and β1+/+Y783F/Y795F cells were adsorbed with reovirus particles at 4°C for 1 h to allow virus binding, incubated at 37°C over a 30-min time course to allow internalization, and analyzed by transmission EM (Fig. 6). Fewer reovirus particles were detected in β1−/− cells than in β1+/+ and β1+/+Y783F/Y795F cells at all time points examined, consistent with the quantitative confocal microscopy data. In β1+/+ cells, and to a much lesser extent in β1−/− cells, reovirus particles were clearly visible in coated-pit and coated-vesicle structures at 0 min postadsorption (Fig. 6A, white arrows, and Fig. 6B). At 10, 20, and 30 min postadsorption, the majority of reovirus particles (Fig. 6A, black arrows, and data not shown) appeared in structures that morphologically resemble early endo-

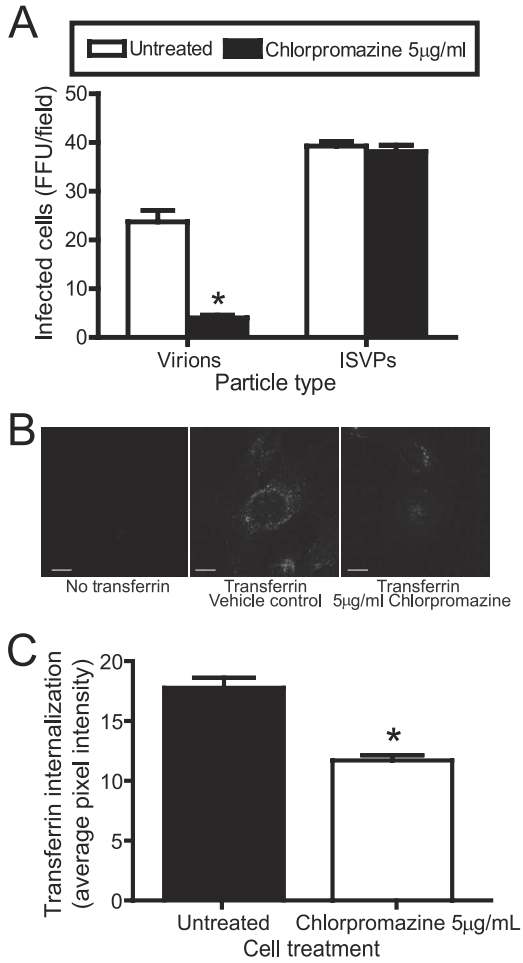

FIG. 4. Uptake of reovirus and transferrin into β1+/+ cells is chlorpromazine sensitive. (A) β1+/+ cells were pretreated with 5 μg of chlorpromazine per ml for 3 h, adsorbed with T1L virions or ISVPs at an MOI of 1 FFU per cell, and incubated at 4°C for 1 h. Cells were washed, complete medium with or without chlorpromazine was added, and cells were incubated at 37°C for 20 h. Cells were fixed and stained by indirect immunofluorescence. Infected cells were quantified by counting cells exhibiting cytoplasmic staining in three visual fields of equivalently confluent monolayers for triplicate samples. The results are expressed as mean FFU per visual field for triplicate samples. Error bars indicate standard deviations. These data are representative of results of three independent experiments performed in triplicate. *, $P < 0.05$ in comparison to untreated cells. (B) β1+/+ cells were pretreated with 5 μg per ml of chlorpromazine for 3 h and incubated with 2.5 μg per ml Alexa Fluor 488-conjugated transferrin in the presence or absence of 5 μg per ml chlorpromazine in incomplete medium at 37°C for 10 min. The medium was removed, and cells were washed, fixed, and imaged by confocal microscopy. Representative digital fluorescence images of untreated and chlorpromazine-treated cells incubated with transferrin are shown. Scale bars, 10 μm. (C) Untreated and chlorpromazine-treated cells were analyzed for fluorescent transferrin internalized into the cytoplasm to determine the average pixel intensity of transferrin per cell. Fluorescent signal localized at the cell periphery was excluded from the analysis. The results are expressed as the average pixel intensity per cell for 10 cells. Error bars indicate standard errors of the means. *, $P < 0.05$ in comparison to untreated cells.

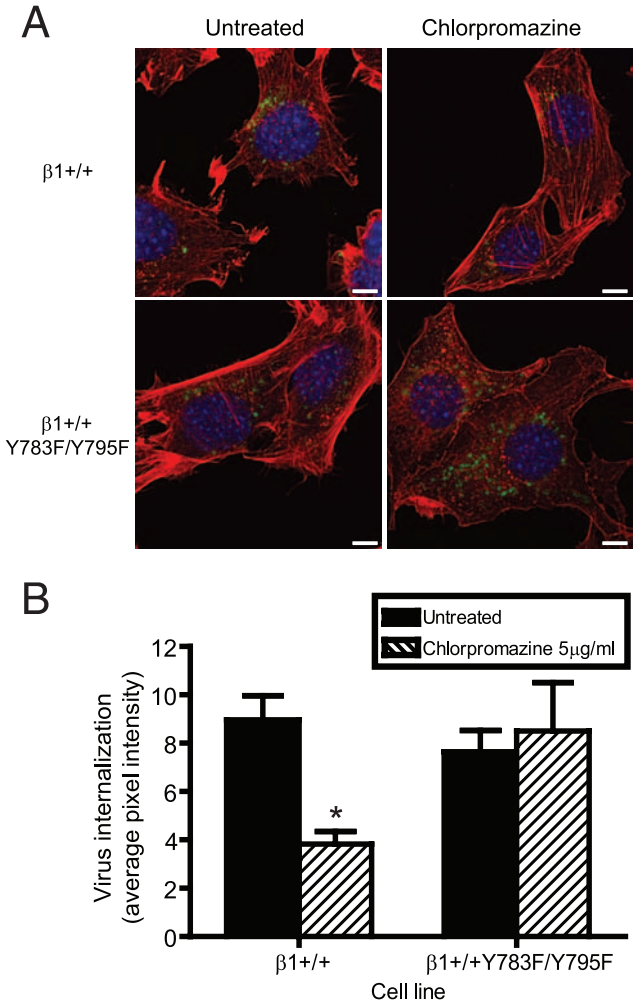

FIG. 5. β1 integrin NPXY motifs are required for functional reovirus internalization. β1+/+ and β1+/+Y783F/Y795F cells were pretreated with 5 μg per ml of chlorpromazine at 37°C for 3 h, adsorbed with 5×10^4 particles per cell of T1L virions in incomplete medium, and incubated at 4°C for 1 h. Cells where washed, complete medium with or without chlorpromazine was added, and cells were incubated at 37°C for 20 min. Cells were fixed, stained for reovirus (green), actin (red), and DNA (blue), and imaged using confocal immunofluorescence microscopy. (A) Representative digital fluorescence images of untreated and chlorpromazine-treated cells at 20 min postadsorption are shown. Scale bars, 10 μm. (B) Fluorescent particles internalized into the cytoplasm were analyzed to determine the average pixel intensity per cell. Fluorescent particles localized at the cell periphery were excluded from the analysis. The results are expressed as the average pixel intensity per cell for five cells. Error bars indicate standard errors of the means. *, $P < 0.05$ in comparison to untreated cells.

somes, which have an electron-lucent appearance, late endosomes, which appear larger and more electron dense, and primary lysosomes, which are small, electron-dense, membrane-bound vesicles. In β1+/+Y783F/Y795F cells, few reovirus particles were observed in coated-pit structures or structures that resemble endosomes. Instead, the majority of reovirus particles in β1+/+Y783F/Y795F cells localized in electron-dense, membrane-bound vesicular structures that morphologically resemble secondary lysosomes or phagolysosomes, which contain a notable amount of heterogeneous material (Fig. 6A and C, black arrowheads). These structures were present in both uninfected and infected β1−/− and β1+/+Y783F/Y795F cells, yet there were a greater number of these structures in the infected β1+/+Y783F/Y795F

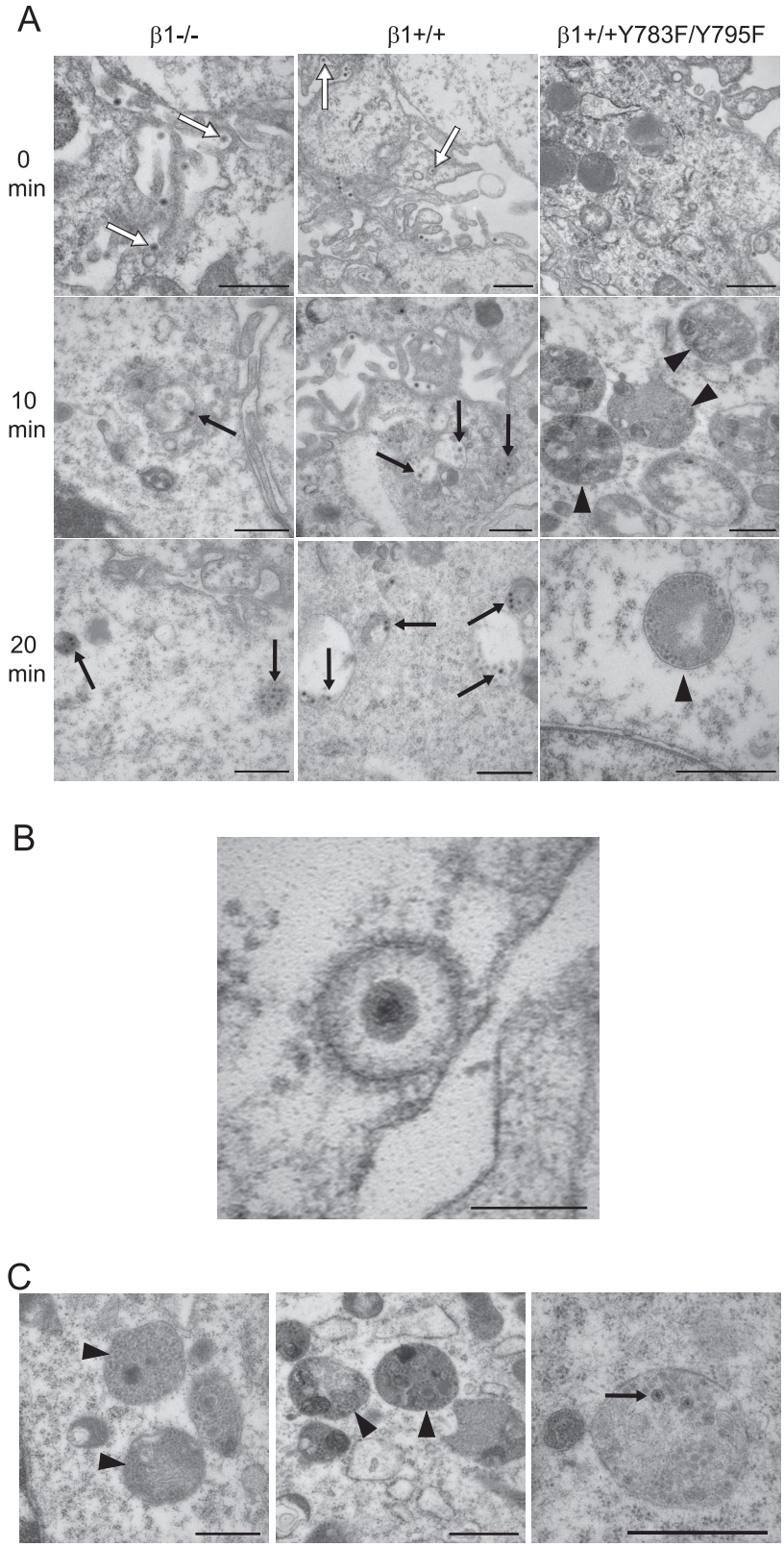

FIG. 6. Ultrastructural analysis of reovirus internalization. (A) β1−/−, β1+/+, and β1+/+Y783F/Y795F cells were adsorbed with 10^5 particles per cell of T1L virions at 4°C for 1 h, washed, and fixed or incubated in complete medium at 37°C. At 10-min intervals, cells were washed, collected by centrifugation, fixed, and stained for EM. Representative images at 0, 10, and 20 min postadsorption are shown. Reovirus virions localized in coated pits and coated vesicles are indicated by white arrows. Reovirus virions localized in structures that resemble early and late endosomes and primary lysosomes are indicated by black arrows. Secondary lysosomes are indicated by black arrowheads. Scale bars, 500 nm. (B) Representative image of reovirus virion in a coated pit structure in β1+/+ cells at 0 min postadsorption. Scale bar, 100 nm. (C) Representative images of organelles resembling secondary lysosomes containing reovirus particles in β1+/+Y783F/Y795F cells at 10, 20, and 30 min postadsorption (left, center, and right, respectively). Reovirus virions are indicated by black arrows. Secondary lysosomes are indicated by black arrowheads. Scale bars, 500 nm.

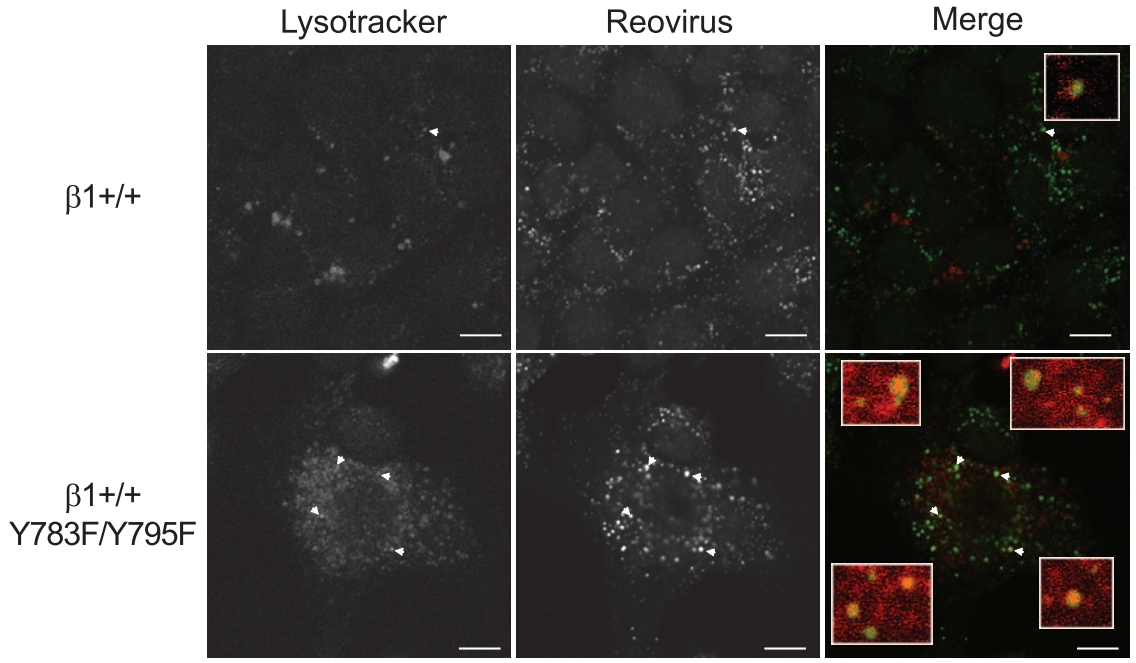

FIG. 7. Intracellular transport of reovirus particles is altered in β1+/+Y783F/Y795F cells. β1+/+ and β1+/+Y783F/Y795F cells were pretreated with Lysotracker-Red DND-99 dye (Lysotracker), adsorbed with 5×10^4 particles per cell of T1L virions (Reovirus), and incubated at 4°C for 1 h. Nonadherent virus was removed, warm medium was added, and cells were incubated at 37°C. Cells were fixed over a time course and stained for reovirus. Images were analyzed for colocalization using ImageJ (version 1.37v) Colocalize RGB plug-in. Representative digital fluorescence images pseudocolored as monochromatic images or fluorescence images of cells fixed at 40 min postadsorption are shown. Lysotracker-Red DND-99 dye is colored red; reovirus is colored green. White arrowheads indicate areas of colocalization, which are magnified in the insets. Scale bars, 10 μm.

cells (Fig. 6A). These findings suggest that NPXY-to-F mutations in the β1 integrin cytoplasmic tail lead to delivery of reovirus virions to an endocytic compartment incapable of either supporting functional capsid disassembly or allowing release of uncoated particles into the cytoplasm.

In a complementary approach to assess the intracellular distribution of reovirus particles following internalization into β1+/+ and β1+/+Y783F/Y795F cells, both cell types were pretreated with the lysosomal-specific marker, Lysotracker-Red DND-99 dye, adsorbed with reovirus virions, and examined by confocal immunofluorescence microscopy (Fig. 7 and data not shown). Reovirus particles appeared in vesicles marked by Lysotracker-Red DND-99 dye in both β1+/+ and β1+/+Y783F/Y795F cells, yet substantially more viral particles were localized to these structures in β1+/+Y783F/Y795F cells at 40 min postadsorption than in β1+/+ cells at that time point (Fig. 7, white arrowheads). These data suggest that while reovirus particles are transported to a lysosomal compartment in both β1+/+ and β1+/+Y783F/Y795F cells, virions in β1+/+ cells egress this compartment to initiate an infectious cycle, while virions in β1+/+Y783F/Y795F cells are trapped and fail to productively infect the cell.

DISCUSSION

The goal of this study was to gain a better understanding of mechanisms by which β1 integrin mediates reovirus internalization. The data demonstrate a function for the β1 integrin NPXY motifs in reovirus endocytosis and endocytic transport. Tyrosine-to-phenylalanine mutation of the β1 integrin NPXY motifs leads to an aberrant pathway of reovirus internalization that does not yield infectious progeny. EM analysis indicates that reovirus virions are internalized into β1+/+Y783F/Y795F cells yet localize in organelles that morphologically resemble secondary lysosomes rather than in endosomes and lysosomes as they do in β1+/+ cells. Reovirus internalization into β1+/+ cells is mediated by a chlorpromazine-sensitive pathway, most likely clathrin-dependent endocytosis, yet particles internalized into β1+/+Y783F/Y95F cells enter by a different route. Collectively, these data indicate that β1 integrin serves to deliver reovirus to the endocytic compartment required to complete subsequent steps in the viral life cycle.

Findings presented in this report provide new insights into mechanisms by which reovirus enters into cells. After attachment to carbohydrate (4, 19, 46, 47) and JAM-A (5, 14, 50), reovirus is internalized into the endocytic pathway by β1 integrin (34). Our results indicate that this process is dependent on signals elicited by the NPXY motifs in the β1 integrin cytoplasmic tail. Since chlorpromazine diminishes reovirus entry and infection in β1+/+ cells, but does not affect reovirus uptake into β1+/+Y783F/Y795F cells, it is likely that the β1 integrin NPXY motifs recruit the endocytic machinery to deliver reovirus to the endocytic organelle required for capsid disassembly and release of the viral core into the cytoplasm.

NPXY motifs recruit clathrin and adaptor proteins and serve as cargo recognition motifs to direct the delivery of cargo to endosomes and lysosomes (10, 37). For example, NPXY motifs recruit AP-2 to the cell surface by directly interacting with the AP-2 μ2

subunit (9). The β2 subunit of AP-2 then binds clathrin subunits (45) and initiates clathrin assembly at the plasma membrane, which leads to accumulation of clathrin at the cell surface for clathrin-mediated endocytosis (44). NPXY motifs also recruit Dab2 (38, 44), which directly interacts with NPXY motifs via the Dab2 phosphotyrosine binding domain (37). Dab2 induces clathrin-mediated endocytosis by binding either to clathrin (37) or to AP-2 (39). Dab2 recognizes either phosphorylated or nonphosphorylated tyrosines of NPXY motifs (37, 38). Therefore, in β1+/+Y783F/Y795F-infected cells, Dab2 could potentially engage β1 integrin with NPXY-to-F mutations and mediate reovirus internalization but direct particles to a nonfunctional endocytic compartment. Since reovirus infection requires acid-dependent proteolytic disassembly (2, 23, 59), virus delivery to an intracellular site other than an endosomal compartment containing the appropriate pH (59) and proteolytic enzymes (23) could result in the failure of reovirus particles to uncoat and penetrate into the cytoplasm. Our experiments using Lysotracker-Red DND-99 dye suggest that reovirus virions distribute to a lysosomal compartment in both β1+/+ and β1+/+Y783F/Y795F cells (Fig. 7). However, this marker does not distinguish between primary and secondary lysosomes, which appear morphologically distinct (Fig. 6). Additional experiments are required to define the intracellular transport pathways traversed by reovirus following uptake into wild-type and mutant cells.

Since phenylalanine residues cannot be phosphorylated, our findings with cells expressing β1 integrin with NPXY-to-F mutations in the cytoplasmic tail raise the possibility that reovirus interactions with β1 integrin lead to tyrosine phosphorylation of the NPXY motifs. In support of this hypothesis, v-*src* transformation of β1+/+ cells but not β1+/+Y783F/Y795F cells results in phosphorylation of β1 integrin (53), suggesting that the NPXY tyrosine residues can serve as substrates for phosphorylation. It is possible that phosphorylation of the β1 integrin NPXY motifs is required for postattachment signaling events required for reovirus endocytosis or other steps in the virus life cycle. For example, phosphorylation of the NPXY tyrosine residues is required for autophosphorylation of focal adhesion kinase (68). Thus, reovirus-β1 integrin interactions may induce phosphorylation and activation of integrin-linked signaling pathways.

It is also possible that the β1 integrin NPXY motifs mediate functional reovirus internalization by an indirect mechanism. The NPXY motifs in the β1 integrin cytoplasmic tail are separated by eight residues that form a tight β turn (3, 63). This region serves as a docking site for phosphotyrosine binding domain-containing proteins (61), including talin (13) and integrin cytoplasmic domain-associated protein 1-α (18). In addition, two of the intervening residues are threonines at positions 788 and 789, and Thr788 is notably essential for integrin activation and ligand engagement (41). Therefore, mutation of the NPXY motifs may result in structural alterations that affect the β1 integrin cytoplasmic tail and preclude engagement of the cytosolic molecules required for reovirus uptake or sorting within the endocytic pathway.

β1+/+Y783F/Y795F cells are surprisingly less permissive for reovirus infection than β1−/− cells (Fig. 2). Since both β1−/− and β1+/+Y783F/Y795F cells express JAM-A on the cell surface, it is possible that reovirus infection of these cells occurs via attachment to JAM-A and internalization via a non-β1-integrin-dependent mechanism, resulting in a low level of infection. However, in the case of β1+/+Y783F/Y795F cells, it is possible that virus interactions with the mutant form of β1 integrin are preferred to non-β1 integrin internalization routes, resulting in delivery of virions to a nonproductive entry pathway as a consequence of the NPXY-to-F mutations. Thus, these data do not exclude the possibility that reovirus utilizes coreceptors other than β1 integrin to internalize into cells after binding to JAM-A. Additionally, it is possible that reovirus internalization may occur via both clathrin-dependent and clathrin-independent mechanisms, which has been reported for influenza virus (56).

Following adsorption to β1+/+Y783F/Y795F cells, reovirus virions localize in electron-dense, membrane-bound vesicular structures that morphologically resemble secondary lysosomes or phagolysosomes (Fig. 6). These structures are present in both uninfected and infected β1−/− and β1+/+Y783F/Y795F cells at all time points analyzed. However, they are not apparent in either uninfected or infected β1+/+ cells. These observations suggest that the lack of β1 integrin signaling or recycling has a detrimental effect on endocytic transport that alters the morphology of endocytic organelles. As probed by analysis of reovirus internalization, these alterations are associated with impairments in the sorting or processing of cargo in the endocytic compartment.

β1 integrin NPXY motifs are required for efficient uptake of *Y. pseudotuberculosis* by clathrin-mediated endocytosis (28, 64). However, mutation of the NPXY motifs to NPXF does not affect internalization of *Y. pseudotuberculosis*; instead, mutation to NPXA leads to abolished *Y. pseudotuberculosis* uptake. Transgenic mice expressing β1 integrin with NPXY-to-F mutations are viable (21), whereas those expressing NPXY-to-A mutations recapitulate the phenotype of β1-null mice and arrest in embryogenesis (21). These data indicate that there are key functional differences mediated by the nature of β1 integrin NPXY motif alterations. In contrast to studies of *Y. pseudotuberculosis*, we found that mutation of NPXY to NPXF results in a nonfunctional route of internalization for reovirus, suggesting that the β1 integrin NPXY motifs play an important regulatory role in endocytic uptake and transport in the endocytic pathway. Our findings, coupled with previous findings made with *Y. pseudotuberculosis* (28, 64), provide support for the idea that β1 integrin NPXY motifs are required for multiple functions in the process of endocytosis. Understanding mechanisms by which integrins engage the endocytic machinery to mediate endocytosis of microbes should provide a useful avenue to investigate integrin cell biology and lead to the identification of new targets for anti-infective drug development.

ACKNOWLEDGMENTS

We thank Pranav Danthi and members of the Dermody laboratory for advice and technical assistance. We thank Elvin Woodruff for performing the EM studies and Agnes Fogo and Anne Kenworthy for assistance in interpretation of the EM images. We thank the Nashville Veterans Hospital Flow Cytometry Core for flow cytometric analysis. Confocal microscopy experiments were performed in part through use of the VUMC Cell Imaging Shared Resource. We thank Deane Mosher (University of Wisconsin, Madison) for providing GD25 cell lines. We thank Beat Imof (Université de Genève) for providing mJAM-A-specific MAb H202-106-7-4.

This research was supported by Public Health Service awards T32 AI007281 (M.S.M.), T32 HL07751 (B.A.M.), T32 HL07526 (A.D.),

T32 AI07611 (E.M.J.), R01 AI32539, the Vanderbilt Research Council (M.S.M.), a Veterans Affairs Merit Award (R.Z.), and the Elizabeth B. Lamb Center for Pediatric Research. Additional support was provided by Public Health Service awards P30 CA68485 for the Vanderbilt-Ingram Cancer Center and P60 DK20593 for the Vanderbilt Diabetes Research and Training Center.

REFERENCES

1. **Agosto, M. A., T. Ivanovic, and M. L. Nibert.** 2006. Mammalian reovirus, a nonfusogenic nonenveloped virus, forms size-selective pores in a model membrane. Proc. Natl. Acad. Sci. USA **103:**16496–16501.
2. **Baer, G. S., and T. S. Dermody.** 1997. Mutations in reovirus outer-capsid protein σ3 selected during persistent infections of L cells confer resistance to protease inhibitor E64. J. Virol. **71:**4921–4928.
3. **Bansal, A., and L. M. Gierasch.** 1991. The NPXY internalization signal of the LDL receptor adopts a reverse-turn conformation. Cell **67:**1195–1201.
4. **Barton, E. S., J. L. Connolly, J. C. Forrest, J. D. Chappell, and T. S. Dermody.** 2001. Utilization of sialic acid as a coreceptor enhances reovirus attachment by multistep adhesion strengthening. J. Biol. Chem. **276:**2200–2211.
5. **Barton, E. S., J. C. Forrest, J. L. Connolly, J. D. Chappell, Y. Liu, F. Schnell, A. Nusrat, C. A. Parkos, and T. S. Dermody.** 2001. Junction adhesion molecule is a receptor for reovirus. Cell **104:**441–451.
6. **Bergelson, J. M., M. P. Shepley, B. M. Chan, M. E. Hemler, and R. W. Finberg.** 1992. Identification of the integrin VLA-2 as a receptor for echovirus 1. Science **255:**1718–1720.
7. **Blanchard, E., S. Belouzard, L. Goueslain, T. Wakita, J. Dubuisson, C. Wychowski, and Y. Rouille.** 2006. Hepatitis C virus entry depends on clathrin-mediated endocytosis. J. Virol. **80:**6964–6972.
8. **Boll, W., H. Ohno, Z. Songyang, I. Rapoport, L. C. Cantley, J. S. Bonifacino, and T. Kirchhausen.** 1996. Sequence requirements for the recognition of tyrosine-based endocytic signals by clathrin AP-2 complexes. EMBO J. **15:**5789–5795.
9. **Boll, W., I. Rapoport, C. Brunner, Y. Modis, S. Prehn, and T. Kirchhausen.** 2002. The μ2 subunit of the clathrin adaptor AP-2 binds to FDNPVY and Yppϕ sorting signals at distinct sites. Traffic **3:**590–600.
10. **Bonifacino, J. S., and L. M. Traub.** 2003. Signals for sorting of transmembrane proteins to endosomes and lysosomes. Annu. Rev. Biochem. **72:**395–447.
11. **Borsa, J., B. D. Morash, M. D. Sargent, T. P. Copps, P. A. Lievaart, and J. G. Szekely.** 1979. Two modes of entry of reovirus particles into L cells. J. Gen. Virol. **45:**161–170.
12. **Borsa, J., M. D. Sargent, P. A. Lievaart, and T. P. Copps.** 1981. Reovirus: evidence for a second step in the intracellular uncoating and transcriptase activation process. Virology **111:**191–200.
13. **Calderwood, D. A., R. Zent, R. Grant, D. J. Rees, R. O. Hynes, and M. H. Ginsberg.** 1999. The Talin head domain binds to integrin β subunit cytoplasmic tails and regulates integrin activation. J. Biol. Chem. **274:**28071–28074.
14. **Campbell, J. A., P. Shelling, J. D. Wetzel, E. M. Johnson, G. A. R. Wilson, J. C. Forrest, M. Aurrand-Lions, B. Imhof, T. Stehle, and T. S. Dermody.** 2005. Junctional adhesion molecule A serves as a receptor for prototype and field-isolate strains of mammalian reovirus. J. Virol. **79:**7967–7978.
15. **Chandran, K., D. L. Farsetta, and M. L. Nibert.** 2002. Strategy for nonenveloped virus entry: a hydrophobic conformer of the reovirus membrane penetration protein μ1 mediates membrane disruption. J. Virol. **76:**9920–9933.
16. **Chandran, K., J. S. Parker, M. Ehrlich, T. Kirchhausen, and M. L. Nibert.** 2003. The delta region of outer-capsid protein μ1 undergoes conformational change and release from reovirus particles during cell entry. J. Virol. **77:**13361–13375.
17. **Chang, C. T., and H. J. Zweerink.** 1971. Fate of parental reovirus in infected cell. Virology **46:**544–555.
18. **Chang, D. D., C. Wong, H. Smith, and J. Liu.** 1997. ICAP-1, a novel β1 integrin cytoplasmic domain-associated protein, binds to a conserved and functionally important NPXY sequence motif of β1 integrin. J. Cell Biol. **138:**1149–1157.
19. **Chappell, J. D., V. L. Gunn, J. D. Wetzel, G. S. Baer, and T. S. Dermody.** 1997. Mutations in type 3 reovirus that determine binding to sialic acid are contained in the fibrous tail domain of viral attachment protein σ1. J. Virol. **71:**1834–1841.
20. **Chu, J. J., and M. L. Ng.** 2004. Interaction of West Nile virus with $\alpha_v\beta_3$ integrin mediates virus entry into cells. J. Biol. Chem. **279:**54533–54541.
21. **Czuchra, A., H. Meyer, K. R. Legate, C. Brakebusch, and R. Fassler.** 2006. Genetic analysis of β1 integrin "activation motifs" in mice. J. Cell Biol. **174:**889–899.
22. **Davis, C. G., M. A. Lehrman, D. W. Russell, R. G. Anderson, M. S. Brown, and J. L. Goldstein.** 1986. The J. D. mutation in familial hypercholesterolemia: amino acid substitution in cytoplasmic domain impedes internalization of LDL receptors. Cell **45:**15–24.
23. **Ebert, D. H., J. Deussing, C. Peters, and T. S. Dermody.** 2002. Cathepsin L and cathepsin B mediate reovirus disassembly in murine fibroblast cells. J. Biol. Chem. **277:**24609–24617.
24. **Ehrlich, M., W. Boll, A. Van Oijen, R. Hariharan, K. Chandran, M. L. Nibert, and T. Kirchhausen.** 2004. Endocytosis by random initiation and stabilization of clathrin-coated pits. Cell **118:**591–605.
25. **Feire, A. L., H. Koss, and T. Compton.** 2004. Cellular integrins function as entry receptors for human cytomegalovirus via a highly conserved disintegrin-like domain. Proc. Natl. Acad. Sci. USA **101:**15470–15475.
26. **Furlong, D. B., M. L. Nibert, and B. N. Fields.** 1988. Sigma 1 protein of mammalian reoviruses extends from the surfaces of viral particles. J. Virol. **62:**246–256.
27. **Guerrero, C. A., E. Mendez, S. Zarate, P. Isa, S. Lopez, and C. F. Arias.** 2000. Integrin $\alpha_v\beta_3$ mediates rotavirus cell entry. Proc. Natl. Acad. Sci. USA **97:**14644–14649.
28. **Gustavsson, A., A. Armulik, C. Brakebusch, R. Fassler, S. Johansson, and M. Fallman.** 2002. Role of the β1-integrin cytoplasmic tail in mediating invasin-promoted internalization of Yersinia. J. Cell Sci. **115:**2669–2678.
29. **Harding, C., J. Heuser, and P. Stahl.** 1983. Receptor-mediated endocytosis of transferrin and recycling of the transferrin receptor in rat reticulocytes. J. Cell Biol. **97:**329–339.
30. **Hewish, M. J., Y. Takada, and B. S. Coulson.** 2000. Integrins α2β1 and α4β1 can mediate SA11 rotavirus attachment and entry into cells. J. Virol. **74:**228–236.
31. **Hynes, R. O.** 2002. Integrins: bidirectional, allosteric signaling machines. Cell **110:**673–687.
32. **Hynes, R. O.** 1992. Integrins: versatility, modulation, and signaling in cell adhesion. Cell **69:**11–25.
33. **Isberg, R. R., and J. M. Leong.** 1990. Multiple β1 chain integrins are receptors for invasin, a protein that promotes bacterial penetration into mammalian cells. Cell **60:**861–871.
34. **Maginnis, M. S., J. C. Forrest, S. A. Kopecky-Bromberg, S. K. Dickeson, S. A. Santoro, M. M. Zutter, G. R. Nemerow, J. M. Bergelson, and T. S. Dermody.** 2006. β1 integrin mediates internalization of mammalian reovirus. J. Virol. **80:**2760–2770.
35. **Maratos-Flier, E., M. J. Goodman, A. H. Murray, and C. R. Kahn.** 1986. Ammonium inhibits processing and cytotoxicity of reovirus, a nonenveloped virus. J. Clin. Investig. **78:**617–625.
36. **Marsh, M., and A. Helenius.** 2006. Virus entry: open sesame. Cell **124:**729–740.
37. **Mishra, S. K., P. A. Keyel, M. J. Hawryluk, N. R. Agostinelli, S. C. Watkins, and L. M. Traub.** 2002. Disabled-2 exhibits the properties of a cargo-selective endocytic clathrin adaptor. EMBO J. **21:**4915–4926.
38. **Morris, S. M., and J. A. Cooper.** 2001. Disabled-2 colocalizes with the LDLR in clathrin-coated pits and interacts with AP-2. Traffic **2:**111–123.
39. **Morris, S. M., M. D. Tallquist, C. O. Rock, and J. A. Cooper.** 2002. Dual roles for the Dab2 adaptor protein in embryonic development and kidney transport. EMBO J. **21:**1555–1564.
40. **Nibert, M. L., A. L. Odegard, M. A. Agosto, K. Chandran, and L. A. Schiff.** 2005. Putative autocleavage of reovirus μ1 protein in concert with outercapsid disassembly and activation for membrane permeabilization. J. Mol. Biol. **345:**461–474.
41. **Nilsson, S., D. Kaniowska, C. Brakebusch, R. Fassler, and S. Johansson.** 2006. Threonine 788 in integrin subunit beta1 regulates integrin activation. Exp. Cell Res. **312:**844–853.
42. **Odegard, A. L., K. Chandran, X. Zhang, J. S. Parker, T. S. Baker, and M. L. Nibert.** 2004. Putative autocleavage of outer capsid protein μ1, allowing release of myristoylated peptide μ1N during particle uncoating, is critical for cell entry by reovirus. J. Virol. **78:**8732–8745.
43. **Ohno, H., J. Stewart, M. C. Fournier, H. Bosshart, I. Rhee, S. Miyatake, T. Saito, A. Gallusser, T. Kirchhausen, and J. S. Bonifacino.** 1995. Interaction of tyrosine-based sorting signals with clathrin-associated proteins. Science **269:**1872–1875.
44. **Oleinikov, A. V., J. Zhao, and S. P. Makker.** 2000. Cytosolic adaptor protein Dab2 is an intracellular ligand of endocytic receptor gp600/megalin. Biochem. J. **347:**613–621.
45. **Owen, D. J., Y. Vallis, B. M. Pearse, H. T. McMahon, and P. R. Evans.** 2000. The structure and function of the β2-adaptin appendage domain. EMBO J. **19:**4216–4227.
46. **Pacitti, A., and J. R. Gentsch.** 1987. Inhibition of reovirus type 3 binding to host cells by sialylated glycoproteins is mediated through the viral attachment protein. J. Virol. **61:**1407–1415.
47. **Paul, R. W., A. H. Choi, and P. W. K. Lee.** 1989. The α-anomeric form of sialic acid is the minimal receptor determinant recognized by reovirus. Virology **172:**382–385.
48. **Pearse, B. M.** 1982. Coated vesicles from human placenta carry ferritin, transferrin, and immunoglobulin G. Proc. Natl. Acad. Sci. USA **79:**451–455.
49. **Pho, M. T., A. Ashok, and W. J. Atwood.** 2000. JC virus enters human glial cells by clathrin-dependent receptor-mediated endocytosis. J. Virol. **74:**2288–2292.
50. **Prota, A. E., J. A. Campbell, P. Schelling, J. C. Forrest, T. R. Peters, M. J. Watson, M. Aurrand-Lions, B. Imhof, T. S. Dermody, and T. Stehle.** 2003.

Crystal structure of human junctional adhesion molecule 1: implications for reovirus binding. Proc. Natl. Acad. Sci. USA **100:**5366–5371.
51. **Reszka, A. A., Y. Hayashi, and A. F. Horwitz.** 1992. Identification of amino acid sequences in the integrin β1 cytoplasmic domain implicated in cytoskeletal association. J. Cell Biol. **117:**1321–1330.
52. **Rubin, D. H., D. B. Weiner, C. Dworkin, M. I. Greene, G. G. Maul, and W. V. Williams.** 1992. Receptor utilization by reovirus type 3: distinct binding sites on thymoma and fibroblast cell lines result in differential compartmentalization of virions. Microb. Pathog. **12:**351–365.
53. **Sakai, T., R. Jove, R. Fassler, and D. F. Mosher.** 2001. Role of the cytoplasmic tyrosines of β1A integrins in transformation by v-src. Proc. Natl. Acad. Sci. USA **98:**3808–3813.
54. **Sakai, T., Q. Zhang, R. Fassler, and D. F. Mosher.** 1998. Modulation of β1A integrin functions by tyrosine residues in the β1 cytoplasmic domain. J. Cell Biol. **141:**527–538.
55. **Schiff, L. A., M. L. Nibert, and K. L. Tyler.** 2007. Orthoreoviruses and their replication, p. 1853–1915. *In* D. M. Knipe, P. M. Howley, D. E. Griffin, R. A. Lamb, M. A. Martin, B. Roizman, and S. E. Straus (ed.), Fields virology, 5th ed., vol. 2. Lippincott Williams & Wilkins, Philadelphia, PA.
56. **Sieczkarski, S. B., and G. R. Whittaker.** 2002. Influenza virus can enter and infect cells in the absence of clathrin-mediated endocytosis. J. Virol. **76:** 10455–10464.
57. **Silverstein, S. C., C. Astell, D. H. Levin, M. Schonberg, and G. Acs.** 1972. The mechanism of reovirus uncoating and gene activation *in vivo*. Virology **47:**797–806.
58. **Smith, R. E., H. J. Zweerink, and W. K. Joklik.** 1969. Polypeptide components of virions, top component and cores of reovirus type 3. Virology **39:**791–810.
59. **Sturzenbecker, L. J., M. L. Nibert, D. B. Furlong, and B. N. Fields.** 1987. Intracellular digestion of reovirus particles requires a low pH and is an essential step in the viral infectious cycle. J. Virol. **61:**2351–2361.
60. **Sun, X., V. K. Yau, B. J. Briggs, and G. R. Whittaker.** 2005. Role of clathrin-mediated endocytosis during vesicular stomatitis virus entry into host cells. Virology **338:**53–60.
61. **Trub, T., W. E. Choi, G. Wolf, E. Ottinger, Y. Chen, M. Weiss, and S. E. Shoelson.** 1995. Specificity of the PTB domain of Shc for β turn-forming pentapeptide motifs amino-terminal to phosphotyrosine. J. Biol. Chem. **270:** 18205–18208.
62. **Turk, V., B. Turk, and D. Turk.** 2001. Lysosomal cysteine proteases: facts and opportunities. EMBO J. **20:**4629–4633.
63. **Ulmer, T. S., B. Yaspan, M. H. Ginsberg, and I. D. Campbell.** 2001. NMR analysis of structure and dynamics of the cytosolic tails of integrin αIIb β3 in aqueous solution. Biochemistry **40:**7498–7508.
64. **Van Nhieu, G. T., E. S. Krukonis, A. A. Reszka, A. F. Horwitz, and R. R. Isberg.** 1996. Mutations in the cytoplasmic domain of the integrin β1 chain indicate a role for endocytosis factors in bacterial internalization. J. Biol. Chem. **271:**7665–7672.
65. **Virgin, H. W., K. L. Tyler, and T. S. Dermody.** 1997. Reovirus, p. 669–699. *In* N. Nathanson (ed.), Viral pathogenesis. Lippincott-Raven, New York, NY.
66. **Virgin, H. W., IV, R. Bassel-Duby, B. N. Fields, and K. L. Tyler.** 1988. Antibody protects against lethal infection with the neurally spreading reovirus type 3 (Dearing). J. Virol. **62:**4594–4604.
67. **Wang, L. H., K. G. Rothberg, and R. G. Anderson.** 1993. Mis-assembly of clathrin lattices on endosomes reveals a regulatory switch for coated pit formation. J. Cell Biol. **123:**1107–1117.
68. **Wennerberg, K., A. Armulik, T. Sakai, M. Karlsson, R. Fassler, E. M. Schaefer, D. F. Mosher, and S. Johansson.** 2000. The cytoplasmic tyrosines of integrin subunit β1 are involved in focal adhesion kinase activation. Molec. Cell Biol. **20:**5758–5765.
69. **Wennerberg, K., R. Fassler, B. Warmegard, and S. Johansson.** 1998. Mutational analysis of the potential phosphorylation sites in the cytoplasmic domain of integrin β1A: requirement for threonines 788–789 in receptor activation. J. Cell Sci. **111:**1117–1126.
70. **Wennerberg, K., L. Lohikangas, D. Gullberg, M. Pfaff, S. Johansson, and R. Fassler.** 1996. β1 integrin-dependent and -independent polymerization of fibronectin. J. Cell Biol. **132:**227–238.
71. **Wetzel, J. D., J. D. Chappell, A. B. Fogo, and T. S. Dermody.** 1997. Efficiency of viral entry determines the capacity of murine erythroleukemia cells to support persistent infections by mammalian reoviruses. J. Virol. **71:**299–306.
72. **Wickham, T. J., P. Mathias, D. A. Cheresh, and G. R. Nemerow.** 1993. Integrins $\alpha_v b_3$ and $\alpha_v b_5$ promote adenovirus internalization but not virus attachment. Cell **73:**309–319.

REFERENCES

1. Marsh, M., and Helenius, A. 2006. Virus entry: open sesame. *Cell* 124:729-740.

2. Chappell, J.D., Prota, A., Dermody, T.S., and Stehle, T. 2002. Crystal structure of reovirus attachment protein σ1 reveals evolutionary relationship to adenovirus fiber. *EMBO J.* 21:1-11.

3. Dryden, K.A., Wang, G., Yeager, M., Nibert, M.L., Coombs, K.M., Furlong, D.B., Fields, B.N., and Baker, T.S. 1993. Early steps in reovirus infection are associated with dramatic changes in supramolecular structure and protein conformation: analysis of virions and subviral particles by cryoelectron microscopy and image reconstruction. *J. Cell Biol.* 122:1023-1041.

4. Ebert, D.H., Deussing, J., Peters, C., and Dermody, T.S. 2002. Cathepsin L and cathepsin B mediate reovirus disassembly in murine fibroblast cells. *J. Biol. Chem.* 277:24609-24617.

5. Zhang, X., Walker, S.B., Chipman, P.R., Nibert, M.L., and Baker, T.S. 2003. Reovirus polymerase λ 3 localized by cryo-electron microscopy of virions at a resolution of 7.6 A. *Nat Struct Biol* 10:1011-1018.

6. Drayna, D., and Fields, B.N. 1982. Activation and characterization of the reovirus transcriptase: genetic analysis. *J. Virol.* 41:110-118.

7. Starnes, M.C., and Joklik, W.K. 1993. Reovirus protein λ3 is a poly(C)-dependent poly(G) polymerase. *Virology* 193:356-366.

8. Tao, Y., Farsetta, D.L., Nibert, M.L., and Harrison, S.C. 2002. RNA synthesis in a cage - structural studies of reovirus polymerase λ3. *Cell* 111:733-745.

9. Kim, J., Parker, J.S., Murray, K.E., and Nibert, M.L. 2004. Nucleoside and RNA triphosphatase activities of orthoreovirus transcriptase cofactor μ2. *J Biol Chem* 279:4394-4403.

10. Noble, S., and Nibert, M.L. 1997. Core protein mu2 is a second determinant of nucleoside triphosphatase activities by reovirus cores. *J. Virol.* 71:7728-7735.

11. Yin, P., Cheang, M., and Coombs, K.M. 1996. The M1 gene is associated with differences in the temperature optimum of the transcriptase activity in reovirus core particles. *J. Virol.* 70:1223-1227.

12. Kirchner, E., Guglielmi, K.M., Strauss, H.M., Dermody, T.S., and Stehle, T. 2008. Structure of reovirus σ1 in complex with its receptor junctional adhesion molecule-A. *PLoS Pathog* 4:e1000235.

13. Liemann, S., Chandran, K., Baker, T.S., Nibert, M.L., and Harrison, S.C. 2002. Structure of the reovirus membrane-penetration protein, μ1, in a complex with its protector protein, σ3. *Cell* 108:283-295.

14. Cleveland, D.R., Zarbl, H., and Millward, S. 1986. Reovirus guanyltransferase is L2 gene product lambda 2. *J. Virol.* 60:307-311.

15. Mao, Z.X., and Joklik, W.K. 1991. Isolation and enzymatic characterization of protein λ2, the reovirus guanylytransferase. *Virology* 185:377-386.

16. Sabin, A.B. 1959. Reoviruses: a new group of respiratory and enteric viruses formerly classified as ECHO type 10 is described. *Science* 130:1387-1389.

17. Rosen, L. 1960. Serologic grouping of reovirus by hemagglutination-inhibition. *American Journal of Hygiene* 71:242-249.

18. Virgin, H.W., Tyler, K.L., and Dermody, T.S. 1997. Reovirus. In *Viral Pathogenesis*. N. Nathanson, editor. New York: Lippincott-Raven. 669-699.

19. Kobayashi, T., Antar, A.A.R., Boehme, K.W., Danthi, P., Eby, E.A., Guglielmi, K.M., Holm, G.H., Johnson, E.M., Maginnis, M.S., Naik, S., Skelton, W.B., Wetzel, J.D., Wilson, G.J., Chappell, J.D., and Dermody, T.S. 2007. A plasmid-based reverse genetics system for animal double-stranded RNA viruses. *Cell Host Microbe* 1:147-157.

20. Chang, C.T., and Zweerink, H.J. 1971. Fate of parental reovirus in infected cell. *Virology* 46:544-555.

21. Sturzenbecker, L.J., Nibert, M.L., Furlong, D.B., and Fields, B.N. 1987. Intracellular digestion of reovirus particles requires a low pH and is an essential step in the viral infectious cycle. *J. Virol.* 61:2351-2361.

22. Borsa, J., Sargent, M.D., Lievaart, P.A., and Copps, T.P. 1981. Reovirus: evidence for a second step in the intracellular uncoating and transcriptase activation process. *Virology* 111:191-200.

23. Silverstein, S.C., Astell, C., Levin, D.H., Schonberg, M., and Acs, G. 1972. The mechanism of reovirus uncoating and gene activation *in vivo*. *Virology* 47:797-806.

24. Borsa, J., Copps, T.P., Sargent, M.D., Long, D.G., and Chapman, J.D. 1973. New intermediate subviral particles in the *in vitro* uncoating of reovirus virions by chymotrypsin. *J. Virol.* 11:552-564.

25. Nibert, M.L., and Fields, B.N. 1992. A carboxy-terminal fragment of protein μ1/μ1C is present in infectious subvirion particles of mammalian reoviruses and is proposed to have a role in penetration. *J. Virol.* 66:6408-6418.

26. Baer, G.S., and Dermody, T.S. 1997. Mutations in reovirus outer-capsid protein σ3 selected during persistent infections of L cells confer resistance to protease inhibitor E64. *J. Virol.* 71:4921-4928.

27. Clark, K.M., Wetzel, J.D., Bayley, J., Ebert, D.H., McAbee, S.A., Stoneman, E.K., Baer, G.S., Zhu, Y., Wilson, G.J., Prasad, B.V.V., and Dermody, T.S. 2006. Reovirus variants selected for resistance to ammonium chloride have mutations in viral outer-capsid protein σ3. *J. Virol.* 80:671-681.

28. Dermody, T.S., Nibert, M.L., Wetzel, J.D., Tong, X., and Fields, B.N. 1993. Cells and viruses with mutations affecting viral entry are selected during persistent infections of L cells with mammalian reoviruses. *J. Virol.* 67:2055-2063.

29. Wetzel, J.D., Chappell, J.D., Fogo, A.B., and Dermody, T.S. 1997. Efficiency of viral entry determines the capacity of murine erythroleukemia cells to support persistent infections by mammalian reoviruses. *J. Virol.* 71:299-306.

30. Lucia-Jandris, P., Hooper, J.W., and Fields, B.N. 1993. Reovirus M2 gene is associated with chromium release from mouse L cells. *J. Virol.* 67:5339-5345.

31. Hooper, J.W., and Fields, B.N. 1996. Role of the μ1 protein in reovirus stability and capacity to cause chromium release from host cells. *J. Virol.* 70:459-467.

32. Schelling, P., Guglielmi, K.M., Kirchner, E., Paetzold, B., Dermody, T.S., and Stehle, T. 2007. The reovirus σ1 aspartic acid sandwich: a trimerization motif poised for conformational change. *J. Biol. Chem.* 282:11582-11589.

33. Bassel-Duby, R., Jayasuriya, A., Chatterjee, D., Sonenberg, N., Maizel, J.V., Jr, and Fields, B.N. 1985. Sequence of reovirus haemagglutinin predicts a coiled-coil structure. *Nature* 315:421-423.

34. Duncan, R., Horne, D., Cashdollar, L.W., Joklik, W.K., and Lee, P.W.K. 1990. Identification of conserved domains in the cell attachment proteins of the three serotypes of reovirus. *Virology* 174:399-409.

35. Fraser, R.D.B., Furlong, D.B., Trus, B.L., Nibert, M.L., Fields, B.N., and Steven, A.C. 1990. Molecular structure of the cell-attachment protein of reovirus: correlation of computer-processed electron micrographs with sequence-based predictions. *J. Virol.* 64:2990-3000.

36. Nibert, M.L., Dermody, T.S., and Fields, B.N. 1990. Structure of the reovirus cell-attachment protein: a model for the domain organization of σ1. *J. Virol.* 64:2976-2989.

37. Gentsch, J.R., and Pacitti, A.F. 1987. Differential interaction of reovirus type 3 with sialylated receptor components on animal cells. *Virology* 161:245-248.

38. Paul, R.W., Choi, A.H., and Lee, P.W.K. 1989. The α-anomeric form of sialic acid is the minimal receptor determinant recognized by reovirus. *Virology* 172:382-385.

39. Paul, R.W., and Lee, P.W.K. 1987. Glycophorin is the reovirus receptor on human erythrocytes. *Virology* 159:94-101.

40. Dermody, T.S., Nibert, M.L., Bassel-Duby, R., and Fields, B.N. 1990. A sigma 1 region important for hemagglutination by serotype 3 reovirus strains. *J. Virol.* 64:5173-5176.

41. Gentsch, J.R., and Pacitti, A.F. 1985. Effect of neuraminidase treatment of cells and effect of soluble glycoproteins on type 3 reovirus attachment to murine L cells. *J. Virol.* 56:356-364.

42. Pacitti, A., and Gentsch, J.R. 1987. Inhibition of reovirus type 3 binding to host cells by sialylated glycoproteins is mediated through the viral attachment protein. *J. Virol.* 61:1407-1415.

43. Rubin, D.H., Wetzel, J.D., Williams, W.V., Cohen, J.A., Dworkin, C., and Dermody, T.S. 1992. Binding of type 3 reovirus by a domain of the σ1 protein important for hemagglutination leads to infection of murine erythroleukemia cells. *J. Clin. Invest.* 90:2536-2542.

44. Martin-Padura, I., Lostaglio, S., Schneemann, M., Williams, L., Romano, M., Fruscella, P., Panzeri, C., Stoppacciaro, A., Ruco, L., Villa, A., Simmons, D., and Dejana, E. 1998. Junctional adhesion molecule, a novel member of the immunoglobulin superfamily that distributes at intercellular junctions and modulates monocyte transmigration. *J. Cell Biol.* 142:117-127.

45. Campbell, J.A., Shelling, P., Wetzel, J.D., Johnson, E.M., Wilson, G.A.R., Forrest, J.C., Aurrand-Lions, M., Imhof, B., Stehle, T., and Dermody, T.S. 2005. Junctional adhesion molecule-A serves as a receptor for prototype and field-isolate strains of mammalian reovirus. *J. Virol.* 79:7967-7978.

46. Borsa, J., Morash, B.D., Sargent, M.D., Copps, T.P., Lievaart, P.A., and Szekely, J.G. 1979. Two modes of entry of reovirus particles into L cells. *J. Gen. Virol.* 45:161-170.

47. Ehrlich, M., Boll, W., Van Oijen, A., Hariharan, R., Chandran, K., Nibert, M.L., and Kirchhausen, T. 2004. Endocytosis by random initiation and stabilization of clathrin-coated pits. *Cell* 118:591-605.

48. Maginnis, M.S., Forrest, J.C., Kopecky-Bromberg, S.A., Dickeson, S.K., Santoro, S.A., Zutter, M.M., Nemerow, G.R., Bergelson, J.M., and Dermody, T.S. 2006. β1 integrin mediates internalization of mammalian reovirus. *J. Virol.* 80:2760-2770.

49. Maginnis, M.S., Mainou, B.A., Derdowski, A.M., Johnson, E.M., Zent, R., and Dermody, T.S. 2008. NPXY motifs in the β1 integrin cytoplasmic tail are required for functional reovirus entry. *J. Virol.* 82:3181-3191.

50. Stehle, T., and Dermody, T.S. 2004. Structural similarities in the cellular receptors used by adenovirus and reovirus. *Viral Immunol.* 17:129-143.

51. Breun, L.A., Broering, T.J., McCutcheon, A.M., Harrison, S.J., Luongo, C.L., and Nibert, M.L. 2001. Mammalian reovirus L2 gene and λ2 core spike protein sequences and whole-genome comparisons of reoviruses type 1 Lang, type 2 Jones, and type 3 Dearing. *Virology* 287:333-348.

52. Seliger, L.S., Zheng, K., and Shatkin, A.J. 1987. Complete nucleotide sequence of reovirus L2 gene and deduced amino acid sequence of viral mRNA guanylyltransferase. *J. Biol. Chem.* 262:16289-16293.

53. Reinisch, K.M., Nibert, M.L., and Harrison, S.C. 2000. Structure of the reovirus core at 3.6 Å resolution. *Nature* 404:960-967.

54. Keroack, M., and Fields, B.N. 1986. Viral shedding and transmission between hosts determined by reovirus L2 gene. *Science* 232:1635-1638.

55. Querbes, W., O'Hara, B.A., Williams, G., and Atwood, W.J. 2006. Invasion of host cells by JC virus identifies a novel role for caveolae in endosomal sorting of noncaveolar ligands. *J. Virol.* 80:9402-9413.

56. Laniosz, V., Holthusen, K.A., and Meneses, P.I. 2008. Bovine papillomavirus type 1: from clathrin to caveolin. *J. Virol.* 82:6288-6298.

57. Georgi, A., Mottola-Hartshorn, C., Warner, A., Fields, B., and Chen, L.B. 1990. Detection of individual fluorescently labeled reovirions in living cells. *Proc. Natl. Acad. Sci. U. S. A.* 87:6579-6583.

58. Rubin, D.H., Weiner, D.B., Dworkin, C., Greene, M.I., Maul, G.G., and Williams, W.V. 1992. Receptor utilization by reovirus type 3: distinct binding sites on thymoma and fibroblast cell lines result in differential compartmentalization of virions. *Microb. Pathog.* 12:351-365.

59. Joklik, W.K. 1972. Studies on the effect of chymotrypsin on reovirions. *Virology* 49:700-715.

60. Smith, R.E., Zweerink, H.J., and Joklik, W.K. 1969. Polypeptide components of virions, top component and cores of reovirus type 3. *Virology* 39:791-810.

61. Canning, W.M., and Fields, B.N. 1983. Ammonium chloride prevents lytic growth of reovirus and helps to establish persistent infection in mouse L cells. *Science* 219:987-988.

62. Maratos-Flier, E., Goodman, M.J., Murray, A.H., and Kahn, C.R. 1986. Ammonium inhibits processing and cytotoxicity of reovirus, a nonenveloped virus. *J. Clin. Invest.* 78:1003-1007.

63. Maxfield, F.R. 1982. Weak bases and ionophores rapidly and reversibly raise the pH in endocytic vesicles in cultured mouse fibroblasts. *J. Cell Biol.* 95:676-681.

64. Ohkuma, S., and Poole, B. 1978. Fluorescence probe measurement of the intralysosomal pH in living cells and the perturbation of pH by various agents. *Proc. Natl. Acad. Sci. U. S. A.* 75:3327-3331.

65. Martinez, C.G., Guinea, R., Benavente, J., and Carrasco, L. 1996. The entry of reovirus into L cells is dependent on vacuolar proton-ATPase activity. *J. Virol.* 70:576-579.

66. Barrett, A.J., Kembhavi, A.A., Brown, M.A., Kirschke, H., Knight, C.G., Tamai, M., and Hanada, K. 1982. L-*trans*-Epoxysuccinyl-leucylamido(4-guanidino)butane (E-64) and its analogues as inhibitors of cysteine proteinases including cathepsins B, H and L. *Biochem. J.* 201:189-198.

67. Chandran, K., and Nibert, M.L. 1998. Protease cleavage of reovirus capsid protein μ1/μ1C is blocked by alkyl sulfate detergents, yielding a new type of infectious subvirion particle. *J. Virol.* 72:467-475.

68. Ebert, D.H., Wetzel, J.D., Brumbaugh, D.E., Chance, S.R., Stobie, L.E., Baer, G.S., and Dermody, T.S. 2001. Adaptation of reovirus to growth in the presence of protease inhibitor E64 segregates with a mutation in the carboxy terminus of viral outer-capsid protein σ3. *J. Virol.* 75:3197-3206.

69. Jané-Valbuena, J., Nibert, M.L., Spencer, S.M., Walker, S.B., Baker, T.S., Chen, Y., Centonze, V.E., and Schiff, L.A. 1999. Reovirus virion-like particles obtained by recoating infectious subvirion particles with baculovirus-expressed σ3 protein: an approach for analyzing σ3 functions during virus entry. *J. Virol.* 73:2963-2973.

70. McAdoo, M.H., Dannenberg, A.M., Jr., Hayes, C.J., James, S.P., and Sanner, J.H. 1973. Inhibition of cathepsin D-type proteinase of macrophages by pepstatin, a specific pepsin inhibitor, and other substances. *Infect Immun* 7:655-665.

71. Kothandaraman, S., Hebert, M.C., Raines, R.T., and Nibert, M.L. 1998. No role for pepstatin-A-sensitive acidic proteinases in reovirus infections of L or MDCK cells. *Virology* 251:264-272.

72. Dermody, T.S. 1998. Molecular mechanisms of persistent infection by reovirus. In *Curr. Top. Microbiol. Immunol.* K.L. Tyler, and M.B.A. Oldstone, editors. Berlin: Springer-Verlag. 1-22.

73. Baer, G.S., Ebert, D.H., Chung, C.J., Erickson, A.H., and Dermody, T.S. 1999. Mutant cells selected during persistent reovirus infection do not express mature cathepsin L and do not support reovirus disassembly. *J. Virol.* 73:9532-9543.

74. Ebert, D.H., Kopecky-Bromberg, S.A., and Dermody, T.S. 2004. Cathepsin B is inhibited in mutant cells selected during persistent reovirus infection. *The Journal of Biological Chemistry* 279:3837-3851.

75. Bond, J.S., and Butler, P.E. 1987. Intracellular proteases. *Annu. Rev. Biochem.* 56:333-364.

76. Gal, S., and Gottesman, M.M. 1986. The major excreted protein (MEP) of transformed mouse cells and cathepsin L have similar protease specificity. *Biochemical & Biophysical Research Communications* 139:156-162.

77. Gottesman, M.M., and Sobel, M.E. 1980. Tumor promoters and Kirsten sarcoma virus increase synthesis of a secreted glycoprotein by regulating levels of translatable mRNA. *Cell* 19:449-455.

78. Kirschke, H., Langner, J., Wiederanders, B., Ansorge, S., and Bohley, P. 1977. Cathepsin L. A new proteinase from rat-liver lysosomes. *Eur. J. Biochem.* 74:293-301.

79. Gal, S., Willingham, M.C., and Gottesman, M.M. 1985. Processing and lysosomal localization of a glycoprotein whose secretion is transformation stimulated. *J. Cell Biol.* 100:535-544.

80. Mason, R.W. 1989. Interaction of lysosomal cysteine proteinases with alpha-2-macroglobulin: conclusive evidence for the endopeptidase activities of cathepsins B and H. *Archives of Biochemistry & Biophysics* 273:367-374.

81. Salminen, A., and Gottesman, M.M. 1990. Inhibitor studies indicate that active cathepsin L is probably essential to its own processing in cultured fibroblasts. *Biochem. J.* 272:39-44.

82. Mach, L., Stuwe, K., Hagen, A., Ballaun, C., and Glossl, J. 1992. Proteolytic processing and glycosylation of cathepsin B. The role of the primary structure of the latent precursor and of the carbohydrate moiety for cell-type-specific molecular forms of the enzyme. *Biochem. J.* 282:577-582.

83. Rowan, A.D., Mason, P., Mach, L., and Mort, J.S. 1992. Rat procathepsin B. Proteolytic processing to the mature form in vitro. *J. Biol. Chem.* 267:15993-15999.

84. Ryan, R.E., Sloane, B.F., Sameni, M., and Wood, P.L. 1995. Microglial cathepsin B: an immunological examination of cellular and secreted species. *J. Neurochem.* 65:1035-1045.

85. Reinheckel, T., Deussing, J., Roth, W., and Peters, C. 2001. Towards specific functions of lysosomal cysteine peptidases: phenotypes of mice deficient for cathepsin B or cathepsin L. *Biol. Chem.* 382:735-741.

86. Halangk, W., Lerch, M., Brandt--Nedelev, B., Roth, W., Ruthenbuerger, M., Reinheckel, T., Domschke, W., Lippert, H., Peters, C., and Deussing, J. 2000. Role of cathepsin B in intracellular trypsinogen activation and the onset of acute pancreatitis. *J. Clin. Invest.* 106:773-781.

87. Guicciardii, M.E., Deussing, J., Miyoshi, H., Bronk, S.F., Svingen, P.A., Peters, C., Kaufmann, S.H., and Gores, G.J. 2000. Cathespin B contributes to TNF-α–mediated hepatocyte apoptosis by promoting mitochondrial release of cytochrome c. *J. Clin. Invest.* 106:1127-1137.

88. Roth, W., Deussing, J., Botchkarev, V., Pauly-Evers, M., Saftig, P., Hafner, A., Schmidt, P., Schmahl, W., Scherer, J., Anton-Lamprechet, I., Von Figura, K., Paus, R., and Peters, C. 2000. Cathepsin L deficiency as molecular defect of furless: hyperproliferation of keratinocytes and perturbation of hair follicle cycling. *FASEB J.* 14:2075-2086.

89. Mizuochi, T., Yee, S.T., Kasai, M., Kakiuchi, T., Muno, D., and Kominami, E. 1994. Both cathepsin B and cathepsin D are necessary for processing of ovalbumin as well as for degradation of class II MHC invariant chain. *Immunol. Lett.* 43:189-193.

90. Matsunaga, Y., Saibara, T., Kido, H., and Katunuma, N. 1993. Participation of cathepsin B in processing of antigen presentation to MHC class II. *FEBS Lett.* 324:325-330.

91. Hsieh, C.S., deRoos, P., Honey, K., Beers, C., and Rudensky, A.Y. 2002. A role for cathepsin L and cathepsin S in peptide generation for MHC class II presentation. *J. Immunol.* 168:2618-2625.

92. Nakagawa, T., Roth, W., Wong, P., Nelson, A., Farr, A., Deussing, J., Villadangos, J.A., Ploegh, H., Peters, C., and Rudensky, A.Y. 1998. Cathepsin L: critical role in Ii degradation and CD4 T cell selection in the thymus. *Science* 280:450-453.

93. Honey, K., Nakagawa, T., Peters, C., and Rudensky, A. 2002. Cathepsin L regulates CD4+ T cell selection independently of its effect on invariant chain: a role in the generation of positively selecting peptide ligands. *J. Exp. Med.* 195:1349-1358.

94. Maehr, R., Mintern, J.D., Herman, A.E., Lennon-Dumenil, A.M., Mathis, D., Benoist, C., and Ploegh, H.L. 2005. Cathepsin L is essential for onset of autoimmune diabetes in NOD mice. *J. Clin. Invest.* 115:2934-2943.

95. Hsing, L.C., and Rudensky, A.Y. 2005. The lysosomal cysteine proteases in MHC class II antigen presentation. *Immunol. Rev.* 207:229-241.

96. Chapman, H.A. 2006. Endosomal proteases in antigen presentation. *Curr. Opin. Immunol.* 18:78-84.

97. Honey, K., Benlagha, K., Beers, C., Forbush, K., Teyton, L., Kleijmeer, M.J., Rudensky, A.Y., and Bendelac, A. 2002. Thymocyte expression of cathepsin L is essential for NKT cell development. *Nat. Immunol.* 3:1069-1074.

98. Golden, J.W., Bahe, J.A., Lucas, W.T., Nibert, M.L., and Schiff, L.A. 2004. Cathepsin S supports acid-independent infection by some reoviruses. *J. Biol. Chem.* 279:8547-8557.

99. Beers, C., Honey, K., Fink, S., Forbush, K., and Rudensky, A. 2003. Differential regulation of cathepsin S and cathepsin L in interferon gamma-treated macrophages. *J Exp Med* 197:169-179.

100. Beers, C., Burich, A., Kleijmeer, M.J., Griffith, J.M., Wong, P., and Rudensky, A.Y. 2005. Cathepsin S controls MHC class II-mediated antigen presentation by epithelial cells in vivo. *J Immunol* 174:1205-1212.

101. Morrison, L.A., Sidman, R.L., and Fields, B.N. 1991. Direct spread of reovirus from the intestinal lumen to the central nervous system through vagal autonomic nerve fibers. *Proc. Natl. Acad. Sci. U. S. A.* 88:3852-3856.

102. Fleeton, M., Contractor, N., Leon, F., Wetzel, J.D., Dermody, T.S., and Kelsall, B. 2004. Peyer's patch dendritic cells process viral antigen from apoptotic epithelial cells in the intestine of reovirus-infected mice. *J. Exp. Med.* 200:235-245.

103. Bass, D.M., Trier, J.S., Dambrauskas, R., and Wolf, J.L. 1988. Reovirus type 1 infection of small intestinal epithelium in suckling mice and its effect on M cells. *Laboratory Investigations* 58:226-235.

104. Rubin, D.H., Kornstein, M.J., and Anderson, A.O. 1985. Reovirus serotype 1 intestinal infection: a novel replicative cycle with ileal disease. *J. Virol.* 53:391-398.

105. Shi, G.P., Munger, J.S., Meara, J.P., Rich, D.H., and Chapman, H.A. 1992. Molecular cloning and expression of human alveolar macrophage cathepsin S, an elastinolytic cysteine protease. *J Biol Chem* 267:7258-7262.

106. Shi, G.P., Webb, A.C., Foster, K.E., Knoll, J.H., Lemere, C.A., Munger, J.S., and Chapman, H.A. 1994. Human cathepsin S: chromosomal localization, gene structure, and tissue distribution. *J Biol Chem* 269:11530-11536.

107. Petanceska, S., Canoll, P., and Devi, L.A. 1996. Expression of rat cathepsin S in phagocytic cells. *J Biol Chem* 271:4403-4409.

108. Riese, R.J., Wolf, P.R., Bromme, D., Natkin, L.R., Villadangos, J.A., Ploegh, H.L., and Chapman, H.A. 1996. Essential role for cathepsin S in MHC class II-associated invariant chain processing and peptide loading. *Immunity* 4:357-366.

109. Nakagawa, T.Y., Brissette, W.H., Lira, P.D., Griffiths, R.J., Petrushova, N., Stock, J., McNeish, J.D., Eastman, S.E., Howard, E.D., Clarke, S.R., Rosloniec, E.F., Elliott, E.A., and Rudensky, A.Y. 1999. Impaired invariant chain degradation and antigen presentation and diminished collagen-induced arthritis in cathepsin S null mice. *Immunity* 10:207-217.

110. Riese, R.J., Shi, G.P., Villadangos, J., Stetson, D., Driessen, C., Lennon-Dumenil, A.M., Chu, C.L., Naumov, Y., Behar, S.M., Ploegh, H., Locksley, R., and Chapman, H.A. 2001. Regulation of CD1 function and NK1.1(+) T cell selection and maturation by cathepsin S. *Immunity* 15:909-919.

111. Shen, L., Sigal, L.J., Boes, M., and Rock, K.L. 2004. Important role of cathepsin S in generating peptides for TAP-independent MHC class I crosspresentation in vivo. *Immunity* 21:155-165.

112. Nibert, M.L., Furlong, D.B., and Fields, B.N. 1991. Mechanisms of viral pathogenesis: distinct forms of reoviruses and their roles during replication in cells and host. *J. Clin. Invest.* 88:727-734.

113. Olland, A.M., Jané-Valbuena, J., Schiff, L.A., Nibert, M.L., and Harrison, S.C. 2001. Structure of the reovirus outer capsid and dsRNA-binding protein σ3 at 1.8 Å resolution. *EMBO J.* 20:979-989.

114. Nason, E.L., Wetzel, J.D., Mukherjee, S.K., Barton, E.S., Prasad, B.V.V., and Dermody, T.S. 2001. A monoclonal antibody specific for reovirus outer-capsid protein σ3 inhibits σ1-mediated hemagglutination by steric hindrance. *J. Virol.* 75:6625-6634.

115. Wetzel, J.D., Wilson, G.J., Baer, G.S., Dunnigan, L.R., Wright, J.P., Tang, D.S.H., and Dermody, T.S. 1997. Reovirus variants selected during persistent infections of L cells contain mutations in the viral S1 and S4 genes and are altered in viral disassembly. *J. Virol.* 71:1362-1369.

116. McCrae, M.A., and Joklik, W.K. 1978. The nature of the polypeptide encoded by each of the ten double-stranded RNA segments of reovirus type 3. *Virology* 89:578-593.

117. Mustoe, T.A., Ramig, R.F., Sharpe, A.H., and Fields, B.N. 1978. Genetics of reovirus: identification of the dsRNA segments encoding the polypeptides of the μ and σ size classes. *Virology* 89:594-604.

118. Wilson, G.J., Nason, E.L., Hardy, C.S., Ebert, D.H., Wetzel, J.D., Prasad, B.V.V., and Dermody, T.S. 2002. A single mutation in the carboxy terminus of reovirus outer-capsid protein σ3 confers enhanced kinetics of σ3 proteolysis, resistance to inhibitors of viral disassembly, and alterations in σ3 structure. *J. Virol.* 76:9832-9843.

119. Jané-Valbuena, J., Breun, L.A., Schiff, L.A., and Nibert, M.L. 2002. Sites and determinants of early cleavages in the proteolytic processing pathway of reovirus surface protein σ3. *J. Virol.* 76:5184-5197.

120. Chandran, K., Walker, S.B., Chen, Y., Contreras, C.M., Schiff, L.A., Baker, T.S., and Nibert, M.L. 1999. In vitro recoating of reovirus cores with baculovirus-expressed outer-capsid proteins μ1 and σ3. *J. Virol.* 73:3941-3950.

121. Danthi, P., Coffey, C.M., Parker, J.S., Abel, T.W., and Dermody, T.S. 2008. Independent regulation of reovirus membrane penetration and apoptosis by the μ1 ϕ domain. *PLoS Pathog* 4:e1000248.

122. Danthi, P., Kobayashi, T., Holm, G.H., Hansberger, M.W., Abel, T.W., and Dermody, T.S. 2008. Reovirus apoptosis and virulence are regulated by host cell membrane-penetration efficiency. *J. Virol.* 82:161-172.

123. Tosteson, M.T., Nibert, M.L., and Fields, B.N. 1993. Ion channels induced in lipid bilayers by subvirion particles of the nonenveloped mammalian reoviruses. *Proc. Natl. Acad. Sci. U. S. A.* 90:10549-10552.

124. Chandran, K., Parker, J.S., Ehrlich, M., Kirchhausen, T., and Nibert, M.L. 2003. The delta region of outer-capsid protein μ1 undergoes conformational change and release from reovirus particles during cell entry. *J. Virol.* 77:13361-13375.

125. Odegard, A.L., Chandran, K., Zhang, X., Parker, J.S., Baker, T.S., and Nibert, M.L. 2004. Putative autocleavage of outer capsid protein μ1, allowing release of myristoylated peptide μ1N during particle uncoating, is critical for cell entry by reovirus. *J. Virol.* 78:8732-8745.

126. Chandran, K., Farsetta, D.L., and Nibert, M.L. 2002. Strategy for nonenveloped virus entry: a hydrophobic conformer of the reovirus membrane penetration protein μ1 mediates membrane disruption. *J. Virol.* 76:9920-9933.

127. Nibert, M.L., Schiff, L.A., and Fields, B.N. 1991. Mammalian reoviruses contain a myristoylated structural protein. *J. Virol.* 65:1960-1967.

128. Nibert, M.L., Odegard, A.L., Agosto, M.A., Chandran, K., and Schiff, L.A. 2005. Putative autocleavage of reovirus μ1 protein in concert with outer-capsid disassembly and activation for membrane permeabilization. *J. Mol. Biol.* 345:461-474.

129. Bodkin, D.K., Nibert, M.L., and Fields, B.N. 1989. Proteolytic digestion of reovirus in the intestinal lumens of neonatal mice. *J. Virol.* 63:4676-4681.

130. Ivanovic, T., Agosto, M.A., Zhang, L., Chandran, K., Harrison, S.C., and Nibert, M.L. 2008. Peptides released from reovirus outer capsid form membrane pores that recruit virus particles. *Embo J* 27:1289-1298.

131. Agosto, M.A., Ivanovic, T., and Nibert, M.L. 2006. Mammalian reovirus, a nonfusogenic nonenveloped virus, forms size-selective pores in a model membrane. *Proc. Natl. Acad. Sci. U. S. A.* 103:16496-16501.

132. Ivanovic, T., Agosto, M.A., Chandran, K., and Nibert, M.L. 2007. A role for molecular chaperone Hsc70 in reovirus outer-capsid disassembly. *J Biol Chem* 282:12210-12219.

133. Bass, D.M., Bodkin, D., Dambrauskas, R., Trier, J.S., Fields, B.N., and Wolf, J.L. 1990. Intraluminal proteolytic activation plays an important role in replication of type 1 reovirus in the intestines of neonatal mice. *J. Virol.* 64:1830-1833.

134. Amerongen, H.M., Wilson, G.A.R., Fields, B.N., and Neutra, M.R. 1994. Proteolytic processing of reovirus is required for adherence to intestinal M cells. *J. Virol.* 68:8428-8432.

135. Wolf, J.L., Dambrauskas, R., Sharpe, A.H., and Trier, J.S. 1987. Adherence to and penetration of the intestinal epithelium by reovirus type 1 in neonatal mice. *Gastroenterology* 92:82-91.

136. Wolf, J.L., Kauffman, R.S., Finberg, R., Dambrauskas, R., Fields, B.N., and Trier, J.S. 1983. Determinants of reovirus interaction with the intestinal M cells and absorptive cells of murine intestine. *Gastroenterology* 85:291-300.

137. Wolf, J.L., Rubin, D.H., Finberg, R., Kaufman, R.S., Sharpe, A.H., Trier, J.S., and Fields, B.N. 1981. Intestinal M cells: a pathway of entry of reovirus into the host. *Science* 212:471-472.

138. Fleeton, M., Contractor, N., Leon, F., He, J., Wetzel, J.D., Dermody, T.S., Iwasaki, A., and Kelsall, B. 2004. Involvement of dendritic cell subsets in the induction of oral tolerance and immunity. *Ann. N. Y. Acad. Sci.* 1029:60-65.

139. Excoffon, K.J.D.A., Guglielmi, K.M., Wetzel, J.D., Gansemer, N.D., Campbell, J.A., Dermody, T.S., and Zabner, J. 2008. Reovirus preferentially infects the basolateral surface and is released from the apical surface of polarized human respiratory epithelial cells. *The Journal of Infectious Diseases* 197:1189-1197.

140. Rubin, D.H. 1987. Reovirus serotype 1 binds to the basolateral membrane of intestinal epithelial cells. *Microb. Pathog.* 3:215-220.

141. Weiner, D.B., Girard, K., Williams, W.V., McPhillips, T., and Rubin, D.H. 1988. Reovirus type 1 and type 3 differ in their binding to isolated intestinal epithelial cells. *Microb. Pathog.* 5:29-40.

142. Bodkin, D.K., and Fields, B.N. 1989. Growth and survival of reovirus in intestinal tissue: role of the L2 and S1 genes. *J. Virol.* 63:1188-1193.

143. Kauffman, R.S., Wolf, J.L., Finberg, R., Trier, J.S., and Fields, B.N. 1983. The σ1 protein determines the extent of spread of reovirus from the gastrointestinal tract of mice. *Virology* 124:403-410.

144. Tyler, K.L., McPhee, D.A., and Fields, B.N. 1986. Distinct pathways of viral spread in the host determined by reovirus S1 gene segment. *Science* 233:770-774.

145. Weiner, H.L., Powers, M.L., and Fields, B.N. 1980. Absolute linkage of virulence and central nervous system tropism of reoviruses to viral hemagglutinin. *J. Infect. Dis.* 141:609-616.

146. Weiner, H.L., Drayna, D., Averill, D.R., Jr, and Fields, B.N. 1977. Molecular basis of reovirus virulence: role of the S1 gene. *Proc. Natl. Acad. Sci. U. S. A.* 74:5744-5748.

147. Antar, A.A.R., Konopka, J.L., Campbell, J.A., Henry, R.A., Perdigoto, A.L., Carter, B.D., Pozzi, A., Abel, T.W., and Dermody, T.S. 2009. Junctional adhesion molecule-A is required for hematogenous dissemination of reovirus. *Cell Host and Microbe* 5:59-71.

148. Tardieu, M., Powers, M.L., and Weiner, H.L. 1983. Age-dependent susceptibility to reovirus type 3 encephalitis: role of viral and host factors. *Ann. Neurol.* 13:602-607.

149. Fan, J.Y., Boyce, C.S., and Cuff, C.F. 1998. T-Helper 1 and T-helper 2 cytokine responses in gut-associated lymphoid tissue following enteric reovirus infection. *Cell Immunol* 188:55-63.

150. London, S.D., Rubin, D.H., and Cebra, J.J. 1987. Gut mucosal immunization with reovirus serotype 1-L stimulates virus-specific cytotoxic T cell precursors as well as IgA memory cells in Peyer's patches. *J. Exp. Med.* 165:830-847.

151. Mathers, A.R., and Cuff, C.F. 2004. Role of interleukin-4 (IL-4) and IL-10 in serum immunoglobulin G antibody responses following mucosal or systemic reovirus infection. *J. Virol.* 78:3352-3360.

152. Cebra, J.J., Periwal, S.B., Lee, G., Lee, F., and Shroff, K.E. 1998. Development and maintenance of the gut-associated lymphoid tissue (GALT): the roles of enteric bacteria and viruses. *Dev Immunol* 6:13-18.

153. Cuff, C.F., Cebra, C.K., Rubin, D.H., and al, e. 1993. Developmental relationship between cytotoxic alpha/beta T cell receptor-positive intraepithelial lymphocytes and Peyer's patch lymphocytes. *Eur. J. Immunol.* 23:1333-1339.

154. London, S.D., Cebra, J.J., and Rubin, D.H. 1989. The reovirus-specific cytotoxic T cell response is not restricted to serotypically unique epitopes associated with the virus hemagglutinin. *Microb. Pathog.* 6:43-50.

155. Major, A.S., and Cuff, C.F. 1997. Enhanced mucosal and systemic immune responses to intestinal reovirus infection in beta2-microglobulin-deficient mice. *J. Virol.* 71:5782-5789.

156. Taterka, J., Cebra, J.J., and Rubin, D.H. 1995. Characterization of cytotoxic cells from reovirus-infected SCID mice: activated cells express natural killer- and lymphokine-activated killer-like activity but fail to clear infection. *J. Virol.* 69:3910-3914.

157. Major, A.S., and Cuff, C.F. 1996. Effects of the route of infection on immunoglobulin G subclasses and specificity of the reovirus-specific humoral immune response. *J. Virol.* 70:5968-5974.

158. Barkon, M.L., Haller, B.L., and Virgin, H.W.t. 1996. Circulating immunoglobulin G can play a critical role in clearance of intestinal reovirus infection. *J. Virol.* 70:1109-1116.

159. George, A., Kost, S.I., Witzleben, C.L., and al, e. 1990. Reovirus-induced liver disease in severe combined immunodeficient (SCID) mice. A model for the study of viral infection, pathogenesis, and clearance. *J. Exp. Med.* 171:929-934.

160. Haller, B.L., Barkon, M.L., Vogler, G.P., and Virgin, H.W., IV. 1995. Genetic mapping of reovirus virulence and organ tropism in severe combined immunodeficient mice: organ-specific virulence genes. *J. Virol.* 69:357-364.

161. Sherry, B., Li, X.Y., Tyler, K.L., Cullen, J.M., and Virgin, H.W. 1993. Lymphocytes protect against and are not required for reovirus-induced myocarditis. *J. Virol.* 67:6119-6124.

162. Virgin, H.W., and Tyler, K.L. 1991. Role of immune cells in protection against and control of reovirus infection in neonatal mice. *J. Virol.* 65:5157-5164.

163. Douville, R.N., Su, R.C., Coombs, K.M., Simons, F.E., and Hayglass, K.T. 2008. Reovirus serotypes elicit distinctive patterns of recall immunity in humans. *J. Virol.* 82:7515-7523.

164. Silvey, K.J., Hutchings, A.B., Vajdy, M., Petzke, M.M., and Neutra, M.R. 2001. Role of immunoglobulin A in protection against reovirus entry into Murine Peyer's patches. *J. Virol.* 75:10870-10879.

165. Tyler, K.L., Virgin, H.W., Bassel-Duby, R., and Fields, B.N. 1989. Antibody inhibits defined stages in the pathogenesis of reovirus serotype 3 infection of the central nervous system. *J. Exp. Med.* 170:887-900.

166. Kramer, D.R., and Cebra, J.J. 1995. Role of maternal antibody in the induction of virus specific and bystander IgA responses in Peyer's patches of suckling mice. *Int Immunol* 7:911-918.

167. Chandran, K., Sullivan, N.J., Felbor, U., Whelan, S.P., and Cunningham, J.M. 2005. Endosomal proteolysis of the Ebola virus glycoprotein is necessary for infection. *Science* 308:1643-1645.

168. Huang, I.-C., Bosch, B.J., Li, F., Li, W., Lee, K.H., Ghiran, S., Vasilieva, N., Dermody, T.S., Harrison, S.C., Dormitzer, P.R., Farzan, M., Rottier, P.J., and Choe, H. 2006. SARS coronavirus, but not human coronavirus NL63, utilizes cathepsin L to infect ACE2-expressing cells. *J. Biol. Chem.* 281:3198-3203.

169. Simmons, G., Gosalia, D.N., Rennekamp, A.J., Reeves, J.D., Diamond, S.L., and Bates, P. 2005. Inhibitors of cathepsin L prevent severe acute respiratory syndrome coronavirus entry. *Proc. Natl. Acad. Sci. U. S. A.* 102:11876-11881.

170. Pager, C.T., and Dutch, R.E. 2005. Cathepsin L is involved in proteolytic processing of the Hendra virus fusion protein. *J. Virol.* 79:12714-12720.

171. Pager, C.T., Craft, W.W., Jr., Patch, J., and Dutch, R.E. 2006. A mature and fusogenic form of the Nipah virus fusion protein requires proteolytic processing by cathepsin L. *Virology* 346:251-257.

172. Meulendyke, K.A., Wurth, M.A., McCann, R.O., and Dutch, R.E. 2005. Endocytosis plays a critical role in proteolytic processing of the Hendra virus fusion protein. *J. Virol.* 79:12643-12649.

173. Morrison, L.A., Fields, B.N., and Dermody, T.S. 1993. Prolonged replication in the mouse central nervous system of reoviruses isolated from persistently infected cultures. *J. Virol.* 67:3019-3026.

174. Barton, E.S., Youree, B.E., Ebert, D.H., Forrest, J.C., Connolly, J.L., Valyi-Nagy, T., Washington, K., Wetzel, J.D., and Dermody, T.S. 2003. Utilization of sialic acid as a coreceptor is required for reovirus-induced biliary disease. *J. Clin. Invest.* 111:1823-1833.

175. Barton, E.S., Connolly, J.L., Forrest, J.C., Chappell, J.D., and Dermody, T.S. 2001. Utilization of sialic acid as a coreceptor enhances reovirus attachment by multistep adhesion strengthening. *J. Biol. Chem.* 276:2200-2211.

176. Wilson, G.A., Morrison, L.A., and Fields, B.N. 1994. Association of the reovirus S1 gene with serotype 3-induced biliary atresia in mice. *J. Virol.* 68:6458-6465.

177. Derrien, M., Hooper, J.W., and Fields, B.N. 2003. The M2 gene segment is involved in the capacity of reovirus type 3Abney to induce the oily fur syndrome in neonatal mice, a S1 gene segment-associated phenotype. *Virology* 305:25-30.

178. Papadimitriou, J.M. 1968. The biliary tract in acute murine reovirus 3 infection. *Am. J. Pathol.* 52:595-601.

179. Phillips, P.A., Keast, D., Papadimitriou, J.M., Walters, M.N., and Stanley, N.F. 1969. Chronic obstructive jaundice induced by reovirus type 3 in weanling mice. *Pathology* 1:193-203.

180. Parashar, K., Tarlow, M.J., and McCrae, M.A. 1992. Experimental reovirus type 3-induced murine biliary tract disease. *J. Pediatr. Surg.* 27:843-847.

181. Sacher, T., Podlech, J., Mohr, C.A., Jordan, S., Ruzsics, Z., Reddehase, M.J., and Koszinowski, U.H. 2008. The major virus-producing cell type during murine cytomegalovirus infection, the hepatocyte, is not the source of virus dissemination in the host. *Cell Host Microbe* 3:263-272.

182. Ernst, H., and Shatkin, A.J. 1985. Reovirus hemagglutinin mRNA codes for two polypeptides in overlapping reading frames. *Proc. Natl. Acad. Sci. U. S. A.* 82:48-52.

183. Jacobs, B.L., and Samuel, C.E. 1985. Biosynthesis of reovirus-specified polypeptides: the reovirus S1 mRNA encodes two primary translation products. *Virology* 143:63-74.

184. Nagata, L., Masri, S.A., Mah, D.C., and Lee, P.W.K. 1984. Molecular cloning and sequencing of the reovirus (serotype 3) S1 gene which encodes the viral cell attachment protein σ1. *Nucleic Acids Res.* 12:8699-8710.

185. Shi, G.P., Villadangos, J.A., Dranoff, G., Small, C., Gu, L., Haley, K.J., Riese, R., Ploegh, H.L., and Chapman, H.A. 1999. Cathepsin S required for normal MHC class II peptide loading and germinal center development. *Immunity* 10:197-206.

186. Katunuma, N., Murata, E., Kakegawa, H., Matsui, A., Tsuzuki, H., Tsuge, H., Turk, D., Turk, V., Fukushima, M., Tada, Y., and Asao, T. 1999. Structure based development of novel specific inhibitors for cathepsin L and cathepsin S in vitro and in vivo. *FEBS Lett* 458:6-10.

187. Yang, M., Zhang, Y., Pan, J., Sun, J., Liu, J., Libby, P., Sukhova, G.K., Doria, A., Katunuma, N., Peroni, O.D., Guerre-Millo, M., Kahn, B.B., Clement, K., and Shi, G.P. 2007. Cathepsin L activity controls adipogenesis and glucose tolerance. *Nat Cell Biol* 9:970-977.

188. Katunuma, N., Tsuge, H., Nukatsuka, M., Asao, T., and Fukushima, M. 2002. Structure-based design of specific cathepsin inhibitors and their application to

protection of bone metastases of cancer cells. *Arch. Biochem. Biophys.* 397:305-311.

189. Diederich, S., Thiel, L., and Maisner, A. 2008. Role of endocytosis and cathepsin-mediated activation in Nipah virus entry. *Virology* 375:391-400.

190. Porotto, M., Orefice, G., Yokoyama, C., Mungall, B., Realubit, R., Sganga, M., Aljofan, M., Whitt, M., Glickman, F., and Moscona, A. 2009. Simulating henipavirus multicycle replication in a screening assay leads to identification of a promising candidate for therapy. *J. Virol.* 83:5148-5155.

191. Tardieu, M., and Weiner, H.L. 1982. Viral receptors on isolated murine and human ependymal cells. *Science* 215:419-421.

192. Tyler, K.L., Mann, M.A., Fields, B.N., and Virgin, H.W., IV. 1993. Protective anti-reovirus monoclonal antbodies and their effects on viral pathogenesis. *J. Virol.* 67:3446-3453.

193. Flamand, A., Gagner, J.P., Morrison, L.A., and al, e. 1991. Penetration of the nervous systems of suckling mice by mammalian reoviruses. *J. Virol.* 65:123-131.

194. Mann, M.A., Knipe, D.M., Fischbach, G.D., and Fields, B.N. 2002. Type 3 reovirus neuroinvasion after intramuscular inoculation: direct invasion of nerve terminals and age-dependent pathogenesis. *Virology* 303:222-231.

195. Campenot, R.B. 1977. Local control of neurite development by nerve growth factor. *Proc Natl Acad Sci U S A* 74:4516-4519.

196. Ch'ng, T.H., and Enquist, L.W. 2006. An in vitro system to study trans-neuronal spread of pseudorabies virus infection. *Vet Microbiol* 113:193-197.

197. Ch'ng, T.H., Flood, E.A., and Enquist, L.W. 2005. Culturing primary and transformed neuronal cells for studying pseudorabies virus infection. *Methods Mol Biol* 292:299-316.

198. Vasiljeva, O., Reinheckel, T., Peters, C., Turk, D., Turk, V., and Turk, B. 2007. Emerging roles of cysteine cathepsins in disease and their potential as drug targets. *Curr. Pharm. Des.* 13:387-403.

199. Haque, A., Banik, N.L., and Ray, S.K. 2008. New insights into the roles of endolysosomal cathepsins in the pathogenesis of Alzheimer's disease: cathepsin inhibitors as potential therapeutics. *CNS Neurol. Disord. Drug Targets* 7:270-277.

200. Mohamed, M.M., and Sloane, B.F. 2006. Cysteine cathepsins: multifunctional enzymes in cancer. *Nat. Rev. Cancer* 6:764-775.

201. Ha, S.D., Martins, A., Khazaie, K., Han, J., Chan, B.M., and Kim, S.O. 2008. Cathepsin B is involved in the trafficking of TNF-alpha-containing vesicles to the plasma membrane in macrophages. *J Immunol* 181:690-697.

202. Tang, Q., Cai, J., Shen, D., Bian, Z., Yan, L., Wang, Y.X., Lan, J., Zhuang, G.Q., Ma, W.Z., and Wang, W. 2009. Lysosomal cysteine peptidase cathepsin L protects against cardiac hypertrophy through blocking AKT/GSK3beta signaling. *J Mol Med* 87:249-260.

203. Matsumoto, F., Saitoh, S., Fukui, R., Kobayashi, T., Tanimura, N., Konno, K., Kusumoto, Y., Akashi-Takamura, S., and Miyake, K. 2008. Cathepsins are required for Toll-like receptor 9 responses. *Biochem Biophys Res Commun* 367:693-699.

204. Puzer, L., Cotrin, S.S., Alves, M.F., Egborge, T., Araujo, M.S., Juliano, M.A., Juliano, L., Bromme, D., and Carmona, A.K. 2004. Comparative substrate specificity analysis of recombinant human cathepsin V and cathepsin L. *Arch Biochem Biophys* 430:274-283.

205. Mori, Y., Yamashita, T., Tanaka, Y., Tsuda, Y., Abe, T., Moriishi, K., and Matsuura, Y. 2007. Processing of capsid protein by cathepsin L plays a crucial role in replication of Japanese encephalitis virus in neural and macrophage cells. *J. Virol.* 81:8477-8487.

206. Maekawa, Y., Himeno, K., Ishikawa, H., Hisaeda, H., Sakai, T., Dainichi, T., Asao, T., Good, R.A., and Katunuma, N. 1998. Switch of CD4+ T cell differentiation from Th2 to Th1 by treatment with cathepsin B inhibitor in experimental leishmaniasis. *J Immunol* 161:2120-2127.

207. Saegusa, K., Ishimaru, N., Yanagi, K., Arakaki, R., Ogawa, K., Saito, I., Katunuma, N., and Hayashi, Y. 2002. Cathepsin S inhibitor prevents autoantigen presentation and autoimmunity. *J Clin Invest* 110:361-369.

208. Alain, T., Kim, T.S., Lun, X., Liacini, A., Schiff, L.A., Senger, D.L., and Forsyth, P.A. 2007. Proteolytic disassembly is a critical determinant for reovirus oncolysis. *Mol. Ther.* 15:1512-1521.

209. Furlong, D.B., Nibert, M.L., and Fields, B.N. 1988. Sigma 1 protein of mammalian reoviruses extends from the surfaces of viral particles. *J. Virol.* 62:246-256.

210. Virgin, H.W., IV, Bassel-Duby, R., Fields, B.N., and Tyler, K.L. 1988. Antibody protects against lethal infection with the neurally spreading reovirus type 3 (Dearing). *J. Virol.* 62:4594-4604.

211. Carmona, E., Dufour, É., Plouffe, C., Takebe, S., Mason, P., Mort, J.S., and Ménard, R. 1996. Potency and selectivity of the cathepsin L propeptide as an inhibitor of cysteine proteases. *Biochemistry* 35:8149-8157.

212. Deussing, J., Roth, W., Saftig, P., Peters, C., Ploegh, H.L., and Villadangos, J.A. 1998. Cathepsins B and D are dispensable for major histocompatibility complex class II-mediated antigen presentation. *Proc. Natl. Acad. Sci. U. S. A.* 95:4516-4521.

213. Rubin, D.H., and Fields, B.N. 1980. Molecular basis of reovirus virulence: role of the M2 gene. *J. Exp. Med.* 152:853-868.

214. Tyler, K.L., Bronson, R.T., Byers, K.B., and Fields, B.N. 1985. Molecular basis of viral neurotropism: experimental reovirus infection. *Neurology* 35:88-92.

215. Virgin, H.W., Dermody, T.S., and Tyler, K.L. 1998. Cellular and humoral immunity to reovirus infection. In *Curr. Top. Microbiol. Immunol.* K.L. Tyler, and M.B.A. Oldstone, editors. Berlin: Springer-Verlag. 147-161.

216. Richardson, B.A., and Overbaugh, J. 2005. Basic statistical considerations in virological experiments. *J. Virol.* 79:669-676.

217. O'Donnell, S.M., Hansberger, M.W., Connolly, J.L., Chappell, J.D., Watson, M.J., Pierce, J.M., Wetzel, J.D., Han, W., Barton, E.S., Forrest, J.C., Valyi-Nagy, T., Yull, F.E., Blackwell, T.S., Rottman, J.N., Sherry, B., and Dermody, T.S. 2005. Organ-specific roles for transcription factor NF-κB in reovirus-induced apoptosis and disease. *J. Clin. Invest.* 115:2341-2350.

218. Barton, E.S., Forrest, J.C., Connolly, J.L., Chappell, J.D., Liu, Y., Schnell, F., Nusrat, A., Parkos, C.A., and Dermody, T.S. 2001. Junction adhesion molecule is a receptor for reovirus. *Cell* 104:441-451.

219. Boll, W., Ohno, H., Songyang, Z., Rapoport, I., Cantley, L.C., Bonifacino, J.S., and Kirchhausen, T. 1996. Sequence requirements for the recognition of tyrosine-based endocytic signals by clathrin AP-2 complexes. *Embo J* 15:5789-5795.

220. Boll, W., Rapoport, I., Brunner, C., Modis, Y., Prehn, S., and Kirchhausen, T. 2002. The μ2 subunit of the clathrin adaptor AP-2 binds to FDNPVY and Yppϕ sorting signals at distinct sites. *Traffic* 3:590-600.

221. Mishra, S.K., Keyel, P.A., Hawryluk, M.J., Agostinelli, N.R., Watkins, S.C., and Traub, L.M. 2002. Disabled-2 exhibits the properties of a cargo-selective endocytic clathrin adaptor. *EMBO J.* 21:4915-4926.

222. Morris, S.M., and Cooper, J.A. 2001. Disabled-2 colocalizes with the LDLR in clathrin-coated pits and interacts with AP-2. *Traffic* 2:111-123.

223. Ohno, H., Stewart, J., Fournier, M.C., Bosshart, H., Rhee, I., Miyatake, S., Saito, T., Gallusser, A., Kirchhausen, T., and Bonifacino, J.S. 1995. Interaction of tyrosine-based sorting signals with clathrin-associated proteins. *Science* 269:1872-1875.